GEOCHEMICAL AND ISOTOPIC STUDIES OF SOME SEDIMENTARY SEQUENCES OF THE VINDHYAN SUPERGROUP, INDIA

A Thesis submitted to

THE MAHARAJA SAYAJIRAO UNIVERSITY OF BARODA

For

THE DEGREE OF DOCTOR OF PHILOSOPHY

In

Geology

By

ANIL DUTT SHUKLA

Physical Research Laboratory
Ahmedabad 380009
India

August, 2011

Dedicated to my parents and family

DECLARATION

This is to certify that the contents of this thesis comprise original research work of the candidate and have at no time been submitted for any other degree or diploma.

Anil Dutt Shukla
(Candidate)

Certified by:

Dr. J. S. Ray
(Guide)
Physical Research Laboratory
Ahmedabad 380 009, India

Prof. L. S. Chamyal
(Co-Guide)
M. S. University of Baroda
Vadodara 390 002, India

Head
Department of Geology
Faculty of Science
M. S. University of Baroda
Vadodara 390 002, India

CONTENTS

List of Tables Page no.

List of Figures **Page No.**

Acknowledgements

I would like to express my gratitude for the inspirations, the support and the help I have got from various persons during the present thesis work, which could have not been possible in the present form. First of all I would like to thank and be indebted for the great amount of encouragements and invaluable support from my supervisor and friend Prof. J. S. Ray, whose consistent pursuance, perseverance and guidance has made this possible. His invaluable suggestions and critical views helped me in enhancing the quality of this work. I would like to pay my high regards and gratitude to Prof. L. S. Chamyal, a teacher, and a true gentleman, for his generosity and always available for any kind of help, suggestions and guidance whenever I have asked for.

I would be highly grateful to Prof. J. N. Goswami, Director, PRL, for his kind support and encouragements and help for completing this work whenever required. I will be highly indebted to Prof. N. Bhandari and Dr. P. N. Shukla, for their kind support and guidance which have taught me the various aspects of research during my association which have shown the intricacies of this sphere of life. I would also like to thank Profs. S. Krishnaswami, A. K. Singhvi, S. V. S. Murty, M. M. Sarin, R. Ramesh, S. K. Singh, D. Banerjee for their suggestions, support and encouragement.

The invaluable scientific discussions and continuous encouragement from my senior and big-brother Dr. N. Juyal were highly refreshing during the course of study for which I am really obliged. Dr. R. Bhushan's witty comments and continuous encouragement are accredited which have helped me a lot in working out the thesis. I accord special thanks to Dr. S. Ramachandran, for his kind and sincere help. My other seniors, colleagues & friends, Drs. M. G. Yadav, R. D. Deshpande, R. Rengarajan, D. Chakraborty, V. Sheel, S. K. Sharma, S. Ganesh, Kuljeet K. Marhas, V. K. Rai, , Mr. Deepak Panda, Mr. K. Dugraprasad, Mr. R. P. Singh, and Mr. Sudheer, Raoji, Pranav and Janiji, are highly appreciated for all their kind help, support and encouragement I got through out the research work. The selfless attitude of J. P. Bhavsar is very much acknowledged who is always ready for help. The students of the Geosciences Division: Alok Kumar, Neeraj Awasthi s help are refreshing & accredited which were always there whenever I have asked during the work and Rehman, Gyanranjan, Vineet, Amzad, Gaurav and Debashish are also acknowledged for their help and support. I would also like to thank to the other members and colleagues of the Geosciences and Planetary Sciences Divisions for their help whenever I have asked. The Computational facility, Workshop, Services, Purchase and Administration people of PRL are acknowledged for their help and support and will be grateful.

I dedicate my thesis to my beloved family and my parents who always stood by me during my thin & thick days. Dipti (wife) has been a source of inspiration with her support and love at home and in my professional work, for which I will be highly obliged. Shivangi and Saanvi my beautiful daughters remain always my source of strength with their cheerful actions, love and affection. I would like to thank my mother and father for providing all their help and support for everything I wanted do in life. I shall remain grateful to my younger brother Anoop and my sisters Anita and Sunita for their love and affection. The kind support and encouragement from my in-laws is also acknowledged. And at the last I would like to thank everybody who has interacted with me during this work.

(Anil Dutt Shukla)

Chapter-1

INTRODUCTION

The sedimentary sequences preserve records of tectonic, climate and biological evolution of our planet. They are the most striking evidence of a wet and dynamic Earth. They are the products of surface processes and store valuable information on processes like weathering, transportation and diagenesis during the Earth's history. (Bio) chemical sediments, precipitated from seawater, preserve information on the chemical evolution of the sea with time and the evolution of life on the Earth. It is therefore, essential that we study and understand the formation of sediments and sedimentary rocks to unravel the mysteries of our planet.

Deciphering the provenance of sediments is one of the most important aspects of any study on sedimentary sequences. Provenance study deals with the history of the sedimentation from their sources, which is basically the reconstruction of the parent-rock compositions from which the assemblages of sediments have been derived and the study of climatic and physiographic conditions under which their formation had taken place. The inference of the sediment provenance from the final product i.e. the sedimentary rocks (sequences), is not straightforward because of the involvement of various agents in the pathways from the source to sink (basin). For a successful provenance analysis one has to understand in greater detail the nature and extent of compositional and textural modifications suffered by the sediments.

Study of sedimentary provenances started as early as in the 19th century with the microscopic investigation of accessory (heavy) minerals of modern sands. Earlier attempts were to trace accessory minerals of recent beach and river sands to their parent rocks (Weltje & Eynatten, 2004, and references therein). The provenance analyses of old sediments using accessory minerals were first attempted by Thürach

(1884). The usage of the petrographic analysis of major framework constituents for the provenance became possible after the invention of thin-section petrography by H.C. Sorby in 1880 and who carried out the first detailed study of various types of quartz. The influence of climate on the preservation of feldspars was recognized as early as 1886 by Judd. Later Mackie (1899a&b), developed criteria for the recognition of quartz grains derived from igneous and metamorphic rocks and tried to interpret feldspars as indicators of prevalent climatic conditions. The early part of 20th century saw the full development of the thin-section sandstone petrography and at the same time quantitative characterization of bulk sediment properties by chemical analysis became popular (see Weltje & Eynatten, 2004).

The first systematic quantitative investigations of sand bulk mineralogy started in the 1930s with modal composition, combining various methods of separation with mounting-and-counting techniques. Later Krumbein and Pettijohn (1938) presented the first comprehensive overview of quantitative methods in sedimentary petrography and in the 1940s, P.D. Krynine and F.J. Pettijohn proposed the first versions of the sandstone classification schemes that are still being used. The importance of tectonic control on the compositional and textural properties of sandstones had been advocated by Krynine. He was inspired by the ideas of his teacher M.S. Shvetsov, who realised already in the 1920s that sandstone mineralogy could be related to tectonic setting (Folk and Ferm, 1966). The invention of a practical point-counting device in 1949 opened the flood gate for the routine measurement of modal composition from thin sections in sandstones and received new impulses through the work of Dickinson (1970), who established clear cut operational definitions for grain types to improve the reproducibility of detrital modes.

The use of geochemistry for the provenance determination started as early as 1916 but its real impetus came in the later part of the 20th century when attempts were made to derive the composition of continental crust (Taylor and McLennan, 1985), and to understand tectonic settings and provenance (Bhatia 1983; Bhatia and Crook, 1986; Roser and Korsch, 1986). It has now been established that chemical composition of sediments (siliciclastic/chemical) can be used effectively to identify the sources of sediments, tectonic settings in the provenance and prevalent climatic conditions. For example, the Rare Earth Elements (REE), which behave as a chemically coherent group due to their similarities in ionic radii and non fractionating behaviour during weathering and diagenesis, are very useful in deriving information about the sources of sediments as well as climatic conditions that prevailed at the time of their deposition (Taylor and McLennan, 1985). Similarly, Nd isotopic ratio is a good indicator of sediment provenance, since Sm and Nd do not get fractionated during weathering/deposition/diagenetic processes (Miller and O'Nions, 1984; Nelson and DePaolo, 1988; Basu et al., 1990; Gleason et al., 1994). Geochronology of sedimentary sequences, in general, is difficult in the absence of dateable igneous material and lack of robust biostratigraphy. In such scenarios, detrital zircon geochronology has proven to be one of the most reliable tools for establishing relative chronology of various formations in a sequence. Detrital zircon geochronology can also reveal a lot about the source rocks, which in turn can be used to develop a depositional model for a sedimentary basin.

1.1 The Proterozoic time on the Earth

The period of Earth's history between 2.5 Ga and 543 Ma is known as the **Proterozoic Eon.** Covering about 43% of Earth's history, it records many of the most exciting geological events of our planet. During this Eon, continents formed over stable cratons and 'modern plate tectonics' began to take control over all geodynamic processes. This exciting period of the Earth has been divided into three subdivisions namely: Paleoproterozoic Era (2500-1600Ma); Mesoproterozoic Era (1600-1000Ma) and Neoproterozoic Era (1000-543Ma). The major events during Proterozoic that shaped our planet are listed in Table 1.1. The table also lists some of the major events of this period in Indian Geology. Some of the important events of the Proterozoic Eon that have caught our imagination are: the global glaciations and the rise of atmospheric oxygen in the Paleoproterozoic and Neoproterozoic (Hoffman et al., 1998; Catling and Claire, 2005; Kopp et al., 2005), the origin of eukaryotes in the Paleoproterozoic (Javaux et al., 2001), and evolution of animals in Neoproterozoic (Yin et al., 2007), and stabilization of the continents (Condie, 1982). The Proterozoic Eon began and ended with episodes of global glaciations (Hoffman et al., 1998; Hoffman and Schrag, 2002; Kopp et al., 2005). The net result of the Paleoproterozoic and Neoproterozoic glaciations was probably a dramatic increase in atmospheric O_2 concentration (Rye and Holland, 1998; Catling and Claire, 2005). Since aerobic respiration and synthesis of membrane lipids (sterols and unsaturated fatty acids) by eukaryotic organisms require certain levels of molecular oxygen, the link between the rise of atmospheric O_2 concentration in the Paleoproterozoic and the appearance of sophisticated morphologies of eukaryotes at ~1800 Ma is appealing. Similarly, multi-cellular life forms like *Ediacara,* resembling the modern day jelly-fish, may have become abundant after the Neoproterozoic glaciations.

In the Proterozoic Eon modern plate tectonics began to govern over other processes in shaping the form of the Earth's crust (Condie, 1982). The first definite proof of the formation of a supercontinent, between 1300-1000 Ma, named as "Rodinia" and its break-up at ~ 750Ma, and various mountain building activities such as Greenville Orogeny have also been reported from this Eon. In India, the evolution of the Aravalli-Delhi mountain belts and the Satpura mountain belt are considered to be of Mesoproterozoic age (see Ramakrishnan and Vaidyanadhan, 2008). It is quite possible that the mantle on which the continental lithospheres floated was hotter, less viscous, and could have been closer to the surface resulting in swift movements of continents. These small continents could have collided quite often and tended to fracture or suture with greater frequency.

Therefore, for understanding the evolution of the Earth, one has to understand the events of the Proterozoic Eon. The Proterozoic sedimentary basins are the best places where the records of these events have been faithfully recorded. The atmosphere, biosphere, hydrosphere, and lithosphere of the Earth affect each other and co-evolve over time, hence for understanding the evolution of the history of the Earth's various systems one needs to unravel the mysteries recorded in the sedimentary deposits.

Table 1.1: Major events of the world and India observed during the Proterozoic Eon*.

A) **Paleoproterozoic Era** (2500 to 1600 Ma)
• Stable continents first appeared. • First free oxygen is found in the oceans and atmosphere around 2500 Ma. • Great Oxidation Event also called the Oxygen Catastrophe: at 2400 Ma. Oxidation precipitates dissolved iron creating banded iron formations. Anaerobic organisms are poisoned by oxygen. • Start of Huronian ice age : 2400 Ma • Opening of the Aravalli basin : 2300Ma • Organisms with mitochondria capable of aerobic respiration appear: 2200 Ma • End of Huronian ice age : 2100 Ma • Intensive orogeny (mountain development) • Meteor impact, 300 km crater Vredefort, South Africa : 2023 Ma • Solar luminosity became 85% of the current level : 2000 Ma • Oxygen starts accumulating in the atmosphere • Major pulse of the Aravalli orogeny : 1900Ma • Meteor impact, 250 km crater Sudbury, Ontario, Canada: 1850 Ma • Complex single-celled life appeared with abundant bacteria • Initiation of sedimentation in the 'Purana Basin's : ~1700 Ma
B) **Mesoproterozoic Era** (1600 to 1000 Ma)
• Photosynthetic organisms proliferate. • Oxygen builds up in the atmosphere above 10%. • Formation of ozone layer starts blocking ultraviolet radiation from the sun. • Eukaryotic (nucleated) cells appear: 1500 Ma Green (Chlorobionta) and red (Rhodophyta) algae abound. • Delhi Orogeny : 1500 Ma • Spore/gamete formation indicates origin of sexual reproduction : 1200 Ma • Formation of the supercontinent ***Rodinia: 1100 Ma*** • Mountain building activity e.g. Greenville orogeny
C) **Neoproterozoic Era** (1000 to 542 Ma)
• Multicellular organisms appear : 1000 Ma • Start of Stuartian-Varangian ice age : 950 Ma • Massive granitization in the Aravalli-Delhi Orogen:1000Ma • **Cryogenian Period** (850 to 630 Ma) • Breakup of Rodinia and formation of the supercontinent ***Pannotia: 750 Ma*** • End of last magnetic reversal : 750 Ma • Mass extinction of 70% of dominant sea plants due to global glaciation *("Snowball Earth"* hypothesis) : 650 Ma • **Ediacaran (Vendian) Period** (630 to 542 Ma) • Soft-bodied organisms (Jellyfish, Tribrachidium, and Dickinsonia) appeared : 580 Ma • End of Stuartian-Varangian ice age : 570 Ma • Pannotia fragmented into Laurasia and Gondwana : 550 Ma

**(Schopf and Klein (1992) and other web resources)*

1.2 Proterozoic Basins of India

The sedimentary sequences started developing over the Indian Peninsula after its emergence as a large shield after accretion of smaller Archean cratons, around 2500Ma ago (Rogers, 1986). The old sedimentary sequences, at present exposed in structurally controlled manner and classified as 'Purana Basins' were formed after the Archean-Proterozoic transition (~2500Ma). These basins are named as the *Aravalli, Delhi, Vindhyan, Bhima, Kaladgi, Indrawati, Chhatisgarh-Raipur, Khariar, Cuddapah, Pranhita-Godavari,* etc. (Fig. 1.1). The Central Indian Tectonic zone (CITZ), which is of Mesoproterozoic age (Acharyya, 2003), divides these basins into northern and southern groups. Numerous basins in southern group are erosional with several major unconformities and were developed on the Dharwar, Baster and Singhbum cratons. In north the largest basin is known as the Vindhyan Basin, and the sedimentary sequences known as the Vindhyan Supergroup, developed on the Bundelkhand and Aravalli cratons.

One of the most intriguing aspects yet to be understood is the places of origin of the sediments for these massive and almost contemporaneous ocean basin deposits. Their coexistence is established by numerous geochronological studies (Rasmussen et al., 2002; Ray et al., 2002, 2003; Sarangi et al., 2004; Ray, 2006; Chakrabarti et al., 2007; Patranabis-Deb et al., 2007; Malone et al., 2008; Bengtson et al., 2009; Turner et al., 2010). Considering the thickness of the various Proterozoic basins, it is quite obvious that massive amounts of sediments poured into these basins and that enormous amount of weathering and erosion must have taken place in various orogens and cratons (e.g. Aravalli-Delhi, Satpuras, Bundelkhand, Dharwar, and Singhbum etc.). Since majority of these Proterozoic sequences are mostly undeformed and unmetamorphosed, they are believed to have preserved intact geological records of the Proterozoic India.

The Vindhyan Supergroup of rocks, deposited in the Vindhyan Basin, cover an aerial extent of ~ 178,000 km^2, spread from Sasaram (Bihar) along the Son river Valley in the east to Chittorgarh, Kota, Bundi, Sawai Madhopur districts of Rajasthan in the west (Fig. 1.1). The basin is bounded by the Aravalli-Delhi orogenic belt (2500-900 Ma) in the west, and by the Satpura orogenic belt (1600–850 Ma) in the south and south-east. Low-grade metamorphic rocks of the Mahakoshal (2400 Ma) and the Bijawar (2100 Ma) Supergroups border its eastern margin. The granite and gneisses of the Bundelkhand craton (3.3-2.5 Ga), which are acting as the basement ridges in the centre divide the basin into eastern (Son valley) and western (Rajasthan) sectors (Prasad and Rao, 2006). The ~4 km thick Vindhyan Supergroup comprises predominantly shallow marine deposits that are mildly deformed and mostly unmetamorphosed. The Supergroup has been divided into the Lower Vindhyans (Semri Group) and the Upper Vindhyans (Kaimur, Rewa and Bhander Groups). This has been done based on a major unconformity between the two divisions (Bhattacharyya, 1996).

The major lithologies of the supergroup are: sandstone, shales and limestones with minor volcaniclastics. The rocks from the eastern sector (i.e. Son Valley) have been subjected to more detailed investigation compared to those in the western sector in Rajasthan. Individual formations of the Vindhyans in the west have been stratigraphically correlated to those in the east based on lithostratigraphy (Prasad, 1984; Soni et al., 1987), the validity of which has been questioned by many workers (e.g. Ray et al., 2003, M. Sharma, personal communication).

The Vindhyan sequences are important because of their vastness in time and space, and as a result they are likely to contain important information on the evolution of the Earth's atmosphere, climate, sedimentary cover and life. Age estimates indicate that the initiation of sedimentation in this basin took place as early as 1721 Ma (Ray, 2006), while the youngest sediments extend up to the Precambrian–Cambrian boundary (Chakraborty, 2006). This duration of sedimentation is considered to be one of the longest amongst all the Proterozoic sequences of the world. These sedimentary sequences have been studied in greater detail for various fossils in form of stromatolites, trace fossils, algae and controversial small shelly fossils etc. (see Venkatchala et al., 1996; Azmi et al., 2006). Discoveries of controversial small shelly

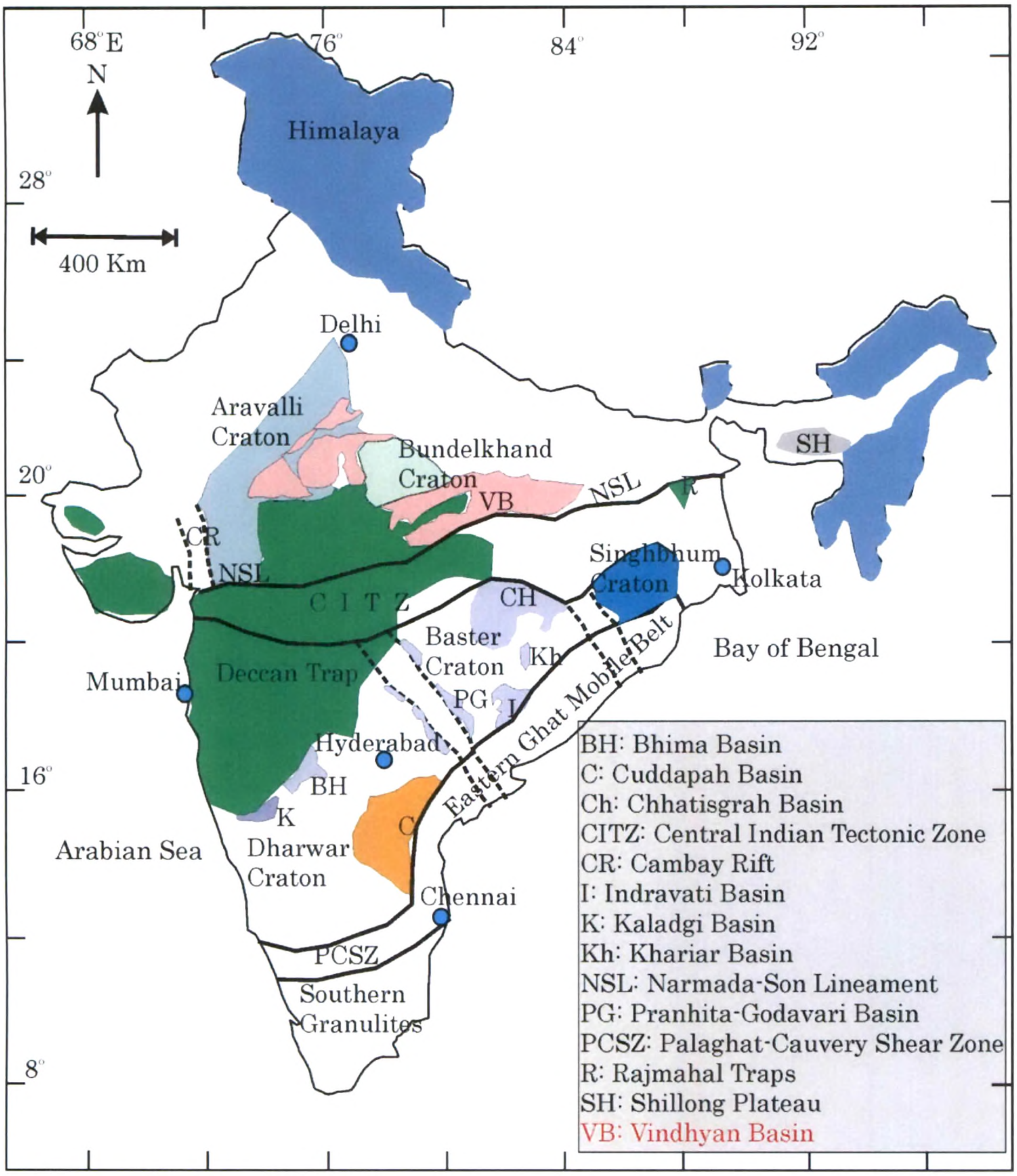

Fig. 1.1: The Proterozoic (Purana) Basins of Indian shield along with major tectonic and geological features (after Ramakrishnan and Vaidyanadhan, 2008).

fauna (Azmi, 1998), the triploblastic metazoan fauna (Seilacher et al., 1998) and numerous plant fossils, and the discovery of Edicara type fossil assemblages (De, 2003, 2006) suggest that the rocks of the Vindhyan Supergroup contain information about the evolution of advanced life on our planet (Bengtson et al., 2009).

The Vindhyan Supergroup in Rajasthan is believed to have been deposited as an infill of the failed rifts on the Aravalli craton (Mondal et al., 2002). In the eastern sector, rifting is along a series of east to west trending faults in a dextral trans-tensional setting in which the volcaniclastic units are obsereved. Chakrabarti et al., (2007) studied the Vindhyans in the Son valley and proposed a "foreland" type setting for the basin on the basis of geochemical signatures of the volcaniclsatic sediments (Porcellanite Formation). Recently Raza et al. (2009) worked on the geochemistry of the basal volcanic sequence (Khairmalia and Jungel) and attributed the formation of the Vindhyan Basin (at~1800 Ma) to a collisional event in the Aravalli-Delhi Fold belt.

Geochemical and isotopic investigations on Vindhyan rocks (Kumar et al., 2002; Ray et al., 2002; Ray et al., 2003; Kumar et al., 2005) have shown that there exists valuable information in these rocks on the Proterozoic environment of global significance. There have been reports of indirect evidences for Neoproterozoic glaciations in the form of negative $\delta^{13}C$ excursions in carbonate rocks of the Upper Vindhyan sequences that generated a lot of interest (Kumar et al., 2002; Ray et al., 2003). The identification of 'Blaini glaciation' event (Kaufman et al., 2007) confirms that Indian subcontinent was under glaciation during the Neoproterozoic, hence it is likely to expect that the Vindhyan Supergroup, which believed to extend well into Neoproterozoic, to contain similar evidences for one or more of these glaciations. Interestingly, in a recent study, Malone et al. (2008), based on detrital zircon geochronology in conjunction with the paleopole position argued that the Vindhyans are older than 1000 Ma and therefore, unlikely to contain any evidence for glaciation. The argument of older age than 1000 Ma for the upper age limit is based on the similarity of paleopole positions for the Rewa and Bhander group of rocks with that derived from the Majhgawan Kimberlite (~1073 Ma old) and not with that derived from the ~770 Ma old Malani Igneous Suite. However, in an earlier work Evans (2009) had observed that *"No field stability tests have been performed on either the Majhgawan kimberlite or the Rewa/Bhander units, so there remains the possibility that these poles represent a two-polarity magnetic print across north-central India" (page 386)*. Hence, the proposal for the above upper age limit of the Vindhyans, from statistically insignificant number of dates from detrital zircon and paleomagnetic pole data, remains doubtful and needs to be tested with new data. Gregory (2008) reconstructed the Apparent Polar Wandering Pole (APWP) for the Indian landmass based on the available age and paleolatitude data (Fig. 1.2). In view of the arguments given by Evans (2009), the reconstruction of Gregory (2008) also remains doubtful.

Geochemical and isotopic studies in the Vindhyan Supergroup are too few and mostly concentrated in the Son Valley sector (Paikaray et al., 2008; Chakrabarti et al., 2007; Mishra and Sen, 2010). The geochemical work of Paikaray et al. (2008) on the shale formations from all across the Vindhyan Supergroup in the Son Valley sector suggested that predominantly granitic sources were responsible for the sediments for the Lower Vindhyans, whereas partial contribution from basaltic sources was envisaged for the Upper Vindhyans. They also argued that the Archean-Paleoproterozoic rocks, exposed beyond the southern basin margin also contributed sediments for these shales. Mishra and Sen (2010) used various discrimination diagrams and elemental ratios for the Kaimur Group of rocks, which are quartz arenite, sublitharenite to litharenite and litharenite to shale, and came to a conclusion that all these rocks were derived from similar source rocks which had undergone severe chemical weathering, under a hot-humid climate in an acidic environment with higher p_{CO2} facilitating high sediment influx in the absence of land plants. The geochemical approach towards deciphering the provenance of the Bhander Sandstone in the Son Valley was attempted recently by Banerjee and Banerjee (2010). They suggested that these sandstones were derived in major part, from granitic sources from the continental interior.

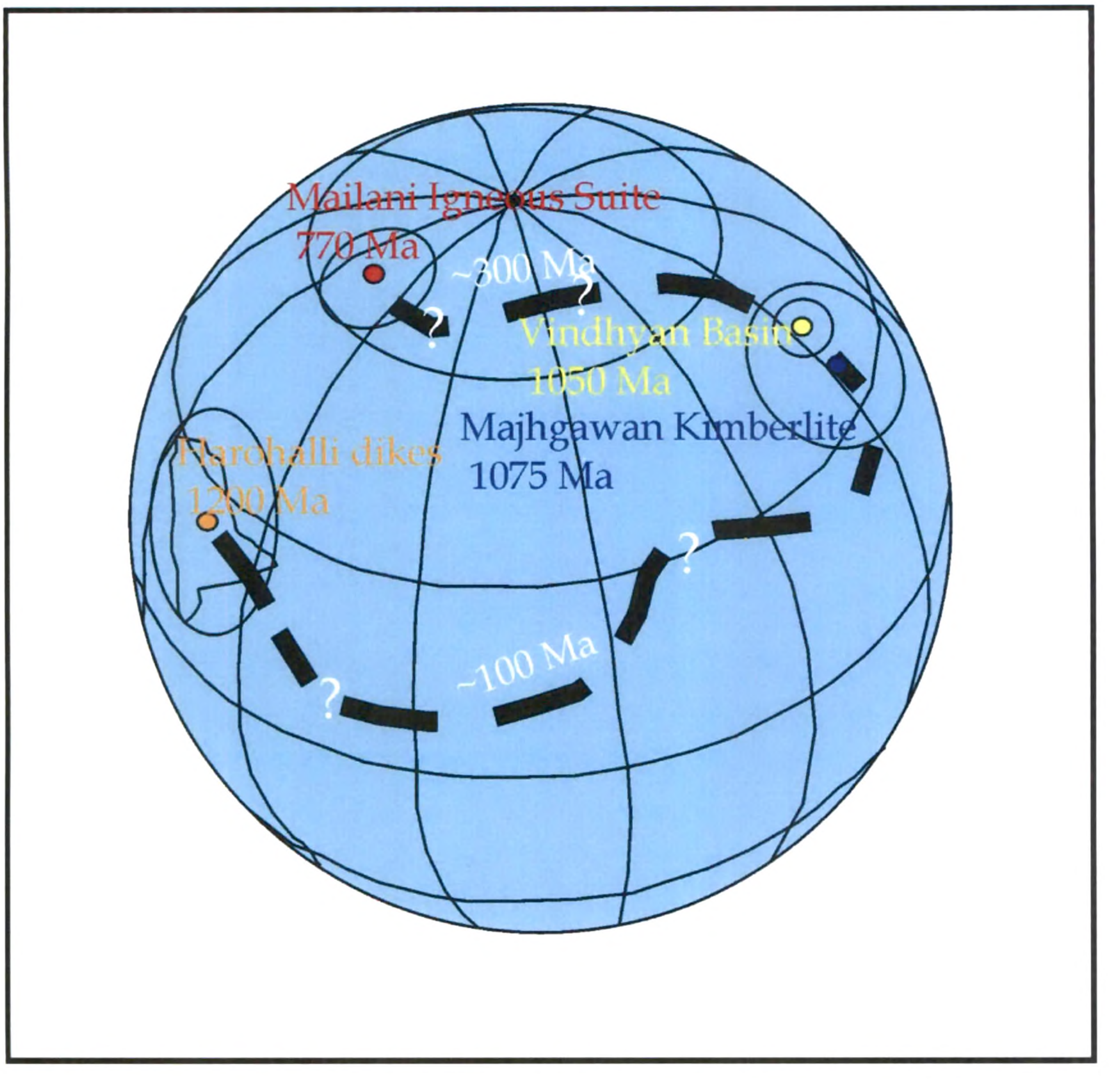

Fig. 1.2: Apparent Polar Wandering Pole (APWP) for India with reliable Proterozoic poles. Poles are from Harohalli Dikes, the Majhgawan Kimberlite, the Mailani Igneous Suite and the Vindhyan Basin (Adapted from Gregory, 2008).

The only Nd-isotopic studies carried out on the Vindhyans of the Son Valley, is by Chakrabarti et al. (2007). They used Nd-isotopic studies in conjunction with trace element geochemistry and inferred that majority of the sediments were derived from a now-extinct Andean-type arc in the south of the basin. This arc, according to them, came into existence as a result of a southerly dipping subduction prior to the collision of the Bhandara and Bundelkhand cratons and the Vindhyan Basin formed as a foreland Basin after the collision.

Unlike the radiogenic isotope studies, there are quite a few studies on C and O isotope systematics in carbonate formations in Vindhyan Supergroup (Kumar et al., 2002, Ray et al., 2003, and Kumar et al., 2005). In this context the studies by Ray et al. (2003) is quite significant and extensive, covering almost all the limestone formations from the western and eastern sectors. According to this work the secular patterns of carbon isotope trends do not support the earlier assumptions that the carbonate sequences at the southern margin correlate with those at the western or northern margins of the Vindhyan Basin. Kumar et al. (2002) believed that they had discovered evidences for one of the Neoproterozoic glaciations in the Lakheri Limestone in the Bundi area in Rajasthan from their observations of a negative excursion in $\delta^{13}C$ profile and presence of a misidentified tilloid unit at the base. Similarly, Kumar et al. (2005) suggested that the Lakheri Limestone of Rajasthan, considered correlatable to the Bhander Limestone of the eastern margin, is stratgraphically older and might have been deposited under the colder climatic conditions that prevailed during the Sturtian glaciations. They further argued that the sedimentation in the Vindhyan Basin ceased around 700 Ma ago and hence the Precambrian-Cambrian transition record is not recorded in them. In a recent work, Sarkar et al. (2009) using the sulphur isotope geochemistry of the various Proterozoic basins including the Vindhyans from the Son Valley argued for prevalence of extreme environmental conditions similar the hypothesized global Proterozoic sulphidic anoxic ocean in the Vindhyan Basin.

As of now, only a limited amount of geochemical work on the Vindhyans (only Semri Group) from the western margin (Rajasthan Vindhyans) is available (Raza et al., 2002, 2010) and results of these studies based on major and trace elements geochemistry suggest that the Banded Gneissic Complex (BGC) of Rajasthan is the major source of the Vindhyan sediments. It is to be noted that only a limited amount of C and O isotopic data (Kumar et al., 2002, Ray et al., 2003), are available for carbonate formations in the Vindhyans of Rajasthan. Worse is the scenario for geochronological information in this sector. Except for an indirect age information from Sr-isotope stratigraphy (Ray et al., 2003) and limited detrital zircon age data (Malone et al., 2008) mostly from the Upper Vindhyans, the ages of depositions of the Vindhyans of Rajasthan are still unknown. The importance of the Vindhyans of Rajasthan also lies in the possibility that these rocks can yield clues for evolution of multi-cellular life on our planet. In the context of Indian Geology, the Vindhyans of Rajasthan are very interesting since they got deposited during the time when the Delhi Basin was also getting filled, and remained largely undeformed and unmetamorphosed. Therefore, it is important to study the Vindhyan Supergroup in Rajasthan for developing a better understanding of the evolutionary history of the vast Vindhyan Basin. Apart from understanding the evolution and history of sedimentation of the Vindhyans, attempts are also necessary to understand the configuration of the Indian shield during the Proterozoic. The present work is an attempt in this direction to understand the above aspects of the Vindhyan Basin using geochemical and isotopic tools.

1.3 Aims of the present investigation:

The major objectives of this Ph. D. work were to:

1) delineate sources of sediments for various formations of the Vindhyan Supergroup using chemical and isotopic tracers,
2) correlate various formations of the western Vindhyans (Rajasthan) with those of the eastern Vindhyans (in Son Valley),

3) understand the causes of breaks in sedimentation within the Vindhyan Super group,
4) establish chronology of carbonate formations using Sr-isotope stratigraphy and that of some siliciclastic formations using detrital zircon dating,
5) understand the variations of $\delta^{13}C$ and $\delta^{18}O$ in carbonate formations in the supergroup and establish their local/global significance, and
6) propose a geodynamic model for the evolution of the Vindhyan Basin and the deposition of the Vindhyan Super group.

1.4 The Structure of the Thesis

To achieve the objectives of the present investigation samples from various formations of the Vindhyan Supergroup in Rajasthan were collected after extensive fieldwork based on available geological maps. Selected samples were subjected to various experimental studies using state of art instruments and results have been interpreted.

The present thesis is divided into four chapters. The **first chapter (Introduction)** introduces the scope of the work and its importance in the present understanding of the Vindhyan Geology. It also discusses the importance of various geochemical tools, such as major and trace element geochemistry, radiogenic isotope studies and stable C-O isotope that are used in this work to characterize the sources of the Vindhyan sediments and understand the evolution of the basin. The major objectives of this work are also outlined and discussed.

The **second chapter (Geological Framework and Analytical Methods)** deals with geology of the study areas (Chittorgarh and Bundi-Lakheri) and our field observations. Geological details of various formations of the Lower and the Upper Vindhyan sequences, exposed in the both the sectors are given. The sampling strategy followed and the details of samples collected during various field excursions are listed in this chapter. Extensive sampling was done in Chittorgarh and Bundi districts with an aim to study the intrabasinal correlations.

Sample preparation methods for various geochemical techniques are discussed in this chapter. X-ray Fluorescence Spectroscopy (XRF) method has been used for major element contents and Inductively Coupled Plasma Mass Spectrometry (ICPMS) for trace element contents. Thermal Ionization Mass Spectrometry (TIMS) for radiogenic isotopic ratios and Isotopic Ratio Mass Spectrometry (IRMS) for C and O isotopic ratios have been used. A detailed account of these techniques is given in this chapter. A brief description of the Sensitive High Resolution Ion Microprobe (SHRIMP) technique utilized (at GSC Canada) for U-Pb dating of detrital zircons, is also given.

The **third chapter** deals with "**Results and Discussion**" which contains all the details of the studies performed and possible inferences. All the results generated during this work which forms a large database of major and trace elements and isotopic ratios in Vindhyan formations have been given. A small but important dataset for U-Pb detrital zircon ages for a lower Vindhyan formation is also presented here. Results of stable C-O isotopic ratio variations in carbonate formations of the Upper Vindhyans are given and their implications are discussed. Our effort to date the topmost carbonate formation by Sr-isotope stratigraphy is also detailed in this chapter.

An attempt has also been made to correlate the sequences in the west with those in the east using geochemical/chronological parameters in terms of provenance sources of the sediments. At the end, the implications of the findings are discussed and a geotectonic model has been proposed for the origin and evolution of the Vindhyan Basin.

The summary of the work with future scope is presented in the **last (fourth) Chapter.**

Chapter-2

GEOLOGICAL FRAMEWORK AND ANALYTICAL METHODS

2. 1. Geological Framework

2.1.1 General Description of the Vindhyan Supergroup

The Vindhyan Supergroup of rocks, deposited in the Vindhyan Basin, cover an aerial extent of ~ 178,000 km^2 (Tandon et al., 1991) spreading from Sasaram (Bihar) along the Son river Valley in the east to Chittorgarh, Kota, Bundi, Sawai Madhopur districts of Rajasthan in the west (Fig. 2.1). It is believed that about 78,000 km^2 of the area is concealed under Deccan Traps, and even a larger area is thought to be lying under the Indo-Gangetic alluvium (Venkatachala et al., 1996). The rocks of the Vindhyan Supergroup overlie unconformably on ~2500 Ma old basement rocks, which include the Bundelkhand Granite, the Bijawar Group, and the Berach Granite (Crawford and Compston, 1970; Mondal et al., 2002, Weidenbeck et al., 1996). The Bundelkhand craton (3.3-2.5 Ga; Mondal et al., 2002), located near the north-central margin of the basin, appears to divide the Vindhyan Basin into two parts: the eastern sector (Son Valley) and the western sector (Rajasthan). A geological map of the Vindhyan Basin, modified after Chakraborty et al. (2010), is given in Fig. 2.1.

In its present configuration, the Vindhyan Basin is bounded to the west by the Aravalli-Delhi orogenic belt (2500-900 Ma; Roy, 1988), to the south by the Satpura orogenic belt (1600–850 Ma; Verma, 1991) and to the east by the low-grade metamorphic rocks of the Mahakoshal Supergroup (2400 Ma; Das et al., 1990) and the Bijawar Supergroup (2100 Ma; Roy and Bandyopadhyay, 1990). The Son-

Narmada lineament (Fig. 2.1) marks the southern tectonic boundary of the Vindhyan Basin. It is believed that this tectonic structure came into existence during the Archean and has remained active throughout its geologic past (Naqvi and Rogers, 1987, Kaila et al., 1989). Further south of this lineament a southerly dipping reverse fault separates the Vindhyans from the Satpura mobile belt (Tewari, 1968, Rogers, 1986). This fault appears to have generated deformations in the sedimentary rocks occurring immediately to its north in the Son Valley, however, these deformations are untraceable to the west, which might be due to the cover of younger rocks (Rogers, 1986). It is believed that the mountain building activity in the Satpuras was underway during the early phases of deposition in the Vindhyan Basin and that at a later stage the folded rocks of the Satpuras were transported onto the Vindhyans (Radhakrishna and Naqvi, 1986, Narain, 1987, Naqvi and Rogers, 1987).

The Great-Boundary Fault (GBF) at the western margin, in Rajasthan, roughly separates the Vindhyans from the Archean/Paleoproterozoic Aravalli/Delhi Fold belt (Fig. 2.1). The strike-length of this fault is over 400 kilometers. Although it was earlier believed that the GBF was purely a pre-Vindhyan fault (Fermor, 1930, Iqbaluddin et al., 1978 and Banerjee and Singh, 1981) that bounded the Vindhyans from the pre-Vindhyan rocks (Murthy and Mishra, 1981, Kaila and Krishna, 1992), there exist ample field evidences which clearly suggest that it had numerous reactivations subsequent to the deposition of the Vindhyans (Sinha-Roy et al., 1986, Srivastava and Sahay, 2003). According to Verma (1996) the GBF started as a normal fault sometime around 2500 Ma and acquired a reverse geometry during the Delhi orogeny, ~1400 million years ago.

The Vindhyan rocks are largely undisturbed, or have gentle dips (~5^{o}), however, deformation features are not uncommon in lower Vindhyans in western and southern margins (Naqvi and Rogers, 1987). The geometry of the basin is in the form of a gentle synclorium with the axis parallel to the arcuate thrust faults, which plunge to the west (Chakraborty and Bhattacharyya, 1996). The sedimentary successions of the Vindhyan Basin consist mostly of unmetamorphosed siliciclastic and carbonate lithologies adding up to a total thickness of 4 km (Prasad 1984, Venkatachala et al., 1996). These rocks are generally believed to be of marine origin, which were deposited in an elongated basin striking East-West and was open to the west (Banerjee, 1974, Chanda and Bhattacharyya, 1982). Both shallow and deep water deposits are common in the basin. The Vindhyan Supergroup is divided into four groups, viz., the Semri, the Kaimur, the Rewa and the Bhander (Table 2.1; Prasad 1984; Sastry and Moitra, 1984; Soni et al., 1987). Each group is further subdivided into formations and members (Table 2.1). The Semri Group of rocks is generally known as the Lower Vindhyans, whereas the other three groups represent the Upper Vindhyans. Typical lithostratigraphic columns of the Vindhyans in the Son Valley and in Rajasthan are presented in Fig. 2.2. The Vindhyan Supergroup does not record any major igneous activity during its deposition except for some minor acidic volcanisms and volcaniclastic deposits related to them (see Venkatachala et al., 1996 and references therein).

The siliciclastic formations of the Vindhyan Supergroup are usually sandstone, shale, and minor conglomerate and volcaniclastic deposits. The carbonate formations (limestones and dolostones) are dominant in the Semri Group and in the Bhander Group. The rocks of the Vindhyan Supergroup in the Son Valley and in Rajasthan are believed to be laterally correlatable (see Table 2.1 and Bhattacharyya, 1996). A major regional unconformity is located between the Lower Vindhyans (Semri Group) and the Upper Vindhyans (Kaimur Group) in the Son Valley, whereas the same appears to be a minor discontinuity in Rajasthan (Oldham, 1893) (Table 2.1). Heron (1936) had suggested that the Lower Vindhyans had a gradational contact with the Upper Vindhyans in Rajasthan. Similarly, many studies carried out in Bundelkhand and Bhopal area also support the suggestion of a conformable relationship between the Lower and Upper Vindhyans (Soni et al., 1987). However, the occurrence of a very thick conglomerate horizon (known as Piparola Conglomerate) near Panna (Fig. 2.1) confirms the general view of a discontinuous relationship between the two groups of rocks (Soni et al., 1987). Furthermore, the intrusion of kimberlite diaterme within the Kaimur Group and its absence in the overlying Rewa Group has been considered as an evidence for an additional depositional hiatus within the Vindhyans, between these two groups of the Upper Vindhyans (e.g., Soni et al., 1987).

The sandstone formations of the supergroup are believed to have been deposited in alluvial fan, braidplain, fan delta, eolian sandsheet, shallow marine and lacustrine environments, while the shale formations represent near shore or off shore deposits (Chakraborty, 2006). Carbonate formations of the supergroup represent various ramp settings (Bhattacharyya, 1996 and Chakraborty, 2006). Based on paleocurrent analysis in the Son Valley it has been suggested that the northerly paleocurrent direction in the southeast Vindhyans is indicative of sediment contribution from the evolving Satpura mountain range, whereas the southerly direction observed in northeast Vindhyans points to sediment sources in the north, to the basement rocks in the Bundelkhand craton (Bundelkhand Granite, Bijawar and Gwalior group of rocks) (Chakraborty, 2006) (Fig 2.1). Post-Vindhyan magmatic activities in the basin are not uncommon. Numerous dolerite dykes are known from the lower part of the Vindhyan Supergroup, and most of them are confined to and trend along the Narmada-Son lineament (Soni et al., 1987).

The Vindhyans of Rajasthan have an average total thickness of ~3.2 km and the basin occupies about 24000 km^2 of area, which is about one fourth of the entire basin and is comparable to its counter parts in the Son Valley (Prasad, 1984). Gokaran et al., (1995), however, suggested, based on magneto-telluric studies, that the Lower Vindhyans are ~3.0 km and the Upper Vindhyans are ~1.2 km in thickness. Therefore, considering this, a total thickness of the Vindhyans in the Rajasthan can be worked out to be ~4.2 km, which is comparable to the Vindhyans of the Son Valley. It is to be noted that some workers have included the Khairmalia volcanics within the Lower Vindhyans (e.g. Prasad, 1984). These volcanics have been considered to be equivalent of the Jungel volcanics in the Son Valley (Raza et al., 2009). However, others believe that the inclusion of the Khairmalia in the Vindhyan Supergroup does not have a geological basis (e.g., Roy and Jakhar, 2002), although the depositions in both sectors appear to have started after the emplacements of the Khairmalia and the Jungel volcanics. These volcanics have been linked to the opening of the Vindhyan Basin by continental rifting (Raza et al., 2009).

The depositional model for the evolution of the Vindhyan basin is largely based on the work carried out at the margins, in particular on the studies carried out in the Son Valley. As of now, two models of basin evolution have been proposed. One of the models suggests that the Vindhyan Basin evolved with a rifting in an intracratonic setting (Jokhan Ram et al., 1996; Bose et al., 1997, 2001) and the second model advocates for an epicratonic foreland setting resulting from a southerly dipping subduction prior to the collision of Bhandara and Bundelkhand cratons (Chakraborty and Bhattacharya, 1996; Chakrabarti et al., 2007).

2.1.2 Lithostratigraphy of the Vindhyans

2.1.2.1 Vindhyans of the Son Valley

The rocks of the Vindhyan Supergroup in the Son Valley sector have been studied in great detail since the beginning of geological investigations in India (Oldham, 1856; Medlicott, 1859; Mallet, 1869). These rocks have been divided into groups and subgroups following the principles of superposition, lithological similarities and breaks in sedimentation. The general stratigraphic classification of the Vindhyans followed in this thesis is presented in Table 2.1, which is mainly based on the compilation by Bhattacharyya (1996), although some of the important features from other studies have also been included.

Medlicott (1859) defined the Semri Series (Group) of Lower Vindhyans on the basis of his work carried out on four formations exposed on the banks of the Semri River near Bijawar, Madhya Pradesh. There are nine formations in the Semri Group, which

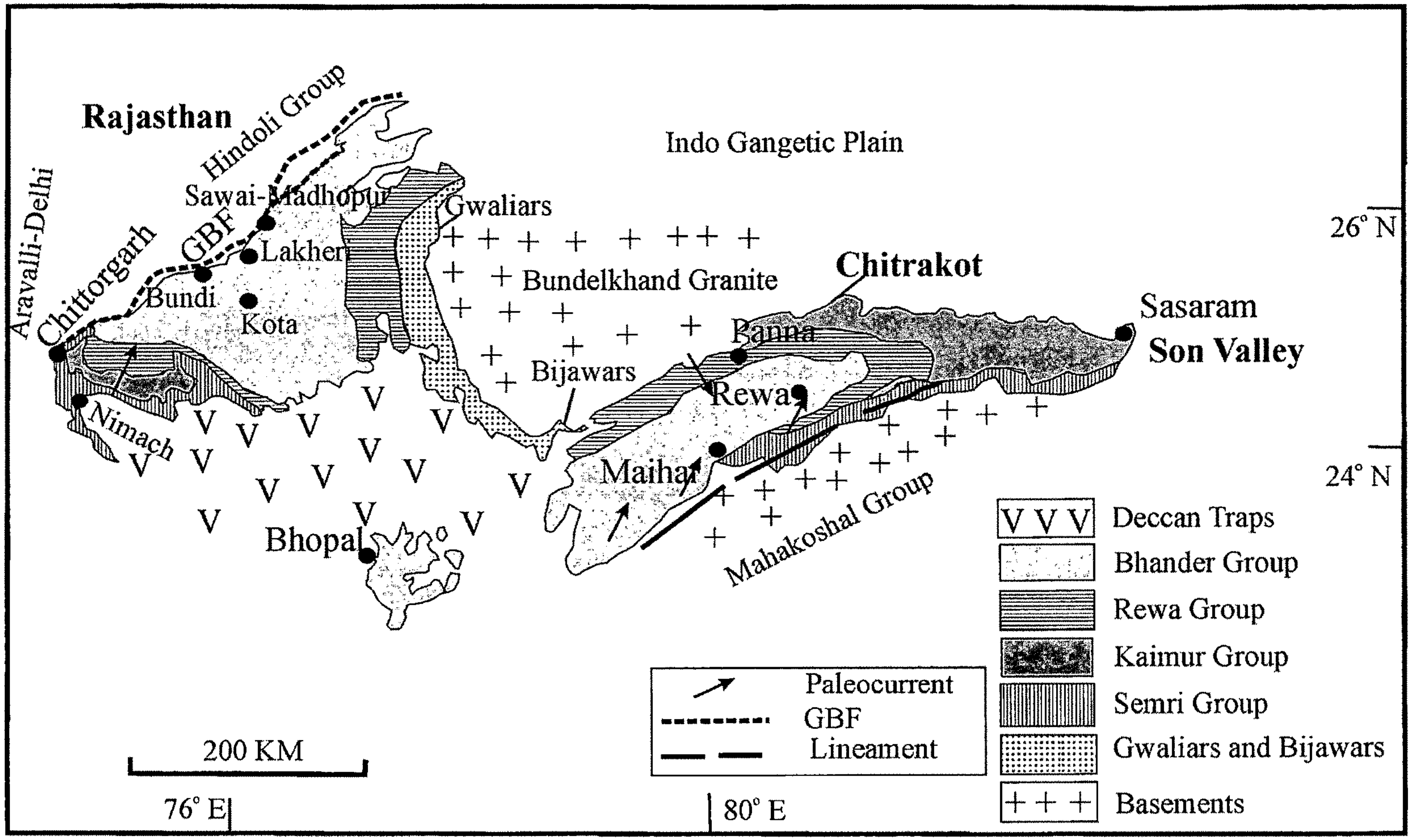

Fig. 2.1. The geological Map of the Vindhyan Supergroup (after Chakaraborty et al., 2010). Paleocurrent directions are from Soni et al. (1987). GBF: Great Boundary Fault; Lineament: Son-Narmada Lineament.

together is about 1.3 km in thickness (Chakraborty, 2006). These nine formations have been grouped into three subgroups namely the Mirzapur, the Kheinjua and the Rohtas according to their order of superposition (Table 2.1). The Vindhyan sequences in the Son Valley starts with a locally developed ~3m thick diamictite at the base of Deoland Formation, which is believed to be of glacial origin by some previous workers (Bose et al., 2001 and references therein). The Mirzapur Subgroup includes the following formations: the Deoland Sandstone, the Arangi Shale, the Kajrahat Limestone and the Deonar Porcellanite. The Deoland Sandstone grades into Arangi Shale on which the Kajrahat Limestone is developed. The Kajrahat Limestone is stromatolitic and dolomitic in nature, and is believed to be shallow marine in origin, and could be correlated with the Bhagwanpura Limestone Formation in Rajasthan (Table 2.1). The Deonar (Porcellanite) Formation, which is made up of volcanic tuff, pyroclatstic surges and flow deposits, is about 500m in thickness. The Kheinjua subgroup is developed over the Porcellanite Formation starting with the dark coloured Koldaha shale consisting of recycled material from the underlying formation (Bose et al., 2001). The Salkhan Limestone which overlies the Koldaha shale is fine grained fawn coloured, dolomitic and cherty (Sharma, 2006). The Chorhat Sandstone Formation, in which fossils of early metazoan life forms have been reported by Seilacher et al. (1998) (see section on biostratigraphy later), is considered to be equivalent of the Salkhan Formation (Chakraborty, 2006). The Rampur Formation overlying the Salkhan Formation is comprised of greenish shale interbedded with sandstones (Chakraborty, 2006). The deposition of the Rohtasgarh Limestone which is massive, plane-laminated and generally devoid of stromatolities marks the beginning of the Rohtasgarh subgroup. The formation becomes a limestone-shale rhythmite towards top. Chakraborty (2006) reported ~ 30m thick volcaniclastic deposits at Jukehi, Satna District, and Madhya Pradesh that directly overlie the Rohtasgarh Limestone. The topmost unit of the Semri Group is called the Bhagwar Shale. The thickness of the Semri Group is estimated to be ~20m in Chandola (Soni et al., 1987) to as thick as ~1.3km (Chakraborty, 2006). This suggests that there exist inherent irregularities on the floor of the Vindhyan Basin. A basin wide unconformity separates the Upper Vindhyans from the Lower Vindhyans (Table 2.1; Fig. 2.2).

The Upper Vindhyans comprising three groups (Kaimur, Rewa and Bhander) containing shale and sandstone formations with one major limestone formation close to the top. Kimberlitic pipes have intruded the Kaimur Group near Panna in the Son Valley. The observed maximum thickness of the Kaimur Group is 400m at the Rohtasgarh (Soni et al., 1987). The Kaimur Group is comprised of sandstones and shales forming six formations. The overlying Rewa Group consists of shales and sandstones appear to rest on the kimberlite pipes with a diamondiferous conglomerate zone in between (Vredenburg, 1906; Krishnan, 1968). The Rewa Group is best developed along the northern margin in the Son Valley. The thickness of this group varies from 109 to 296m (Soni et al., 1987). The Bhander Group, the uppermost division of the Vindhyan Supergroup, starts with the Ganurgarh Shale which grades into the Lakheri (or the Bhander) Limestone (> 100m thick) followed by the deposition of the Lower Bhander (Bundi Hill) Sandstone. This group of rocks is best developed in the central part of the basin. Another diamondiferous conglomerate separates the Rewa and Bhander Group near Panna. The Simrawal Shale marks the initiation of deposition of the Bhander Group in this area, which is considered equivalent to the Ganurgarh Shale (Soni et al., 1987). The Lakheri Limestone is stromatolitic in nature, which indicates that its deposition took place in a shallow shelf region (Sarkar et al., 1998). The Bundi Hill Sandstone overlying the Lakheri Limestone is the most impersistent formation (Soni et al., 1987). The Sirbu Shale which is best exposed in Sirbu hills near Rewa town is about 120 to 320m thick and occurs on the top of the Bundi Hill Sandstone. The Upper Bhander Sandstone or the Maihar Sandstone (or the Shikaoda Sandstone) that forms the topmost Vindhyan formation in the Son Valley is exposed along the central axis of the Vindhyan basin.

2.1.2.2 *Vindhyans of Rajasthan*

The Vindhyan Supergroup in Rajasthan commences with the eruption of the Khairmalia volcanics belonging to the lower part of the Sand subgroup, comprising of andesites and pyroclastics (Table 2.1). The total thickness mapped for the Sand subgroup is ~1000m thick which include the earlier classified Satola subgroup containing the lower 835m of sediments and volcanics (Prasad, 1984). A minor porcellanite formation which is considered to be equivalent to its counterpart in the Son Valley is mapped as part of the Palri Shale formation of the Sand subgroup (Table 2.1 and Prasad, 1984). The Kalmia Sandstone and the Binota Shale form the Lasrawan subgroup that overlies the Sand subgroup. The Khorip subgroup that marks the end of the deposition in the Semri is made up of three major formations: the Bari (or the Nimbahera) Shale, the Nimbahera Limestone and the Suket Shale (Table 2.1). The total thickness of the Khorip subgroup is ~475meter (Prasad, 1984). The cumulative thickness of the Semri Group is determined to be ~ 1.7 km , which is comparable to that in the Son Valley.

The Upper Vindhyans of Rajasthan start with the deposition of the Kaimur Group in which only one formation in the form of sandstone is present, in comparison to the six formations of different rock types in the Son Valley. The Badanpur Conglomerate below the Kaimur Group, in the Bundi district, which is about 8-10 meter thick, developed locally on the Pre Aravalli or the Hindoli Group of rocks (Prasad, 1984). The Rewa Group is comprised of four formations: the Panna Shale, the Indergarh Sandstone (or the Lower Rewa Sandstone), the Jhiri Shale and the Taragarh Fort Sandstone (the Upper Rewa Sandstone), with a maximum thickness of ~285m (Prasad, 1984). Deposition of the Bhander Group started with the Ganurgarh Shale (200m) followed by the Lakheri Limestone (150m). The Lakheri Limestone is not stromatolitic like its counterpart in the Son Valley. The Samaria Shale that overlies the Lakheri Limestone has patches of dolomite bearing stromatolitic limestones, and is found only in Rajasthan. The Bundi Hill Sandstone (or the Lower Bhander sandstones) overlies the Samaria Shale formation. These formations i.e. Ganurgarh, Lakheri, Samria, Bundi Hill Sandstone and the Sirbu Shale constitute the lower portion of the Bhander Group (Prasad, 1984), whereas the Upper portion of the group is represented by the Maiher (or the Shikaoda) Sandstone, the Balwan Limestone, and the Dholpur (Bhavpura) Shale units marking the closure of the Vindhyan sedimentation in Rajasthan. Interestingly, the latter two formations are not observed/reported from the Vindhyans of the Son Valley. The Shikaoda Sandstone is best developed in Bundi area, and is about 780m thick (Soni et al., 1987). The Bhander Group shows thickening from east to west in Bundi. This group is best developed in Bundi- Ranthambhore-Sapotra-Karauli sector.

2.1.3 Biostratigraphy of the Vindhyans

Biostratigraphy of the Vindhyans are not well established for a simple reason that most of the supergroup is Paleo-Mesoproterozoic in age when life was not so well developed. However, the Vindhyans are famous for numerous interesting and controversial fossil discoveries. In this section I made an attempt to compile some of the important findings. A compilation of the fossil findings and their implications towards the age of the Vindhyan is presented in Table 2.2. In one of the earliest studies, Valdiya (1969) reported *Kussiella* type stromatolites from the Kajrahat Limestone in Son valley and the Bhgawanpura Limestone in Rajasthan that showed development of columnar-branching within the domal and laminated forms. According to this work, the stromatolites of Chitrakoot, which show passive branching and upward swelling columns, represent early forms of Lower Riphean (1650 -1350 Ma) stromatolites within *Kussiella* assemblage.

The *Chuaria* and *Tawuia* fossils have generally been reported from the upper Vindhyans, particularly from the Bhander and the Rewa groups (see Table 2.2), however, they are also known to occur in the Suket Shale of the lower Vindhyans (Kumar, 2001). The ages of these fossil assemblages are believed to be in the range of 1100-700 Ma (Hoffman, 2005). Seilacher et al. (1998) reported trace fossils of

Table 2.1: The stratigraphic classification of the Vindhyan Supergroup (after Bhattacharyya 1996).

			Typical Vindhyan Basin (adapted for Son Valley)		Vindhyan Basin in Rajasthan (used in the present work)
UPPER VINDHYAN	BHANDER GROUP		Shikaoda (Maihar) Sandstone		Bhavpura (Dholpur) Shale
					Balwan Limestone
					Shikaoda Sandstone
			Sirbu Shale		Sirbu Shale
			Bundi Hill Sandstone		Bundi Hill Sandstone
			Lakheri (Bhander) Limestone		Lakheri Limestone
			Ganurgarh Shale		Ganurgarh Shale
	REWA GROUP		Govindgarh Sandstone		Taragarh Fort Sandstone
			Dramondganj Sandstone		
			Jhiri Shale		Jhiri Shale
			Asan Sandstone		Indergarh Sandstone
			Panna Shale		Panna Shale
	KAIMUR GROUP		Dhandraul Sandstone		
			Mangesar Formation		
			Bijaigarh Shale		
			Ghaghar Sandstone		
			Susni Breccia		
			Sasaram Formation		Kaimur Sandstone with Conglomerate
LOWER VINDHYAN	SEMRI GROUP	Rohtas Subgroup	Bhagwar Shale	Khorip Subgroup	Suket Shale
					Nimbahera Limestone
			Rohtasgarh Limestone		Bari (Nimbahera)Shale
		Kheinjua Subgroup	Rampur Formation		
			Salkhan Limestone	Larsrawan Subgroup	Binota Shale
			Koldaha Shale		Kalmia Sandstone
		Mirzapur Subgroup	Deonar Formation	Sand Subgroup	Palri Shale (with Porcellanite)
			Kajrahat Limestone		Sawa Sandstone with Congolomerate
			Arangi Formation		Bhagwanpura Limestone
			Deoland Formation		Khardeola Sandstone
					Khairmalia Andesite
Aravalli/Bhilwara Supergroup/Berach Granite/ Bundelkhand Granite/Jungel volcanics/Bijawar Group of rocks					

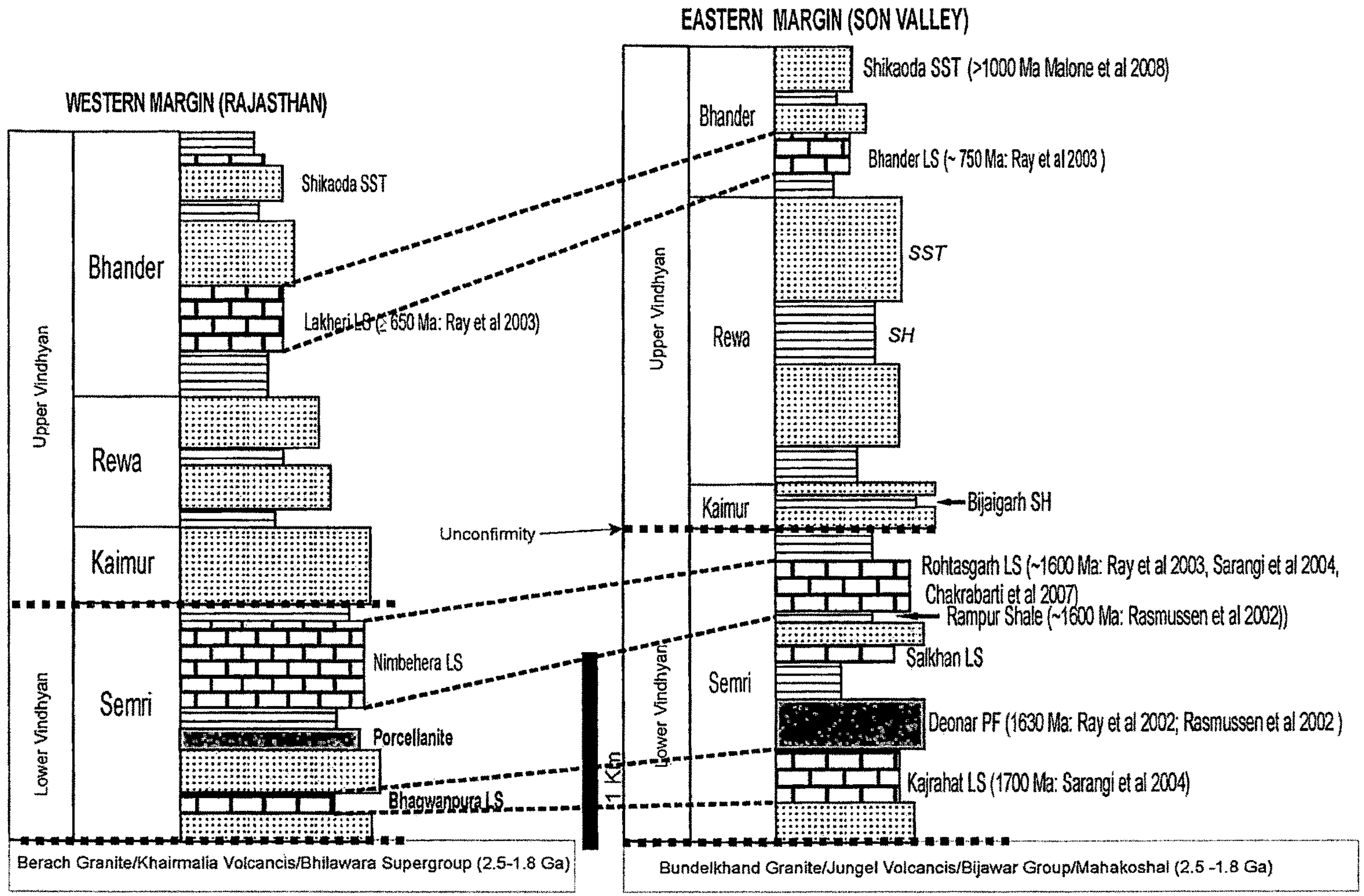

Fig. 2.2: Stratigraphic logs for the Vindhyan Supergroup in Rajasthan and in the Son Valley. The dashed lines connect correlatable limestone formations across the basin (Source: Ray et al., 2003). Recent radiometric ages and sources are given in the brackets. PF: Porcellanite Formation; SST: Sandstone; LS Limestone and SH: Shale.

Table 2.2: The fossil evidences with age connotation in Vindhyans.

Formation	Fossil Assemblages	Age Inferred (Ma)	References
	Upper Vindhyans		
Bhander Group			
Dholpur Shale	*Chuaria-Tawuia*		Srivastava, (2002)
Balwan Limestone	*cynobacterial affinity-algal mats*	late Neoproterozoic	Kumar & Pandey (2008)
Shikoada (Maihar) Sandstone	*Skolithos* and complex *Planolites* burrows		Maitra and De (1998)
Sirbu Shale	*Trachyhystrichosphaer*	Cryogenian (850–630 Ma)	Srivastava (2009)
Bundi Hill Sandstone			
Lakheri Limestone , Son valley	Sponge *spicule*		Kumar (1999)
Lakheri Limestone , Son valley	*Chuaria-Tawuia*	1100-700	Kumar & Srivastava (1997, 2003)
Lakheri Limestone, Rajasthan	*Ediacara* type	Ediacaran-Cambrian	De (2003, 2006)
Lakheri Limestone, Rajasthan	Stromatolites *Baicalia and Tungussia, Minjaria, Maslowviella & Linella*		Prasad (1980)
Lakheri Limestone, Maihar (Son valley)	Bioherm built Stromatolites (*Baicalia and Tungussia)*		Valdiya (1969)
Rewa Group			
Dramondganj Sandstone	*Planolites* burrows		Maitra and De (1998)
Jhiri Shale	Fossil*(Chuaria-Tawuia)*	1100-700	Rai et al. (1997)
Kaimur Group			
Kaimur Sandstone and Shale	*Skolithos* and Meandering traces *Planolites*		Kulkani & Borakar (1996); Maitra and De (1998)
	Lower Vindhyans		
Semri Group			
Rohtasgarh Limestone	Bedding planes of shales carbonaceous discs and filaments *Chuaria, Tawula, Sekwia*		Sahni (1936), Mishra (1969) Maithy and Babu (1988), Kumar (1995), Sharma (1996), Kumar (2001)
	annulated tubes, embryo like globules with polygonal surface pattern, and filamentous and coccoidal microbial fabrics similar to *Girvanella* and *Renalcis*	~1,650	Bengtson et al. (2009)
	Grypaenia spirals	~1600	Sarangi et al. 2004
	Small Shelly fossils		Azmi (1998), Azmi et al. (2006)
Chorhat Sandstone (Salkhan Formation)	*Triploblastic* metazoan burrows/worm like	> 1000	Seilacher et al. (1998)
	Horizontal Burrows		Sarkar et al. (1996)
	Planolites Serpens		Maitra and De (1998)
Salkhan Limestone	Conical Stromatolites (*Comophyton & Maslowviella*)		Mathur et al. (1958) Valdiya (1969)
	Obruchevella		Rai and Singh, (2004)
Koldaha Shale	*Acritarch*		Anbarasu (2001)
	Primitive no-vascular plant spores		Ghosh and Bose (1950)
Kajrahat Limestone, Son valley, Bhagwanpura Limestone in Rajasthan	Columnar branching Stromatolites *(Kussiella type)*	1650-1350	Valdiya (1969)

triploblastic animals in Chorhat Sandstone, which were believed to be worm-like metazoan. Azmi (1998) reported small shelly fossils (SSFs) from the Rohtasgarh Limestone from the Semri Group and claimed these to be similar to the fauna those are usually found near the Precambrian-Cambrian transition. These findings generated a debate among the workers about the age of the Vindhyan supergroup. Eventually, this led to a renewed interest among the various workers to settle the issue pertaining to the age of these rocks and the authenticity of the fossil discoveries. The main issue that needed to be resolved was that if the fossils were true then, these were the first ever finds of Ediacara in Mesoproterozoic rocks of the Vindhyans.

The renewed interest to date these sedimentary sequences by available geochronological tools resulted in publication of good age estimates of the Lower Vindhyans from the Son Valley (Rasmussen et al., 2002, Ray et al., 2002, Ray et al., 2003, Sarangi et al., 2004, Chakrabarti et al., 2007, Bengtson et al., 2009). The most recent work of Bengtson et al. (2009) re-ascertained the claims of fossil findings of Azmi et al. (2006) from the Lower Vindhyans and therefore has pushed back the age of metazoan evolution. These authors have also dated the fossilifeorus phosphorite horizons in Tirohan Dolostone (equivalent to Rohtasgarh Limestone) from Janaki Kund in Chitrakoot by Pb-Pb isochron technique, and reported an age of 1,650 ± 89 (2σ).

In the Upper Vindhyans of Rajasthan De (2003; 2006) reported 'Ediacaran-*like*' organisms with doubtful preservation characteristics in the Lakheri Limestone, suggesting that the age of this limestone could be younger than the latest Cryogenian (i.e. <620Ma). The authenticity of these findings further may be questioned by the recent study of Srivastava (2009), who reported 850-630Ma old fossils of *Trachyhystrichosphaer* an acritarch, in a dolomitic limestone member of the Sirbu Shale Formation. All these findings, although remains controversial, hint at the possibility that parts of the Upper Vindhyans in Rajasthan may actually have been deposited during the Cryogenian epoch of the Neoproterozoic.

2.1.4. Geochronology in the Vindhyans

The duration of the sedimentation within the Vindhyan basin is a controversy that has remained unresolved for over one hundred years (Venkatachala et al., 1996). The Table 2.3 presents a synoptic view on the existing reliable age information from the Vindhyan Supergroup. From the table it is evident that the age of the Lower Vindhyans i.e. Semri Group is well constrained compared to the Upper Vindhyans. From the existing age information it appears that the sedimentation in the Son Valley must have started prior to 1721 Ma (Sarangi et al., 2004), the oldest age estimate for the Kajrahat Formation based on Pb-Pb dating. Lack of robust age data restricts us to make such an inference for the Vindhyans of Rajasthan; however the upper age limit for initiation of the sedimentation could be put at 1850 Ma, the age of the underlying volcanic rocks (Deb et al., 2002).

The geochronological data for the Lower Vindhyan sequences (Table 2.3) are derived from U-Pb zircon ages from the Deonar Porcellanite Formation that yielded dates: 1628±8 Ma, and 1630.7±0.4 Ma (Rasmussen et al., 2002; Ray et al., 2002). The Rohtashgarh Limestone has been dated by various groups using Pb-Pb dating method, and the results fall in the range between 1514-1650 Ma (Ray et al., 2003, Sarangi et al., 2004, Chakrabarti et al., 2007, Bengtson et al., 2009). Unlike the Lower Vindhyans, the age of deposition for the Upper Vindhyan sequences has remained unresolved (see Table 2.2 and 2.3) due to lack of robust radiometric age data. A very poorly defined Pb-Pb age on the Bhander Limestone of 650±700 (2σ) Ma was reported by Ray et al. (2003) and this date has remained as the only direct radiometric age information for the Bhander Group. Based on the Sr-isotope stratigraphy Ray et al. (2003) suggested that the age of Bhander Limestone could be anywhere between 750 and 650 Ma, which the authors believe is consistent with the data for carbon isotope stratigraphy during this period.

Table 2.3 Radiometric Age data for the Vindhyan Supergroup

Formation	Method	Age (Ma)	Reference
		Upper Vindhyans	
Bhander Group			
Dholpur Shale	K-Ar	550	Vinogradov et al. (1964)
Shikaoda Sandstone	Detrital zircon (Pb-Pb)	>1000 ?	Malone et al. (2008)
Lakheri Limestone, Rajasthan	Sr Isotope stratigraphy	≤650	Ray et al. (2003)
Lakheri Limestone, Son Valley	Pb-Pb	650 ± 700 ?	Ray et al. (2003)
Lakheri Limestone, Son valley	Sr isotope stratigraphy	≤750	Ray et al. (2003)
Kaimur Group			
Kaimur Conglomerate	K-Ar	940	Vinogradov et al. (1964)
	F-T	1071 ± 169	Srivastava and Rajagopalan, (1986)
	F-T	1070 ± 160	Srivastava and Rajagopalan, (1986)
Bhagain (Kaimur)Sandstone	Rb-Sr	>1067	Based on the Age of Kimberlite intrusion (1067±31 Ma), Kumar et al. (1993)
		Lower Vindhyans	
Semri Group			
Rohtasgarh Limestone	Pb-Pb	1601 ± 130	Ray et al. (2003)
	Pb-Pb	1599±48	Sarangi et al. (2004)
	Pb-Pb	1514 ±120	Chakrabarti et al. (2007)
Tirohan Dolostone	Pb-Pb	1650 ± 89	Bengtson et al. (2009)
Rampur Shale (Rampur Formation), Son Valley	U-Pb	1599 ± 8	Rasmussen et al. (2002)
Deonar Porcellanites, Son Valley	U-Pb	1628 ±8	Rasmussen et al. (2002)
		1630 ± 1	Ray et al. (2002)
Glauconitic Sandstone, Chitrakoot	Rb-Sr	1504-1409	Kumar et al. (2001)
Kajrahat Limestone, Son Valley	Pb-Pb	1721± 90	Sarangi et al. (2004)
Basement Rocks			
Hindoli volcanics	U-Pb	1850	Deb et al. (2002)
Khairmalia	Rb-Sr	> 1000	Crawford & Compston, (1970)
Berach Granite	Pb-Pb	2440 ± 8	Wiedenbeck et al. (1996)
Bundelkhand Granite	Pb-Pb	2492 ± 10	Mondal et al. (2002)

A late Neoproterozoic or Cambrian age for the Bhander-Rewa was supported by a comparison of paleomagnetic directions found in the rocks with those from Late Proterozoic-Cambrian age sedimentary rocks in the Salt Ranges of Pakistan (McElhinny et al., 1978; Meert and Torsvik, 2003). Klootwijk et al. (1986) suggested that although the paleomagnetic poles from the Salt Range rocks are similar to the Bhander-Rewa directions, significant vertical axis rotation of units in the Salt Ranges during the Tertiary Era casts doubt on this proposed correlation. Additional evidences forwarded in support of a Neoproterozoic age for the Rewa and Bhander groups are generally indirect and inconclusive.

Recent attempt of Malone et al. (2008) using Pb-Pb dating of detrital zircon and paleomagnetic pole analysis in Bhander Group in the Son Valley as well as in Rajasthan suggests a lower age limit of ~1000 Ma for the topmost sandstone formation, the Shikoada (Maihar) Sandstone. This inference was based on the observation that the zircon population from the Shikoada Sandstone did not contain zircons younger than 1000 Ma. Using this evidence in the paleopole data that suggested identical pole position to the Majhgawan kimberlite intrusion, Malone et al. (2008) went on to infer that the deposition in Vindhyan Basin had seized much before 1000 Ma. However, we feel that the zircon data of Malone et al. (2008) is statistically insignificant (the 1000 Ma peak contains only 1 grain!), and hence, conclusions of this studies should not be considered seriously.

The findings of Malone et al. (2008) have made things more complicated because the uppermost Bhander Group is generally considered to be late Neoproterozoic (750-650 Ma; Kumar et al., 2002; Ray et al., 2003). Unfortunately, the most striking features of Late Neoproterozoic sequences worldwide - the presence of glacial diamictites (Evans, 2000) is not known from the Upper Vindhyans.

These are, however, some indirect (chemical) evidences which have been suggested to represent one or more of these Neoproterozoic glacial events. A large negative excursions in $\delta^{13}C$ of carbonates observed in the Lakheri Limestones of Rajasthan (by

Kumar et al., 2002) and in the Bhander Limestone (Ray et al., 2003) have been interpreted to represent one of the Neoproterozoic global glaciations. If true, then the age of the Lakheri/Bhander Limestones should lie between 750-635 Ma, which is supported by minimum ages obtained by Ray et al. (2003) from Sr-isotope stratigraphy.

2.2 Field Relationships and sampling

Since the focus of this work was the Vindhyans of Rajasthan, two localities were selected for sampling where all the groups of the supergroups were accessible in a small domain. After thorough field survey based on the existing geological maps and district resource maps prepared by Geological Survey of India (GSI), it was found that the Lower Vindhyans and the Upper Vindhyans were best exposed around Chittorgarh (Fig 2.3) and Bundi-Lakheri sectors (Fig. 2.4), respectively.

2.2.1 Field relationship

In the Chittorgarh district the general strike of the Vindhyan formations are N-S and these formations terminate against GBF, which runs NE to SW along the Berach River (Fig. 2.3 & 2.5). They are bounded by the Deccan Traps in the south, and by the Berach Granite in the north. The general stratigraphic younging direction is towards east from the contact with the Berach Granite and the Hindoli Group of rocks. In Chittorgarh region large scale folds occur in the Vindhyan formations, with synclines occupying the topographic highs and the anticlines forming the valleys (Srivastava & Sahay, 2003, Fig. 2.5). The axes of the numerous large scale folds, form parallel ridges and valleys, trend oblique to the GBF (Fig.2.5). Figure 2.6 represents eastern limb of such a folded anticline within the Nimbahera Limestone Formation that the topographic lows at Chittorgarh. Interestingly this folding pattern changes its orientation (axial) to NE-SW from N-S and becomes parallel to the GBF in the eastern sector towards Bundi and beyond, in Rajasthan. Near Chittorgrah the GBF forms the boundary between the Vindhyans and the Berach Granite in the NW and western margins and traced through the Vindhyans in the northern margin (Fig. 2.3 & 2.5).

Berach Granite (Fig. 2.7) forms the basement of the Vindhyan Basin at Chittorgarh, and the Bhagwanpura Limestone represents the beginning of the deposition of the Vindhyan Super group. The topmost Vindhyan formation in this area is Panna Shale which occupies the ridges atop the Kaimur Sandstone of the Upper Vindhyans. The contact between the Suket Shale (Semri Group) and Kaimur Sandstone (Kaimur Group) has been observed in the Chittorgarh Fort Hill where it appears to be conformable, in contrast to the observations elsewhere in the basin. Near the contact zone of GBF and the Vindhyans, the rocks of the supergroup have been deformed as a result of the reactivatiuon of the fault (Sahay & Srivastava, 2005). Multiphase deformations in the Nimbahera Shale at Berach river section (Fig. 2.8) is an evidence of the post Vindhyan reactivation of the GBF.

In the Bundi-Lakheri sector only the upper Vindhyans are exposed in the form of hills and ridges, those run parallel to the ENE-WSW strike of the GBF. These ridges many of which are anticlines are affected by secondary faults parallel to and at an angle to the GBF (Fig. 2.4). A majestic fault scarp that runs for > 60 km from Bundi to Lakheri within the Vindhyans provides a testimony for the reactivation of the GBF subsequent to the filling of the Vindhyan Basin. Further towards Sapotra in NE the GBF bifurcates into two major faults. The main fault of the GBF marks the boundary between the Hindoli supracrustals and the Vindhyans, however, patches of Kaimur sandstone are emplaced onto the Hindolis through secondary faults (Fig. 2.9). The GBF is displaced about 1.5km near Satur. The continuity of the GBF is truncated and displaced for ~ 2km towards SSE near Mohanpura south of Indergarh town, by a right lateral cross fault. An example of cross fault cutting across the Bundi-Indergarh ridge near Khatgarh is shown in Fig 2.8. One can observe that the formations of the Bhander Group occur in repetitive manner all along the Bundi-Indergarh road in form of linear ridges below the fault scarp. The Lakheri limestone formation occupies most of the linear anticlines and also deformed at a smaller scale too, an example of which is shown in Fig. 2.10. The Vindhyan formations continue further towards north parallel to the GBF in Sawai-Madhopur and the Sapotra-Karauli sub-basin, where some formations of the Lower Vindhyans are also exposed.

The top three formations of the Bhander Group, which are not exposed along the Bundi-Lakheri section, are exposed along a 15 km long patch, south-east of Lakheri near Indergarh (Fig. 2.4). The topmost formation of the Vindhyans in Rajasthan, the Dholpur Shale outcrops along a faulted contact with the Sirbu Shale-the most extensive formation below the alluvium in the Bundi District of Rajasthan. The Shikaoda (Maihar) Sandstone formation occurs on a ridge (Fig. 2.4). The Balwan Limestone formation, which is ~100-120m thick, forms a necklace around the sandstone ridge in the north east and disappears along with two other formations in the south west. The Balwan Limestone is stromatolitic at the base and at the top with a conglomerate horizon in between. Interestingly the Balwan Limestone is not exposed in the Balwan Village, which is situated almost at the centre of the ridge. A detailed geological map of this region is given in Fig. 2.11.

It is believed that the Vindhyan Supergroup of rocks was deposited on peneplained Archeans and Paleoproterzoic basements with irregular topography. The occurrence of a conglomerate as an outlier (named Badanpur Conglomerate) of the Kaimur Group directly over the folded Pre-Aravallis, north of the GBF, between Bundi and Indergarh (see Fig 2.4) and absence of the Lower Vindhyans in this sector while partial presence of the Lower Vindhyans in Karauli-Sapotra region, indicate the irregularities in the basement topography. The transition of Suket Shale (Lower Vindhyans) to the Kaimur sandstones (Upper Vindhyans) at Chittorgarh fort suggests a conformable nature. These observations indicate that the non deposition of Lower Vindhyans at the margins could be due to the highland and ridges like topography. This could have been a result of Pre-Vindhyan geological events such as the formation of Aravalli-Delhi mountain ranges.

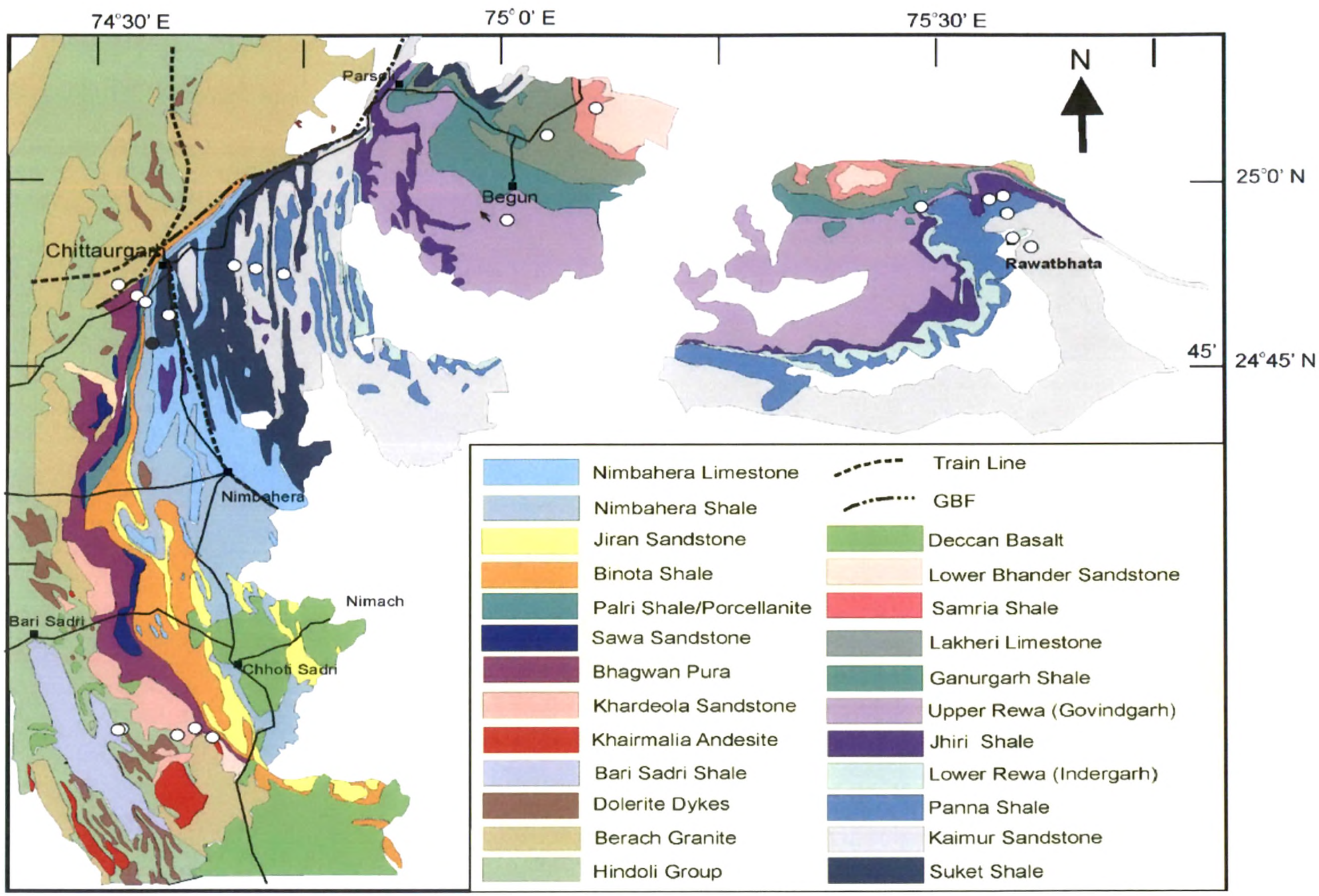

Fig. 2.3: The Geological map of the Chittorgarh district (after DRM, courtesy: GSI). Samples collected from Vindhyan formations and the basement rocks are marked as white circles.

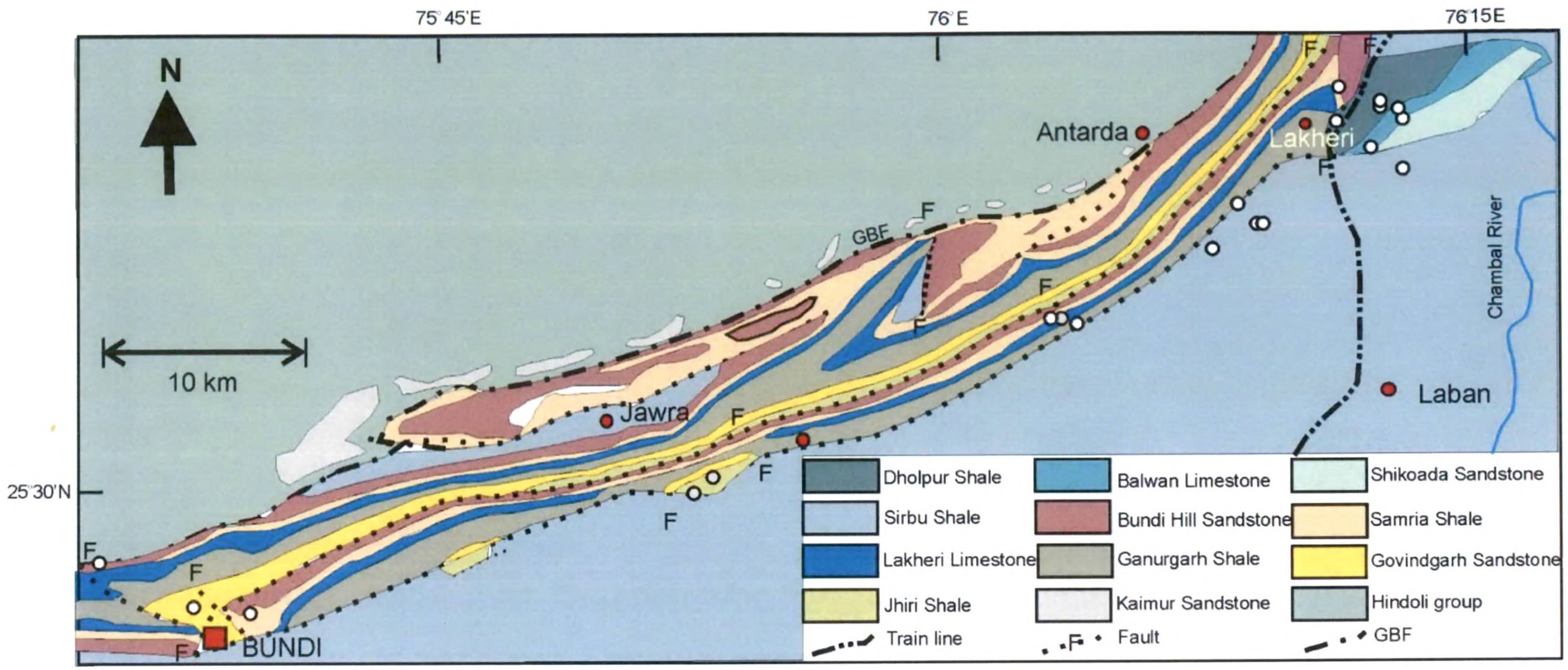

Fig.2.4: Geological map of Vindhyans in the Bundi-Lakheri sector (after DRM: courtesy GSI). Samples collected from various formations are marked as white circles.

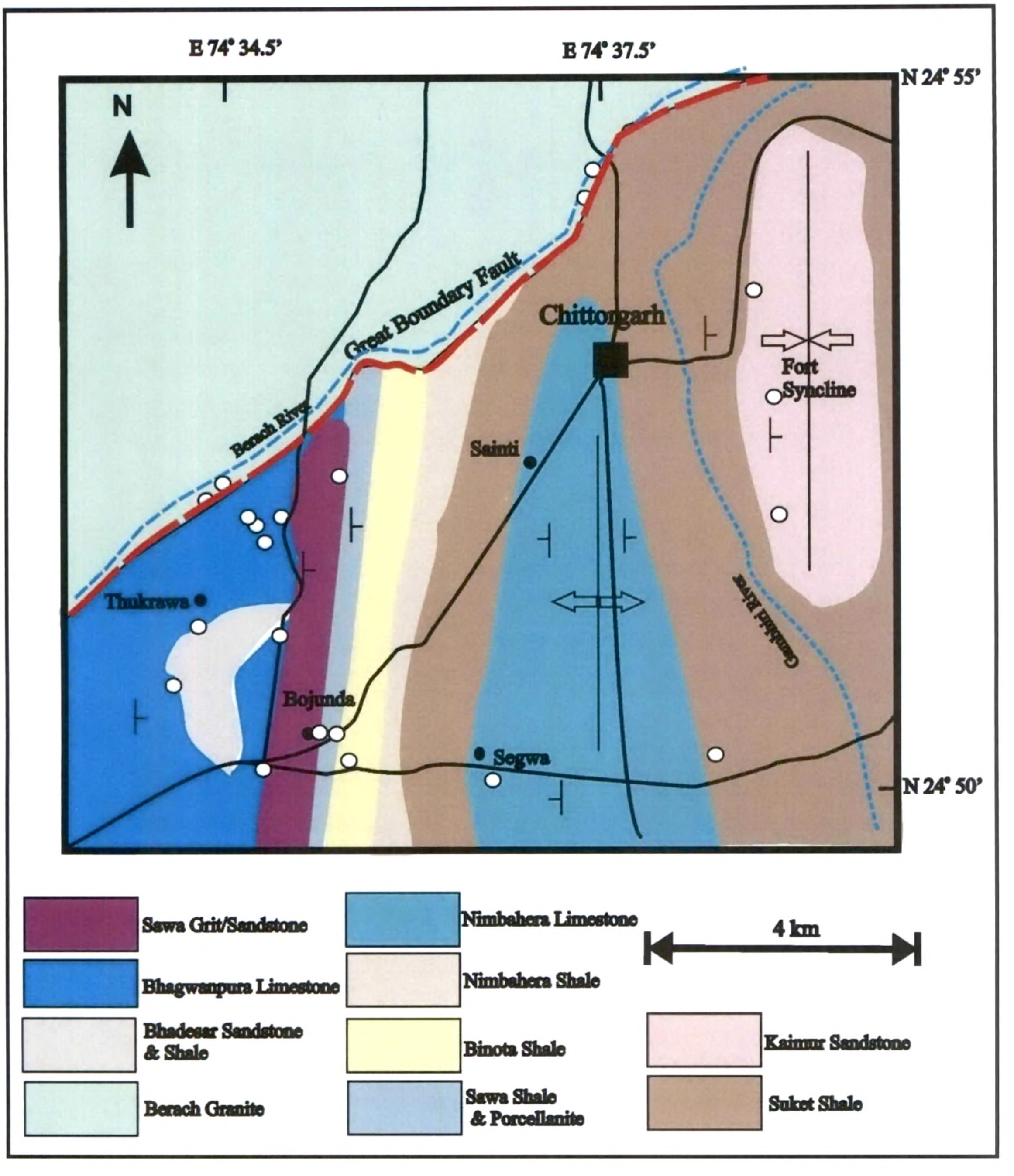

Fig. 2.5: Detailed geological map around Chittorgarh modified from Srivastava and Sahay (2003).

Fig. 2.6: East dipping beds of the Nimbahera Limestone at Chittorgarh. These beds represent the eastern limb of a regional anticlinal fold.

Fig 2.7: Outcrop of the Berach Granite exposed along the banks of the Berach River near Chittorgarh.

Fig. 2.8: Complexly folded Nimbahera Shale Formation along the Great Boundary Fault Zone at Chittorgarh.

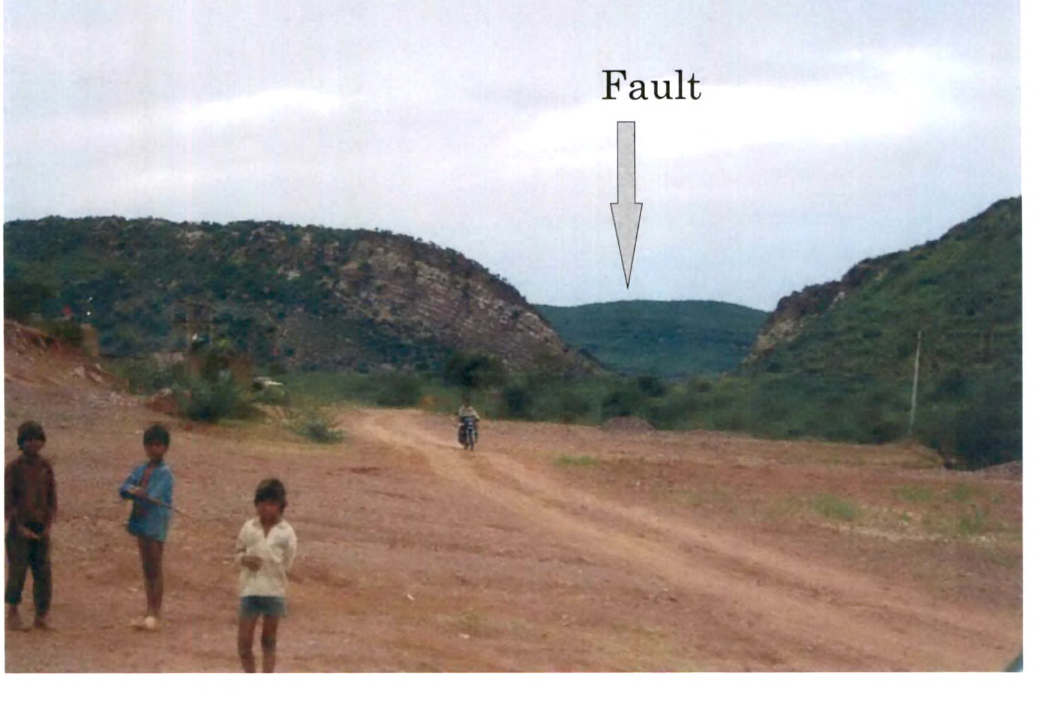

Fig.2.9: A fault within the upper Vindhyans at Khatgarh that cut across the GBF at an angle.

Fig.2.10: Folding in the Lakheri Limestone near Gandoli Village on the Bundi-Indergarh road.

2.2.2 Sampling Strategy and Sample details

Our work required sampling of siliciclastic formations for provenance study and therefore one or two representative samples from each formation were considered sufficient. For sampling the Lower Vindhyans the area south and south west of Chittorgarh town was selected. The samples were collected starting from the Berach River with the Berach Granite and following an east-west transect towards the Chittorgarh Fort, where the Kaimur group (Kaimur Sandstone) is exposed. This total transect is about 5 km across the general strike. Also to determine the chemistry of possible source rocks for the Vindhyan sediments we collected samples of various Pre-Vindhyan rocks near Chittorgarh. These include the Berach Granite and several meta-volcanic rocks of the Hindoli supracrustals. Our sampling locations are marked

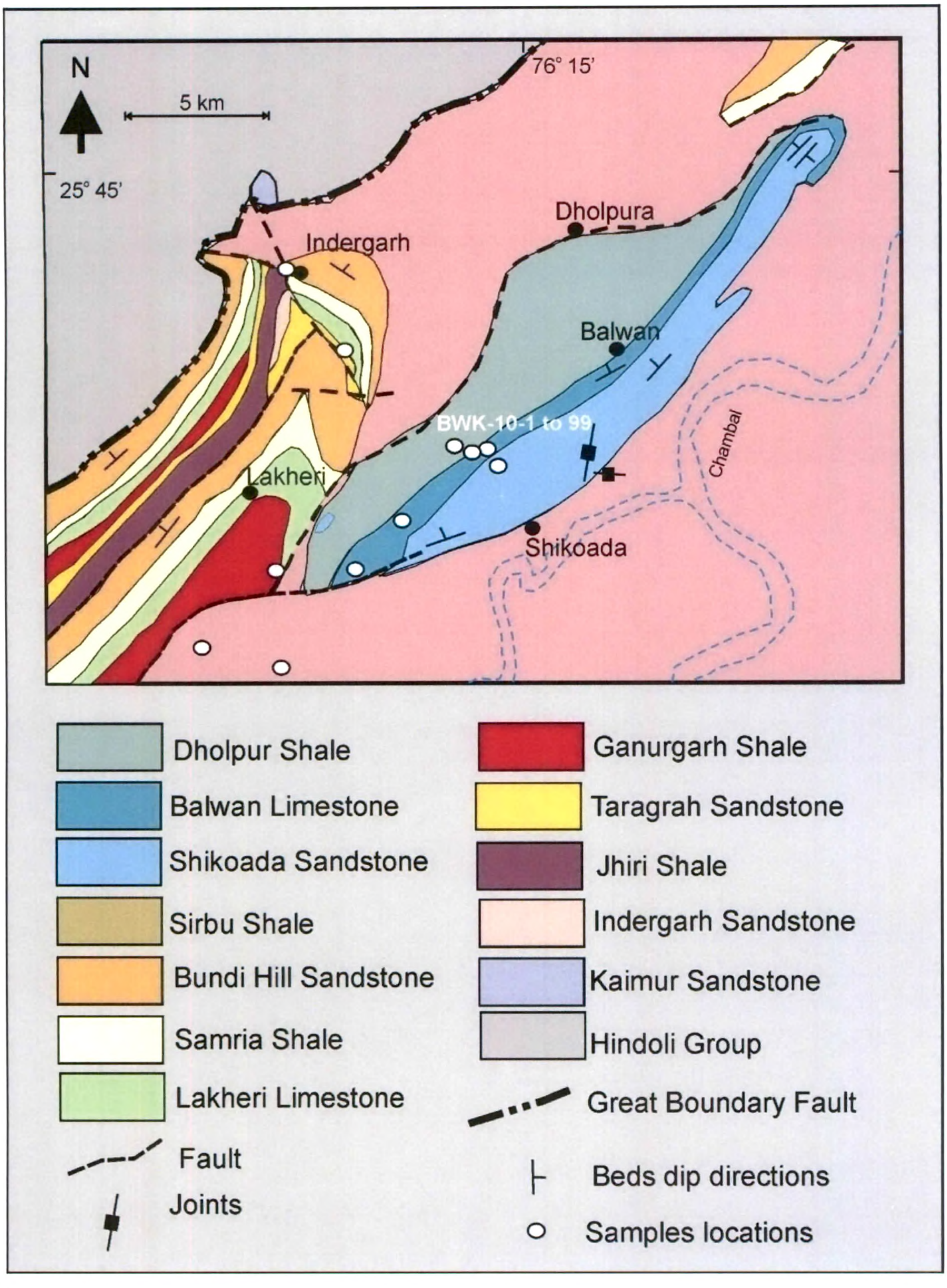

Fig. 2.11: Detailed map of the Lakheri-Indergarh area, after Prasad (1984).

in Fig. 23. & 2.5. Furthermore, some of the lowermost formations of the Lower Vindhyans including Khairmalia Andesites were sampled near Chhoti Sadri (Fig 2.3). Sample of various formations of the upper Vindhyans were collected in Begun, Rawatbhata, Bundi and Lakheri sectors (Fig 2.3, 2.4). As discussed earlier stratigraphic correlations between various formations of the Vindhyans of Rajasthan and those in the Son Valley remains problematic. In an attempt to shed some light on these issues we took the help of detrital zircon geochronology. Considering the fact that the Lower Vindhyans of Chittorgarh contains a formation (Sawa Sandstone) that is believed to be equivalent of the ~1630 Ma Deonar porcellanite Formation of the Son Valley (Prasad, 1984) an attempt was made to date this formation using the above method. For this purpose samples were collected from this formation near Bojunda (N24°50.434′E74°35.528′ Table 2.5). As has been demonstrated by many workers (e.g. Ray et al., 2003), Sr-isotope stratigraphy is a useful tool to determine minimum depositional ages of limestone formations in cases where direct dating methods and biostratigraphy either are absent or fail. In an effort to establish the chronology of the topmost limestone unit of the Vindhyans in Rajasthan, the Balwan Limestone, we employed this method and for this purpose careful sampling was done to reduce least altered samples. We also worked on C and O isotope compositions of these limestone formations in order to understand their depositional environments/diagenetic history. For C and Sr isotope stratigraphy high resolution sampling was done, with ~ 5cm sampling interval, in the Balwan Limestone from two transects across the strike (Fig.2.4 & 2.12).

Our samples were collected from the large exposures of various formations after selecting fresh outcrops to avoid the weathered domains. Lists of the samples with their locations and other relevant information are presented in Tables 2.4, 2.5, and 2.6. Table 2.4 presents samples collected from the Vindhyan formations exposed in the Chittorgarh district, whereas Table 2.5 deals with the samples collected from Bundi district. The samples collected from the Balwan Limestone near Lakheri town in Bundi district are presented in Table 2.6. The locations of the samples are marked on the geological maps in Figs. 2.3, 2.4, 2.5 &2.12.

Table 2.4: Samples collected from the Vindhyan formations and pre-Vindhyan rocks exposed in Chittorgarh district.

Sample	Location	Formation	Description/Remarks
CHITTOR-09-12	N25°07.207'; E75°07.954' Near Menaal on NH 76	Bhander Shale	Fine grained, yellow color with sandy intercalations
CHITTOR-09-9	N25°02.877'; E75°08.880'	Ganurgarh Shale (Black Shale)	Thinly laminated black shale, from a well
CHITTOR-09-8	N24°57.587'; E75°04.410'	Ganurgarh Shale (Black Shale)	Hard, thinly laminated, black colour, from a well
CHITTOR-09-13	N25°08.099'; E75°07.304'	Samaria Shale	Greenish-gray thinly laminated
CHITTOR-09-07	N24°58.916'; E75°29.689' Rawat Bhata	Ganurgarh Shale	Compact, greenish colour
CHITTOR-09-06	N24°57.934'; E75°33.434'	Jhiri Shale	Green color, thinly laminated, fissile
CHITTOR-09-05	N24°57.188'; E75°33.714'	Jhiri/Panna Shale	Purple & greenish colour, thinly laminated
CHITTOR-09-03	N24°55.562'; E75°35.667'	Indergarh Sandstone	Light colour with brown bands
CHITTOR-09-17	N24°54.512'; E74°46.706' Gorasiya village	Panna Shale (Black Shale)	Black shale with evident pyrite crystal
CHITTOR-09-15	N24°54.465'; E74°42.044'	Panna Shale	Greenish-yellow with sandy intercalations
CHITTO-09-02	N24°58.074'; E75°35.064'	Panna Shale	Brownish, thinly laminated, fragile
CHITTOR-09-16	N24°54.913'; E74°42.130'	Panna Shale	compacted, laminated with sandy layer, dark green colour
CGB07-20	N24°51.914'; E74°38.719'	Kaimur Sandstone	White hard, quartz-feldspar bearing rock
CGB07-21	N24°52.437'; E74°38.752'	Kaimur Sandstone	White, hard, quartz-feldspar, bearing fine grained rock
CGB07-22B	N24°53.305'; E74°38.524'	Suket Shale	Banded, yellowish shale, with lenticular structure
CGB07-22A	N24°53.305'; E74°38.524'	Suket Shale	Red bands in yellowish shale

Table 2.4 continued...

CGB07-19	N24°50.037'; E74°37.569'	Suket Shale	Yellowish
CGB07-18	N24°50.049'; E74°36.328'	Nimbahera Limestone	Fine, grayish
CGB07-23	N24°53.597'; E74°36.855'	Nimbahera Shale	Dark gray
CGB07-24	N24°54.226'; E74°37.364'	Nimbahera Shale	Light gray
CHITTOR-09-21	N24°26.510'; E74°37.692'	Palri (Binota) shale	Gray/greenish, yellow ting, finely laminated
CGB07-17	N24°50.205'; E74°35.453'	Binota Shale	Greenish
CGB07-01	N24°52.1'; E74°35. 6' Bojunda	Sawa Grit	Coarse grained, grayish with weathered material.
CGB07-02	N24°52.1'; E74°35. 6'	Sawa Grit	Fine grained, grayish with white infillings
CGB07-09	N24°51.75; E74°34.96'	Sawa Shale	Buff colour compact
CGB07-10	N24°51.662'; E74°34.903'	Sawa Shale	Grayish ,hard
CGB07-15	N24°50.434'; E74°35.528'	Sawa Sandstone/	Coarse grained, Black
CGB07-16	N24°50.496'; E74°35.515'	Sawa sandstone	Coarse, quartz, feldspar(pink)
CGB07-13	N24°51.00'; E74°35'	Bhagwanpura Limestone	Fine grained, grayish, stromatolitic, silicified
CGB07-14	N24°50.257'; E74°35.019'	Bhagwanpura Limestone	Fine grained, grayish, hard, stromatolitic
CGB07-05	N24°52.051'; E74°34.554'	Bhagwanpura Limestone	Grayish, fine grained, hard.
CGB07-04	N24°52.051'; E74°34.554'	Quartzite	Grey granite with quartzite bands.
CHITTOR-09-20	N24°25.399'; E74°40.002'	Khardeola Sandstone	Fine grained, purple with brown solution features
CGB07-08	N24°51.8'; E74°34.8'	Metabasalt	Coarse grained, black
CHITOR-09-24	N24°16.606'; E74°36.678'	Khairmalia Andesite	Coarse grained, black
CHITOR-09-25	N24°16.606'; E74°36.678'	Light colored basic rock	Green colour
CHITOR-09-26	N24°16.606'; E74°36.678'	Khairmalia Andesite?	Gray colour rock

Table 2.4 continued...			
CHITOR-09-23B	N24°16.850'; E74°35.827'	Mafic rock	Black in colour, very fine grained
CGB07-07	N24°51.12'; E74°34.33'	Bhadesar Quartzite	Yellowish white
CGB07-11	N24°50.71'; E74°34.21'	Bhadesar Quartzite	White with yellow and black bands
CGB07-12	N24°51.8'; E74°34.8'	Bhadesar Quartzite	Coarse grained, quartz & feldspar bearing
CGB07-6	N24°52.051'; E74°34.554'	Berach Granite	Coarse, quartz with pink feldspar
CGB07-3	N24°51.99'; E74°34.48'	Berach Granite	Coarse, gray with quartz-feldspar

Table 2.5: Samples collected from Vindhyan formations exposed in Bundi District.

Sample	Location	Formation	Descriptionn/Remarks
BUNDI-09-06	N25°41.175'; E76°14.512' Kavarpura	Dholpur Shale	Thinly laminated, yellowish brown in colour
BUNDI-09-07	N25°41.345'; E76°14.568'	Dholpur Shale	Laminated yellow in colour
BUNDI-09-03	N25°40.993'; E76°14.602'	Balwan Limestone	Stromatolitic, pinkish white calcites
BUNDI-09-04	N25°40.993'; E76°14.602'	Balwan Dolomite	Light pink, coarse grained
BUNDI-09-05	N25°40.821'; E76°14.722'	Upper Bhander Sandstone	Purple colour fine grain with dark brown bands
BUNDI-09-10	N25°40.701'; E76°12.433'	Sirbu Shale	Thinly laminated, yellowish colour
LAK07-02	N 25°37.06'; E 76° 07.46'	Black shale (Sirbu)	From a well dump
LAK07-08	N 25°38.577'; E 76°9.093'	Gray shale ~22feet thick below the soil in the well (Sirbu)	Gray colour from a fresh dump from a well
LAK07-09	-do-	Black shale (Sirbu)	Dull Black in occurs below the above inside the well
LAK07-10	-do-	Black shale (Sirbu)	Black Shale below occurs below the above inside the well
LAK07-11	N 25°38.297'; E 76° 08.893'	Black shale (Sirbu)	Black shale from a well
LAK07-12	N 25°38.009'; E 76° 08.538'	Black shale (Sirbu)	Black shale from a well
LAK07-13	N 25°37.023'; E 76° 07.438'	Black shale (Sirbu)	Black shale from a well
LAK07-14	N 25°36.554'; E 76° 06.882'	Black shale (Sirbu)	Black shale from a well
SAT-07-23	N 25°28.260'; E 75° 33.133'	Bundi Hill Sandstone	Maroon colour ferruginous with solution features
BUNDI-09-08	N25°43.450'; E76°11.421'	Bundi Hill Sandstone	Purple colour with light brown bands, fine grained
SAT-07-22	N 25°28.260'; E 75° 33.133'	Dolostone (Samaria)	Stromatolitic yellow colour
SAT-07-21	N 25°28.260'; E 75° 33.133'	Samaria Shale	Thinly laminated yellow colour
BUNDI-09-13	N25°27.178'; E75°38.510'	Samaria Shale	Purple, compact
BUNDI-09-01	N25°32.639'; E75°58.274'	Samaria Shale	Compact, thinly laminated, creamish
BUNDI-09-02	N25°32.639'; E75°58.274'	Samaria Shale	Purple, pinkish, thinly laminated

Table 2.5 continued...			
BUNDI-09-09	N25°42.983'; E76°11.461'	Shale (Samria) below sandstone	Sandy horizon within shale, yellow colour
SAT-07-01	N 25°28.260'; E 75° 33.133'	Samaria Shale	Thinly laminated yellow colour
SAT-07-02 to SAT-07-20 and SAT-07-25 & 26	N 25°28.260'; E 75° 33.133'	Lakheri Limestone	Pinkish /purple/grey colour
Gandoli-1 to Gandoli-23	N 25°32.65'; E 75° 58.33'	Lakheri Limestone	Pinkish /purple/gray colour
LAK07-07	N 25°28.260'; E 75° 33.133'	Ganurgarh shale	Thinly laminated grey colour
LAK07-01	N 25°35.389'; E 76° 4.928'	Ganurgarh shale	Yellowish, grey friable
BUNDI-09-10	N25°40.701'; E76°12.433'	Ganurgarh Shale	Yellowish, grey friable
BUNDI-09-14	N25°27.140'; E75°38.007'	Taragarh Fort Sandstone	Light pink fine grained compact
LAK07-16	N 25°30.520'; E 75° 52.072'	Taragarh Fort Sandstone	Reddish, compact, ferruginous
BUNDI-09-11	N25°32.086'; E75°56.161'	Upperr Rewa Sandstone	Reddish, compact, ferruginous
BUNDI-09-12	N25°32.086'; E75°56.161'	Jhiri Shale	Reddish brown laminated with folding

Table 2.6: Samples from the Balwan Limestone Formation near Lakheri town in Bundi district.

Sample	Relative Position	Description/Remarks
Transect-1		
	Towards older formation	(~ 2km from Kavarpura Village towards east on the Bagishwar Mahadev road left side) N25°40.993'; E 76 °14.602'
BWK-10-1	0 m	Stromatolitic, in contact with Dholpur Shale
BWK-10-2	15 m	pink coloured, stromatolitic
BWK-10-3	30 m	-do-
BWK-10-4	35 m	-do-
BWK-10-5	40 m	-do-
BWK-10-6	50 m	-do-
BWK-10-7	52 m	Colour change from pink to yellowish Limestone
BWK-10-8	55 m	intraclastic limestone
BWK-10-9	57 m	intraclastic limestones with chert
BWK-10-11	58.5 m	intraclastic limestone
BWK-10-12	61.5 m	Limestone Clast-1
BWK-10-13	61.5 m	Limestone Clast-2
BWK-10-14	64.5 m	intraclastic limestone
BWK-10-15	69.5 m	dolomitic, grainy
BWK-10-16	79.5 m	dolomitic, with intraclasts
BWK-10-17		Black ,sandy, clast bearing limestone
BWK-10-18		Limestone with large intraclasts
BWK-10-19		Limestone conglomerate
	N 25° 40.938'; E 76 °14.580'	
BWK-10-38		Light pink coloured
BWK-10-39		A limestone clast
BWK-10-42		Limestone conglomerate
BWK-10-41	1m	pink coloured
BWK-10-40	0m	Stromatolitic, pink coloured dolostone
N 25° 41.047'; E 76°, 14.559'		
BWK-10-90	Close to the contact with Shikaoda Sandstone	
BWK-10-91	Limestone in contact with Dholpur Shale (~30m above BWK-10-1)	
Transect-2		
N 25° 41.064'; E 76°; 14.727'		
(~200 m north of the Transect -1 along the strike)		
BWK-10-34	0m	Stromatolitic –top of the formation
BWK-10-33	5m	No Stromatolites
BWK-10-32	6.5m	Pink colour
BWK-10-31	7.6m	Pink colour
BWK-10-30	8.5m	Pink colour

Table 2.6 continued...		
BWK-10-29	10m	Pink colour
BWK-10-28	11m	Limestone with chert pebbles
BWK-10-27A	11.6m	Stromatolitic, with chert pebbles
BWK-10-27B	11.6m	Stromatolitic , with chert pebbles
BWK-10-26	13.1m	Limestone with chert clasts
BWK-10-25	14.1m	Limestone with chert clasts
BWK-10-24	15.9m	Intraclastic
BWK-10-23	17.4m	Intraclastic
BWK-10-22	19.9m	Intraclastic
BWK-10-35	44.9m	Cherty horizen
BWK-10-36	59.9m	Abundant Molar Tooth structures
BWK-10-37	67.9m	Pinkish, molar tooth structures
N 25° 41.064'; E 76° 14.727'		
(Re-sampling at same location with high resolution)		
BWK-10-67	0m	With stromatolitic intraclasts
BWK-10-66	0.7m	Non stromatolitic
BWK-10-65	1.2m	Stromatolitic
BWK-10-64	2m	Stromatolitic
BWK-10-63	2.1m	Stromatolitic
BWK-10-62	2.8m	Stromatolitic
BWK-10-61	3.9m	Limestone with sandy pebbles
BWK-10-60	4.8m	Intraclastic (=BWK-10-27)
BWK-10-68	9.6m	Intraclastic
BWK-10-69	11.1m	Intraclastic
BWK-10-70	26.1m	Intraclastic
BWK-10-71	29.6m	Intraclastic
BWK-10-72	30.6m	Intraclastic
BWK-10-73	31.1m	Intraclastic
BWK-10-74	32.1m	Cherty horizen
BWK-10-75	34m	Without stromatolites
BWK-10-76	35m	Without stromatolites
BWK-10-77	43m	Without stromatolites
BWK-10-78	45m	Stromatolitic
BWK-10-79	47.5m	Stromatolitic
BWK-10-80	48.5m	Stromatolitic
BWK-10-81	51.5m	Stromatolitic
BWK-10-82	53.5m	Stromatolitic
BWK-10-83	54.5m	Stromatolitic
BWK-10-84	56.5m	Stromatolitic
BWK-10-85	60m	Stromatolitic
BWK-10-86	62m	Stromatolitic
BWK-10-87	68m	Stromatolitic
BWK-10-88	69m	Stromatolitic
BWK-10-89	79m	Molar Tooth structures
Transect-3		
N 25° 40.195'; E 76° 12.880'		
Along the left side of the Lakheri- Shikaoda road, near ACC quarry		
BWK-10-45	0 m	Stromatolitic

Table 2.6 continued…

BWK-10-46	3m	Stromatolitic
BWK-10-47		Stromatolitic at same position of BWK-10-46
BWK-10-44	5 m	Stromatolitic
BWK-10-43	7.5 m	Above the chert intercalated horizon
BWK-10-53	8 m	Limestone with cherty intercalations
BWK-10-54	10 m	Limestone Conglomerate
BWK-10-55	12 m	Chert bearing horizon
BWK-10-56	17 m	yellow colour
BWK-10-57	27m	Yellowish colour
BWK-10-48	30m/100m	compacted
BWK-10-20		Pink color, stromatolitic from the near-by quarry
BWK-10-21		Black color, stromatolitic from the near-by quarry
N 25° 40.278'; E 76° 12.874'		
BWK-10-49	Cherty horizon below the pink stromatolitic top unit	
BWK-10-50	Below sandy horizon	
BWK-10-51	Pink Limestone above sandy BWK-10-50	
BWK-10-52	same at BWK-10- 51 level ~ 15 m away	
N 25°40.220'; E 76° 12.876'		
BWK-10-92	0m	Stromatolitic, pink colour
BWK-10-93	0.5m	Above the sand intercalated horizon
BWK-10-94	2.0m	Limestone with sandy intercalation
BWK-10-95	3.5m	Clast bearing unit of the limestone (=BWK-10-56)
BWK-10-96	9.5m	Chert bearing
BWK-10-97	11.5m	Chert bearing
BWK-10-98	12.5m	Chert bearing (=BWK-10-57)
N 25° 40.938'; E 76° 14.580'		
BWK-10-99	Cherty Limestone on the left side of the Shikaoda road (Dip of the beds are changing)	
N 25° 24.584'; E 75° 35.229'		
BWK-10-100	Limestone within Sirbu Shale Formation at 6 km milestone Bundi- Bijolia	

2.3 Experimental Methods

The objectives of the current work were achieved by carrying out necessary field studies, collecting suitable rock samples and performing various analyses petrographic and chemical in the laboratory. Petrography was done on all the samples and subset of these was selected for geochemical and isotopic studies. Care was taken to avoid weathered and altered materials. Petrography was done on thin sections, where as geochemical studies were performed on powder samples. Powdering was done using an Agate mortar and an automated milling system (Fisher-Type). Major element analyses were carried out using X-ray Fluorescence (XRF) method and trace element content were measured using Inductively Coupled Plasma Mass Spectrometry (ICPMS). Sr and Nd isotopic ratios were analyzed with the help of Thermal Ionization Mass Spectrometer (TIMS) and the stable C-O isotope analyses for carbonates, were done using gas source mass spectrometry. In the next sections detailed description of these methodologies are given.

2.3.1 Petrography

The major objectives of this study were to identify various minerals present in sandstone (e.g. quartz, feldspar etc.), determine the carbonate mineralogy in limestones/dolostones, determine the degree of alteration, determine the micro structures generated by biology and most importantly select a region of least alteration in limestones for micro sampling for C-O-Sr isotope analyses.

Calcite and dolomite phases and their variants (e.g. Fe/Mn rich varieties) were identified in limestone samples using the standard staining procedure on thin sections. The staining solution was prepared following the standard protocol using Potassium Ferricyanide and Alizarine Red S (Tucker et al. 1990) in the following manner:

- A 500 ml 0.5% HCl solution was prepared, and divided into two parts: a 300ml solution -Part A and a 200ml solution-Part B.

- 1.5g of Potassium Ferricyanide was added to Part A and thoroughly mixed and left for 24 hours.
- 0.2gm Alizarine Red S to Part B thoroughly mixed and left for 24 hours.
- After 24 hours both the solution were mixed and used for staining a portion of a thin section.

In general, calcites are stained to pink or purple (Fe-rich), while dolomites remain either colourless or stained blue. After identifying carbonate minerals on thin section the same were sampled from a polished slab, which represents the counterpart (mirror image) of thin section, using a micro drill. This sample powders were then processed for C, O and Sr isotopic ratio analyses. Preference was given to least altered calcite minerals for the geochemical work. Petrographical studies of sandstones were also carried out to understand the mineral composition that was expected to help in understanding the geochemical variations and ultimately deciphering the provenances. All the petrographical studies of thin sections of sandstones and carbonates were done using a Nikon Eclipse LV100POL microscope and Stereo Microscopes at PRL.

2.3.2. Major element analysis

Major element concentrations were measured by X-ray Fluorescence (XRF) Spectrometry method in an automated Philips AXIOS X-ray Spectrometer fitted with an Rh X-ray tube, operated at 50 kV and 55 mA, of 4kW power. The instrument is a National Facility for Planetary Science and Exploration Program (PLANEX) of Indian Space Research Organisation (ISRO) housed at Physical Research Laboratory, Ahmedabad. This instrument was set-up and installed and calibrated for routine measurements of rock samples under this research activity (Ray et al., 2008). The analyses for this work were done on pressed pellets of sample powders. For calibration purpose several international rock standards, as listed in Table 2.7, were used. Appropriate set of standards were used for a given set of samples to avoid interferences and absorptions caused by matrix. For example, sedimentary samples were analyzed using sedimentary rock or sediment standards, while igneous rocks were analyzed with calibration using igneous rock standards. Fig 2.12 gives typical calibration curves for major element oxides and two trace elements.

Pressed Pellets of our samples and rock standards were prepared using wax binder. A finely powdered sample (2.0 gm) was mixed homogeneously with 0.5 gm of wax binder in an agate mortar. The mixture was then transferred into 37 mm standard aluminum cups and subjected to 150kN pressure using a hydraulic press for about a minute. The pressure was removed slowly and pellets were recovered for analysis. The precision of measurements at 2σ level, based on repeated analyses of sample/standard, for major oxides is better than 5% and for trace elements it is better than 15%, except for Ni for which it is ~25%.

During the analyses one of the sedimentary standards Cody-Shale (SCo-1), which was not part of the calibration, was used as unknown for accuracy check (Table 2.8). The measured values (average of 20 measurements) are in good agreement with the reported values within the 2σ level of error.

2.3.3 Loss on Ignition (LOI) analysis

The concentration of volatile matter (e.g. water in the form of hydrates or labile hydroxyl ions; carbon dioxide from the carbonates etc.) in rocks or sediments is reported as Loss on Ignition (LOI). For this purpose, ~ 2 gm of a sample powder was taken in a silica crucible after drying down at 110^{o}C for 4-5 hours. The silica crucible was inserted into a furnace preheated to 1070^{o}C and sample was ignited. After igniting the sample for an hour, furnace was switched off, and was allowed to cool down to room temperature. The difference in the weight (in% loss) of sample powder before and after ignition is determined and tabulated as LOI.

Table 2.7: International rock standards used in various analytical techniques during the generation of major and trace elements data.

Name of Standard	Rock Type	Supplier
AGV-1	Andesite	USGS*
BCR-2	Basalt	USGS
BHVO-2	Hawaiian Basalt	USGS
COQ-1	Carbonatite	USGS
G-2	Granite	USGS
JB-2	Japanese Basalt	GJS**
JG-2	Granite	GJS
JGb-1	Gabbro	GJS
JGb-2	Gabbro	GJS
JLS-1	Limestone	GJS
JDO-1	Dolomite	GJS
JMS-2	Marine Mud	GJS
MAG-1	Marine sediments	USGS
SCO-1	Cody-Shale	USGS
SDO-1	Shale	USGS
W-2	Diabase	USGS

**USGS= United State Geological Survey & **GJS= Japanese Geological Survey*

Table 2.8: A comparison of measured and reported concentrations for various elements in SCo-1 standard.

	Measured (n=20)		Reported*	
		±2σ		±2σ
Al_2O_3 (wt %)	14.0	0.65	13.7	0.42
CaO (wt %)	2.79	0.02	2.62	0.4
Fe_2O_3 (wt %)	5.06	0.11	5.13	0.36
K_2O (wt %)	2.72	0.01	2.77	0.16
MgO (wt %)	2.83	0.02	2.72	0.36
MnO (wt %)	0.05	0.00	0.053	0.008
Na_2O (wt %)	0.99	0.02	0.9	0.12
P_2O_5 (wt %)	0.20	0.01	0.21	0.04
SiO_2 (wt %)	63.1	0.22	62.8	1.32
TiO_2 (wt %)	0.66	0.01	0.63	0.12
Rb (ppm)	117	5.36	110	8
Sr (ppm)	180	2.10	170	32
Zr (ppm)	163	1.59	160	60
Ni (ppm)	28.1	7.00	27	8
Y (ppm)	24.5	1.50	26	8
Cr (ppm)	84.1	11.77	68	10

*(*Certificate of Analysis supplied by USGS: Abbey, (1983), Flanagan, (1976); Gladney & Roelandts (1988); Govindaraju, (1994)).*

2.3.4 Analysis of Trace Elements including Rare Earth Elements (REE)

Inductively coupled plasma-mass spectrometry (ICP-MS) is a well established rapid and precise method for the determination of concentration of trace elements including rare earth elements (REEs) in geological samples (Lichte et al., 1987; Jarvis, 1988; Longerich et al., 1990). Trace elements Sc, V, Cr, Co, Ni, Zn, Rb, Sr, Zr, Nb, Ba, Hf, Ta, Th and 14 REEs (La, Ce, Pr, Nd, Sm, Eu, Gd, Tb, Dy, Ho, Er, Tm, Yb and Lu) in our samples were measured using a Thermoelectron X-Series^{II} ICPMS, which is installed recently at the National Facility for Planetary Science and Exploration Program (PLANEX) of ISRO at Physical Research Laboratory, Ahmedabad. This instrument was set-up and installed and calibrated for routine measurements for rock samples during this work (Ray et al., 2008).

Samples and a couple of rock standards (G2 and BHVO-2) (~50mg each) were dissolved using ultra-pure acids following standard HF-HNO3 dissolution technique in Savillex Teflon vials. Care was taken for complete dissolution of rock powders. The stock solutions were prepared in 2% HNO_3 with ~1000 dilution factor. The analyses were performed on highly diluted samples prepared from the stock solution, to avoid matrix effect. Calibration curves were generated using blank and various dilutions of G-2 and BHVO-2 standards. Normally calibration curves are drawn in the range of 0 to 50 ppb concentrations. A few typical calibration curves are presented in Figure 2.13. The isotopes ^{139}La, ^{140}Ce, ^{141}Pr, ^{146}Nd,^{147}Sm, ^{153}Eu, ^{157}Gd, ^{159}Tb, ^{163}Dy, ^{165}Ho, ^{166}Er, ^{169}Tm, ^{172}Yb, ^{175}Lu,^{45}SC, ^{51}V, ^{52}Cr, ^{59}Co, ^{60}Ni, ^{66}Zn, ^{85}Rb, ^{88}Sr, ^{90}Zr, ^{93}Nb, ^{137}Ba, ^{178}Hf, ^{181}Ta, and ^{232}Th, were analyzed for their respective elements. Reproducibility (external precision) of our measurements, based on repeated analyses of a sample, were better than 2% at 2σ level, for all trace elements reported here. For accuracy check analyses of various dilutions of the international standard BHVO-2 were performed at regular intervals. As can been seen in Table 2.9, the measured data agree well with the reported values (within the reproducibility) for all the elements analyzed.

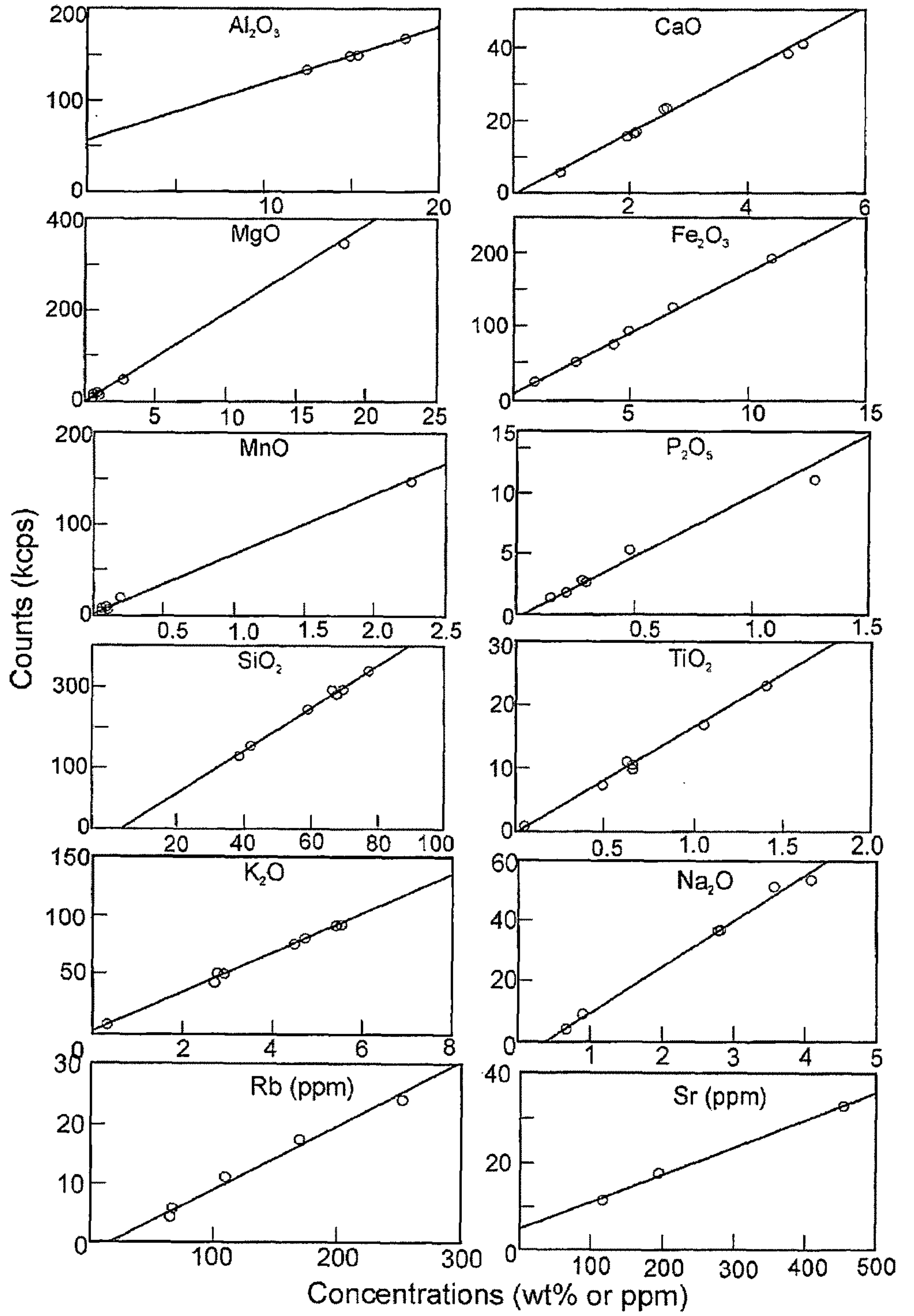

Fig. 2.12: Typical calibration curves generated using XRF for 10 major element oxides and two trace elements using several international rock standards.

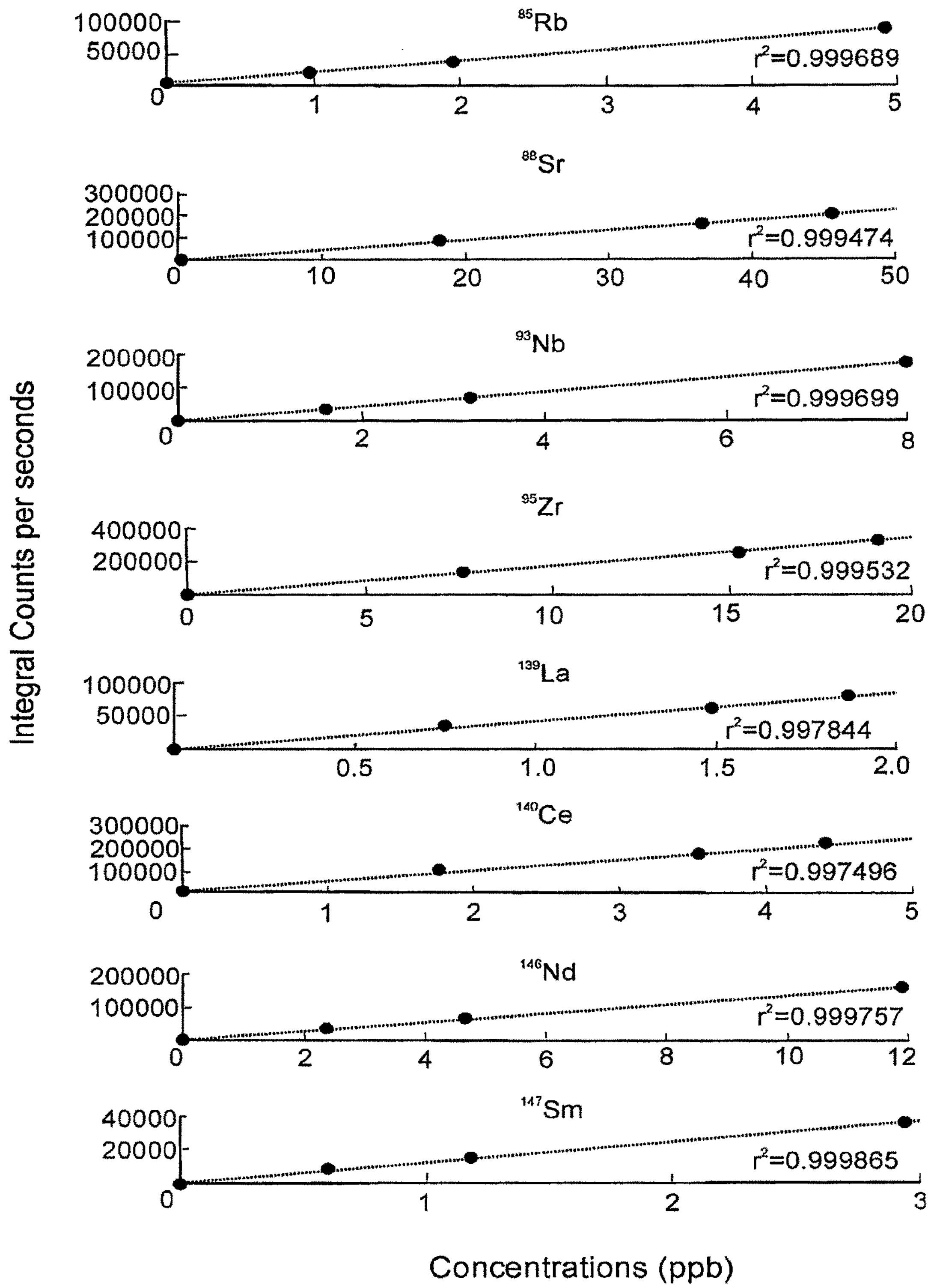

Fig. 2.13: Typical calibration curves generated by diluting the BHVO-2 USGS rock standard for analyzing the trace elements by ICPMS.

Table 2.9: Measured Trace element concentrations in BHVO-2 compared with their reported values.

Elements	Measured (n=10) (ppm)		Reported* (ppm)	
		±2σ		±2σ
Sc	31.6	3.6	31	2
V	330	36	329	18
Cr	290	31	285	28
Co	48.1	5.4	47	4
Ni	114	13.8	112	18
Rb	10.5	1.1	10.1	1.2
Cs	0.11	0.02	0.11	0.02
Sr	383	36	382	20
Y	23.0	2.4	23	2
Zr	159	17	160	16
Nb	16.3	1.9	16.4	0.1
Ba	129	1.0	128	8
La	15.1	1.5	15.6	0.1
Ce	37.3	3.6	37	2
Pr	5.35	0.86	5	0.6
Nd	24.4	3.3	24	2
Sm	6.10	0.76	5.8	1.0
Eu	2.06	0.23	2.0	0.2
Gd	6.24	0.78	5.9	0.8
Tb	0.82	0.17	0.86	0.06
Dy	5.37	0.58	4.9	0.8
Ho	0.93	0.07	0.91	0.12
Er	2.59	0.27	2.3	0.2
Tm	0.31	0.03	0.3	0.1
Yb	1.95	0.24	2.0	0.4
Lu	0.29	0.01	0.26	0.08
Hf	4.13	0.39	4.1	0.8
Ta	0.93	0.12	0.94	0.14
Pb	1.61	0.10	1.4	0.4
Th	1.12	0.19	1.18	0.18
U	0.41	0.07	0.44	0.06

**Gao et al. (2002); Kent et al. (2004); Raczek et al. (2003)*

2.3.5 Analysis of Radiogenic Isotope Ratios

Sr and Nd isotopic ratios ($^{87}Sr/^{86}Sr$ and $^{143}Nd/^{144}Nd$) were measured in selected samples from all the siliciclastic formations of the Vindhyan Supergroup from Chittorgarh as well as Bundi area. The sample powders were dissolved in 17 ml Savillex^{R} teflon vials using the standard HF-HNO_3-HCl acid dissolution protocol (see Table 2.10). Sr and REE were separated from other elements by standard cation exchange chromatography using 2N HCl as elutant (Table 2.11). Nd was separated from the rest of the REE fraction using Ln -specific resin from Eichrom^{R} and diluted (0.18N) HCl acid as elutant (Table 2.12).

Table 2.10: The dissolution procedure for silicate rocks.

Step 1: About 50-100mg sample powder weighed into pre cleaned Savillex^{R} Teflon vials

Step 2: ~1.5ml of HF: HNO_3 (3:1) mixture was added to the sample

Step 3: Samples were agitated through ultrasonication

Step 4: After 24 hours of dissolution- samples were completely dissolved. After complete dissolution samples were dried down at slow heat (~80°C) and taken back in ~ 1ml of 8N HNO_3

Step 5: Dissolution in 1ml HNO3 and drying down were repeated 3 times to oxidize the elements completely.

Step 6: 2ml of 6N HCl was added and dried down to convert the elements to chloride.

Step 7: Final solution was prepared in 1ml in 2N HCl and kept for column chemistry.

Table 2.11: Protocol for Sr and REE separation from sample solution.

Step 1: The primary columns (~15 cm length) were filled with Dowex 50 cation exchange resin
Step 2: Columns were conditioned with 6ml 2N HCl
Step 3: 1ml of the dissolved sample in 2N HCl was loaded on to a column
Step 4: 1ml of 2N HCl passed to allow complete loading
Step 5: 36 ml of 2N HCl was passed and discarded-(removal of Fe, K, Na, Ca, Rb etc)
Step 6: Collect 12ml of 2N HCl was passed and collected for Sr
Step 7: 18ml of 2N HCl passed and collected for REE-dried down and taken up in 100µl of 0.18N HCL-ready for REE column chemistry
Step 8: The collected Sr cut (12ml) was dried down-ready for mass spectrometry
Step 9: columns were cleaned 2 times with full volume of 6N HCl and regenerated with water

Table 2.12: Protocol for Nd separation from rest of the REE.

Step 1: Setting up of REE columns using Ln-specific resin (~9cm length)
Step 2: Columns were conditioned with 2ml 0.18N HCl each. The REE cuts from the primary columns were loaded (100µl of sample in 0.18N HCl)
Step 3: Another 100µl of 0.18N HCl was loaded after washing the vial for each sample
Step 4: Wash- 19 ml of 0.18 N HCl was passed (removal of La, Ce, Pr)
Step 5: Collection - 7ml of 0.3N HCl was eluted for collection of Nd
Step 6: Columns were washed with 6N HCl to remove other REEs and full column volume with water to regenerate the resin
Step 7: The collected 7ml Nd cut was dried down and stored for Nd- analysis

Sr-isotopic ratio analyses in the selected carbonate samples from the limestone formations were also carried out. For these Sr was separated from other elements by

Sr- Sr-Specific resin from Eichron^R. In brief, the selected carbonate sample powders were leached with 40μl Acetic Acid (glacial) and 3ml of Milli-Q water, in a clean 15ml centrifuge tube. These tubes were ultrasonicated for 30 minutes and centrifuged for 15 minutes to separate the solution from residue. 2ml each of the solutions were collected in a clean 7ml Savillex^R Teflon vials and dried down. The samples were then converted into nitrate by adding 0.5 ml of 3N HNO_3 twice and drying down. The final solution was prepared in 2ml 3N HNO_3, which was then processed for Sr preconcentration through column chemistry using the Sr-Specific resin as shown in Table 2.13.

Table 2.13: Protocol for Sr-separation using Sr-specific resin column chemistry.

Step 1: Specific Resin (100-150μm) cleaned with MilliQ water and was stored in MilliQ water
Step 2: The 2ml BioRad polypropylene disposable columns (with frits) were cleaned with warm HNO_3 (3N) and MilliQ water before use
Step 3: About 200 μl resin was loaded onto each column
Step 4: Columns were conditioned with 1ml of 3N HNO_3
Step 5: Samples in 3N HNO_3 were loaded onto the resin
Step 5: Wash -columns were washed 3 times with 0.5ml of 3 N HNO_3
Step 6: Sr collection: Elution of Sr with 4 times of 0.5ml of MilliQ water
Step 7: The collected Sr was dried down and proceeds for mass spectrometry

The mass spectrometric analyses for Sr and Nd isotopic ratios were carried out on a new generation solid source, thermal ionization mass spectrometer (TIMS) Isoprobe-T, at PRL. Sr samples were loaded on pre-degasses, oxidized single Ta filaments and analyzed in static multi collection mode. Small samples were loaded on single Re filaments and a Ta activator. Mass fractionation correction was done by normalizing $^{86}Sr/^{88}Sr$ to 0.1194. Typical Sr loads were 2-4 μg, yielding ^{88}Sr beams of 2-3 V. The 4 years average (n=40) of $^{87}Sr/^{86}Sr$ for international standard NBS 987 is 0.71023

±0.00001 (2σ). Nd samples were loaded on the outer Ta filament of the triple (Ta-Re-Ta) filament settings. Data collection was done in a static mode. Typical Nd loads were 500-1000 ng yielding ^{146}Nd beams of 0.5-2V. Mass fractionation correction was done by normalizing 144Nd/146Nd to its natural ratio of 0.7219. The 2 year average (n-20) of $^{143}Nd/^{144}Nd$ for an international standard is 0.512104±0.000008 (2σ). This corresponds to a value of 0.511847 for much commonly used La Jolla Nd-standard (Tanaka et al., 2000). In addition to running international isotopic ratio standards on mass spectrometer a rock standard, BHVO-2 from USGS, was also processed regularly with samples and analyzed for Sr and Nd isotopic ratios. The average values for $^{87}Sr/^{86}Sr$ and $^{143}Nd/^{144}Nd$ for 12 runs during the course of this work respectively are 0.703458 ± 0.00003 (2σ) and 0.512975 ± 0.000010(2σ). These are well in agreement with the reported values of 0.703462 and 0.512983 respectively (Raczek et al., 2003).

2.3.6 Stable C and O isotopic ratio analysis

Carbon and oxygen isotopic ratios of limestone samples, microdrilled from the slabs were carried out in PRL and the analyses were performed by Dr. J. S. Ray. Samples were weighed (~10 mg) into side-arm (35 cc) vessels with the arm filled with ~2 cc of 100% H_3PO_4. After evacuation, vessels were kept in a constant-temperature water bath at 25°C for a couple of hours and then reacted. In case of pure calcite samples, CO_2 was extracted after 12 hours of reaction at 25°C, while in case of pure dolomites, CO_2 extraction was carried out after 72 hours of reaction. CO_2 extraction was done using in-house fabricated glass system. During the extraction the vessels were kept at 25°C using small water baths.

The $\delta^{13}C$ and $\delta^{18}O$ of CO_2 were measured on a Europa-2020 mass spectrometer against a pre-calibrated laboratory standard CO_2 (prepared from foraminifers) and then converted to PDB and SMOW, respectively. The 25°C acid fractionation factors used for $\delta^{18}O$ of calcite and dolomite were from Friedman and O' Neel (1977) and Rosenbaum and Sheppard (1986) respectively. Reproducibility measured as 1σ for eight analyses of NBS-19 ($\delta^{13}C_{PDB}$ = 1.95 and $\delta^{18}O_{PDB}$ = −2.3‰) and a local dolomite standard ($\delta^{13}C_{PDB}$ = 0.7 and $\delta^{18}O_{PDB}$ = −9.2‰), during the course of the measurements, was better than 0.1‰ for both $\delta^{13}C$ and $\delta^{18}O$. The analyses were carried with respect to pre-calibrated internal laboratory standard CO_2 and then converted to PDB and SMOW respectively.

2.3.7. Detrital Zircon Geochronology

The detrital zircon geochronology on the zircons separated from the Sawa Sandstone Formation was carried out by Dr. J. S. Ray at Geological Survey of Canada at Ottawa using a Sensitive High Resolution Ion Micro Probe (SHRIMP) following the analytical protocol described by Stern (1997), with standards and U-Pb calibration methods following Stern and Amelin (2003). Zircons were mounted in a 2.5cm diameter epoxy mounts along with fragments of the GSC laboratory standard zircon (z6266, with $^{206}Pb/^{238}U$ age = 559 Ma). The zircon grains were exposed by polishing using 9, 6, and 1-μ diamond compound. The mount surfaces were evaporatively coated with 10nm of high-purity Au. All the analyses were carried out using a $^{16}O^{-}$ primary beam. The area on the zircon grains used for analysis was between 15 to 25μ. The data was processed off-line using customized in-house software. The characterizations of the zircons were carried out using scanning electron microscopy (SEM) for the clean and unaltered areas which were used for analyses. The Pb-isotope data was not subjected to fractionation correction. The common Pb correction was taken account the Pb composition of the surface blank (Stern, 1997). The Isoplot v. 3.00 (Ludwig, 2003) was used to calculate weighted means and cumulative probability diagrams were generated using the Age-Display workbook for MS-Excel (Sircombe, 2004). The 1σ external errors of $^{206}Pb/^{238}U$ ratios reported in the data table incorporate a minimum ±1.0% error in calibrating the standard zircon.

Chapter-3

RESULTS AND DISCUSSION

The results of geochemical and isotopic studies carried out in samples from various formations of the Vindhyan Supergroup in Rajasthan are presented in this chapter. Attempts have been made to interpret these results in terms of their implications for the sources of the sediments and for the tectonic evolution of the Vindhyan Basin during the Proterozoic Eon. Apart for our own results, geochemical data from other sources, especially those for the basement and older rocks surrounding the basin, have also been used in discussion.

3.1 Results

3.1.1 Geochemical Data

The data for major element and trace element contents, radiogenic isotopic ratios, stable isotopic ratios in carbonates and U-Pb dating of zircon are presented in various tables in the following pages. The data tables are arranged according to the stratigraphic order of the groups and formations. Concentrations of major elements are presented in 'wt%' of their oxides, whereas those of trace elements are in 'ppm'. Sr and Nd isotopic ratios measured in our samples are presented as $^{87}Sr/^{86}Sr_m$ and $^{143}Nd/^{144}Nd_m$. Since the variations in $^{143}Nd/^{144}Nd$ are extremely low, we make use of the $\varepsilon_{Nd}(0)$ parameter which is defined as:

$$\varepsilon_{Nd}(0) = \left[\frac{\left({}^{143}Nd / {}^{144}Nd \right)_s^p}{\left({}^{143}Nd / {}^{144}Nd \right)_{CHUR}^p} - 1 \right] \times 10^4$$

$$\varepsilon_{Nd}(T) = \left[\frac{\left({}^{143}Nd / {}^{144}Nd \right)_s^T}{\left({}^{143}Nd / {}^{144}Nd \right)_{CHUR}^T} - 1 \right] \times 10^4$$

where subscript 's' and 'CHUR', respectively stand for sample and Chondritic Uniform Reservoir and superscript 'p' and 'T' stand for present day and at T years respectively. The present day $^{143}Nd/^{144}Nd$ ratio in the CHUR is 0.512638 (Depaolo and Wasserburg, 1976).

The Sm-Nd model dates, calculated for the various Vindhyan formations, are also presented in the tables with respect to CHUR and depleted mantle (DM). The model dates T_{CHUR} and T_{DM} respectively are calculated using the following relations,

$$T_{CHUR} = (1/\lambda)ln \left[1 + \frac{\left(\frac{^{143}Nd}{^{144}Nd} \right)_S - \left(\frac{^{143}Nd}{^{144}Nd} \right)_{CHUR}}{\left(\frac{^{147}Sm}{^{144}Nd} \right)_S - \left(\frac{^{147}Sm}{^{144}Nd} \right)_{CHUR}} \right]$$

$$T_{DM} = (1/\lambda)ln \left[1 + \frac{\left(\frac{^{143}Nd}{^{144}Nd} \right)_S - \left(\frac{^{143}Nd}{^{144}Nd} \right)_{DM}}{\left(\frac{^{147}Sm}{^{144}Nd} \right)_S - \left(\frac{^{147}Sm}{^{144}Nd} \right)_{DM}} \right]$$

where $(^{143}Nd/^{144}Nd)_{CHUR}$ = 0.512638 and $(^{147}Sm/^{144}Nd)_{CHUR}$= 0.1967; after DePalo & Wasserburg (1976) and $(^{143}Nd/^{144}Nd)_{DM}$=0.513114 and $(^{147}Sm/^{144}Nd)_{DM}$= 0.222; after Michard et al. (1985).

The parameter $f_{Sm/Nd}$, presented in the tables was calculated using the following relationship:

$$f_{\frac{Sm}{Nd}} = \left[\frac{\left(\frac{^{147}Sm}{^{144}Nd}\right)_S}{\left(\frac{^{147}Sm}{^{144}Nd}\right)_{CHUR}} - 1 \right]$$

For normalization of data we have utilized data for various hypothetical reservoirs such as CHUR, Primitive Mantle (PM), Post Archean Average Australian Sedimentary Rocks (PAAS) and Upper Continental Crust (UCC). The sources of these data are from McDonough & Sun (1995), McLennan et al. (1989) and Taylor and McLennan (1985), respectively. Table 3.1 through 3.5 present the geochemical data for Pre-Vindhyan rocks and various formations of the Vindhyan Supergroup in Rajasthan.

3.1.2 U-Pb analytical data for detrital zircons

Detrital zircons from the Sawa Sandstone Formation from Chittorgarh area were dated using U-Pb method on a SHRIMP-II. The analytical data: concentration of U, Th, Pb and various isotopic ratios are presented in Table 3.6. Table 3.6 also presents the $^{207}Pb/^{206}Pb$ apparent ages and percent discordance of the data.

3.1.3 $\delta^{13}C$ and $\delta^{18}O$ data from limestones

The stable isotopic compositions of C and O from the two limestone formations are presented in form of the change in the isotopic ratios of C and O in comparison to those in the Pee Dee Belemnite (PDB) standard. The stable isotope data are presented as $\delta^{13}C$ and $\delta^{18}O$ in permil. These are defined as follows:

$$\delta\,^{13}C_{PDB} = \left[\frac{\left(\frac{^{13}C}{^{12}C}\right)_{Sample}}{\left(\frac{^{13}C}{^{12}C}\right)_{PDB}} - 1 \right] * 1000$$

$$\delta\,^{18}O_{PDB} = \left[\frac{\left(\frac{^{18}O}{^{16}O}\right)_{Samp\,le}}{\left(\frac{^{18}O}{^{16}O}\right)_{PDB}} - 1 \right] * 1000$$

During the analyses of our samples measurements were also done routinely for an international standard, NBS-19, from the International Atomic Energy Agency (IAEA) and for a local laboratory standard, the Makarana Marble (MMB), which were pre-calibrated against PDB. The results for the standards are presented in Table 3.7.

The $\delta^{13}C$ and $\delta^{18}O$ data for the Lakheri Limestone Formation are presented in Table 3.8. The Balwan Limestone Formation was sampled in more detailed fashion considering its stratigraphic position within the Vindhyan Supergroup. The results of C and O isotope analyses for this formation are given in Table 3.9.

3.1.4 $^{87}Sr/^{86}Sr$ data from limestones

For Sr isotopic stratigraphy samples of the Lakheri Limestone and the Balwan Limestone formations were selected based on their $\delta^{13}C$ and $\delta^{18}O$ compositions and trace element contents. The trace elements ratios (Table 3.10), such as Mn/Sr, were used as a proxy for alteration and samples with lowest values of Mn/Sr were analysed for $^{87}Sr/^{86}Sr$. These samples essentially represent least altered carbonate components in the whole rock samples. The $^{87}Sr/^{86}Sr$ ratio data are presented in Table 3.11.

Table 3.1: Geochemical data for Pre-Vindhyan rocks and basal volcanics of the Vindhyans near Chittorgarh.

	CGB07-03 Berach Granite	*CGB07-06 Berach Granite*	*CHITTOR-09-23B Metavolcanics*	*CGB07-08 Metavolcanics*	*CHITTOR-09-26 Khairmalia*	*CHITTOR-09-25 Khairmalia*	*CHITTOR-09-24 Metavolcanics*
SiO_2	61.10	56.66	47.82	42.06	61.86	55.13	44.71
TiO_2	0.43	0.66	0.74	1.36	0.12	0.55	1.73
Al_2O_3	13.95	12.25	13.04	9.80	3.28	13.90	10.72
Fe_2O_3	3.61	4.99	8.58	14.98	bdl	5.38	14.51
MnO	0.02	0.06	0.04	0.11	0.03	0.09	0.15
MgO	2.48	2.62	3.33	9.27	10.85	5.52	5.36
CaO	0.22	1.72	0.35	2.60	11.58	1.71	8.45
Na_2O	bdl	2.38	bdl	0.29	bdl	2.89	1.77
K_2O	6.63	3.86	4.93	3.72	2.25	2.76	0.97
P_2O_5	0.09	0.18	0.11	0.17	0.07	0.18	0.21
LOI	1.67	1.99	3.87	4.38		3.19	1.91
TOTAL	90.21	87.35	82.81	88.73	105.44	91.29	90.49
Rb	259	103	301	109	53.9	151	36.2
Sr	17.1	142	145	133	112	237	220
Ba	1172	1206	390	1624	313	816	235
Y	14.3	15.0	19.3	18.9	1.92	1bdl	23.65
Zr	125	63.4	123	137	18.1	98.8	89.0
Hf	4.05	1.99	3.45	3.79	0.56	2.59	2.61
Nb	12.6	12.9	13.0	10.0	1.66	5.85	8.90
Ta	0.84	0.86	1.01	0.61	0.15	0.41	0.49
Th	31.6	6.44	21.9	3.07	5.44	11.9	2.71
U	4.02	2.10	2.96	0.52	0.39	1.91	0.54
La	16.9	31.0	55.1	20.7	9.66	38.2	17.5
Ce	31.9	63.1	107	42.1	16.27	71.5	38.0
Pr	2.76	7.29	11.8	4.45	1.63	7.71	5.14
Nd	12.8	31.8	41.8	21.9	4.95	27.4	21.7
Sm	2.50	5.68	8.65	4.75	0.89	5.48	5.27
Eu	0.51	1.26	1.34	1.98	0.21	1.15	1.61
Gd	2.70	4.49	6.57	4.85	0.64	3.93	5.53
Tb	0.44	0.58	0.72	0.74	0.05	0.40	0.80
Dy	2.82	3.02	4.17	4.44	0.40	2.19	5.23
Ho	0.58	0.57	0.76	0.84	0.07	0.37	0.96
Er	1.73	1.58	2.44	2.20	0.23	1.16	2.86
Tm	0.27	0.23	0.34	0.30	0.03	0.15	0.36
Yb	2.03	1.68	2.40	2.11	0.23	1.11	2.39
Lu	0.29	0.23	0.36	0.28	0.04	0.17	0.34
Sc	0.02	3.98	18.6	37.18	bdl	8.36	28.37
V	bdl	18.01	88.5	360	3.17	73.4	291
Cr	bdl	bdl	111	166	bdl	18.4	66.0
Co	bdl	4.53	27.1	43.1	0.94	11.8	41.6
Ni	bdl	0.29	43.5	44.34	bdl	7.36	34.88
Pb	21.9	11.1	6.24	93.1	3.84	6.25	4.14
Cs			9.17		0.82	2.85	1.58
$^{87}Sr/^{86}Sr_m$	1.05362	0.76331	1.96917	0.75992	0.85778	0.74595	0.71769
$^{143}Nd/^{144}Nd_m$	0.510999	0.511091	0.511291		0.510919	0.510964	0.512015
$\varepsilon_{Nd}(0)$	-32.0	-30.2	-26.3		-33.5	-32.7	-12.2
T_{CHUR}	3.16	2.65	2.86		2.97	3.35	1.90
T_{DM}	3.08	2.69	2.85		2.94	3.22	2.22
$f_{Sm/Nd}$	-0.40	-0.45	-0.36	-0.33	-0.45	-0.38	-0.25

Table 3.2: Geochemical data for samples from various formations of the Semri Group.

	CHITTOR-09-20 Khardeola SST	*CGB07-11 Bhadesar QTZ*	*CGB07-12 Bhadesar QTZ*	*CGB07-04 Quartzite*	*CGB07-07 Bhadesar QTZ*
SiO_2	79.41	97.66	75.98	90.67	85.09
TiO_2	0.04	0.09	0.04	0.18	0.08
Al_2O_3	1.44	0.00	3.29	4.54	0.00
Fe_2O_3	1.30	0.41	0.12	0.11	1.96
MnO	0.02	0.00	0.02	0.00	0.01
MgO		0.02	0.18	0.00	0.40
CaO		0.00	0.02	0.25	0.23
Na_2O		0.00	0.19	0.00	0.00
K_2O	0.05	0.00	4.21	1.46	0.67
P_2O_5		0.02	0.01	0.00	0.30
LOI	0.44	0.19	0.74	0.81	0.66
TOTAL	82.70	98.39	84.79	98.01	89.40
Rb	1.63		107.48	42.21	
Sr	89.18		30.52	4.13	
Ba	20.90		627.20	157.50	
Y	3.15		1.19	1.29	
Zr	38.73		29.55	9.30	
Hf	1.08		0.82	0.32	
Nb	0.52		0.85	0.28	
Ta	0.04		0.07	0.05	
Th	2.32		9.15	1.27	
U	0.64		1.13	2.55	
La	9.93		6.52	4.89	
Ce	20.48		12.34	8.00	
Pr	2.27		0.52	bdl	
Nd	7.77		4.74	2.71	
Sm	1.60		0.59	0.32	
Eu	0.24		0.19	0.07	
Gd	1.11		0.38	0.23	
Tb	0.11		0.04	0.03	
Dy	0.69		0.18	0.15	
Ho	0.13		0.04	0.04	
Er	0.42		0.13	0.14	
Tm	0.06		0.02	0.02	
Yb	0.41		0.18	0.17	
Lu	0.07		0.03	0.02	
Sc	0.68		bdl	bdl	
V	17.43		6.78	bdl	
Cr	4.46		bdl	bdl	
Co	0.00		bdl	0.80	
Ni	4.36		bdl	bdl	
Pb	2.26		19.85	9.54	
Cs	0.14				
$^{87}Sr/^{86}Sr_m$	0.73557		0.92481	0.92304	
$^{143}Nd/^{144}Nd_m$	0.511579		0.511658	0.510928	
ε_{Nd} (0)	-20.7		-19.1	-33.4	
T_{CHUR}	2.23		1.22	2.07	
T_{DM}	2.39		1.50	2.20	
$f_{Sm/Nd}$	-0.37		-0.62	-0.64	

QTZ: Quartzite; SST: Sandstone; SH: Shale and LST: Limestone

Table 3.2 continued...

	CGB07-14 Bhagwanpura LST		*CGB07-05 Bhagwanpura LST*		*CGB07-13 Bhagwanpura LST*
SiO_2	16.65		9.39		14.13
TiO_2	0.11		0.11		0.12
Al_2O_3	0.00		0.00		0.00
Fe_2O_3	0.97		1.67		1.28
MnO	0.03		0.20		0.04
MgO	12.79		1.04		13.64
CaO	36.38		63.76		38.75
Na_2O	0.00		0.00		0.00
K_2O	0.77		0.00		0.81
P_2O_5	0.03		0.07		0.03
LOI	-		-		-
TOTAL	67.73		76.24		68.80
	Sil.	Carb.	Sil.	Carb.	
Rb				1.01	
Sr				290.90	
Ba				8.32	
Y				21.73	
Zr				bdl	
Hf				0.01	
Nb				bdl	
Ta				bdl	
Th				0.19	
U				bdl	
La				29.46	
Ce				38.26	
Pr				3.43	
Nd				17.17	
Sm				3.61	
Eu				2.23	
Gd				4.13	
Tb				0.52	
Dy				2.80	
Ho				0.55	
Er				1.43	
Tm				0.19	
Yb				1.31	
Lu				0.17	
Sc				bdl	
V				bdl	
Cr				4.78	
Co				1.71	
Ni				0.80	
Pb				5.87	
Cs					
$^{87}Sr/^{86}Sr_m$	0.81884	0.71446	0.75906	0.75906	
$^{143}Nd/^{144}Nd_m$		0.511412	0.511241	0.511241	
$\varepsilon_{Nd}(0)$		-23.9	-27.3	-27.3	
T_{CHUR}		2.68	3.04	3.04	
T_{DM}		2.72	2.99	2.99	
$f_{Sm/Nd}$	-0.35		-0.35	-0.35	

Table 3.2 continued..					
	CGB07-09 Khardeola SH	CGB07-10 Khardeola SH	CGB07-02 Sawa Grit	CGB07-15 Sawa SST	CGB07-16 Sawa SST
SiO_2	56.39	55.90	100.15	74.17	86.95
TiO_2	0.69	0.69	0.08	0.66	0.01
Al_2O_3	23.34	22.98	0.28	8.13	0.00
Fe_2O_3	5.66	5.62	0.38	3.50	0.20
MnO	0.02	0.02	0.00	0.01	0.01
MgO	1.54	1.53	0.04	0.00	0.07
CaO	0.15	0.15	0.00	0.21	0.08
Na_2O	0.29	0.30	0.00	0.00	0.17
K_2O	6.12	6.09	0.11	1.32	0.00
P_2O_5	0.08	0.08	0.02	0.00	0.00
LOI	2.92	3.18	0.86	1.48	0.53
TOTAL	97.19	96.52	101.92	89.47	88.02
Rb	263.60	302.50		35.57	6.87
Sr	43.64	40.19		0.99	Bdl
Ba	580.30	416.80		62.25	13.92
Y	35.93	26.49		16.68	0.62
Zr	121.30	106.90		195.00	12.86
Hf	3.63	3.31		5.49	0.44
Nb	14.08	12.84		5.29	0.06
Ta	1.27	1.11		0.31	0.01
Th	26.19	24.63		14.56	1.97
U	4.73	3.72		1.98	0.69
La	47.56	60.25		12.13	2.54
Ce	90.09	105.30		22.73	4.20
Pr	9.82	12.49		2.20	Bdl
Nd	38.85	47.17		11.70	1.68
Sm	7.37	8.57		2.56	0.21
Eu	1.40	1.62		0.62	0.03
Gd	7.26	7.37		3.21	0.13
Tb	1.07	0.95		0.49	0.02
Dy	6.46	5.06		2.83	0.05
Ho	1.28	0.96		0.54	0.02
Er	3.53	2.61		1.49	0.05
Tm	0.51	0.36		0.21	0.01
Yb	3.53	2.67		1.55	0.10
Lu	0.48	0.36		0.22	0.02
Sc	14.50	15.85		0.92	bdl
V	69.33	77.45		14.73	bdl
Cr	90.42	100.10		8.76	bdl
Co	15.62	6.41		0.02	bdl
Ni	27.43	24.94		2.34	bdl
Pb	14.81	8.16		11.62	10.84
Cs					
$^{87}Sr/^{86}Sr_m$	1.07899	0.99102		0.88497	0.82709
$^{143}Nd/^{144}Nd_m$	0.511314	0.51143		0.511439	0.511481
$\varepsilon_{Nd}(0)$	-25.8	-23.6		-23.4	-22.6
T_{CHUR}	2.43	2.14		2.80	1.44
T_{DM}	2.53	2.31		2.81	1.68
$f_{Sm/Nd}$	-0.42	-0.44		-0.33	-0.62

Table 3.2 continued..					
	CHITTOR-09-21 Sawa (Palri) SH	*CGB07-17 Binota Shale*	*CHITTOR-09-19 Binota Shale*	*CGB07-23 NimbaheraSH*	*CGB07-24 Nimbahera SH*
SiO_2	58.45	73.43	61.04	65.46	54.59
TiO_2	0.75	0.51	0.70	0.76	0.98
Al_2O_3	12.41	6.57	13.13	15.05	24.43
Fe_2O_3	3.72	1.28	5.29	3.41	4.73
MnO	0.02	0.02	0.02	0.04	0.02
MgO	0.44	0.80	0.44	0.69	0.91
CaO		0.58	-0.08	0.18	0.21
Na_2O	0.35	0.19	0.30	0.53	0.72
K_2O	3.00	2.46	3.15	2.95	3.92
P_2O_5	0.02	0.37	0.01	0.03	0.03
LOI	3.83	2.81	3.89	3.21	4.57
TOTAL	82.99	89.02	87.90	92.29	95.09
Rb	185.45	113.75		167.05	
Sr	165.50	187.10		61.14	
Ba	378.00	351.90		438.80	
Y	26.56	26.77		20.15	
Zr	192.20	101.50		151.00	
Hf	5.12	3.21		4.69	
Nb	5.20	7.85		14.94	
Ta	0.37	0.60		1.14	
Th	19.54	11.31		21.00	
U	3.46	6.77		3.32	
La	55.80	14.56		47.14	
Ce	120.40	28.80		106.30	
Pr	12.82	4.14		10.00	
Nd	46.59	22.81		37.06	
Sm	9.79	5.54		6.43	
Eu	1.48	1.13		1.13	
Gd	7.25	4.96		5.24	
Tb	0.85	0.71		0.72	
Dy	5.16	4.33		4.06	
Ho	0.96	0.93		0.81	
Er	3.15	2.85		2.36	
Tm	0.44	0.46		0.36	
Yb	3.19	3.59		2.70	
Lu	0.48	0.53		0.38	
Sc	15.23	8.30		10.72	
V	109.30	373.70		73.84	
Cr	54.75	41.86		52.35	
Co	8.69	4.29		4.91	
Ni	17.67	47.37		3.89	
Pb	17.83	22.73		19.61	
Cs	8.52				
$^{87}Sr/^{86}Sr_m$	0.82945	0.74781		0.82574	
$^{143}Nd/^{144}Nd_m$	0.51169	0.511975		0.511645	
ε_{Nd} (0)	-18.5	-12.9		-19.4	
T_{CHUR}	2.07	2.02		1.65	
T_{DM}	2.28	2.30		1.91	
$f_{Sm/Nd}$	-0.35	-0.25		-0.47	

Table 3.2 continued..				
	CGB07-18 Nimbahera LST	*CGB07-19 Suket SH*	*CGB07-22A Suket SH*	*CGB07-22B Suket SH*
SiO_2	23.41	65.13	64.44	73.15
TiO_2	0.13	0.70	0.62	0.62
Al_2O_3	0.00	6.59	9.66	7.02
Fe_2O_3	0.95	7.52	6.17	3.68
MnO	0.03	0.02	0.00	0.00
MgO	0.63	1.18	0.75	0.56
CaO	56.29	0.21	0.07	0.04
Na_2O	0.08	0.20	0.00	0.00
K_2O	0.76	1.32	1.50	1.22
P_2O_5	0.34	0.03	0.02	0.03
LOI		3.03	2.60	1.95
TOTAL	82.61	85.91	85.82	88.28
Rb	6.61	68.47		
Sr	239.90	16.90		
Ba	39.78	203.20		
Y	16.46	14.68		
Zr	bdl	154.70		
Hf	0.06	4.83		
Nb	bdl	6.38		
Ta	bdl	0.56		
Th	5.10	13.77		
U	0.28	2.41		
La	16.85	19.03		
Ce	29.68	36.99		
Pr	2.72	3.64		
Nd	14.87	16.63		
Sm	2.84	3.19		
Eu	0.56	0.63		
Gd	2.96	3.18		
Tb	0.43	0.49		
Dy	2.67	2.94		
Ho	0.54	0.58		
Er	1.48	1.64		
Tm	0.21	0.25		
Yb	1.44	1.93		
Lu	0.19	0.27		
Sc	0.83	4.50		
V	bdl	33.91		
Cr	bdl	18.92		
Co	3.02	5.69		
Ni	5.96	20.49		
Pb	29.28	14.07		
Cs				
$^{87}Sr/^{86}Sr_m$	0.71033	0.81791	0.82299	0.81018
$^{143}Nd/^{144}Nd_m$	0.511881	0.511795	0.510894	0.51176
ε_{Nd} (0)	-14.8	-16.4	-34.0	-17.1
T_{CHUR}	1.42	1.59	3.27	0.98
T_{DM}	1.76	1.89	3.17	1.28
$f_{Sm/Nd}$	-0.41	-0.41	-0.41	-0.69

Table 3.3: Geochemical data for samples from the Kaimur Group.

	CGB07-20 *Kaimur SST*	*CGB07-21* *Kaimur SST*
SiO_2	97.47	95.43
TiO_2	0.02	0.10
Al_2O_3		
Fe_2O_3	0.14	0.44
MnO	0.01	
MgO	0.03	0.03
CaO	0.10	
Na_2O	0.16	
K_2O		
P_2O_5	0.01	0.02
LOI	0.29	0.29
TOTAL	98.24	96.31
Rb		2.19
Sr		5.76
Ba		12.45
Y		1.68
Zr		24.23
Hf		0.40
Nb		0.17
Ta		0.01
Th		0.97
U		0.18
La		10.58
Ce		25.48
Pr		0.58
Nd		7.54
Sm		0.76
Eu		0.11
Gd		0.50
Tb		0.05
Dy		0.16
Ho		0.04
Er		0.12
Tm		0.02
Yb		0.15
Lu		0.02
Sc		bdl
V		bdl
Cr		bdl
Co		bdl
Ni		bdl
Pb		1.58
Cs		
$^{87}Sr/^{86}Sr_m$		0.72875
$^{143}Nd/^{144}Nd_m$		0.511703
$\varepsilon_{Nd}(0)$		-18.2
T_{CHUR}		1.05
T_{DM}		1.33
$f_{Sm/Nd}$		-0.69

SST: Sandstone

Table 3.4: Geochemical data for samples from various formations of the Rewa Group.

	CHITTO-09-02 Panna SH	CHITTOR-09-16 Panna SH	CHITTOR-09-17 Panna SH	CHITTOR-09-18 Panna SH	CHITTOR-09-11 Panna SH
SiO_2	42.56	59.14	55.28	62.57	61.16
TiO_2	0.66	0.59	0.92	0.68	1.01
Al_2O_3	11.54	8.00	12.14	11.20	12.89
Fe_2O_3	8.23	5.25	6.92	3.33	8.31
MnO	0.25	0.02	0.06	0.02	0.07
MgO	1.64	0.55	1.34	0.53	2.62
CaO	29.36				1.96
Na_2O					
K_2O	3.13	2.11	3.14	3.54	3.60
P_2O_5	0.08	0.03	0.12	0.03	0.07
LOI	-	2.54	6.73	6.37	4.75
TOTAL	97.45	78.25	86.64	88.26	96.43
Rb	154.85		318.17		
Sr	203.90		427.37		
Ba	496.30		1245.06		
Y	25.10		60.61		
Zr	83.61		655.68		
Hf	2.61		6.11		
Nb	6.24		22.55		
Ta	0.51		0.83		
Th	13.62		18.03		
U	2.00		3.07		
La	29.81		106.88		
Ce	60.56		216.63		
Pr	8.31		8.21		
Nd	31.71		29.51		
Sm	7.19		6.27		
Eu	1.36		1.01		
Gd	6.59		5.01		
Tb	0.86		0.64		
Dy	5.31		4.07		
Ho	0.95		0.76		
Er	2.89		2.44		
Tm	0.39		0.34		
Yb	2.69		2.49		
Lu	0.40		0.38		
Sc	12.33		39.05		
V	65.16		217.62		
Cr	40.79		162.87		
Co	13.89		189.47		
Ni	26.47		269.33		
Pb	7.39		59.62		
Cs	15.55		9.75		
$^{87}Sr/^{86}Sr_m$	0.78567		0.89992		
$^{143}Nd/^{144}Nd_m$	0.511859		0.511765		
$\varepsilon_{Nd}(0)$	-15.2		-17.0		
T_{CHUR}	1.99		1.95		
T_{DM}	2.25		2.19		
$f_{Sm/Nd}$	-0.30		-0.35		

SST: Shale; SST: Sandstone and LST: Limestone

Table 3.4 continued..					
	CHITTOR-09-15 Panna SH	*BUNDI-09-08 Indergarh SST*	*CHITTOR-09-03 Indergarh SST*	*CHITTOR-09-05 Jhiri/Panna SH*	*CHITTOR-09-06 Jhiri SH*
SiO_2	62.77	75.44	73.27	61.61	64.70
TiO_2	0.72	0.08		0.99	0.77
Al_2O_3	9.09	2.00	1.08	13.13	10.55
Fe_2O_3	3.30		4.95	5.68	3.52
MnO	0.04	0.02	0.16	0.02	0.03
MgO	0.53			1.65	1.31
CaO				0.11	1.82
Na_2O					0.20
K_2O	2.77	0.56	0.12	5.70	4.42
P_2O_5	0.02		0.03	0.03	0.05
LOI	2.63	0.40	1.15	4.07	3.50
TOTAL	81.88	78.51	80.74	92.99	90.88
Rb	132.80	14.00	2.77		176.20
Sr	153.70	125.00	128.20		166.90
Ba	290.30	27.14	76.64		368.50
Y	17.62	2.46	1.99		20.46
Zr	206.30	58.72	14.86		234.80
Hf	6.23	1.72	0.43		6.74
Nb	9.76	0.25	0.13		7.87
Ta	0.75	0.01	0.02		0.62
Th	17.19	2.48	1.27		17.02
U	2.93	0.66	0.40		2.98
La	39.04	9.02	12.05		33.08
Ce	97.76	21.87	27.41		67.32
Pr	10.41	2.42	3.51		8.03
Nd	38.42	8.77	13.47		29.15
Sm	8.06	1.98	2.91		6.22
Eu	1.15	0.29	0.47		1.01
Gd	5.61	1.15	1.92		5.11
Tb	0.66	0.11	0.14		0.66
Dy	4.06	0.73	0.67		4.26
Ho	0.75	0.14	0.10		0.80
Er	2.47	0.44	0.27		2.55
Tm	0.35	0.07	0.03		0.35
Yb	2.56	0.50	0.23		2.54
Lu	0.39	0.08	0.04		0.39
Sc	8.90	0.34	0.70		11.59
V	61.10	6.08	4.15		66.32
Cr	36.19	0.00	0.00		38.06
Co	12.24	0.00	0.32		14.54
Ni	16.65	0.00	0.00		21.29
Pb	27.27	1.01	1.31		16.16
Cs	8.47	0.32	0.17		8.16
$^{87}Sr/^{86}Sr_m$	0.81198	0.75932	0.71890		0.84885
$^{143}Nd/^{144}Nd_m$	0.511727		0.511888		0.511755
$\varepsilon_{Nd}(0)$	-17.8		-14.6		-17.2
T_{CHUR}	1.98		1.72		1.98
T_{DM}	2.21		2.04		2.22
$f_{Sm/Nd}$	-0.36		-0.34		-0.34

Table 3.4 continued..				
	BUNDI-09-12 Jhiri SH	BUNI-09-11 Taragarh SST	LAK07-16 Taragarh SST	BUNDI-09-14 Taragarh SST
SiO_2	63.73	97.37	93.2	93.02
TiO_2	0.88	0.41	0.21	0.00
Al_2O_3	14.15	1.68	3.89	1.32
Fe_2O_3	7.34		0.17	
MnO	0.02	0.02	0.01	0.02
MgO	1.47	0.00		
CaO	0.31			
Na_2O				
K_2O	3.33	0.29	0.11	0.09
P_2O_5	0.08	0.01	0.03	
LOI	3.54	0.72	1.07	0.20
TOTAL	94.84	100.50	98.68	94.65
Rb	413.85	16.25	4.78	2.59
Sr	581.85	144.70	147.30	133.60
Ba	830.31	18.58	176.50	54.42
Y	70.56	12.33	5.18	2.38
Zr	558.28	276.50	89.71	16.55
Hf	5.80	9.01	2.68	0.53
Nb	25.26	2.00	1.25	0.19
Ta	1.02	0.04	0.08	0.02
Th	21.51	11.58	5.72	1.28
U	3.10	2.22	1.27	0.33
La	125.70	18.38	7.42	4.08
Ce	258.47	38.95	15.98	9.42
Pr	11.38	5.53	1.91	1.50
Nd	41.25	20.52	7.03	5.98
Sm	8.90	4.49	1.76	1.37
Eu	1.42	0.69	0.43	0.23
Gd	7.33	3.67	1.66	1.00
Tb	0.92	0.44	0.18	0.11
Dy	5.68	2.72	1.24	0.68
Ho	1.03	0.51	0.23	0.12
Er	3.25	1.66	0.78	0.34
Tm	0.45	0.23	0.12	0.04
Yb	3.16	1.68	0.90	0.29
Lu	0.47	0.26	0.15	0.05
Sc	40.07	0.07	1.00	0.00
V	263.82	0.74	18.30	0.00
Cr	187.47	3.80	1.35	0.00
Co	43.26	0.00	0.00	0.00
Ni	87.30	0.00	0.91	0.00
Pb	11.60	2.46	1.49	4.03
Cs	16.27	0.54	0.23	0.13
$^{87}Sr/^{86}Sr_m$	0.78285		0.74155	1.05282
$^{143}Nd/^{144}Nd_m$	0.511733		0.511841	0.511879
$\varepsilon_{Nd}(0)$	-17.7		-15.5	-14.8
T_{CHUR}	2.08		1.26	1.11
T_{DM}	2.29		1.60	1.45
$f_{Sm/Nd}$	-0.56		-0.49	-0.53

Table 3.5: Geochemical data for samples from various formations of the Bhander Group.

	GANDOLI-1 Lakheri LST	*CHITTOR-09-07 Ganurgarh SH*	*BUNDI-09-10 Ganurgarh SH*	*LAK07-01 Ganurgarh SH*	*GANDOLI-3 Lakheri LST*	*GANDOLI-2 Lakheri LST*
SiO_2	34.85	58.43	68.90	79.75	32.67	31.66
TiO_2	0.36	1.37	0.93	0.65	0.38	0.30
Al_2O_3	5.47	15.43	16.39	9.11	5.48	4.53
Fe_2O_3	3.61	9.58	4.15	3.59	4.95	3.69
MnO	0.41	0.02	0.03	0.07	0.38	0.45
MgO	0.88	2.89	1.66	1.00	0.83	0.82
CaO	42.01	0.14		0.39	38.78	47.21
Na_2O			0.12	0.15		
K_2O	1.40	5.00	3.15	1.40	1.49	1.12
P_2O_5	0.05	0.12	0.02	0.02	0.07	0.06
LOI		5.16	4.37	3.77		
TOTAL	89.04	98.14	99.71	99.90	85.02	89.84
Rb	11.29	221.05	194.90	80.55		
Sr	798.40	172.20	193.50	168.30		
Ba	6720.00	361.00	346.50	501.90		
Y	129.90	27.08	18.64	16.49		
Zr	0.10	186.50	181.50	177.00		
Hf	0.03	5.09	5.54	5.34		
Nb	0.00	15.45	12.61	4.96		
Ta	0.00	1.07	1.01	0.38		
Th	27.21	17.73	22.89	15.87		
U	0.71	3.36	4.52	3.79		
La	42.83	25.75	48.71	26.95		
Ce	97.40	54.64	95.31	59.53		
Pr	10.40	7.31	11.53	7.25		
Nd	48.72	30.12	39.01	26.01		
Sm	13.82	7.40	7.38	5.43		
Eu	3.48	1.50	0.92	0.82		
Gd	15.28	6.80	4.77	4.31		
Tb	2.13	0.89	0.58	0.57		
Dy	13.19	5.72	4.03	3.76		
Ho	2.33	1.04	0.81	0.69		
Er	6.82	3.26	2.76	2.25		
Tm	0.86	0.44	0.40	0.32		
Yb	5.97	3.05	2.95	2.31		
Lu	0.86	0.45	0.45	0.35		
Sc	28.39	20.41	14.51	6.46		
V	12.75	130.40	93.02	63.44		
Cr	19.53	67.65	68.03	28.64		
Co	33.81	14.18	11.98	14.22		
Ni	82.88	30.00	34.65	17.54		
Pb	15.25	9.66	16.97	34.67		
Cs	0.52	12.83	11.57	3.81		
$^{87}Sr/^{86}Sr_m$		0.86238	0.79315	0.76140		
$^{143}Nd/^{144}Nd_m$		0.51175	0.51161	0.511762		
$\varepsilon_{Nd}(0)$		-17.3	-20.1	-17.1		
T_{CHUR}		2.80	1.30	1.19		
T_{DM}		2.81	1.57	1.49		
$f_{Sm/Nd}$		-0.24	-0.61	-0.57		

SST: Sandstone; SH: Shale and LST: Limestone

Table 3.5 continued..

	GANDOLI-12 Lakheri LST	*GANDOLI-11 Lakheri LST*	*GANDOLI-7 Lakheri LST*	*GANDOLI-5 Lakheri LST*		*GANDOLI-4 Lakheri LST*
SiO_2	22.97	24.09	23.41	31.73		34.11
TiO_2	0.06	0.07	0.11	0.27		0.33
Al_2O_3	1.72	1.94	2.19	4.38		5.28
Fe_2O_3	1.13	1.52	1.79	2.92		3.71
MnO	0.12	0.14	0.32	0.47		0.41
MgO	0.46	0.62	0.62	0.75		0.85
CaO	67.33	70.66	63.22	47.43		43.64
Na_2O						
K_2O	0.36	0.36	0.41	1.10		1.33
P_2O_5	0.12	0.12	0.07	0.05		0.05
LOI				-		
TOTAL	94.27	99.52	92.15	89.08		89.69
				Sil.	Carb.	
Rb				25.28	1.12	
Sr				14.69	19.36	
Ba				587.50	65.59	
Y				1.24	2.14	
Zr				6.54	0.33	
Hf				0.67	0.03	
Nb				1.57		
Ta				0.18	0.00	
Th				2.26	1.31	
U				0.60	0.08	
La				2.35	0.83	
Ce				3.64	1.46	
Pr				1.72	0.94	
Nd				5.65	4.43	
Sm				1.06	1.23	
Eu				0.25	0.28	
Gd				0.91	1.39	
Tb				0.11	0.19	
Dy				0.75	1.21	
Ho				0.15	0.22	
Er				0.52	0.65	
Tm				0.08	0.08	
Yb				0.55	0.59	
Lu				0.09	0.09	
Sc				0.52	0.57	
V				3.40		
Cr				2.25		
Co				1.03	0.48	
Ni				2.86	1.25	
Pb				1.60	1.40	
Cs				1.42	0.11	
$^{87}Sr/^{86}Sr_m$				0.78300		
$^{143}Nd/^{144}Nd_m$				0.51160		
$\varepsilon_{Nd}(0)$				-20.2		
T_{CHUR}				1.30		
T_{DM}				1.57		
$f_{Sm/Nd}$				-0.62		

Table 3.5 continued..						
	SATUR-12 Lakheri LST		*GANDOLI-13 Lakheri LST*	*BUNDI-09-09 Samaria SH*	*BUND-09I-13 Samaria SH*	*CHITTOR-09-13 Samaria SH*
SiO_2	10.00		24.12	72.00	63.66	52.95
TiO_2	0.12		0.07	0.24	0.79	0.88
Al_2O_3	2.39		1.63	7.64	12.52	16.59
Fe_2O_3	1.21		0.65	1.57	4.17	4.96
MnO	0.06		0.11	0.02	0.07	0.02
MgO	0.52		0.45	1.17	1.38	1.38
CaO	69.57		70.24		0.18	0.02
Na_2O						
K_2O	0.69		0.33	1.65	4.12	6.04
P_2O_5	0.07		0.04	0.01	0.06	0.05
LOI	-			1.87	11.24	5.68
TOTAL	84.62		97.64	86.15	98.19	88.58
	Sil.	Carb.				
Rb	9.06	1.25				522.40
Sr	11.02	16.31				180.80
Ba	5.20	2.19				494.00
Y	0.19	0.31				37.79
Zr	1.96	0.23				140.00
Hf	0.20	0.02				3.96
Nb	0.45					13.10
Ta	0.05	0.00				1.05
Th	0.27	0.46				29.20
U	0.25	0.09				7.57
La	0.16	0.38				68.66
Ce	0.32	0.82				135.50
Pr	0.12	0.36				15.51
Nd	0.41	1.33				56.31
Sm	0.09	0.29				11.92
Eu	0.02	0.04				1.64
Gd	0.08	0.25				9.06
Tb	0.01	0.03				1.09
Dy	0.11	0.21				7.04
Ho	0.03	0.04				1.33
Er	0.09	0.12				4.30
Tm	0.01	0.02				0.59
Yb	0.10	0.10				4.05
Lu	0.02	0.02				0.60
Sc	0.10	0.07				25.34
V	0.98					158.80
Cr	0.67					108.30
Co	0.01	0.06				3.67
Ni	0.13	0.34				40.16
Pb	0.42	0.50				7.36
Cs	0.51	0.13				26.07
$^{87}Sr/^{86}Sr_m$	0.73810					0.96337
$^{143}Nd/^{144}Nd_m$	0.511777					0.511843
$\varepsilon_{Nd}(0)$	-16.8					-15.5
T_{CHUR}	1.25					1.76
T_{DM}	1.56					2.05
$f_{Sm/Nd}$	-0.53					-0.35

Table 3.5 continued..					
	SATUR07-22 Samaria-LST	*SATUR07-01 Samaria SH*	*SATUR07-21 Samaria SH*	*BUNDI-09-01 Samaria SH*	*BUNDI-09-02 Samaria SH*
SiO_2	17.21	64.57	55.02	38.61	55.37
TiO_2	0.02	0.92	0.76	0.44	0.74
Al_2O_3	1.49	15.35	11.89	7.36	15.66
Fe_2O_3	4.76	4.93	5.98	7.37	7.22
MnO	0.11	0.02	0.05	0.27	0.05
MgO	18.62	2.30	2.36	1.31	1.41
CaO	45.66	0.38	16.79	36.43	4.02
Na_2O					
K_2O	0.42	5.18	3.55	1.41	4.14
P_2O_5	0.01	0.16	0.15	0.09	0.04
LOI	-	4.47	3.41	24.85	9.80
TOTAL	88.3	98.27	99.95	118.14	98.45
Rb		272.20			260.40
Sr		137.50			195.40
Ba		387.60			1320.00
Y		29.15			24.37
Zr		160.20			104.20
Hf		4.31			3.24
Nb		17.15			11.07
Ta		1.24			0.88
Th		21.72			26.61
U		3.03			1.80
La		50.15			51.93
Ce		98.34			103.90
Pr		12.31			12.25
Nd		45.89			43.42
Sm		10.11			8.70
Eu		1.60			1.28
Gd		8.19			6.31
Tb		1.01			0.77
Dy		6.08			5.02
Ho		1.07			0.94
Er		3.36			3.06
Tm		0.45			0.43
Yb		3.13			3.04
Lu		0.45			0.45
Sc		18.09			16.01
V		94.87			63.42
Cr		76.25			49.94
Co		10.80			14.60
Ni		41.80			29.53
Pb		6.61			12.88
Cs		12.15			15.72
$^{87}Sr/^{86}Sr_m$		1.02725			0.82376
$^{143}Nd/^{144}Nd_m$		0.511829			0.511734
$\varepsilon_{Nd}(0)$		-15.8			-17.6
T_{CHUR}		1.14			1.82
T_{DM}		1.47			2.08
$f_{Sm/Nd}$		-0.55			-0.38

Table 3.5 continued...

	Satur-23 Bundi Hill SST	LAK07-14 Black SH	CHITOR-09-11 Black SH	CHITTOR-09-12 Black SH	CHITTOR-09-9 Black SH	CHITTOR-09-8 Black SH
SiO_2	95.37	65.19	61.16	65.15	59.92	44.81
TiO_2	0.26	0.92	1.01	0.55	1.22	0.63
Al_2O_3	1.93	15.98	12.89	12.00	16.88	9.83
Fe_2O_3	0.53	3.59	8.31	3.70	8.65	5.10
MnO	0.02	0.03	0.07	0.03	0.03	0.14
MgO		1.56	2.62	0.98	2.99	8.26
CaO	0.02		1.96	0.02	0.22	15.92
Na_2O		0.32				
K_2O	0.16	3.35	3.60	3.70	4.95	2.86
P_2O_5	0.07	0.01	0.07	0.02	0.07	0.04
LOI	1.13	8.20	4.75	4.04	4.79	-
TOTAL	99.49	99.15	96.43	90.19	99.71	87.58
Rb	6.54			213.60	212.05	
Sr	79.59			182.40	112.10	
Ba	193.20			329.30	328.90	
Y	10.09			22.57	25.96	
Zr	207.50			125.60	163.00	
Hf	6.16			3.71	4.67	
Nb	3.78			6.94	15.72	
Ta	0.28			0.61	1.19	
Th	6.34			17.05	20.99	
U	1.91			3.36	3.33	
La	12.39			33.81	29.42	
Ce	28.43			68.48	73.23	
Pr	3.96			8.27	9.46	
Nd	15.28			29.94	36.34	
Sm	3.22			6.35	7.93	
Eu	0.55			1.07	1.33	
Gd	2.55			5.12	6.63	
Tb	0.33			0.66	0.87	
Dy	2.19			4.39	5.61	
Ho	0.41			0.84	1.04	
Er	1.34			2.75	3.32	
Tm	0.19			0.38	0.46	
Yb	1.43			2.66	3.20	
Lu	0.22			0.40	0.47	
Sc	2.76			13.34	19.98	
V	7.92			78.58	127.60	
Cr	8.96			49.22	79.91	
Co	0.11			10.32	20.18	
Ni	0.43			32.84	29.54	
Pb	1.73			32.71	10.25	
Cs	0.20			13.35	14.25	
$^{87}Sr/^{86}Sr_m$	0.75253			0.86776	1.07818	
$^{143}Nd/^{144}Nd_m$	0.511891			0.511723	0.511798	
$\varepsilon_{Nd}(0)$	-14.6			-17.8	-16.4	
T_{CHUR}	1.02			2.03	1.97	
T_{DM}	1.36			2.25	2.22	
$f_{Sm/Nd}$	-0.57			-0.35	-0.33	

Table 3.5 continued..						
	LAK07-09 Black SH	*LAK07-02 Black SH (Sirbu-SH)*	*LAK07-10 Black SH*	*LAK07-11 Black SH*	*LAK07-12 Grey SH*	*LAK07-13 Black SH*
SiO_2	62.42	65.62	65.04	73.83	74.61	69.07
TiO_2	0.96	0.92	0.85	0.86	0.87	0.92
Al_2O_3	17.3	15.9	16.06	13.25	14.25	15.89
Fe_2O_3	3.84	4.13	4.46	3.00	3.46	4.49
MnO	0.03	0.03	0.03	0.07	0.03	0.04
MgO	1.63	1.70	1.72	1.61	1.53	1.72
CaO				0.51		
Na_2O	0.09	0.50	0.13	0.93	0.53	0.75
K_2O	3.79	3.25	3.53	2.31	2.78	2.89
P_2O_5	0.02	0.03	0.02	0.01	0.01	0.03
LOI	8.28	10.2	6.52	4.72	3.30	5.00
TOTAL	98.35	102.32	98.36	101.10	101.37	100.79
Rb		214.25				
Sr		177.50				
Ba		360.90				
Y		31.14				
Zr		165.40				
Hf		5.22				
Nb		14.40				
Ta		1.14				
Th		22.61				
U		4.97				
La		49.75				
Ce		105.30				
Pr		14.48				
Nd		55.10				
Sm		11.50				
Eu		1.56				
Gd		8.00				
Tb		1.07				
Dy		7.01				
Ho		1.31				
Er		4.13				
Tm		0.55				
Yb		3.74				
Lu		0.54				
Sc		16.21				
V		100.00				
Cr		75.04				
Co		11.48				
Ni		29.79				
Pb		23.31				
Cs		16.65				
$^{87}Sr/^{86}Sr_m$		0.80083				
$^{143}Nd/^{144}Nd_m$		0.511725				
$\varepsilon_{Nd}(0)$		-17.8				
T_{CHUR}		1.23				
T_{DM}		1.53				
$f_{Sm/Nd}$		-0.57				

Table 3.5 continued...

	BUNDI-09-05 Shikaoda SST	*BUNDI-09-3 Balwan LST*		*BUNDI-9-04 Balwan LST*	*BUNDI-09-06 Dholpur SH*	*BUNDI-09-07 Dholpur SH*
SiO_2	98.06	11.86		7.40	81.21	70.32
TiO_2	0.01	0.12			0.41	0.87
Al_2O_3	1.51	2.77		1.11	6.20	14.1
Fe_2O_3	0.16	1.90		1.65	3.47	3.39
MnO	0.02	0.25		0.15	0.28	0.02
MgO		0.57		12.9	0.91	1.34
CaO		74.73		50.0	1.69	0.00
Na_2O						
K_2O	0.22	0.55		0.08	1.06	3.12
P_2O_5	0.00	0.01			0.03	0.02
LOI	0.35				3.52	3.47
TOTAL	100.32	92.75		73.32	98.78	96.66
		Sil.	Carb.			
Rb	7.35	8.66	0.97	2.19	54.23	176.20
Sr	97.61	10.52	11.52	99.19	162.90	184.00
Ba	13.43	6.72	20.84	53.32	521.40	252.10
Y	4.04	0.14	0.58	0.00	16.73	22.94
Zr	38.00	0.34	0.06	0.00	181.60	192.40
Hf	1.09	0.05	0.01	0.00	5.31	5.86
Nb	0.70	0.30		0.03	5.07	11.51
Ta	0.06	0.04		0.01	0.52	0.91
Th	3.24	0.09	0.28	0.00	10.82	20.34
U	0.76	0.20	0.03	3.96	2.53	3.55
La	10.01	0.29	0.38	0.44	18.22	40.20
Ce	23.28	0.32	0.57	0.00	41.27	81.60
Pr	2.50	0.26	0.43	0.17	5.11	9.99
Nd	9.11	1.05	1.91	0.70	19.60	35.39
Sm	1.94	0.23	0.45	0.14	4.76	7.18
Eu	0.26	0.04	0.09	0.02	0.94	1.08
Gd	1.29	0.20	0.46	0.08	4.86	5.48
Tb	0.13	0.02	0.06	0.00	0.68	0.73
Dy	0.82	0.18	0.37	0.03	4.21	4.86
Ho	0.15	0.04	0.07	0.01	0.72	0.92
Er	0.48	0.12	0.19	0.01	2.15	3.00
Tm	0.07	0.02	0.02	0.00	0.29	0.42
Yb	0.47	0.10	0.14	0.00	2.04	2.98
Lu	0.07	0.02	0.02	0.00	0.30	0.45
Sc	0.12	0.01	0.03	0.00	5.83	12.30
V	7.67	1.29		6.85	26.02	76.40
Cr	2.61	0.86		0.17	21.22	58.64
Co	0.03	0.14	0.11	17.53	15.24	7.44
Ni	0.00	0.68	0.61	2.34	14.62	30.25
Pb	1.55	1.56	1.49	27.58	14.93	12.53
Cs	0.26	0.71	0.07	0.12	5.83	11.48
$^{87}Sr/^{86}Sr_m$	0.72537	0.86464		0.70818	0.80527	0.77186
$^{143}Nd/^{144}Nd_m$	0.511773	0.511642			0.511683	0.511908
$\varepsilon_{Nd}(0)$	-16.9	-19.4			-18.6	-14.2
T_{CHUR}	1.19	1.49			1.27	1.12
T_{DM}	1.50	1.77			1.55	1.48
$f_{Sm/Nd}$	-0.56	-0.52			-0.58	-0.50

Table 3.6: U-Pb Analytical data for detrital zircons from the Sawa Sandstone, Bojunda, and Chittorgarh.

Labels-Spot	U (ppm)	Th (ppm)	Th/U	± Th/U	Pb* (ppm)	204Pb (ppb)	204Pb/ 206Pb	± ^{204}Pb/ 206Pb	f (206)^{204}	208Pb*/ 206Pb*	±^{208}Pb*/ 206Pb*	207Pb*/ 235U	±^{207}Pb*/ 235U	206Pb*/ 238U	±^{206}Pb*/ 238U	Corr. Coeff.	207Pb*/ 206Pb*	±^{207}Pb*/ 206Pb*	Apparent Age 207Pb/ 206Pb	Apparent Age ±^{207}Pb/ 206Pb	% DISC
Bojunda05-01	(N 24° 50.431'; E74° 35.526')																				
9017-24.1	81.66	53.6	0.678	0.015	30	3	1.13E-04	3.18E-05	1.97E-03	0.195	3.07E-03	5.172	0.112	0.330	6.54E-03	0.951	0.114	7.70E-04	1860.3	12.3	1.3
9017-1.1	111.03	101.79	0.947	0.020	66	1	3.04E-05	1.82E-05	5.30E-04	0.264	3.48E-03	11.354	0.226	0.485	8.73E-03	0.944	0.170	1.12E-03	2557.0	11.11	0.4
9017-2.1	103.15	102.95	1.031	0.021	62	1	1.55E-05	2.05E-05	2.70E-04	0.302	3.98E-03	11.099	0.243	0.472	9.17E-03	0.934	0.171	1.34E-03	2563.5	13.2	2.8
9017-9.1	135.12	236.98	1.812	0.037	91	10	1.88E-04	5.69E-05	3.25E-03	0.519	3.75E-03	10.885	0.227	0.465	8.67E-03	0.937	0.170	1.25E-03	2555.5	12.39	3.7
9017-10.1	249.52	195.04	0.808	0.016	135	18	1.89E-04	2.26E-05	3.27E-03	0.213	2.33E-03	10.693	0.193	0.456	7.86E-03	0.982	0.170	5.90E-04	2559.2	5.83	5.4
9017-12.1	149.92	226.84	1.563	0.032	93	5	9.38E-05	1.87E-05	1.63E-03	0.431	4.92E-03	10.459	0.195	0.450	7.93E-03	0.975	0.169	7.10E-04	2544.3	7.03	5.9
9017-14.1	229.38	91.13	0.410	0.009	117	4	4.45E-05	1.27E-05	7.70E-04	0.113	9.80E-04	10.813	0.204	0.460	8.32E-03	0.983	0.170	5.90E-04	2562.0	5.84	4.8
9017-33.1	110.78	67.83	0.633	0.013	41	2	5.74E-05	2.67E-05	9.90E-04	0.184	2.58E-03	5.210	0.114	0.328	5.84E-03	0.875	0.115	1.23E-03	1880.2	19.34	2.6
9017-34.1	124.82	103.37	0.856	0.018	72	2	3.77E-05	2.16E-05	6.50E-04	0.237	1.82E-03	11.119	0.209	0.475	8.41E-03	0.973	0.170	7.50E-04	2555.5	7.38	2
9017-36.1	97.63	81.51	0.863	0.020	37	3	9.74E-05	5.28E-05	1.69E-03	0.259	5.58E-03	5.034	0.108	0.324	5.68E-03	0.878	0.113	1.16E-03	1840.8	18.82	1.6
9017-37.1	91.34	58.36	0.660	0.014	34	1	5.15E-05	3.35E-05	8.90E-04	0.192	2.71E-03	5.141	0.108	0.328	6.05E-03	0.925	0.114	9.20E-04	1860.0	14.66	1.7
9017-41.1	126.7	221.48	1.806	0.037	85	44	8.65E-04	5.96E-05	1.50E-02	0.494	3.41E-03	10.939	0.231	0.466	8.91E-03	0.945	0.170	1.19E-03	2558.6	11.74	3.5
9017-43.1	236.46	166.84	0.729	0.015	131	1	1.00E-05	1.00E-05	1.70E-04	0.203	1.25E-03	10.964	0.210	0.469	8.48E-03	0.974	0.170	7.40E-04	2552.8	7.33	2.9
9017-45.1	152.75	108	0.730	0.015	55	6	1.49E-04	2.59E-05	2.59E-03	0.200	1.82E-03	4.982	0.099	0.319	5.75E-03	0.947	0.113	7.30E-04	1850.0	11.71	3.4
9017-48.1	275.1	203.87	0.766	0.020	155	3	2.96E-05	1.08E-05	5.10E-04	0.200	1.23E-03	11.173	0.309	0.479	1.30E-02	0.995	0.169	4.60E-04	2551.0	4.53	1.2
9017-49.1	138.29	65.47	0.489	0.011	57	2	3.48E-05	2.33E-05	6.00E-04	0.138	1.55E-03	6.911	0.132	0.379	6.71E-03	0.960	0.132	7.10E-04	2126.5	9.45	2.5
9017-52.1	93.29	226.79	2.511	0.052	51	3	9.32E-05	3.72E-05	1.61E-03	0.728	4.61E-03	5.866	0.126	0.345	6.07E-03	0.877	0.123	1.29E-03	2004.3	18.65	4.6
9017-53.1	105.15	64.11	0.630	0.013	57	4	8.49E-05	2.54E-05	1.47E-03	0.175	1.81E-03	10.925	0.210	0.472	8.41E-03	0.960	0.168	9.10E-04	2535.2	9.18	1.6
9017-55.1	264.46	78.34	0.306	0.006	149	2	1.78E-05	1.06E-05	3.10E-04	0.086	7.10E-04	13.318	0.235	0.514	8.89E-03	0.993	0.188	4.00E-04	2723.7	3.48	1.8
9017-56.1	127.27	71.83	0.583	0.013	46	2	6.01E-05	2.18E-05	1.04E-03	0.165	1.68E-03	5.147	0.099	0.327	5.82E-03	0.958	0.114	6.40E-04	1865.8	10.09	2.2
9017-58.1	249.39	134.1	0.556	0.012	122	258	2.63E-03	1.06E-04	4.56E-02	0.138	5.06E-03	9.834	0.296	0.438	8.14E-03	0.707	0.163	3.49E-03	2484.8	36.63	5.7
9017-60.1	96.09	60.61	0.652	0.015	35	0	1.00E-05	1.00E-05	1.70E-04	0.194	2.04E-03	5.192	0.106	0.326	6.18E-03	0.963	0.115	6.40E-04	1885.6	10.03	3.4
9017-25.1	136.89	206.63	1.559	0.032	90	0	4.46E-06	1.32E-05	8.00E-05	0.443	5.59E-03	11.095	0.213	0.472	8.57E-03	0.973	0.171	7.60E-04	2563.1	7.45	2.8
9017-62.1	84.76	58.99	0.719	0.015	32	1	2.35E-05	2.89E-05	4.10E-04	0.207	2.89E-03	5.306	0.134	0.334	6.23E-03	0.815	0.115	1.70E-03	1885.6	26.76	1.6
9017-63.1	318.17	153.1	0.497	0.010	127	3	3.40E-05	8.55E-06	5.90E-04	0.139	1.24E-03	6.434	0.123	0.366	6.44E-03	0.956	0.127	7.30E-04	2063.4	10.08	2.5
9017-64.1	105.5	82.8	0.811	0.017	46	13	3.61E-04	8.21E-05	6.26E-03	0.185	4.43E-03	7.223	0.168	0.383	6.82E-03	0.833	0.137	1.78E-03	2185.3	22.84	4.3
9017-66.1	107.96	73.08	0.699	0.015	39	1	4.33E-05	3.22E-05	7.50E-04	0.203	2.48E-03	5.033	0.116	0.323	6.14E-03	0.882	0.113	1.24E-03	1850.9	19.99	2.6
9017-68.1	34.73	18.71	0.557	0.012	12	2	2.46E-04	1.46E-04	4.26E-03	0.150	6.28E-03	4.928	0.163	0.321	6.22E-03	0.679	0.111	2.72E-03	1821.1	45.05	1.4
9017-69.1	156.98	97.5	0.642	0.013	56	1	3.23E-05	2.05E-05	5.60E-04	0.185	2.60E-03	5.039	0.102	0.319	5.76E-03	0.937	0.115	8.20E-04	1874.6	12.98	4.9
9017-75.1	216.22	160.42	0.766	0.016	121	1	1.44E-05	1.69E-05	2.50E-04	0.219	2.52E-03	10.812	0.196	0.468	8.13E-03	0.982	0.167	5.80E-04	2531.8	5.86	2.2
9017-81.1	219.77	99.36	0.467	0.010	115	2	2.37E-05	1.04E-05	4.10E-04	0.128	1.26E-03	10.841	0.195	0.469	8.11E-03	0.985	0.168	5.30E-04	2534.0	5.34	2.1
9017-82.1	127.48	68.01	0.551	0.012	45	1	2.31E-05	3.96E-05	4.00E-04	0.158	3.25E-03	5.057	0.102	0.324	5.82E-03	0.937	0.113	8.00E-04	1849.4	12.84	2.1
9017-84.1	96.48	101.55	1.087	0.024	57	4	1.08E-04	3.03E-05	1.87E-03	0.294	2.46E-03	10.831	0.229	0.467	8.94E-03	0.948	0.168	1.14E-03	2541.2	11.38	2.8

Labels-Spot	U (ppm)	Th (ppm)	Th/U	± Th/U	Pb* (ppm)	204Pb (ppb)	204Pb/ 206Pb	± ^{204}Pb/ 206Pb	f (206)^{204}	208Pb*/ 206Pb*	±^{208}Pb*/ 206Pb*	207Pb*/ 235U	± ^{207}Pb*/ 235U	206Pb*/ 238U	± ^{206}Pb*/ 238U	Corr. Coeff.	207Pb*/ 206Pb*	± ^{207}Pb*/ 206Pb*	Apparent Age 207Pb/ 206Pb	± ^{207}Pb/ 206Pb	% DISC
9017-88.1	215.27	139.49	0.669	0.014	120	1	1.55E-05	2.86E-05	2.70E-04	0.186	1.54E-03	11.090	0.207	0.476	8.46E-03	0.979	0.169	6.50E-04	2546.9	6.45	1.4
9017-89.1	101.97	114.79	1.163	0.024	61	0	1.00E-05	1.00E-05	1.70E-04	0.319	3.60E-03	10.596	0.227	0.465	8.99E-03	0.944	0.165	1.18E-03	2509.3	12.04	1.9
9017-93.1	142.89	61.51	0.445	0.009	61	6	1.24E-04	9.51E-06	2.15E-03	0.123	4.45E-03	7.225	0.166	0.391	7.17E-03	0.860	0.134	1.59E-03	2149.4	20.86	0.9
9017-94.1	143.94	89.96	0.646	0.015	52	3	7.65E-05	3.60E-05	1.33E-03	0.190	2.58E-03	5.027	0.104	0.322	5.87E-03	0.928	0.113	8.80E-04	1850.2	14.06	2.7
9017-99.1	152.08	124.3	0.844	0.017	88	0	7.52E-06	1.90E-05	1.30E-04	0.236	2.94E-03	11.258	0.271	0.478	1.09E-02	0.975	0.171	9.10E-04	2566.6	8.98	1.9
9017-100.1	146.51	43.79	0.309	0.007	50	1	3.55E-05	2.28E-05	6.20E-04	0.089	1.97E-03	5.250	0.101	0.329	5.78E-03	0.956	0.116	6.60E-04	1892.6	10.28	3.2
9017-102.1	103.92	50.74	0.504	0.011	62	2	3.54E-05	2.41E-05	6.10E-04	0.132	2.95E-03	14.095	0.264	0.522	9.26E-03	0.974	0.196	8.40E-04	2791.0	7.04	2.9
9017-103.1	305.08	152.7	0.517	0.011	167	2	1.46E-05	8.25E-06	2.50E-04	0.145	9.00E-04	11.084	0.207	0.484	8.75E-03	0.988	0.166	4.90E-04	2519.6	4.91	-1
9017-109.1	105.36	69.11	0.678	0.015	55	2	4.48E-05	3.68E-05	7.80E-04	0.190	2.77E-03	9.933	0.194	0.453	8.10E-03	0.952	0.159	9.60E-04	2445.8	10.26	1.5
9017-111.1	154.75	83.93	0.560	0.012	82	2	3.23E-05	2.11E-05	5.60E-04	0.156	1.55E-03	10.805	0.204	0.468	8.24E-03	0.966	0.168	8.30E-04	2533.1	8.3	2.3
9017-113.1	95.35	129.46	1.403	0.029	59	4	1.15E-04	3.45E-05	1.99E-03	0.394	5.64E-03	10.328	0.207	0.462	8.57E-03	0.962	0.162	8.90E-04	2479.7	9.26	1.3
Bojunda05-02	**(N 24° 50.431'; E74° 35.526')**																				
9018-2.1	241.66	139.08	0.595	0.012	82	8	1.26E-04	3.12E-05	2.18E-03	0.177	1.72E-03	4.602	0.091	0.307	5.37E-03	0.930	0.109	8.00E-04	1778.3	13.48	3
9018-4.1	74.48	97.33	1.350	0.031	46	4	1.33E-04	4.59E-05	2.30E-03	0.362	4.60E-03	10.760	0.215	0.470	8.24E-03	0.925	0.166	1.27E-03	2518.3	12.96	1.4
9018-3.1	67.46	105.13	1.610	0.036	45	4	1.31E-04	4.22E-05	2.28E-03	0.458	7.62E-03	11.009	0.245	0.471	9.13E-03	0.921	0.169	1.48E-03	2551.2	14.73	2.4
9018-6.1	104.85	63.42	0.625	0.013	32	3	1.11E-04	3.79E-05	1.93E-03	0.179	4.40E-03	3.880	0.088	0.277	5.25E-03	0.892	0.102	1.05E-03	1654.4	19.25	4.8
9018-7.1	72.26	79.95	1.143	0.024	43	2	6.85E-05	2.83E-05	1.19E-03	0.317	4.31E-03	10.931	0.235	0.470	8.65E-03	0.910	0.169	1.51E-03	2545.5	15.12	2.5
9018-8.1	256.53	115.77	0.466	0.010	93	4	4.80E-05	1.34E-05	8.30E-04	0.134	1.19E-03	5.323	0.100	0.336	5.94E-03	0.973	0.115	5.00E-04	1877.0	7.86	0.5
9018-37.1	119.63	77.41	0.669	0.014	40	4	1.23E-04	3.07E-05	2.13E-03	0.190	4.15E-03	4.401	0.092	0.301	5.63E-03	0.942	0.106	7.50E-04	1734.0	13.01	2.2
9018-28.1	215.67	94.79	0.454	0.010	75	1	1.98E-05	2.44E-05	3.40E-04	0.132	1.45E-03	5.148	0.100	0.326	5.72E-03	0.945	0.115	7.30E-04	1874.9	11.56	3.1
9018-33.1	160.19	115.99	0.748	0.016	52	6	1.42E-04	3.39E-05	2.47E-03	0.209	2.27E-03	4.056	0.086	0.288	5.29E-03	0.922	0.102	8.40E-04	1665.6	15.33	2.2
9018-35.1	258.48	122.89	0.491	0.010	79	3	4.12E-05	1.66E-05	7.10E-04	0.140	1.36E-03	4.042	0.075	0.285	4.99E-03	0.969	0.103	4.80E-04	1674.2	8.59	3.3
9018-13.1	147.8	73.09	0.511	0.012	80	1	2.03E-05	2.56E-05	3.50E-04	0.144	2.72E-03	11.218	0.244	0.479	8.69E-03	0.890	0.170	1.70E-03	2555.7	16.83	1.3
9018-12.1	171.27	149.84	0.904	0.019	99	1	1.75E-05	2.49E-05	3.00E-04	0.250	1.77E-03	11.007	0.223	0.473	8.42E-03	0.926	0.169	1.31E-03	2546.8	13.03	2
9018-17.1	160.06	63.39	0.409	0.009	84	1	1.00E-05	1.00E-05	1.70E-04	0.109	1.08E-03	11.336	0.292	0.474	1.08E-02	0.931	0.173	1.64E-03	2590.3	15.89	3.4
9018-22.1	136.11	134.92	1.024	0.022	79	1	2.23E-05	1.71E-05	3.90E-04	0.291	7.93E-03	10.685	0.466	0.462	1.45E-02	0.796	0.168	4.47E-03	2536.8	45.37	3.6
9018-50.1	66.18	102.74	1.604	0.034	26	0	1.00E-05	1.00E-05	1.70E-04	0.454	4.78E-03	4.181	0.100	0.294	5.53E-03	0.855	0.103	1.29E-03	1683.3	23.16	1.4
9018-51.1	63.78	33.7	0.546	0.012	36	2	6.32E-05	3.25E-05	1.10E-03	0.147	2.85E-03	12.473	0.335	0.499	9.71E-03	0.801	0.181	2.93E-03	2665.4	27.06	2.1
9018-48.1	289.42	147.72	0.527	0.011	101	3	4.13E-05	1.30E-05	7.20E-04	0.150	2.44E-03	5.007	0.095	0.322	5.67E-03	0.965	0.113	5.70E-04	1842.2	9.11	2.2
9018-43.1	207.57	138.53	0.689	0.014	68	3	6.00E-05	1.92E-05	1.04E-03	0.194	1.68E-03	4.261	0.095	0.294	5.21E-03	0.859	0.105	1.21E-03	1713.8	21.31	2.9
9018-50.1.2	56.88	87.16	1.583	0.072	23	1	7.49E-05	5.46E-05	1.30E-03	0.473	1.01E-02	4.181	0.103	0.291	5.73E-03	0.866	0.104	1.29E-03	1700.2	22.98	3.1
9018-51.1.2	64.95	34.55	0.550	0.012	37	1	3.04E-05	4.96E-05	5.30E-04	0.150	3.16E-03	12.613	0.276	0.502	1.01E-02	0.958	0.182	1.15E-03	2671.6	10.47	1.8
9018-48.1.2	282.24	145.31	0.532	0.011	97	0	3.09E-06	1.97E-05	5.00E-05	0.155	1.47E-03	4.914	0.100	0.316	6.00E-03	0.967	0.113	5.90E-04	1846.5	9.52	4.2
9018-43.1.2	214.06	143.63	0.693	0.014	71	2	3.12E-05	2.92E-05	5.40E-04	0.204	3.75E-03	4.324	0.096	0.296	5.66E-03	0.911	0.106	9.80E-04	1730.2	17.06	3.4
9018-42.1	162.75	89.82	0.570	0.012	54	2	4.40E-05	2.27E-05	7.60E-04	0.172	2.51E-03	4.426	0.092	0.301	5.78E-03	0.962	0.107	6.00E-04	1742.7	10.43	2.7
9018-39.1	56.53	40.15	0.734	0.017	17	2	1.76E-04	1.41E-04	3.05E-03	0.212	6.32E-03	3.702	0.120	0.270	5.08E-03	0.673	0.100	2.41E-03	1616.0	45.81	4.8

Labels-Spot	U (ppm)	Th (ppm)	Th/U	± Th/U	Pb* (ppm)	204Pb (ppb)	204Pb/ 206Pb	± ^{204}Pb/ 206Pb	f (206)^{204}	208Pb*/ 206Pb*	± ^{208}Pb*/ 206Pb*	207Pb*/ 235U	± ^{207}Pb*/ 235U	206Pb*/ 238U	± ^{206}Pb*/ 238U	Corr. Coeff.	207Pb*/ 206Pb*	± ^{207}Pb*/ 206Pb*	Apparent Age 207Pb/ 206Pb	± ^{207}Pb/ 206Pb	% DISC
9018-38.1	95.63	59.03	0.638	0.014	52	0	7.76E-06	3.36E-05	1.30E-04	0.173	3.18E-03	10.985	0.206	0.471	8.23E-03	0.965	0.169	8.40E-04	2548.7	8.34	2.4
9018-29.1	255.32	178.06	0.720	0.015	140	2	2.19E-05	7.63E-06	3.80E-04	0.202	2.25E-03	10.615	0.196	0.465	8.14E-03	0.973	0.165	7.10E-04	2511.5	7.22	1.9
9018-53.1	114.86	52.18	0.469	0.010	37	1	4.20E-05	3.93E-05	7.30E-04	0.135	2.46E-03	4.461	0.099	0.303	5.61E-03	0.893	0.107	1.07E-03	1746.9	18.47	2.4
9018-57.1	108.85	59.24	0.562	0.013	39	3	9.53E-05	2.96E-05	1.65E-03	0.165	2.21E-03	5.115	0.109	0.322	6.03E-03	0.927	0.115	9.30E-04	1880.8	14.62	4.2
9018-58.1	205.06	68.03	0.343	0.007	124	2	2.54E-05	1.68E-05	4.40E-04	0.093	1.03E-03	15.324	0.281	0.541	9.40E-03	0.976	0.206	8.30E-04	2871.4	6.56	3
9018-62.1	248.94	76.49	0.317	0.007	84	0	5.97E-06	1.79E-05	1.00E-04	0.093	1.54E-03	5.116	0.093	0.326	5.61E-03	0.974	0.114	4.70E-04	1862.3	7.54	2.4
9018-64.1	201.1	47.41	0.244	0.005	70	3	4.86E-05	1.60E-05	8.40E-04	0.072	1.16E-03	5.607	0.117	0.337	6.22E-03	0.928	0.121	9.50E-04	1965.8	14.09	4.7
9018-65.1	44.19	33.77	0.789	0.021	16	2	1.91E-04	7.54E-05	3.32E-03	0.223	5.45E-03	5.003	0.126	0.322	6.13E-03	0.827	0.113	1.61E-03	1844.3	26.06	2.5
9018-67.1	204.38	74.78	0.378	0.008	70	2	4.16E-05	1.91E-05	7.20E-04	0.105	2.02E-03	5.191	0.101	0.326	5.91E-03	0.963	0.116	6.10E-04	1888.7	9.51	3.7
9018-66.1	116.33	55.73	0.495	0.010	59	1	1.94E-05	2.31E-05	3.40E-04	0.144	1.71E-03	10.037	0.210	0.452	8.74E-03	0.962	0.161	9.30E-04	2467.9	9.76	2.6
9018-71.1	166.02	70.54	0.439	0.010	58	4	7.94E-05	2.18E-05	1.38E-03	0.127	1.52E-03	5.234	0.103	0.328	5.91E-03	0.952	0.116	7.10E-04	1888.8	11.04	3.1
9018-72.1	164.91	98.74	0.619	0.013	58	1	2.97E-05	1.85E-05	5.10E-04	0.181	2.70E-03	4.948	0.098	0.317	5.82E-03	0.964	0.113	6.00E-04	1850.3	9.6	4
9018-76.1	88.17	83.97	0.984	0.021	30	1	5.72E-05	8.87E-05	9.90E-04	0.286	6.14E-03	4.005	0.099	0.283	5.01E-03	0.793	0.103	1.56E-03	1673.1	28.31	4
9018-78.1	76.91	101.1	1.358	0.029	48	3	9.05E-05	4.28E-05	1.57E-03	0.379	3.91E-03	10.643	0.212	0.467	8.41E-03	0.945	0.165	1.08E-03	2509.1	11.03	1.5
9018-80.1	108.14	101.68	0.971	0.020	42	2	8.04E-05	3.10E-05	1.39E-03	0.277	4.36E-03	5.190	0.101	0.325	5.70E-03	0.943	0.116	7.50E-04	1890.1	11.72	3.9
9018-82.1	131.32	104.97	0.826	0.017	73	2	3.04E-05	2.03E-05	5.30E-04	0.228	2.35E-03	10.805	0.214	0.460	8.63E-03	0.975	0.170	7.50E-04	2559.9	7.42	4.6
9018-87.1	209.02	140.27	0.693	0.014	115	1	1.78E-05	1.58E-05	3.10E-04	0.196	1.54E-03	10.879	0.209	0.466	8.48E-03	0.975	0.169	7.30E-04	2550.1	7.25	3.3
9018-89.1	193.88	123.32	0.657	0.014	62	0	8.63E-06	1.71E-05	1.50E-04	0.187	2.03E-03	4.280	0.089	0.287	5.43E-03	0.945	0.108	7.40E-04	1766.7	12.62	7.9
9018-90.1	258.46	34.66	0.139	0.003	77	3	4.59E-05	2.66E-05	7.90E-04	0.037	1.13E-03	4.573	0.087	0.304	5.36E-03	0.961	0.109	5.80E-04	1787.2	9.78	4.4
9018-91.1	82.02	37.89	0.477	0.010	46	4	1.05E-04	3.47E-05	1.83E-03	0.130	3.45E-03	12.717	0.241	0.496	8.72E-03	0.961	0.186	9.80E-04	2706.0	8.76	4
9018-96.1	142.51	85.61	0.621	0.014	44	5	1.30E-04	4.44E-05	2.25E-03	0.162	2.35E-03	4.155	0.092	0.285	5.46E-03	0.917	0.106	9.40E-04	1724.5	16.37	6.1
9018-97.1	126.03	175.61	1.439	0.030	54	1	3.26E-05	2.95E-05	5.70E-04	0.405	3.09E-03	5.153	0.112	0.328	6.24E-03	0.926	0.114	9.40E-04	1862.6	14.97	1.8
9018-106.1	193.65	101.78	0.543	0.012	64	3	5.27E-05	2.19E-05	9.10E-04	0.159	1.59E-03	4.445	0.083	0.303	5.28E-03	0.964	0.107	5.40E-04	1741.5	9.29	2.2
9018-110.1	74.89	64.59	0.891	0.019	29	1	3.92E-05	4.32E-05	6.80E-04	0.254	4.20E-03	5.094	0.107	0.325	5.91E-03	0.916	0.114	9.70E-04	1859.1	15.47	2.4

Spot name follows the convention x-y-z; where x = sample number, y = grain number and z = spot number. Multiple analyses in an individual spot are labeled as x-y.z.z
Uncertainties reported at 1s (absolute) and are calculated by numerical propagation of all known sources of error
f206^{204} refers to mole fraction of total ^{206}Pb that is due to common Pb, calculated using the ^{204}Pb-method;
common Pb composition used is the surface blank (4/6: 0.05770; 7/6: 0.89500; 8/6: 2.13840)
* refers to radiogenic Pb (corrected for common Pb)
Discordance relative to origin = 100 * (1-(^{206}Pb/^{238}U age)/ (^{207}Pb/^{206}Pb age))
Calibration standard 6266; U = 910 ppm; Age = 559 Ma; ^{206}Pb/^{238}U = 0.09059
Error in ^{206}Pb/^{238}U calibration 1.0 - 1.7% depending on analytical session
UO/Zr$_2$O 5.83660; Pb*/UO$_2$ 0.10335, Error 1.70
Th/U calibration: F = 0.03900*UO + 0.85600

Table 3.7: $\delta^{13}C$ and $\delta^{18}O$ of the international standard NBS-19 and the local standard MMB.

	$\delta^{13}C_{PDB}$ (‰)	±1σ	$\delta^{18}O_{PDB}$ (‰)	±1σ
NBS-19				
Recommended	1.95	0.05	-2.20	0.10
Measured (n=20)	1.97	0.05	-2.31	0.09
MMB				
Recommended	3.90	0.05	-10.70	0.10
Measured (n=20)	3.87	0.05	-10.79	0.10

Table 3.8: C and O isotopic compositions in samples from the Lakheri Limestone.

Sample	Depth (m)	$\delta^{13}C_{PDB}$(‰)	$\delta^{18}O_{PDB}$(‰)
Gandoli-1	0	1.22	-12.22
Gandoli-2	0.1	1.13	-12.05
Gandoli-4	0.5	1.23	-12.16
Gandoli-5	0.9	1.2	-12.52
Gandoli-6	3	-0.23	-10.36
Gandoli-10	13	1.66	-11.9
Gandoli-11	25	5.96	-10.24
Gandoli-18	60	4.12	-9.26
Gandoli-21	76	5.97	-8.36
Gandoli-23	86	4.13	-11.64

Table 3.9: C and O isotopic compositions in samples from the Balwan Limestone.

Sr. No.	Sample	$\delta^{13}C_{PDB}$ (‰)	$\delta^{18}O_{PDB}$ (‰)
1	BWK-10-1	0.03	-8.43
2	BWK-10-2	3.33	-8.22
3	BWK-10-3A	3.96	-9.98
4	BWK-10-3B	4.18	-8.17
5	BWK-10-4	2.08	-8.94
6	BWK-10-5	4.50	-8.08
7	BWK-10-6	4.05	-4.17
8	BWK-10-7	3.72	-2.69
9	BWK-10-8	-0.64	-3.25
10	BWK-10-9	2.63	-2.34
11	BWK-10-13B	-0.17	-2.42
12	BWK-10-14	-0.75	-5.60
13	BWK-10-15	0.09	-4.26
14	BWK-10-16	3.30	-4.17
15	BUNDI-09-04	3.66	-2.63
16	BWK-10-20	4.13	-9.31
17	BWK-10-21	3.91	-10.70
18	BWK-10-22	1.36	-5.92
19	BWK-10-23	-0.38	-5.10
20	BWK-10-24	0.47	-2.76
21	BWK-10-25	3.83	-8.21
22	BWK-10-26	4.14	-4.79
23	BWK-10-27A	4.41	-5.72
24	BWK-10-28	3.92	-4.79
25	BWK-10-29	1.45	-5.39
26	BWK-10-30	1.56	-5.88
27	BWK-10-31	6.63	-3.71
28	BWK-10-32	3.95	-7.36
29	BWK-10-33	2.84	-5.14
30	BWK-10-34	3.41	-9.60
31	BWK-10-35A	-3.72	-9.00
32	BWK-10-35A-II	-3.65	-6.62
33	BWK-10-35B	-3.43	-7.78
34	BWK-10-36	1.55	-2.79
35	BWK-10-37	1.37	-2.05
36	BWK-10-39	2.50	-3.78
37	BWK-10-40	3.61	-8.58
38	BWK-10-41	4.50	-6.88
39	BWK-10-43	1.13	-6.93
40	BWK-10-44	4.05	-6.09
41	BWK-10-45	4.10	-7.93
42	BWK-10-46	1.53	-6.49
43	BWK-10-47	3.08	-4.02
44	BWK-10-48	0.90	-3.97
45	BWK-10-50	2.16	-5.37
46	BWK-10-51	4.19	-5.79
47	BWK-10-52	2.82	-5.58
48	BWK-10-53	3.27	-6.63
49	BWK-10-55	-2.84	-5.34
50	BWK-10-56	-3.06	-3.29
51	BWK-10-57	1.87	-1.23
52	BWK-10-60	3.98	-5.56
53	BWK-10-61	3.80	-4.87
54	BWK-10-62	2.62	-4.38
55	BWK-10-63	3.94	-6.26
56	BWK-10-64	3.97	-7.10
57	BWK-10-65	4.15	-6.19
58	BWK-10-66	4.17	-6.84
59	BWK-10-67	4.27	-7.88
60	BWK-10-68	-0.58	-2.30
61	BWK-10-69	-1.32	-5.00
62	BWK-10-70	2.50	-2.47
63	BWK-10-71	-0.58	-3.95
64	BWK-10-72	-0.51	-5.70
65	BWK-10-73	-4.93	-10.00
66	BWK-10-73-2	-0.82	-2.32
67	BWK-10-73-3	-1.46	-3.53
68	BWK-10-74	-3.48	-8.51
69	BWK-10-75	-0.57	-3.28

70	BWK-10-76	0.20	-2.35
71	BWK-10-77	-0.79	-5.92
72	BWK-10-78	1.21	-3.37
73	BWK-10-79	0.35	-3.40
74	BWK-10-80	0.59	-2.98
75	BWK-10-81	0.05	-3.67
76	BWK-10-82	1.17	-2.60
77	BWK-10-83	0.39	-5.74
78	BWK-10-84	1.15	-2.62
79	BWK-10-85	0.70	-2.70
80	BWK-10-86	0.68	-1.37
81	BWK-10-87	-0.80	-5.97
82	BWK-10-88	1.33	-4.21
83	BWK-10-89	0.39	-3.33
84	BWK-10-90	1.57	-3.23
85	BWK-10-92	-2.33	-5.48
86	BWK-10-93	-3.08	-5.58
87	BWK-10-94	-3.38	-5.99
88	BWK-10-95	-3.55	-5.09
89	BWK-10-96	2.83	-3.10
90	BWK-10-96-R	3.10	-3.14
91	BWK-10-97	-0.48	-4.66
92	BWK-10-98	2.30	-3.56
93	BWK-10-99	-0.96	-4.46

Table 3.10: Trace element data for selected samples from the Balwan Limestone.

	Mn/Sr	(Sr/Ca)×10^{-4}	(Mg/Ca)×10^{-3}	(Fe/Ca)×10^{-3}
BWK-10-1	35.54	3.49	21.40	28.49
BWK-10-2	9.05	6.51	43.73	31.45
BWK-10-3	5.17	7.01	29.48	15.65
BWK-10-4	16.94	4.27	37.73	27.44
BUNDI-09-04	11.03	7.42	1203.84	35.76
BWK-10-5	4.82	8.39	80.53	3.68
BWK-10-8	87.79	2.49	36.46	48.59
BWK-10-9	88.25	6.05	973.24	68.14
BWK-10-13B	28.71	9.88	1382.01	62.71
BWK-10-15	9.33	7.68	832.27	31.31
BWK-10-20	5.41	8.33	26.81	12.28
BWK-10-21	4.35	8.31	31.66	10.19

Table 3.11: Sr isotopic ratio data for carbonate components from limestone formations of the Upper Vindhyans.

	Sample	$^{87}Sr/^{86}Sr$	2 sigma	$(^{87}Sr/^{86}Sr)^{norm}$
Balwan Limestone	BWK-10-1	0.72599	0.00006	0.72601
	BWK-10-2	0.71430	0.00002	0.71432
	BWK-10-3A	0.71571	0.00002	0.71573
	BWK-10-3B	0.71449	0.00008	0.71451
	BWK-10-4	0.72814	0.00009	0.72816
	BWK-10-5	0.70674	0.00001	0.70676
	BWK-10-6	0.70828	0.00002	0.70830
	BWK-10-13B	0.70903	0.00001	0.70905
	BWK-10-20	0.70682	0.00002	0.70684
	BWK-10-21	0.71031	0.00002	0.71033
Lakheri Limestone	Gandoli--3	0.71520	0.00003	0.71522
	Gandoli--4	0.71885	0.00006	0.71887
	Gandoli--6	0.71556	0.00004	0.71558
	Gandoli--8	0.71526	0.00001	0.71528
	Gandoli--10	0.71312	0.00002	0.71314
	Gandoli--11	0.71078	0.00003	0.71080
	Gandoli--18	0.71884	0.00008	0.71886
	Gandoli--23	0.71803	0.00003	0.71805

$(^{87}Sr/^{86}Sr)_{norm}$ = $^{87}Sr/^{86}Sr$ ratio normalized with respect to a value of 0.71025 of the international standard NBS 987. The long term average of this value for our lab is 0.71023.

3.2 Discussion

3.2. 1 Pre-Vindhyan rocks

To understand the provenance and evolution of a sedimentary basin it is necessary to document the possible source rocks in the vicinity of the basin. In the Rajasthan sector of the Vindhyans, the possible source rocks are the various pre-Vindhyan igneous, metamorphic and sedimentary rocks of the Aravalli mountain ranges. The nature of contact between the Vindhyans and the pre-Vindhyans in the area south/southeast and in the north-east of Chittorgarh is not very well defined due to post-Vindhyan tectonic activities, which have eliminated the primary signatures (Prasad, 1984). This contact is defined by Prasad (1984) as disconformity with the Berach Granite and the Hindoli Group of rocks. These rocks could have been the most prominent sources for sediments to the Vindhyan Basin. Similarly, the occurrences of the Khairmalia volcanics in the vicinity, considered as a basal volcanics, which is now included within the Vindhyan Supergroup, might have been one of the active sources of the sediments during the deposition of the Vindhyans in this sector. Apart from these, the Aravalli-Delhi Supergroups which are exposed in the Aravalli-Delhi mountain chain at the western margin of the basin could also have contributed sediments. Since chemical characterization of all possible sources was beyond the scope of this work, we concentrated on a few pre-Vindhyan magmatic rocks which could have had significant contributions to the sediment budget for the Vindhyan Basin. The geochemical data for these rocks are presented in Table 3.1 and their implications are discussed in the following sections.

3.2.1.1 *The Berach Granites*

The Berach Granites are considered as basement inliers within the Aravalli supracrustals, and believed to have undergone a very low-grade metamorphism during the Proterozoic tectonothermal events (Roy and Jakhar, 2002). The Berach

Granites belong to the Mewar Gneissic Complex and form part of the Archean basement of the Aravalli Supergroup. Described as Chittor Granites by Hacket (1881), Gupta (1934) correlated them with the Bundelkhand Granites and Gneisses occurring in Central India. Gupta (1934) identified that these represent the pre-Aravalli land surface on which the rocks of Aravalli Supergroup lie with a definite erosional unconformity. The geochronological studies on the Berach Granites using the Pb-Pb isochron analysis by Weidenbeck et al. (1996) provided a minimum age of crystallization of 2440±8 Ma, which is similar to the estimated age for the Bundelkhand granites and gneisses given by Mondal et al. (2002).

The texture of these granites varies from coarse porphyritic to highly foliated gneissic type in thin sections. Minerals found in these are quartz, feldspar, biotite and ferromagnesian minerals parallel to the foliation. Two samples (CGB-07-03 and CGB-07-06) of this granite were collected from the Berach River section near Chittorgarh. One of the samples was slightly weathered (CGB07-03) as is evident from its low contents of Na and Ca (Table 3.1). The major difference between the Berach granites and the other Archean granites in the nearby region such as Untala and Gingla is in the amount of SiO_2, which is lower in Berach. A comparative study between the Berach granites and the data generated on Bundelkhand granites and gneisses (Hussain et al., 2004) suggests that although the chemical compositions are similar, the chondrite normalized Rare Earth Elements (REE) patterns of Berach granites are somewhat different from that of the Bundelkhand granites (Fig. 3.1 A). Further, the multi-element spiderograms normalized to the primitive mantle (PM), in which the elements are arranged according to their incompatibility, are presented in Fig 3.2. The samples from the Berach granites show typical enrichment in Pb and depletion in Sr values compared to their Bundelkhand counter parts (Fig. 3.1A). These observations suggest that though compositionally similar, these two granites have evolved in different tectonic settings, with the Berach granites representing a magmatic arc (subduction zone) setting.

The $\varepsilon_{Nd}(0)$ values for the two Berach granite samples are -32 and -30 with T_{CHUR} age of 3.16 and 2.65 Ga and T_{DM} ages of 3.08 and 2.69 Ga (Table 3.1). These model ages are older than the crystallization age of the granites, i.e. 2.5 Ga. Model ages essentially reflect the age of mantle extraction for the samples, hence are older than their crystallization ages.

3.2.1.2 *Mafic igneous rocks*

The Khairmalia volcanics are reported from the western margins of the Vindhyan Basin. These are described as intermediate amygdaloidal andesitic flows including pyroclastics which occur unconformably over the Berach Granite and over the Pre-Aravalli metamorphics (i.e. Bhilwara Supergroup) (Prasad, 1984). The thickness of the flows is 40 to 100 m. The Khairmalia volcanics are mainly fine grained and dark purple, pink, greenish or greenish brown in colour. The amygdales are of millimeter to centimeter in size, filled with silicate-chloritic, calcite, siderite, chert and quartz. Although the precise age of emplacement of these rocks is not yet known.

Raza et al. (2009) carried out detailed geochemical studies on the Khairmalia volcanics and suggested that these represent Continental Flood Basalt (CFB) except for one sample which showed signatures of Ocean Island Basalt (OIB). They also worked on the Jungel volcanics from the Son Valley and identified them as OIBs. Five samples of mafic igneous rocks were collected from Khairmalia volcanics south-west of Chittorgarh between Badi Sadri and Dholapani, separated by 30 km. The results of geochemical analyses are given in Table 3.1.

Based on total alkali and silica (TAS) diagram (Fig 3.3) these rocks are classified as andesite to dacite, with two of the samples falling within the field of basalt. It is highly likely that these rocks came from the same ourcrops that are sampled by Raza et al. (2009). However, in the present study these have been identified as metavolcanics with evidences of metamorphic recrystallization textures.

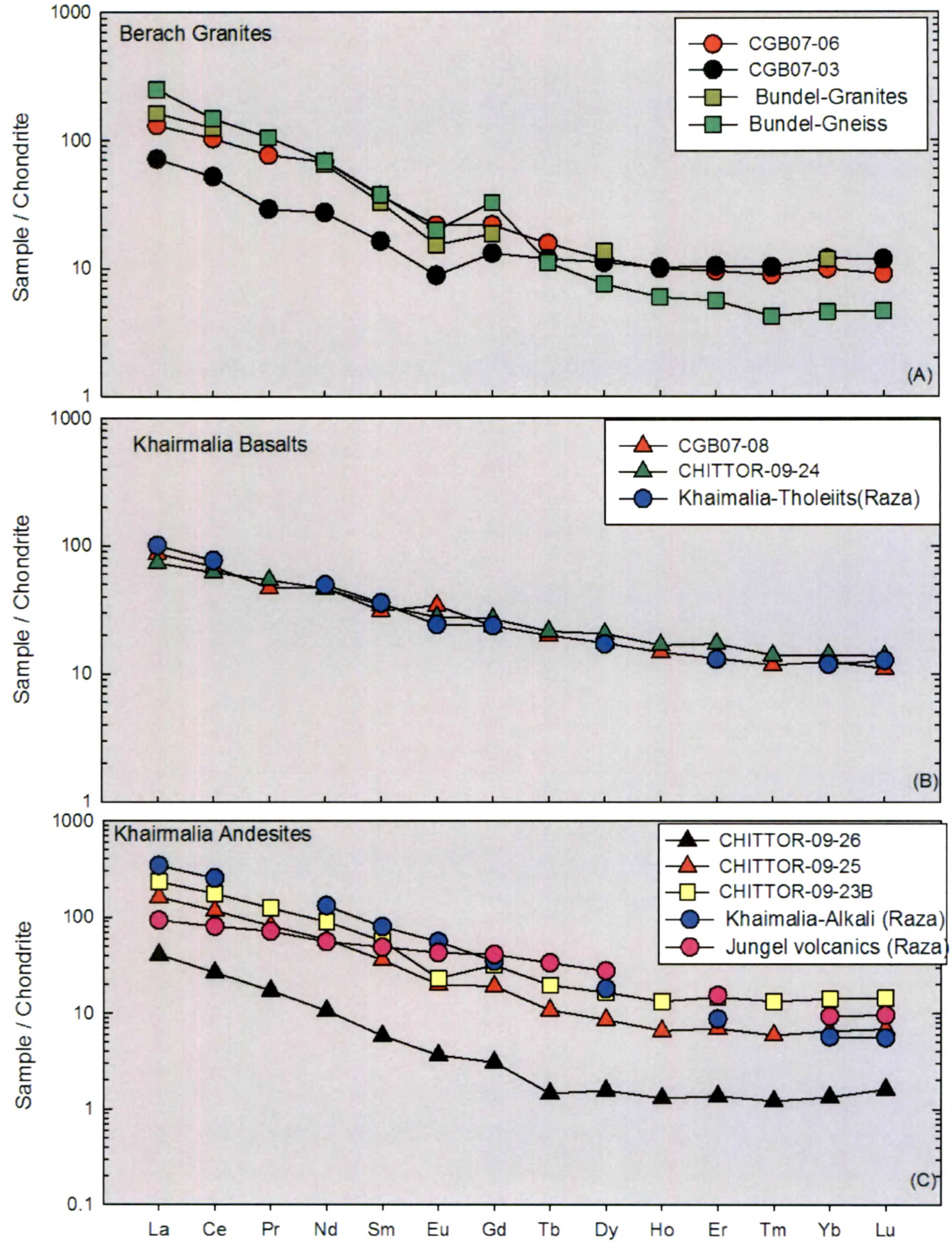

Fig. 3.1: Chondrite normalized REE patterns for various pre-Vindhyan granites and mafic igneous rocks. Data sources: Table 3.1, Hussain et al. (2004) and Raza et al. (2009).

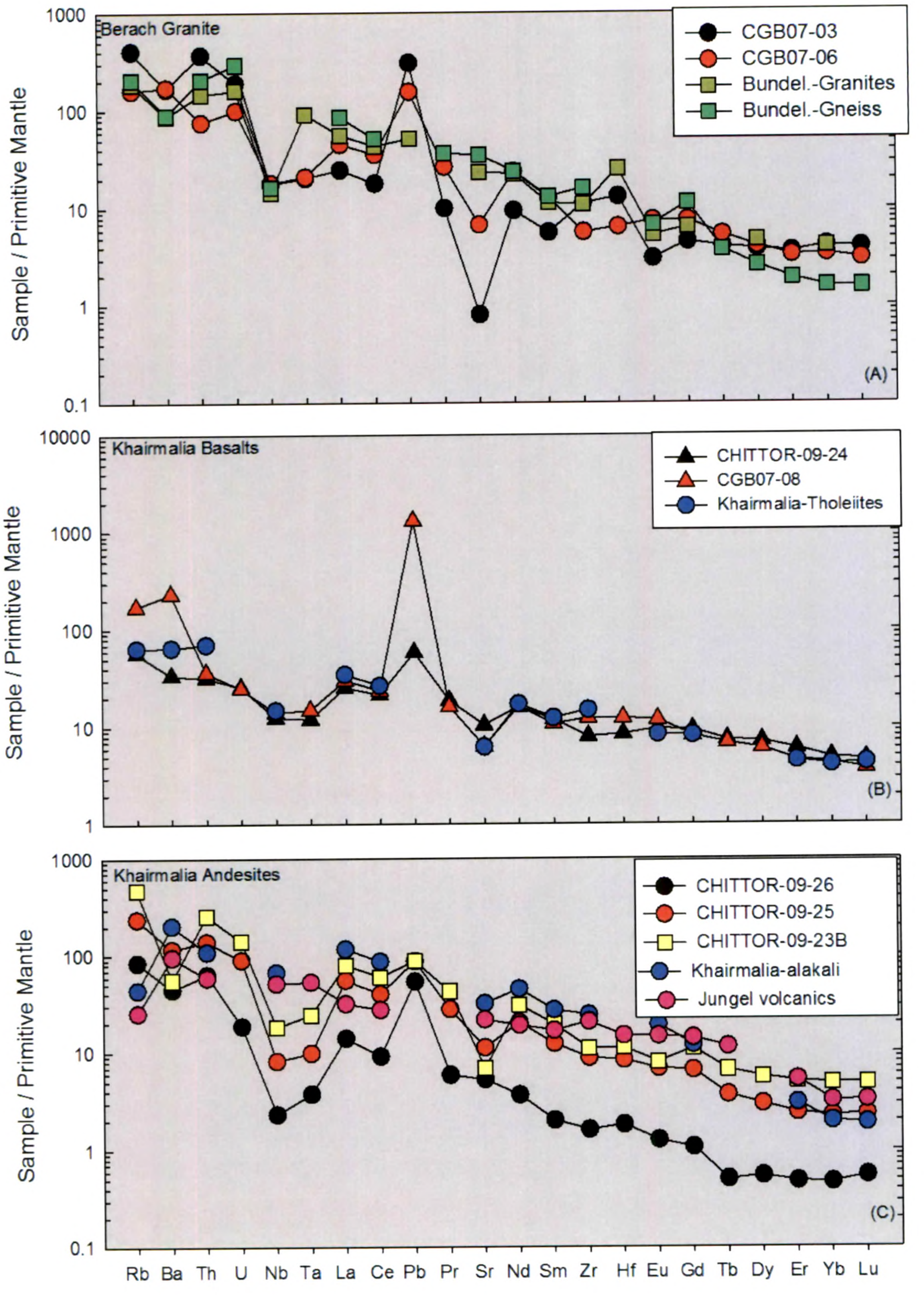

Fig. 3.2: Primitive Mantle normalized multi-element content variations in pre-Vindhyan granites and mafic igneous rocks. Data sources: same as in Fig. 3.1.

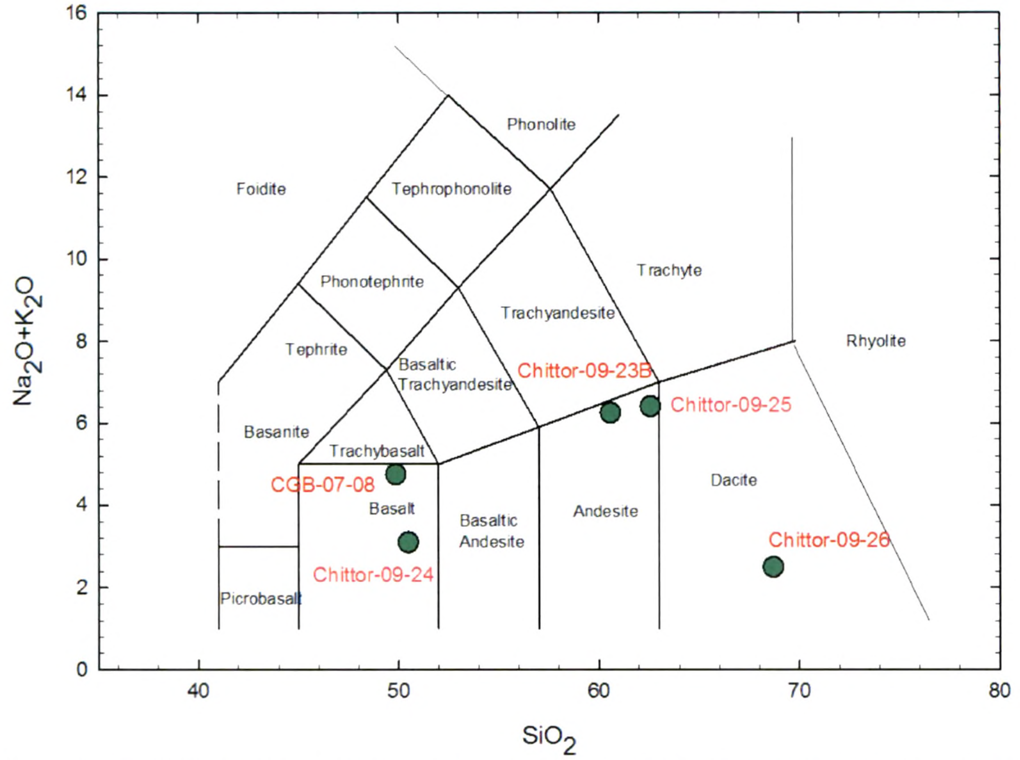

Fig. 3.3: Total Alkali- Silica diagram and classification of the Khairmalia volcanics. Classification scheme after Lee Bas et al. (1990).

For comparison, the average values of REE concentrations in Khairmalia tholeiites and alkali basalts and those in the Jungel volcanics (Raza et al., 2009) have been plotted along with our data from Khairmalia metavolcanics in Fig. 3.1 B & C. One can see that the two of our mafic metavolcanic samples, identified as basalts (Fig. 3.3), are similar to the Khairmalia tholeiites of Raza et al. (2009) (Fig. 3.1B). Similarly, most of our samples classified as andesite and dacite (Fig. 3.3) have higher total REE contents and show LREE enrichment and appear to be different from Jungel volcanics (Fig. 3.1C).

Further to identify the source characteristics, multi-element variation diagrams were utilized, where trace and rare earth element contents were plotted after normalizing them to primitive mantle (PM) compositions. Samples with affinity towards andesite and dacite show enrichments in large ion lithophile elements (LILE) and depletion in Nb, Ta, and Sr and enrichments in Pb (Fig. 3.2 B & C). Such features are typical for island/magmatic arc igneous rocks (Winter, 2001) and therefore, hint at a subduction zone setting during Khairmalia magmatism. We envisage that a subduction zone setting existed at the western margin of the Vindhyan Basin during Paleoproterozoic (2500-2200Ma) and that the Khairmalia volcanics represent the mature arc magmatism. Such a scenario is supported by several previous studies (Sarkar et al. 1989; Mishra et al. 2000; Leelanandam et al.; 2006).

Ahmad et al. (2008a) carried out geochemical studies on the Proterozoic mafic volcanic rocks from the Aravalli-Delhi orogeny and suggested that all the metavolcanic rocks within the supracrustal belts of Aravalli, Bhilwara, Jharol and Delhi were of typical tholeiitic in composition except for the rocks in Basantgarh area of Delhi belt, which were cal-alkaline in composition. The Bhilwara and Aravalli samples showed enriched LREE, while Delhi belt samples showed flat to fractionated REE patterns. The incompatible element ratios were similar in Bhilwara and Aravalli volcanics, while Delhi belt samples showed large variations. Comparison of trace element patterns of these rocks with those of the Khairmalia volcanics reveals that the metavolcanics of the Delhi Supergroup have similar chemical affinities (e.g. depletions of Nb & Ta) and going by conclusions made by Ahmad et al (2008a) both should represent island arc settings, though the locations of the subduction zones and their timing could have been different.

The measured $^{87}Sr/^{86}Sr$ ratios in these rocks are highly radiogenic (0.718 to 1.969) and so are the initial ratios, which clearly point to incorporation of radiogenic Sr during metamorphism. The measured $^{143}Nd/^{144}Nd$ isotopic ratios vary from 0.510919 to 0.512015 (corresponding $\varepsilon_{Nd}(0)$ varies from -33.5 to -12.2; Table 3.1), which confirm the radiogenic nature of Nd in them. The Nd model ages (T_{DM}) vary from 3.22 to 2.22 Ga. It appears that there have been different episodes of this activity with rocks having higher model ages representing magmas affected by continental derived material at the source or were crustally contaminated. The sample that has the lowest $^{87}Sr/^{86}Sr$ (0.71769) and $\varepsilon_{Nd}(0)$ (-12.2) possibly represents the least contaminated lava within the Khairmalia volcanics. There exists a finite probability that some of our metavolcanics may actually represent pre-Khairmalia magmatism.

3.2.2 Vindhyan Sedimentary Sequences

The chemical compositions of the clastic sediments have been widely used as provenance indicators (McLennan et al., 1995, 2003), since these are directly controlled by their original source rocks. Chemistry of siliciclastic sediments has also been used for understanding the weathering histories and the past climate changes (e.g., Nesbitt & Young, 1982; Fedo et al., 1995). These also help to understand secondary processes such as hydraulic sorting and diagenesis (e.g. McLennan et al., 1993) and tectonic history of the depositional environments (Bhatia, 1983; Bhatia & Crook, 1986; Naqvi et al., 1988). Chemistry of sediments also plays an important role in the evaluation of the composition of the continental crust (Condie, 1993). Therefore, geochemistry of the sedimentary rocks/sediments is essential for unraveling the mysteries for the evolutionary processes of the planet Earth.

The composition of sedimentary rocks is controlled by the source rock compositions and the sedimentary processes responsible for sediment generation and its deposition in a basin. Further, diagenesis of sediments, which is responsible for conversion of sediments into sedimentary rocks, also plays a crucial role in determining the chemical compositions of the sedimentary rocks. Some of the geochemical signatures of the source rocks get obliterated by diagenetic processes, in such scenario isotopic ratios come in handy in provenance determination.

The geochemical studies on the finest fraction of sediments (i.e. clay size fraction) are believed to yield good results for understanding the provenance of the sediments since they faithfully record the sedimentary history of the basin. Shales (mudstones), due to their impermeability, retain the minerals from the source rocks (Blatt, 1985; Graver and Scott, 1995) and hence preserve the near original composition of the sources. These rocks record the elemental abundances of the relatively immobile elements (e.g. REE, Th, Nb, Sc, Zr etc.), transferred quantitatively through the sedimentary processes from the parent rocks into the clastic sediments (Taylor & McLennan, 1985; Condie, 1991). According to these workers the abundances as well as the ratios of these elements remain intact during the diagenesis as well as low grade metamorphism. The provenance signal get well represented in case of the mud/shale due to effective mixing of the sources during suspension transport comparative to the sand size, which, in generals transported as bed load. Therefore, geochemical study of finer clastic sediments (i.e. shales/pelites) is useful in deciphering the source compositions of the sediments in a basin.

Daly (1909) first identified that Ca/Mg ratios varied over the geological history. Subsequently, numerous geochemical investigations were carried out to identify secular trends in major and trace elements in siliciclatsics as well as carbonate rocks. The parameters controlling these secular variations are the mixed responses of sediment recycling and preservation of the changes in the composition due to weathering/diagenesis as well as the evolution of continental crust (McLennan and Hemming, 1992). Sedimentary processes tend to mask the signatures of the provenance and direct correlation with the source rocks is not straightforward. In such a scenario combination of elemental geochemistry and isotopic studies specifically of Nd isotopic ratios have proved to be useful.

The Nd isotopic ratios and rare earth element (REE) concentrations have widely been used in shales for understanding the sedimentary provenance. Since shales are believed to be true representatives of the parent materials because of their fine grained and well-mixed nature. It is believed that the REE concentration of the

Upper Crust is represented by average shales, with low organic content, which show uniform REE pattern with narrow range of Sm/Nd ratio (typically varying between 0.10 and 0.12; Taylor and McLennan, 1985; McLennan et al.,1989). As discussed earlier the REE content of shales remain unchanged during weathering, re-working, re-suspension, and re-deposition and hence the relative abundances of Sm and Nd do not change during deposition and very early diagenesis of shales due to their group chemistry. However, some workers have demonstrated that diagenesis can significantly mobilize/fractionate REEs (Milodowski and Zalasiewicz, 1991; Ohr et al., 1994; Lev et al., 1999; Lev and Filer, 2004). It may lead to disparities between the whole rock geochemical signature of shales and that of the presumed parent material. In this case a preferential loss of the REEs during diagenesis can significantly alter the Sm/Nd ratio and hence the Nd-isotopic signature of the sediments relative to the source rock (McLennan et al., 1989; Bock et al., 1994; Hannigan and Basu, 1998).

3.2.2.1 *Petrography of Sandstones*

The Vindhyan sedimentation in Rajasthan started with the deposition of the Khardeola Sandstone in which volcanic clasts have been reported (Prasad, 1984). Our petrographical study on these sandstones reveals that these do not show any signature of metamorphism. However, in some of the samples we observed sub-parallel fractures in quartz grains with associated high relief. We believe that it might be due to the effect of tectonics associated with the nearby faults (in the GBF zone) on these grains. The most dominant mineral after quartz is feldspar, which are mostly orthoclase. These rocks also contain opaque minerals, predominantly reddish brown in colour, which are most likely hematite (Fig. 3.4). The immature status of these sandstones is evident from the presence of abundant lithic fragments, with large amount of accessory phases of Fe bearing minerals.

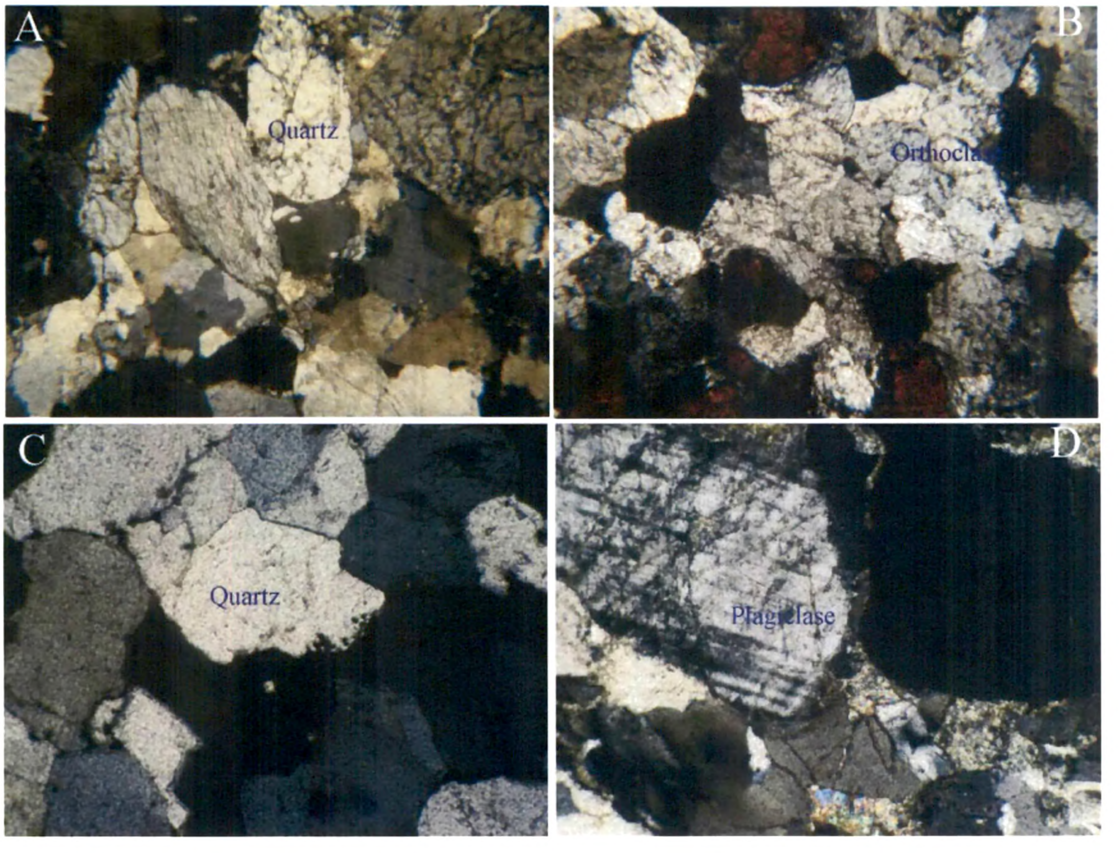

Fig. 3.4: Photomicrographs of thin sections of the Lower Vindhyan sandstones under crossed polars: A) Khardeola Sandstone; B) Bhadesar Quartzite; C) Sawa Sandstone; D) Sawa Sandstone/Porcellanite.

The Bhadesar Quartzite/Sandstone Formation, which is considered equivalent to the Khardeola Formation by Srivastava and Gyanchand (1984) and Soni et al. (1987), is included in the Hindoli Group of rocks by Prasad (1984). The pterographical examination of samples of Bhadesar Formation collected from hillocks of Thukrawa village near Bojunda town reveals that these too contain lithic fragments of volcanic materials, and feldspars. Also, the fractured nature of grains (Fig 3.4b) is very much like those observed in the Khardeola sandstone.

The Sawa Sandstone Formation is gritty in nature. It contains, apart from quartz, plagioclase feldspars and iron oxides with minor lithic fragments (Fig 3.4 C&D).

These observations hint at inclusion of igneous material within this formation. A thin porcellanite formation has been reported to be occurring between this and the overlying Sawa Shale Formation. In the field, however, we found it difficult to identify the porcellanite lithology.

The Kaimur Sandstone contains almost uniform, sub-rounded quartz and orthoclase feldspar grains with low amount of cements (Fig 3.5A) suggesting maturity. Up in the stratigraphical column, the Taragarh Sandstone of the Rewa Group, contains angular quartz grains and plenty of lithic clasts (Fig 3.5.B). The grains are finer compared to the underlying Kaimur Sandstone and the overlying Bundi Hill Sandstone of the Bhander Group (Fig 3.5C). The texture of the Bundi Hill Sandstone has similarity with the Kaimur Sandstone but have smaller mineral grains. The Shikoada Sandstone (i.e. Maihar Sandstone) occurring above the Lower Bhander Sandstone contains a lot of angular clasts within a dirty matrix (Fig. 3.5 D).

The petrographical studies suggest that the sandstone formations from the Lower Vindhyans have signatures of immaturity which is evident from the presence of plagioclase feldspars, lithic clasts and opaques. This suggests that the location of the sources could not have been far off from the place of deposition. Similarly, in the Upper Vindhyans the Taragarh Sandstone of the Rewa Group also shows the incorporation of igneous material from the nearby sources as the angularity of the grains hints at a short distance transport for the quartz grains.

3.2.2.2 Clues from Major Elements

The sandstone and shale formations from the Lower Vindhyans (Semri Group) are plotted in the chemical classification diagram of Heron (1988) (Fig 3.6). It is noted that most of the Vindhyan shales/mudstones plot in the field of wacke suggesting that the shales are slightly coarser than a typical shale. The Binota Shale of the Semri Group of the Lower Vindhyans is found to be Fe-rich and falls in Fe-sand field (Fig. 3.6). These observations suggest that the deposition of the Lower Vindhyan mud

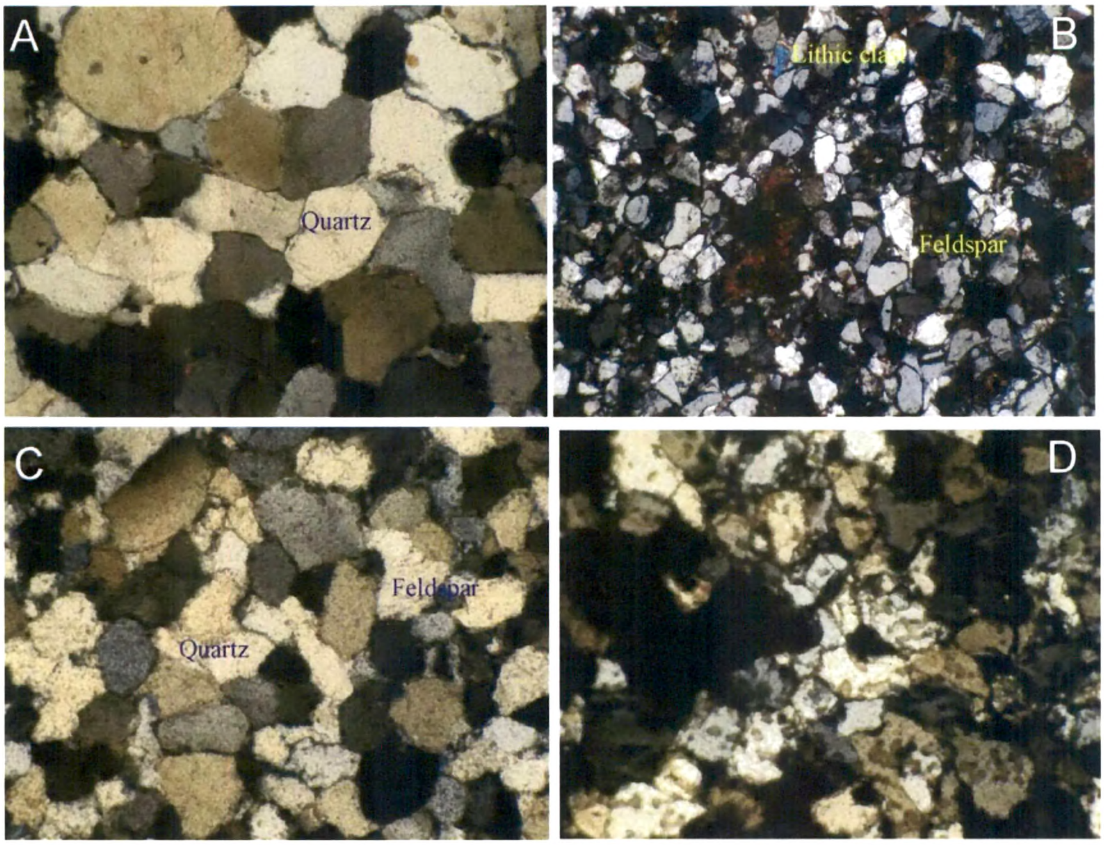

Fig. 3.5: Photomicrographs of thin sections of Upper Vindhyan sandstones under crossed polars; A) Kaimur Sandstone; B) Taragarh Fort Sandstone; C) Bundi Hill Sandstone and D) Shikoada Sandstone. Scale: 1cm = 500 μm.

rocks did not take place in a deep water regime and not far away from the provenances. The latter is reflected in the lack of sorting of grains. The sandstones of the Lower Vindhyans, except for the Sawa Grit Formation, fall in less mature fields (Fig. 3.6), which is a result of the presence of lithic and feldspathic fragments in them.

The Kaimur sandstones are composed of >95% of SiO_2, and Al and Fe contents are below the detection limits. The composition itself suggests that it is a Quartz Arenite. Our petrographical studies also indicate it to be a super mature sandstone with the presence of well rounded quartz grains and no feldspar grains (Fig 3.5). Most of the sandstones from the Rewa and Bhander Groups are of subarkose and sublitharenite type. The Sawa Grit Formation of the Semri Group and the Shikoada Sandstone of the Bhander Group are typical quartz arenites and contain > 95% of quartz. The Taragarh Sandstone contains lithic fragments while the Indergarh Sandstone plots at the boundary of Fe-sands and quartz arenite. The survival of the lithic/rock fragments and feldspar in the sandstones as well as within the coarse-grained shales suggest that the sources of these rocks were near the depositional sites within the basin.

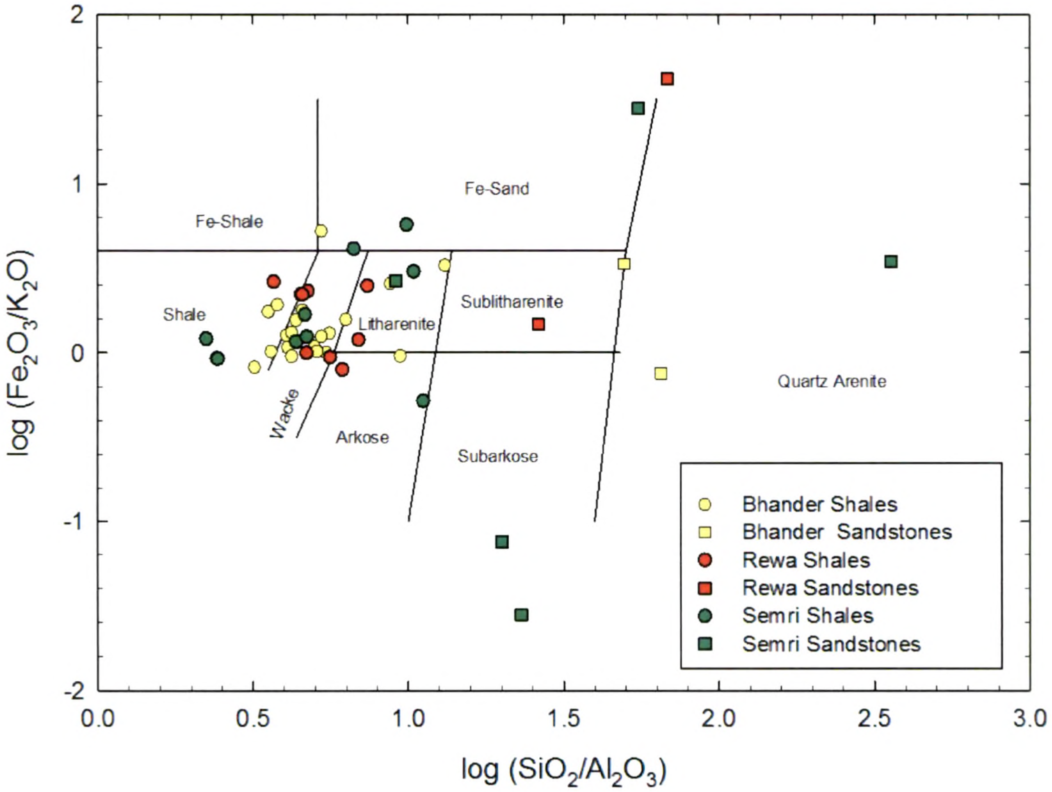

Fig. 3.6: Chemical classification of shale and sandstone formations of various groups of Rajasthan Vindhyans using the scheme of Heron (1988).

The Chemical Index of Alteration (CIA) proposed by Nesbitt & Young (1982) has been most widely used in understanding of weathering in the source area. This index is defined as follows using molecular proportions:

$$CIA = [Al_2O_3/ (Al_2O_3+CaO^*+Na_2O+K_2O)] \times 100$$

where CaO* is the amount of CaO incorporated in the silicate fractions of the rocks and a correction should be carried out for carbonates and apatite contents.

The CIA value of the Khardeola Sandstone is calculated to be 97 while the samples from the Bhadesar Quartzite (CGB-07-12) have values ranging from 40 to 70. The low value of 40 could be explained by higher content resulting from K-metasomatism (Fedo et al., 1995). The Sawa Sandstone and Porcellanite formations have CIA values varying between 70.2 and 87.7, suggesting a moderate to high degree of weathering at the source regions prior to the derivation of these sediments. The CIA calculated data for the Khardeola/Bhadesar formations support that the source areas have experienced high degree of weathering. On the A-CN-K (Al_2O_3-CaO^*+Na_2O-K_2O) plot of Nesbitt & Young (1984), in which the oxides are represented as molar proportions and the CaO* represents the carbonate free CaO, the sandstones from the Semri Group plot near the field of illite clay minerals along the A-K axis (Fig. 3.7). This suggests high degree of weathering in the source region, however, the large spread could be a result of involvement of multiple sources.

The sediments from the Upper Vindhyan formations are also plotted on A-CN-K diagram in Fig 3.8. The CIA vales for the shales from the Upper Vindhyans vary between 59.5 to 81.9 and the sandstones between 76.7 and 96.9. These observations also suggest moderate to high degree of chemical weathering in the source region of these sediments prior to their deposition. On the A-CN-K diagram (Fig. 3.8) all the sandstones and shales, except a few, fall along the A-K axis suggesting the presence

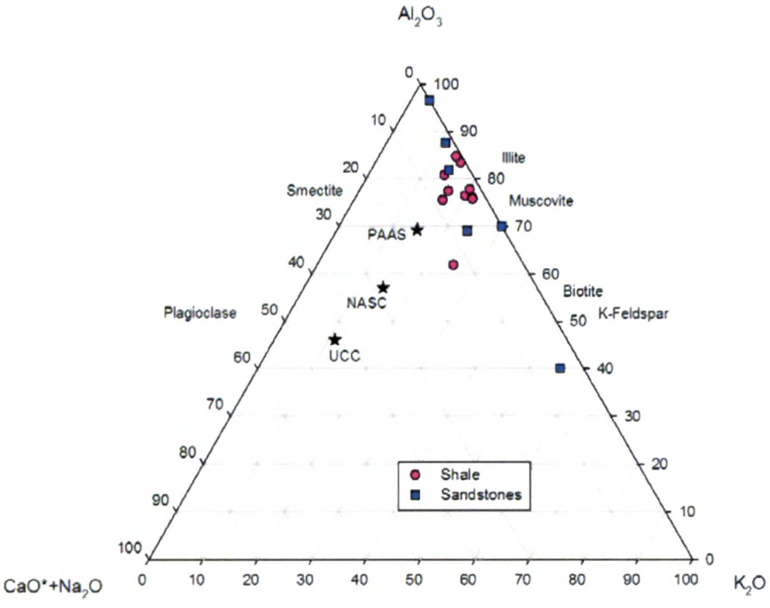

Fig 3.7: Shales and sandstones from the Lower Vindhyans (Semri Group) plotted on A-CN-K diagram of Nesbitt & Young (1984). Also shown are the compositions of PAAS (Post Archean Australian Sediments), NASC (North American Shale Composite) and UCC (Upper Continental Crust).

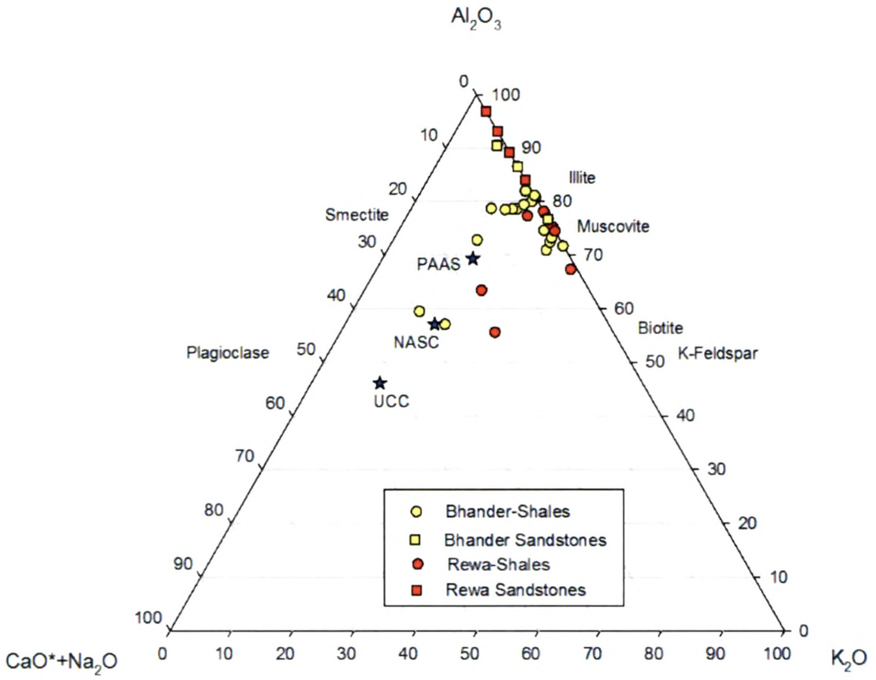

Fig. 3.8: Shales and sandstones from the Upper Vindhyans plotted on A-CN-K diagram of Nesbitt & Young (1984).

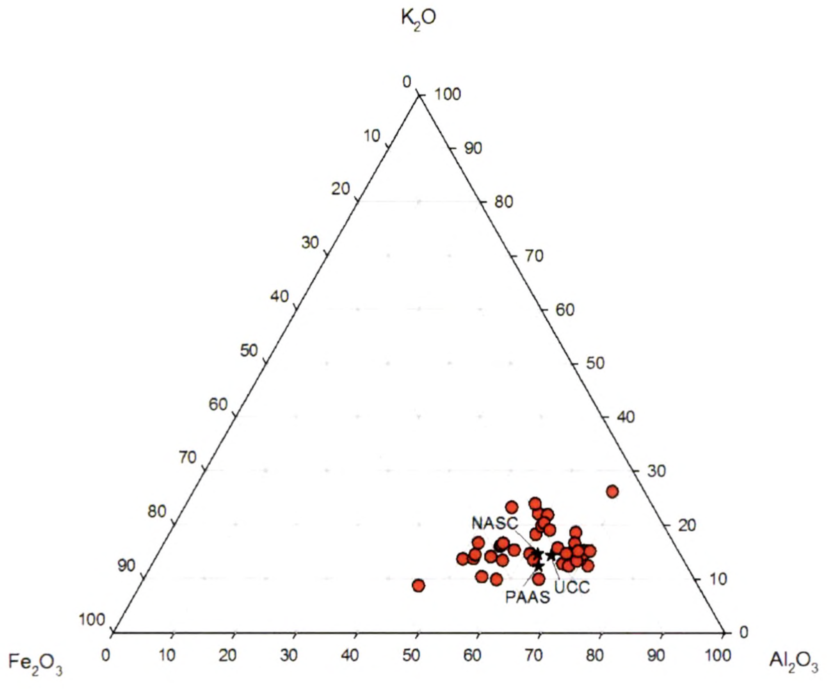

Fig. 3.9: Al_2O_3-K_2O-Fe_2O_3 diagram for the shales from the Vindhyans of Rajasthan.

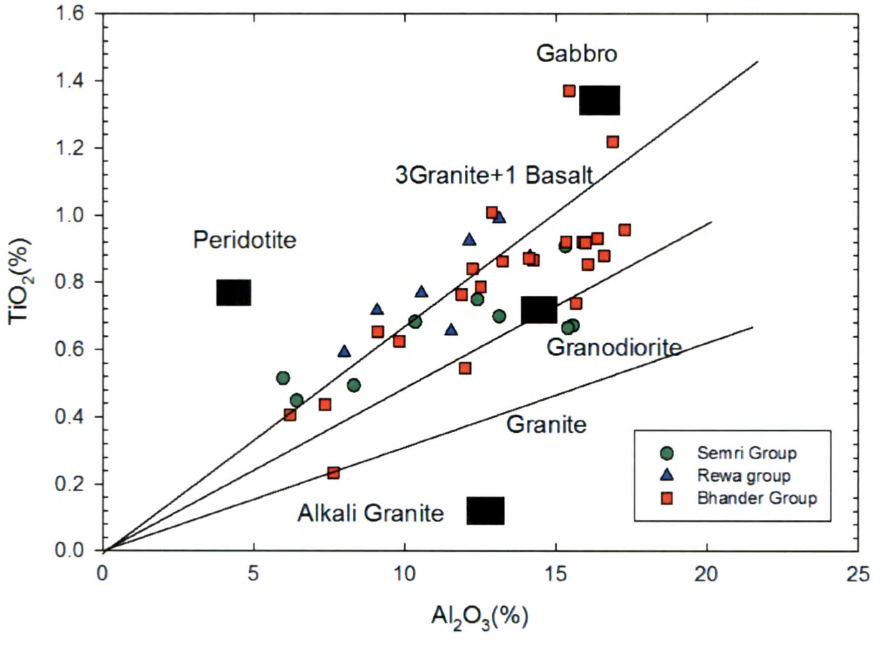

Fig. 3.10: TiO_2 vs. Al_2O_3 plot of McLennan et al. (1980) for sedimentary rocks on which data from the Vindhyan sediments of Rajasthan are plotted. The 'granite' and '3Granite+1 Basalt' lines are from Schieber (1992).

of illite/muscovite. The near absence of Al in the Kaimur Group of sandstone samples restricts us reconstructing the weathering history of the sediment sources.

The computed CIA data in conjunction with the A-CN-K compositional triangular diagram provide valuable information about weathering and tectonic history. The weathering and post depositional diagenetic changes could be ascertained by plotting weathering trends in the A-CN-K plots. No clear trend has been observed for shales of Vindhyans of Rajasthan, except their spread along the A-K axis. This suggests that their sources had undergone high degree of weathering, as during early stages of weathering the samples follow the trend parallel to A-CN line due to loss of Ca and Na form the plagioclase feldspar and later shifting of the trend towards A-apex due to breakdown of K-feldspars (Nesbitt & Young, 1982).

The molecular proportion of Al_2O_3-K_2O and Fe_2O_3 of the shales are plotted in the compositional space in Fig. 3.9. The majority of the data plotted fall close to Al_2O_3 suggesting clay minerals control the compositions (Wronkiewicz and Condie, 1987). The shales from Rajasthan Vindhyans also show significant variation in iron content (Fig. 3.9).

The chemical resistant behaviour of Al and Ti during weathering has also been used to identify the source signatures by plotting a bivariate plot between TiO_2 vs. Al_2O_3 (McLennan et al., 1980; Schieber, 1992), which has been reproduced in Fig. 3.10. In this plot the data of the Rajasthan Vindhyans fall closer to the mixing line of "3 granite+1 basalt' line of Schieber (1992) and the 'granodiorite' field. Even some samples fall closer to the 'gabbro'field.

3.2.2.3 Clues from Trace Elements

Concentration variations of trace elements have been very useful in understanding provenance, weathering, transportation, diagenesis and metamorphic history of sedimentary rocks. The low mobility of trace elements like Ti, Zr, Y, Nb, Th, Sc and rare earth elements (REEs) in fluids make them good tracers for understanding the sources of sediments. Trace element geochemistry including the REEs in the fine grained sediments i.e. mud and mudstones (shales) have been extensively used in deciphering history of sediments. The REEs, due to their group behaviour, immobility in natural waters, and almost nonexistent inter-element fractionation, faithfully preserve the source compositions (McLennan et al., 1989). Elements like Th and Sc have similar behaviour in sedimentary environments and hence considered useful for provenance studies (Taylor and McLennan, 1985). The increase of Th/Sc ratio in sediments subsequent to the Archean-Proterozoic transition has been attributed to derivation of sediments from more differentiated felsic material compared to undifferentiated mafic material in Archean (McLennan and Hemming, 1992). Similar trends also have been observed in La/Sc and La/Yb ratios and are believed to be controlled again by felsic material. Various workers have tried to utilize the Sm/Nd ratio over the geological time scale to understand the compositional of the Upper Crust from mafic to felsic (Miller and O'Nions, 1985; Goldstein and Jacobsen, 1988; Dia et al., 1990). However, contrary to a predicted decrease in this ratio it was found to have increased in sedimentary rocks (Goldstein and Jacobsen, 1988; Depaolo, 1988), which suggests a complex evolutionary history for the Upper Crust. Hence, there exist drawbacks in such type of work while relating the trends in sediment compositions to the possible changes in the source rocks.

Chondrite normalised patterns of REE, more specifically of the light rare earth elements (from La to Nd) have been extensively used in sedimentary provenance studies (McLennan et al., 1980). The chondrite normalized REE patterns of shales and sandstones from all the four groups of the Vindhyan Supergroup are presented in Fig. 3.11 and Fig. 3.12. The chondrite normalized patterns are almost similar for all the shales with typical negative Eu anomaly (Fig. 3.11) except for the Nimbahera and Suket Shale of the Semri Group these show slightly depleted LREE patterns (Fig. 3.13). From these patterns it is clear that these shales show homogenous nature reflecting mixed source signatures. The negative Eu anomaly seen in the Vindhyan shales is quite common in sediments that have been formed after stabilization of the continental crust. The sandstones from all the four groups of the Vindhyan Supergroup show similar LREE enriched patterns as shales except that these have overall lower REE contents and not so pronounced Eu anomalies (Fig. 3.12). From the REE patterns various sandstones within the various groups can be differentiated based on the extent of LREE enrichment. For example, the Bundi Hill Sandstone (Sample No. Satur-23; Fig. 3.12A) has higher REE content compared to that in the Shikoada Sandstone (BUNDI-09-05;-Fig. 3.12A). The REE patterns for the Indergarh Sandstone (BUNDI-09-08) collected, near Indergarh town in Bundi district, is quite similar to that of the sample of same formation collected near Rawatbhata town in Chittorgarh district (CHITTOR-09-03), separated by more than 100 km. This suggests that the sources of the sediments to both the places may not have been very different.

For comparison, normalized REE patterns of shales and sandstones were also plotted against the Post Archean Australian Sedimentary Rocks (PAAS: McLennan et al., 1989) in Fig. 3.13 and 3.14 respectively. The REE patterns of Nimbahera Shale and Suket Shale show prominent LREE depletion (Fog. 3.13C) and so do a few formations of the Bhander Group. This might be due to changes in sources or lesser input from felsic igneous components. The rest of the samples show either a flat or LREE enriched pattern suggesting that the sources for the Vindhyan sediments represented an average, post Archean continental crust.

To further understand the sources of Vindhyan sediments, their normalized trace element contents were plotted in multi-element spidergrams. Normalization was done using compositions of the primitive mantle (PM) and PAAS (Fig. 3.15 to Fig. 3.18). In these diagrams the elements are arranged according to their decreasing incompatibility in mafic igneous systems. The shales are plotted in Fig. 3.15 and 3.16 and sandstones are plotted in Fig. 3.17 and 3.18. The most striking features in the PM normalized diagram plots are: 1) depletion in Nb and Ta; 2) enrichment in Pb; and 3) depletion in Sr (Fig. 3.15 &3.17). Such patterns are typical of crustal rocks but

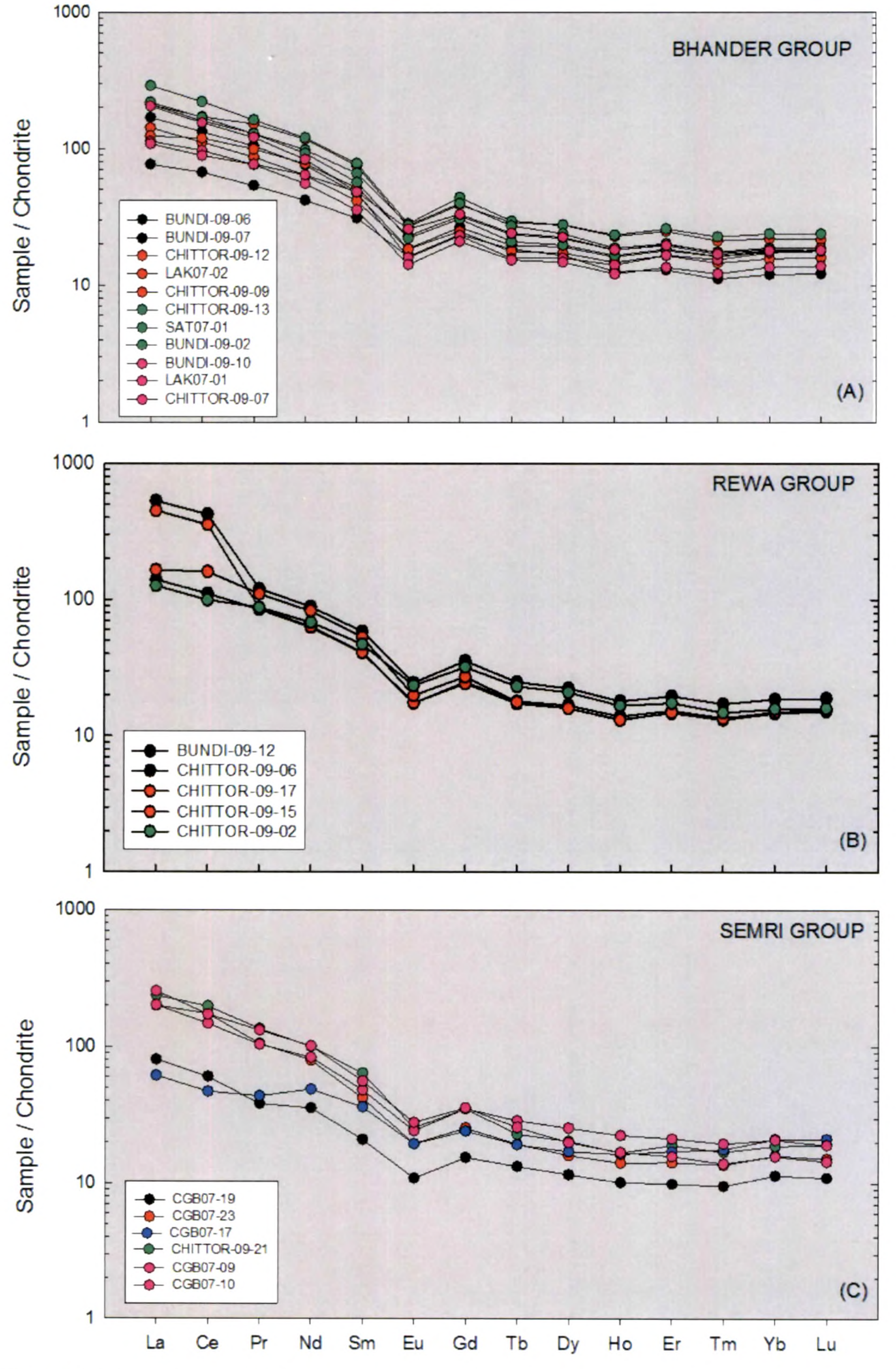

Fig. 3.11: Chondrite normalized REE patterns of shales from the Vindhyans of Rajasthan.

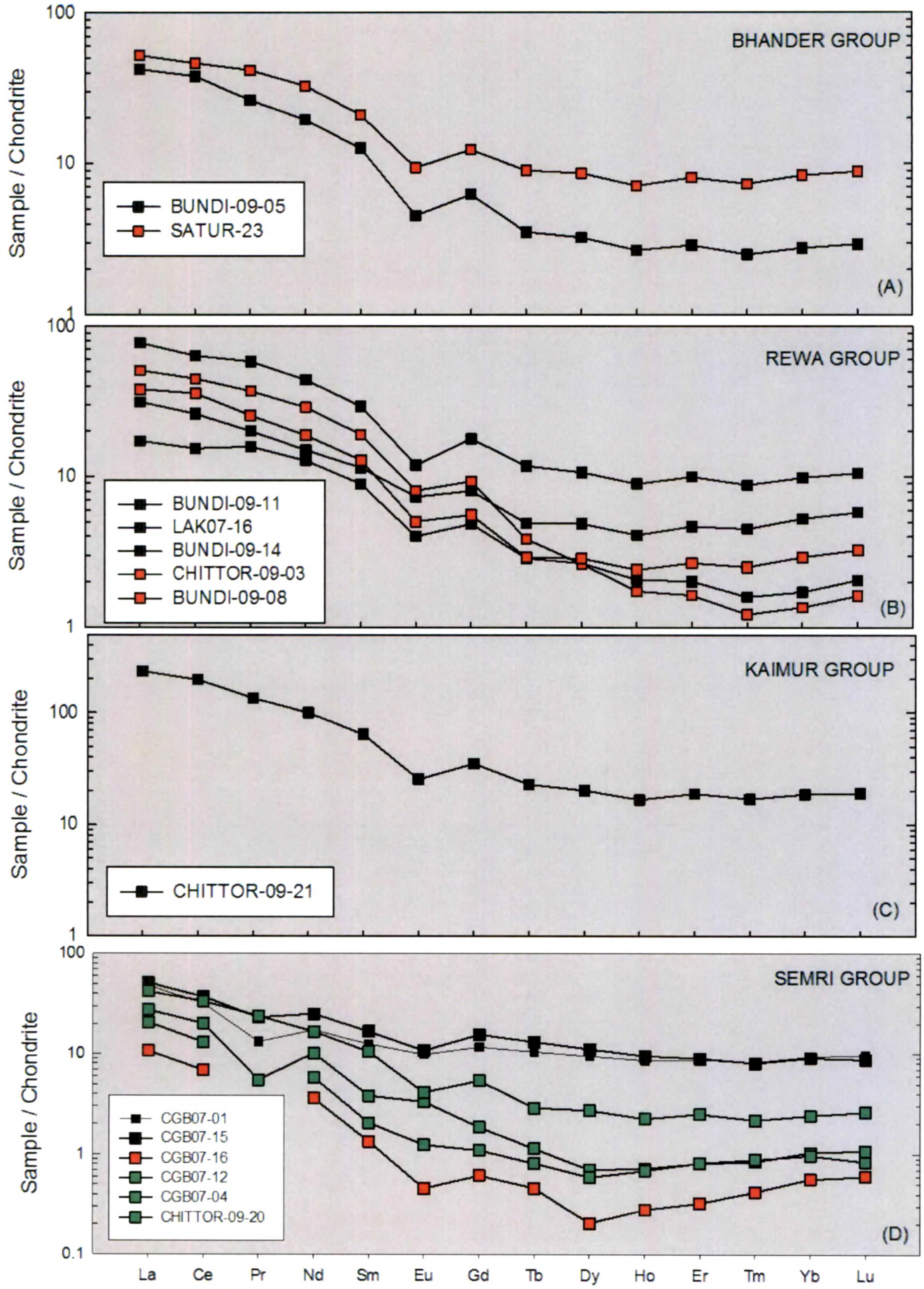

Fig. 3.12: Chondrite normalized REE patterns of sandstones from the Vindhyans of Rajasthan.

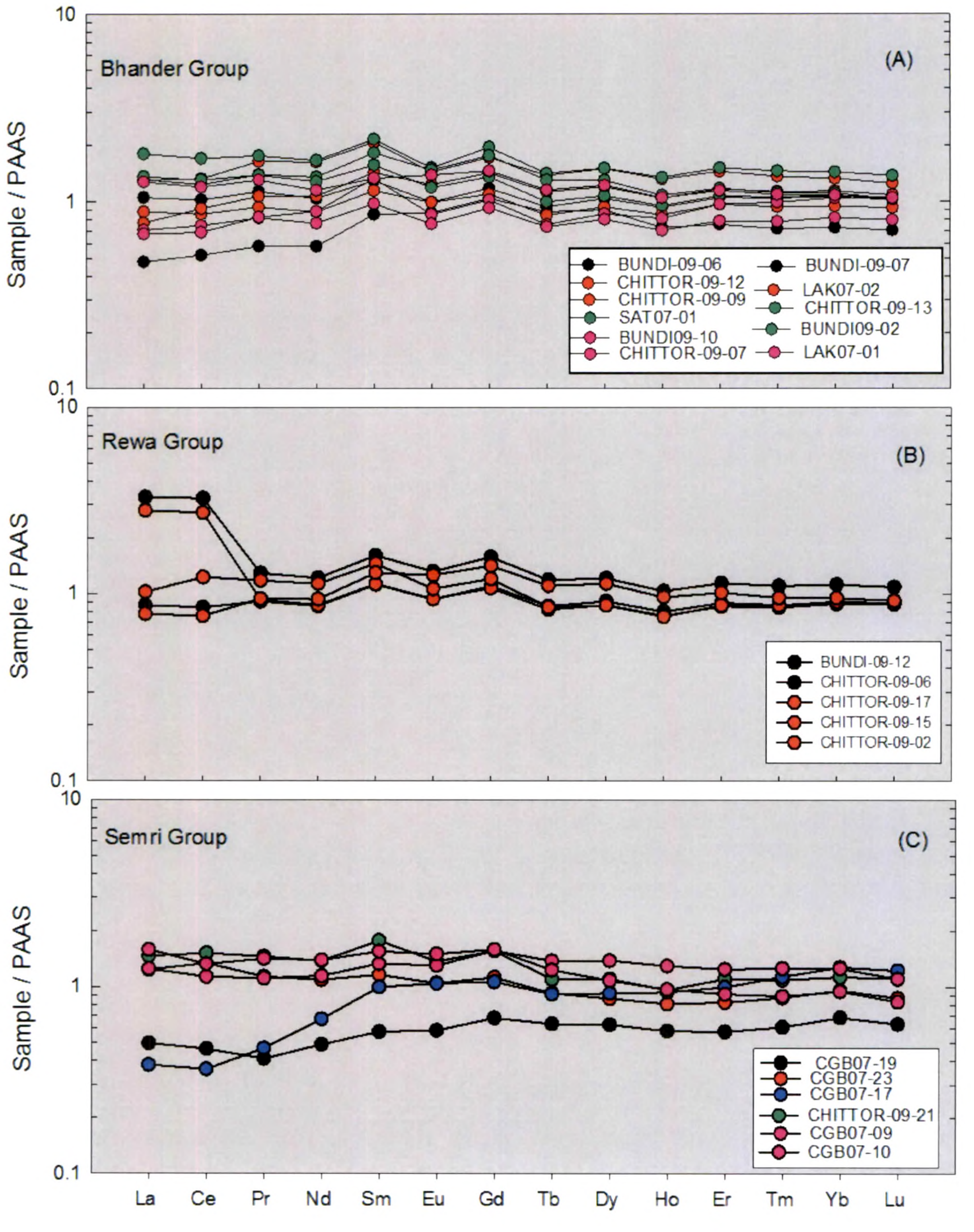

Fig. 3.13: PAAS normalized REE patterns for shale formations of the Vindhyan Supergroup, Rajasthan.

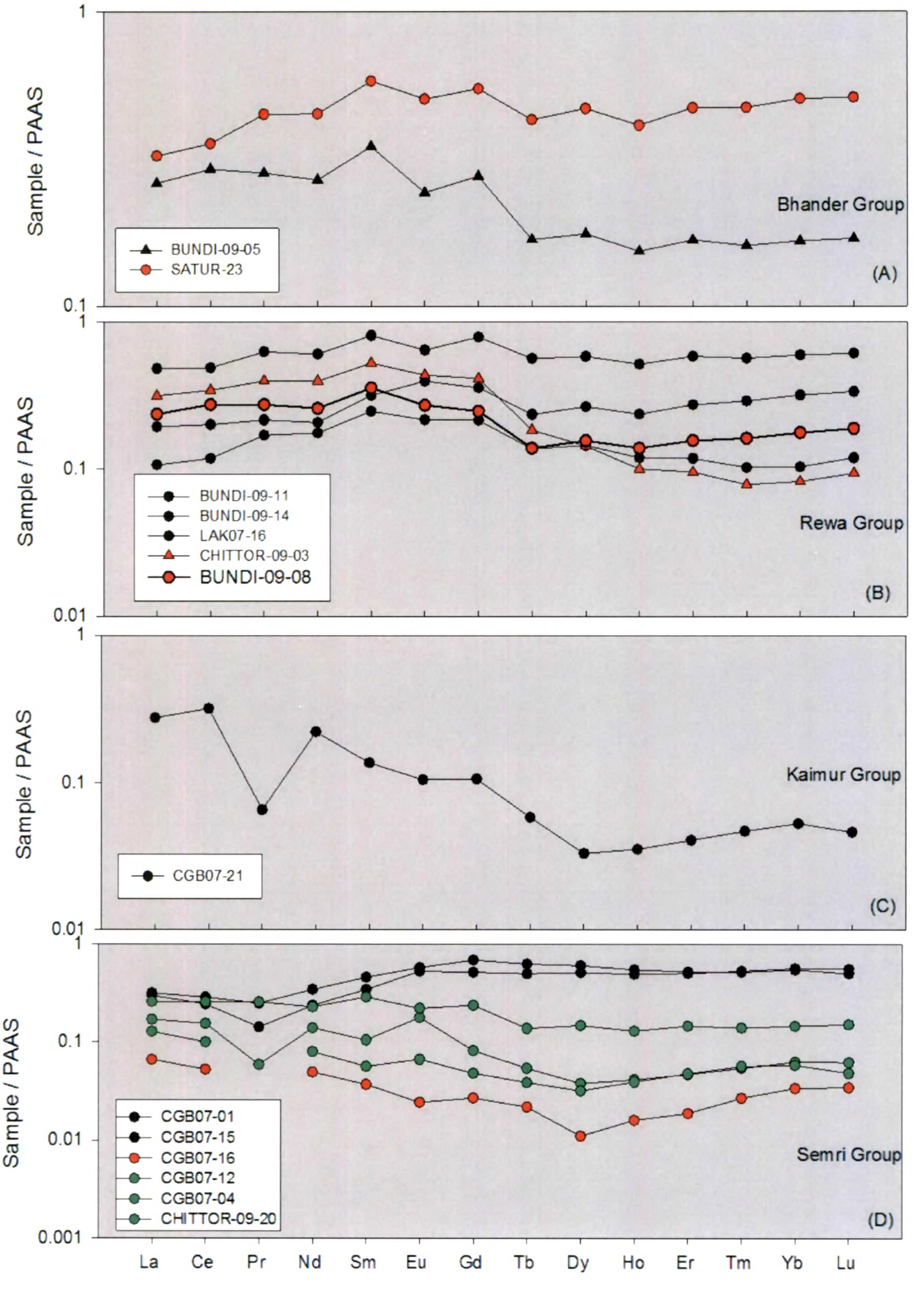

Fig. 3.14: PAAS normalized REE patterns for sandstone formations of the Vindhyan Supergroup, Rajasthan

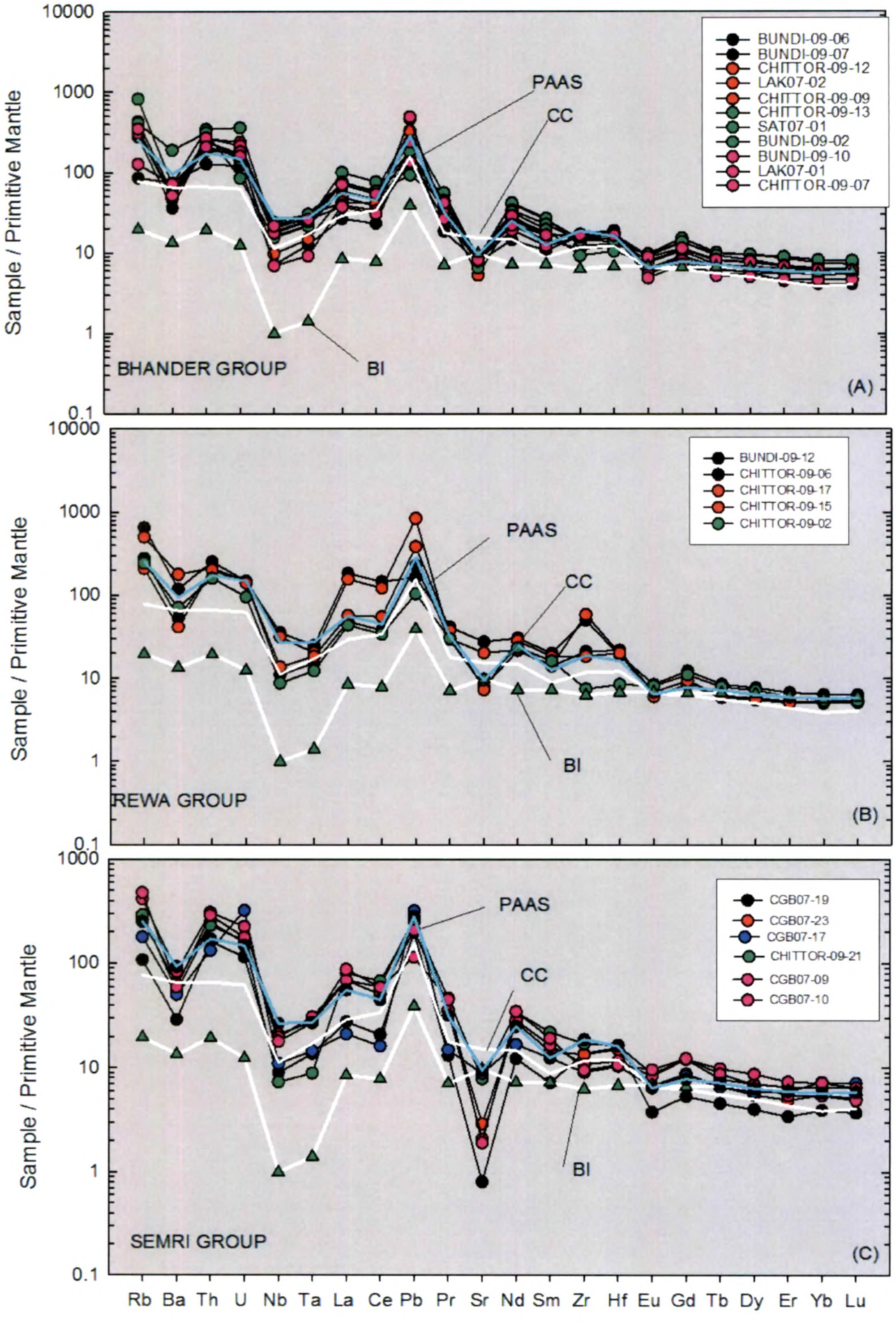

Fig. 3.15: Primitive Mantle normalized multi element spiderograms for the Vindhyan Shales. Also plotted are the patterns for PAAS, Average Continental Crust (CC) and average compositions of Barren Island lavas (BI: a modern volcano in the Andamans).

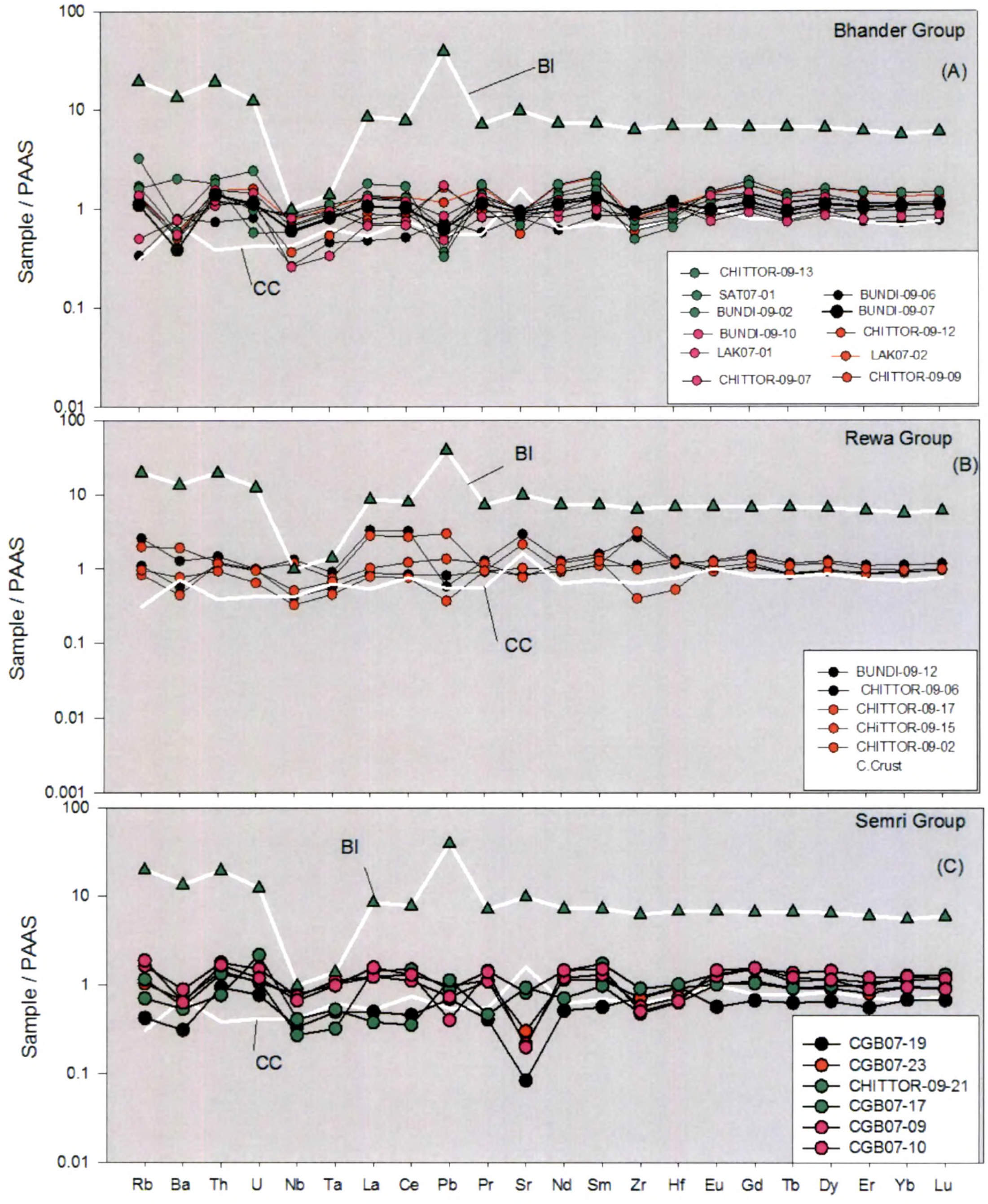

Fig. 3.16: PAAS normalized multi element spiderograms for the Vindhyan shales.

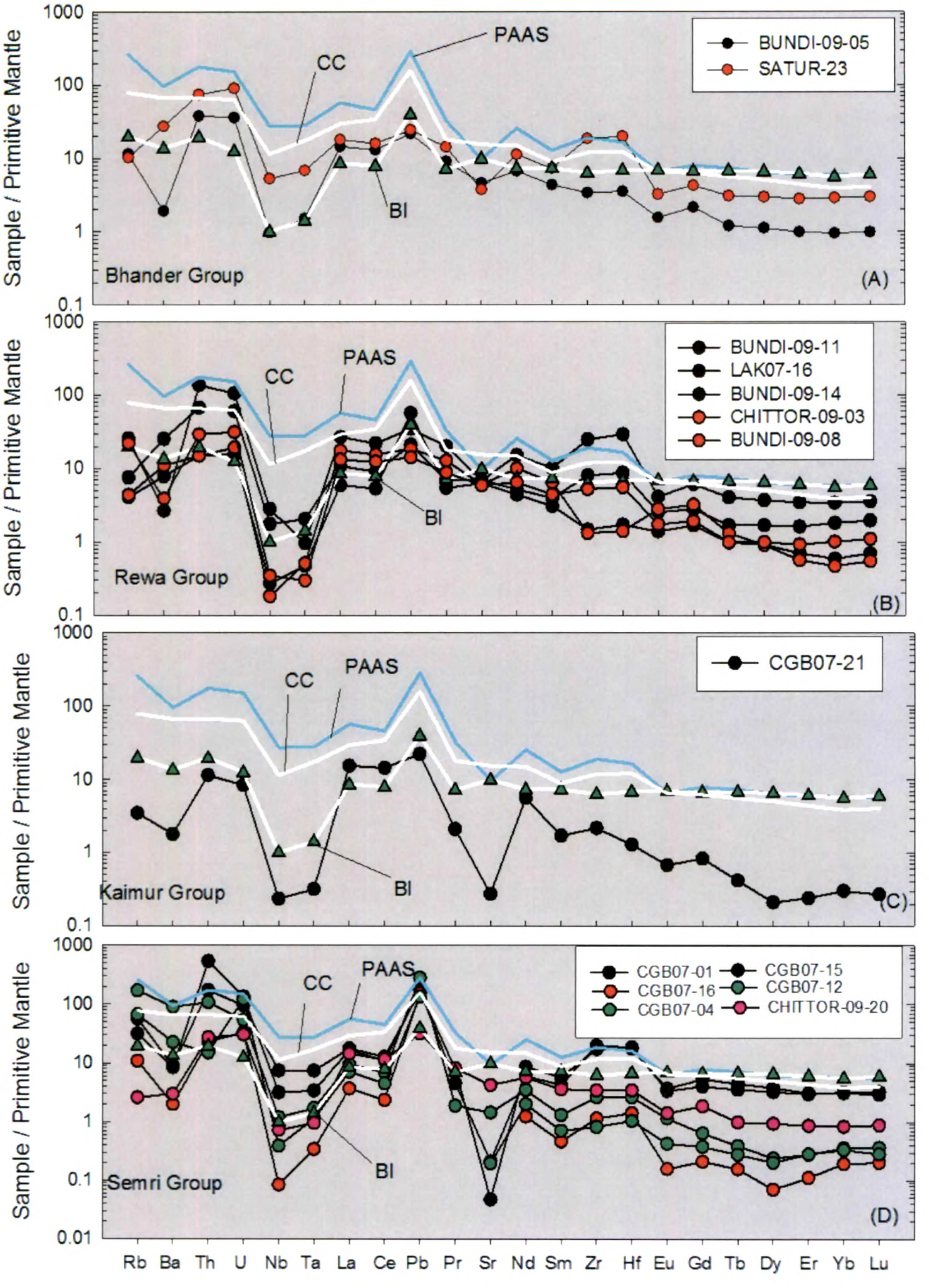

Fig. 3.17: PM normalized multi-element spiderograms for the Vindhyan sandstones.

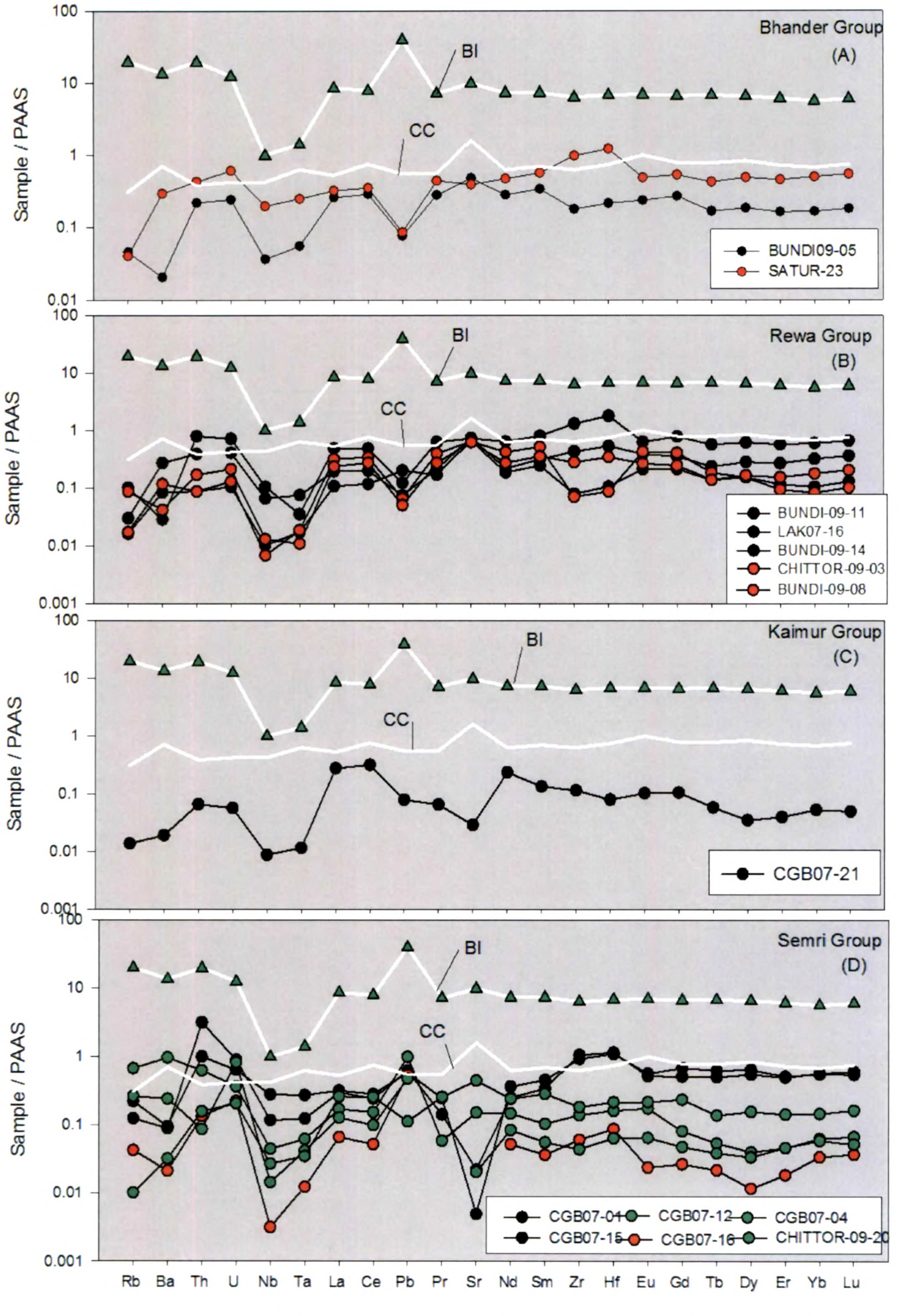

Fig. 3.18: PAAS normalized multi-element spiderograms for the Vindhyan sandstones.

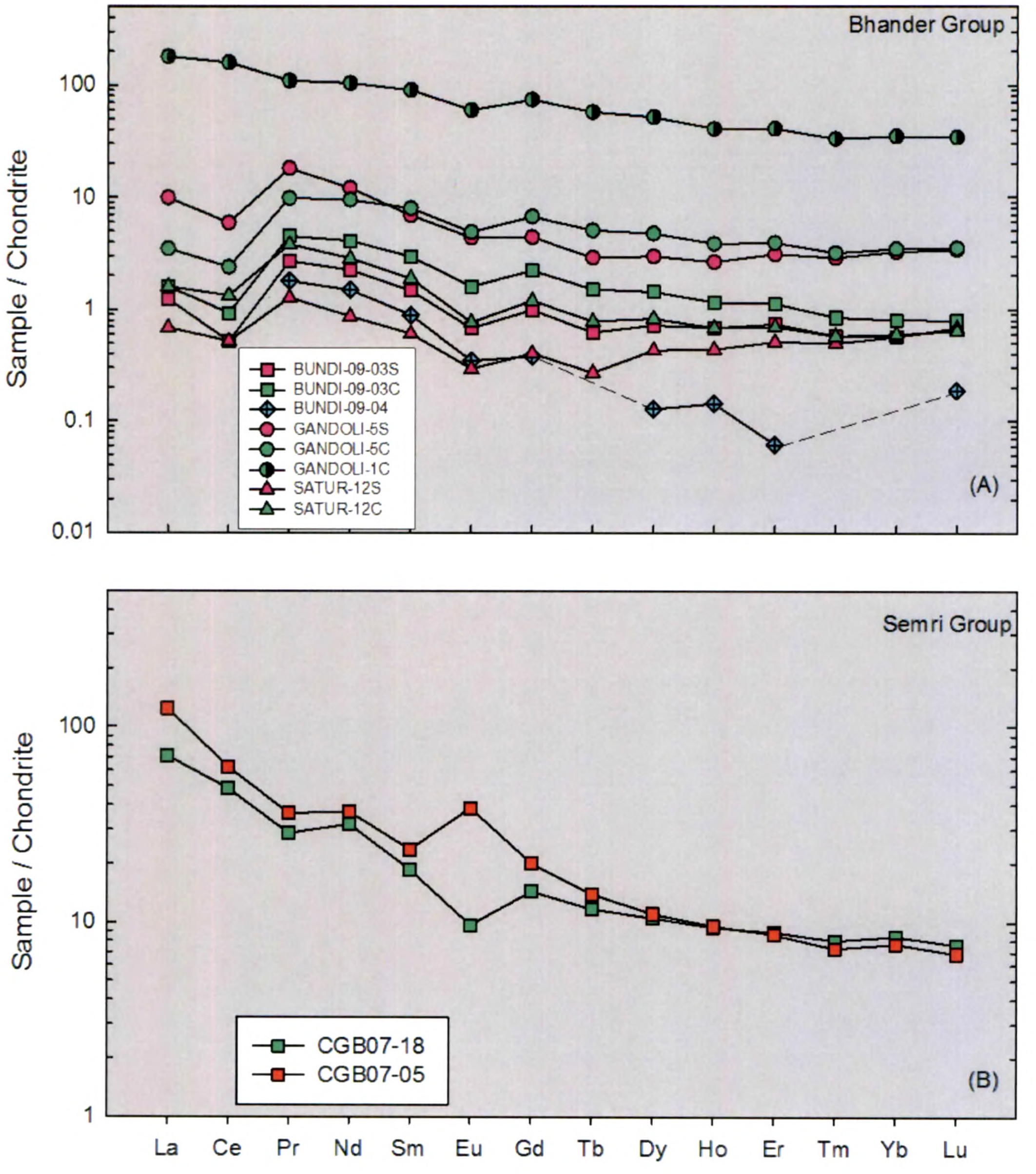

Fig. 3.19: Chondrite normalized REE patterns for carbonate (C) and silicate (S) fractions of limestone/dolostones of the Vindhyans of Rajasthan.

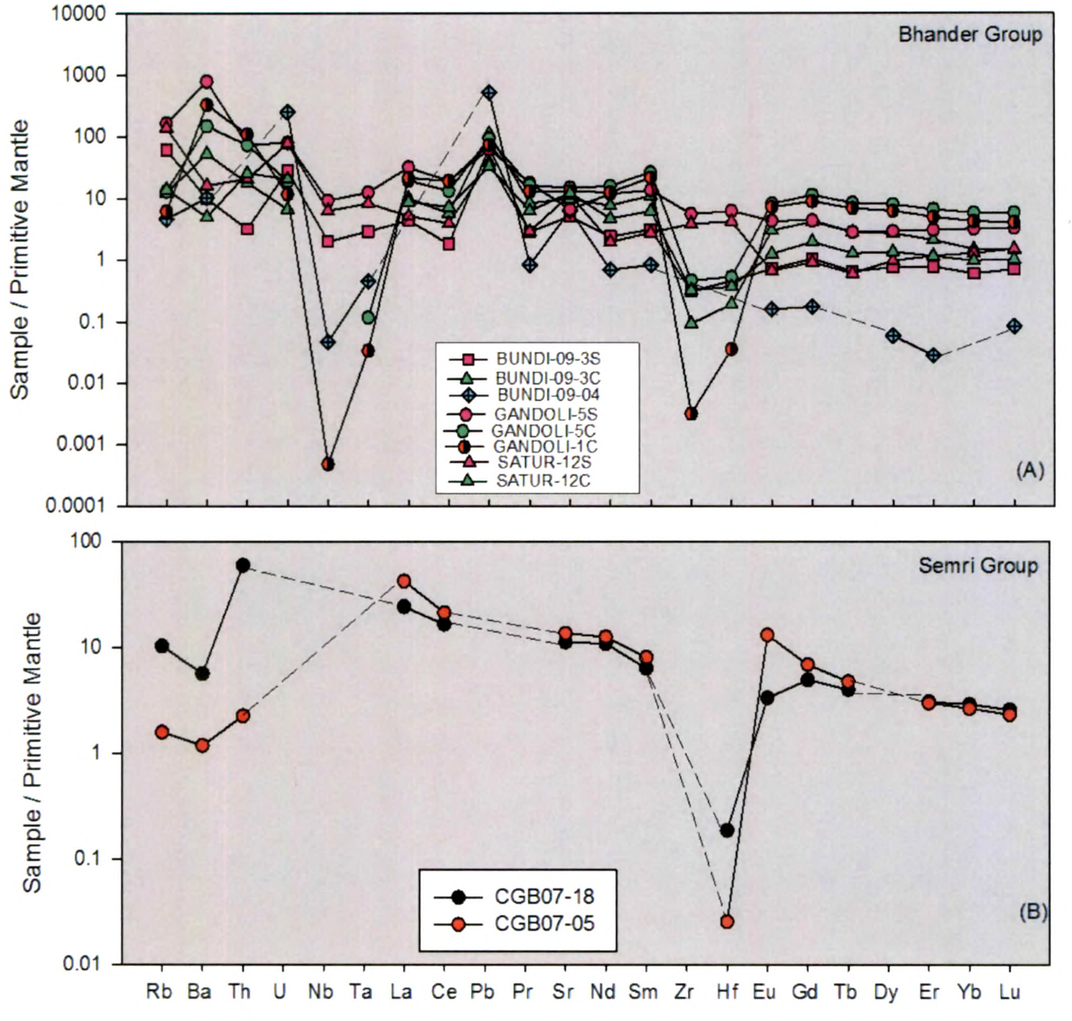

Fig. 3.20: The PM normalized multi-element spiderograms for carbonate (C) and silicate (S) fractions of the carbonate formations of the Vindhyans of Rajasthan.

more pronounced in material derived from subduction zone magmatism (Winter, 2001). For comparison with the modern day subduction zone magmatism an average composition (N=28) of lavas from Barren Island Volcano, Andaman Sea (Luhr & Haldhar, 2006) have also been plotted along with an average composition of continental crust (Taylor & McLennan, 1985). The typical shape of the patterns in all formations across the Vindhyans is similar to that of the Barren Island lavas. There are quite a few samples of shales that show depletion of several elements compared to PAAS (Fig. 3.16) and almost all the sandstones show large depletions in most elements compared to PAAS and Barren Island lavas (Fig. 3.18). The prominent depletion features that are characteristic of subduction zone mafic magmatism persisted even on PAAS normalized plots (Fig. 3.18), which clearly suggests that Vindhyan sandstones had contributions from subduction zone igneous rocks that existed in close proximity of the basin. We, therefore, postulate that a subduction zone setting existed in the vicinity of the basin, and sediments for the basin derived from magmatic arc that contained mafic igneous rocks like Khairmalia volcanics.

Limestone formations of the Vindhyan Supergroup are important members as they record changes in the depositional environment and patterns. Some of the limestones are impure and contain siliciclastic sediments. To shed some light on the source of non-carbonate matrix, these rocks also are analyzed for their trace element contents. Figure 3.19 and 3.20 show chondrite normalized REE patterns and PM normalized trace element patterns in these rocks. These limestone formations have high REE contents in both carbonate and silicate fractions (Fig. 3.19), which suggest incorporation of REE into carbonate matrix during deep burial diagenesis and or recrystallization. Interestingly, the silicate fractions in these limestone show Nb, and Ta depletions and Pb enrichments (Fig. 3.20) similar to those observed in shale and sandstone formations, which suggest that the clastic sediment sources did not change much even when the carbonate was getting deposited.

Trace element ratios such as Nb/Ta, Zr/Sm and Ce/Pb can also be used as tracers for sediment sources (Miller et al., 1994). These ratios in the Vindhyan sediments of

Rajasthan also support their derivation from island or magmatic arc igneous rocks and their derivatives (Fig. 3.21 and 3.22). To further characterize the sources of siliciclastic sediments in the Vindhyan Supergroup of Rajasthan a bivariate plot of Chondrite normalized ratios: La/Yb versus Yb/Gd has been utilized (Fig. 3.23). A three component mixing envelope is generated using the Khairmalia Tholeiites, older metavolcanics from the Hindoli Group and the Berach Granite as end members. We observed that most of the Vindhyan sediments from Chittorgarh and Bundi districts fall within this envelope, which suggests that the surrounding rocks to the west and south of the Vindhyan Basin in Rajasthan played a major role in supplying sediments for the supergroup. Sediments from mafic igneous rocks dominated the Upper Vindhyans.

An attempt was made to decipher existence of any temporal change in contribution from felsic and mafic components to the Vindhyans using the elemental ratios La/Th and Th/Yb (Fig. 3.24). In general, La/Th increases and Th/Yb decreases with the increase in incorporation of mafic/basic igneous materials (McLennan et al., 1980; Wang et al., 1986). Our observations (Fig. 3.24) suggest that the contributions from mafic igneous rocks started to rise around the upper part of the Semri Group and become very strong during the deposition of the Kaimur Group (La/Th=11 and Th/Yb=6.5) and in the Rewa Group (La/Th=3.8 and Th/Yb=6.2).

All the geochemical results from Vindhyan sequences of Rajasthan suggest that these were possibly deposited in a foreland basin developed adjacent to a subduction zone. The presence of Khairmalia Andesite, an arc derived lava flow, at the base of the Vindhyans in Chittorgarh region supports the above hypothesis. The subduction zone or zones might be located within the Aravalli craton. The materials for the Vindhyans were clearly derived from the Aravalli-Delhi Supergroups, along with other basement rocks which were exposed on topographically higher regions. Such a scenario is also supported by the field based sedimentological studies on the Vindhyan basin that indicate that basin was open from the west (Banerjee, 1974). In fact, the Porcellanite Formation in the Semri Group in the Son Valley has also been identified as a direct product of arc volcanism, and it has been proposed that the eastern margin of the Vindhyan Basin in the Son valley was developed as a foreland basin with southerly dipping subduction of oceanic plate attached to the Bundelkhand craton under the Bhandara craton in the south (Chakrabarti et al., 2007).

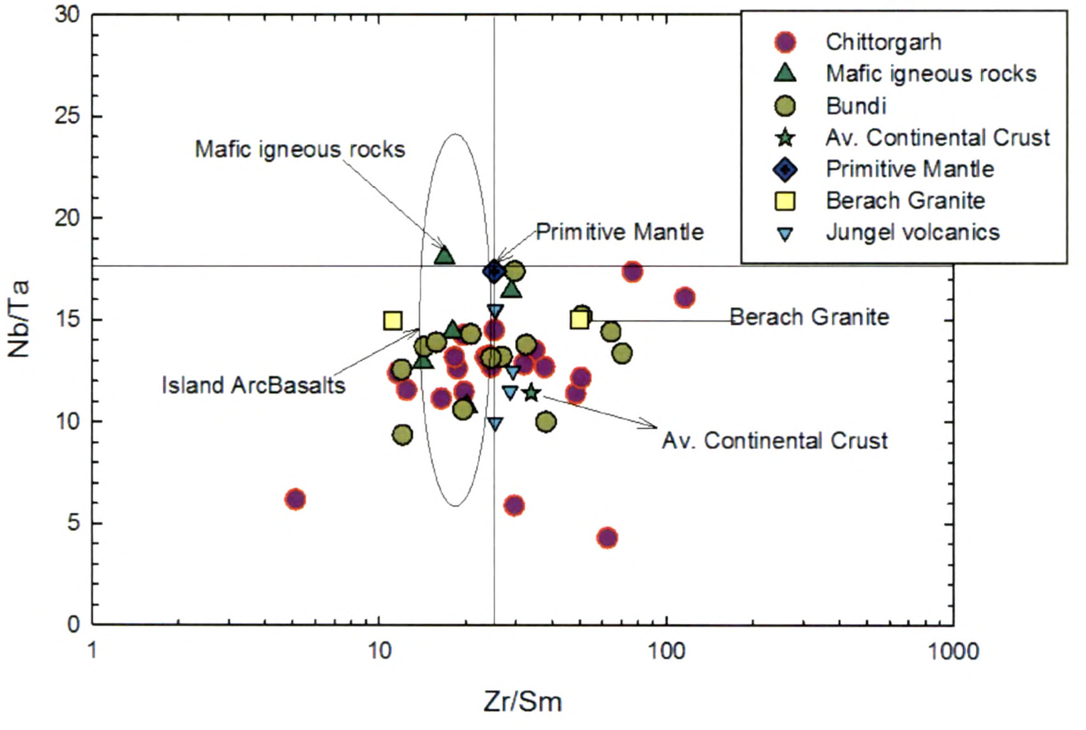

Fig. 3.21: Nb/Ta vs. Zr/ Sm variation in Vindhyan sediments and pre-Vindhyan mafic igneous rocks, Berach Granite and Jungel volcanics. Fields are after Foley et al. (2002).

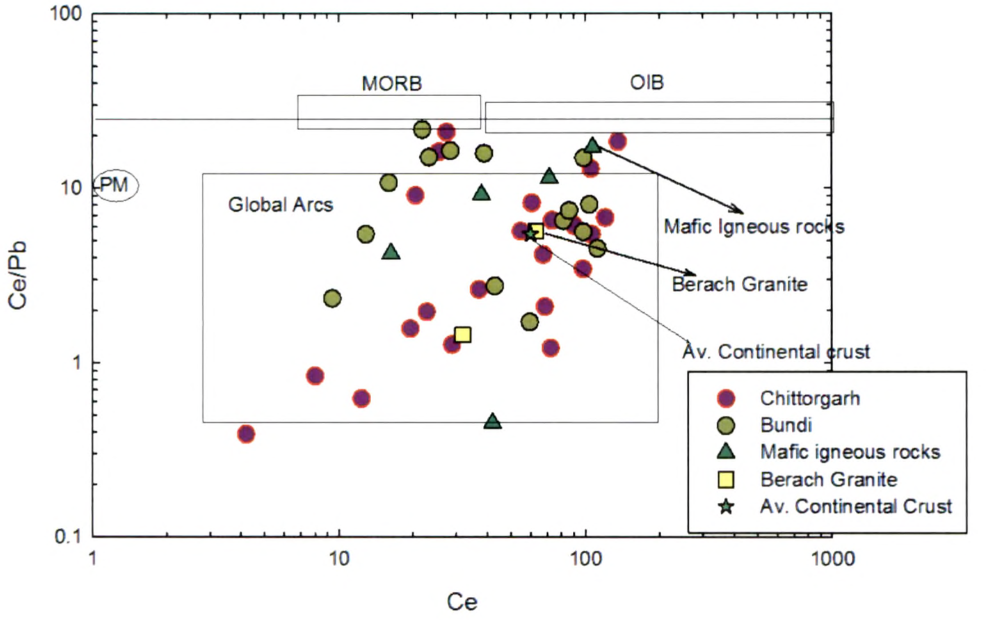

Fig. 3.22: Ce/Pb versus Ce in Vindhyan sediments from various sectors of the basin. Also plotted are the data from pre-Vindhyan granite, mafic igneous rocks and average continental crust. Fields are after Foley et al. (2002).

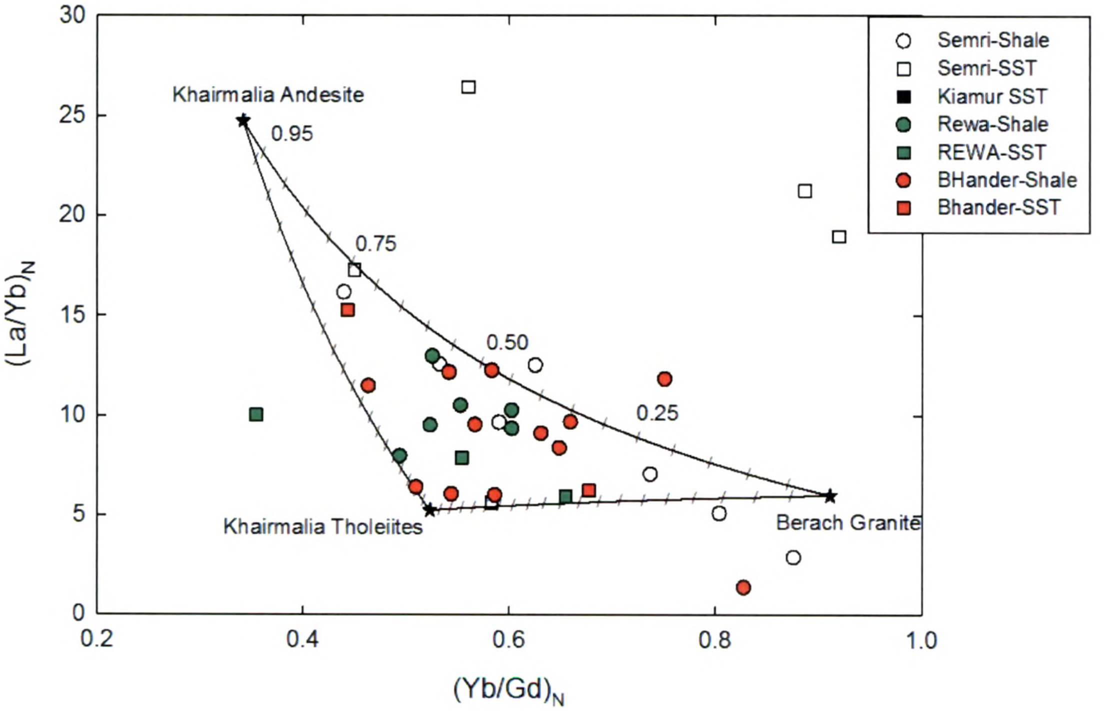

Fig.3.23: Chondrite normalized La/Yb versus Yb/Gd plot for Vindhyan sediments superimposed on model curves for mixing between three end members.

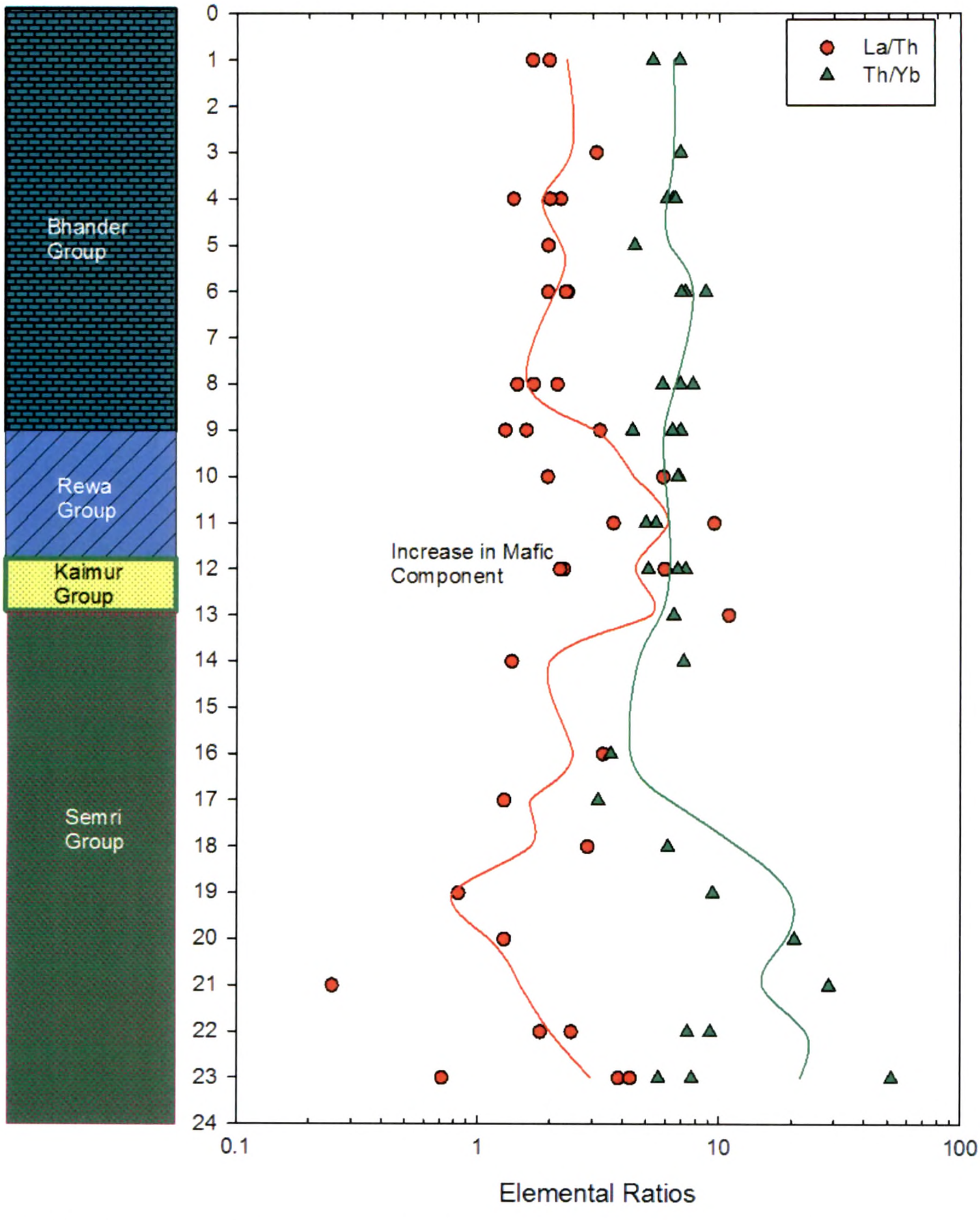

Fig. 3.24: La/Th and Th/Yb profiles along the startigraphical column of the Vindhyan Supergroup, Rajasthan. The scale along the depth/height profile is arbitrary. The lines are drawn using a 3-points average statistics.

3.2.2.4 *The Radiogenic isotope studies*

The radiogenic isotopic studies of Nd and Sr have been used in deciphering the source compositions of the detrital sedimentary rocks, using their chemical properties as well as the advantages of the radioactive decay of ^{147}Sm to ^{143}Nd and ^{87}Rb to ^{87}Sr. McCulloch and Wasserburg (1978) suggested that the Sm/Nd ratios of shale and other sediments are constant and similar to their parent rocks and it does not change appreciably during sedimentary processes (as discussed earlier in trace elements section) and hence Sm-Nd model dates of sedimentary rocks relative to Chondritic Uniform Reservoir (CHUR) or Depleted Mantle (depleted in large ion lithophile elements) are ages of mantle extraction of the original igneous source rocks from which the first sediments were derived. This aspect of the Nd-isotope systematics helps us in understanding the provenance. The Rb/Sr ratios in shale are highly variable due to the absorption of Rb by clay minerals and mostly higher than their parent rocks, and Sr isotopes are less reliable, particularly for very old rocks, in provenance determination. The Sm-Nd model dates of sedimentary rocks can be seen as time elapsed since the Nd separation from CHUR or DM. Hence the model ages are "crustal residence ages" and could be used for understanding crust mantle interaction through the time. The crustal residence ages of the Proterozoic and Phanerozoic shales are generally older than their depositional ages suggesting that the recycled crustal material which separated from CHUR or DM long before the formation of their parent rocks, got incorporated in shales. These ages decrease whenever young volcanic materials get mixed with older terrigenous sediments (Faure, 1986).

The Sr-isotope data from the Vindhyan Supergroup suggest that the highly radiogenic Sr is present in almost all the siliciclastic formations, while in limestones and dolostones it is moderately radiogenic. The obsereved $^{87}Sr/^{86}Sr$ variation is between 0.70818 (Blawan Dolostone) and 1.07899 (Khardeola Shale). A histogram of

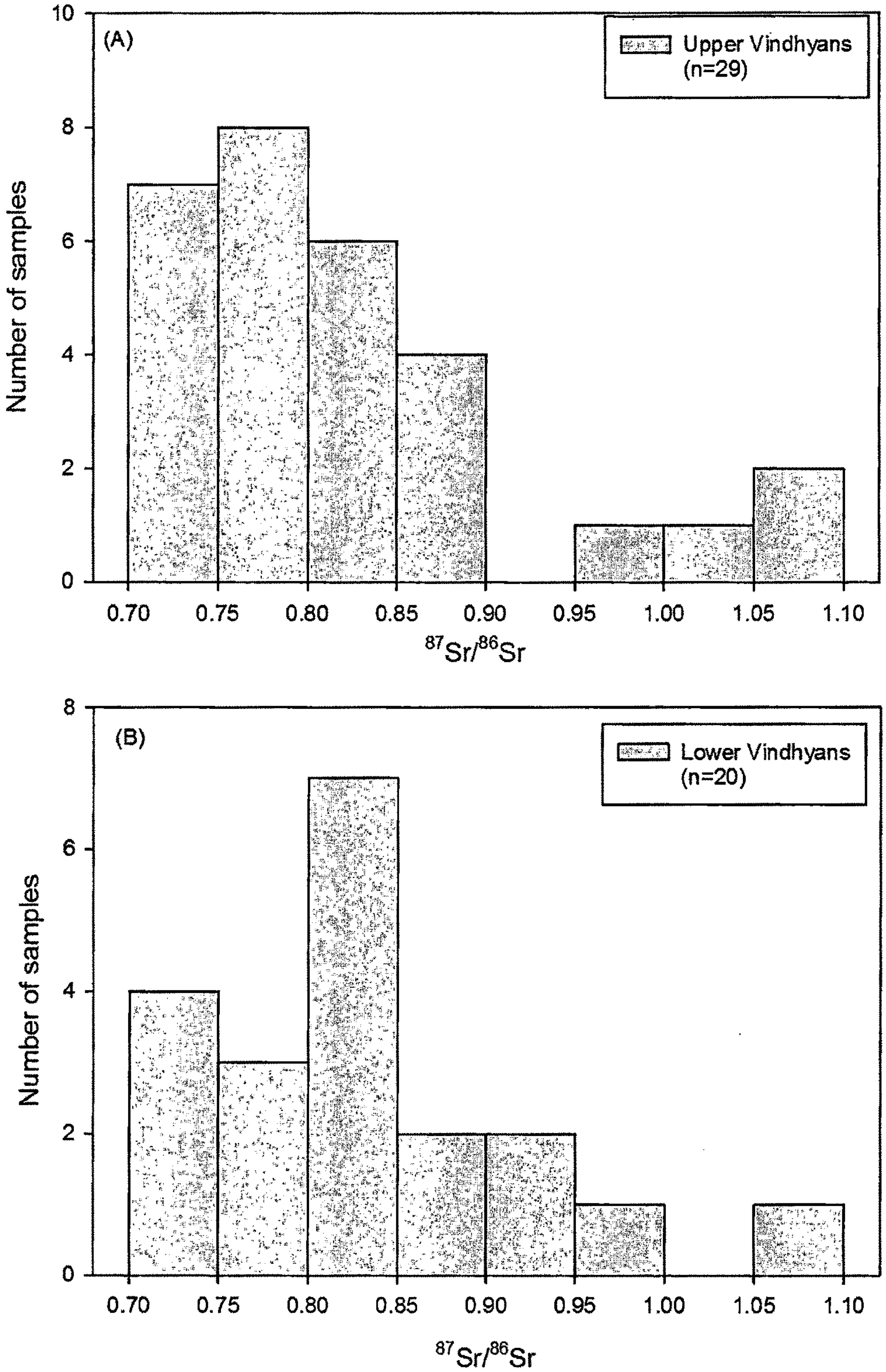

Fig. 3.25: Histograms showing frequency distribution of $^{87}Sr/^{86}Sr$ ratios in the Upper Vindhyans (A) and the Lower Vindhyans (B) of Rajasthan.

$^{87}Sr/^{86}Sr$ ratios variations in the Vindhyans of Rajasthan is presented in Fig. 3.25 (A: Upper Vindhyans and B: Lower Vindhyans). From the frequency distribution pattern one can observe that the ratios are highly radiogenic and values for the Lower and the Upper Vindhyans overlap. Threfore, extractions of any valuable information about provenance is difficult. The $^{87}Sr/^{86}Sr$ ratio, in sedimentary rocks, is readily affected by diagenesis and other fluid mediated port-diagentic processes due to the reactive nature of Rb & Sr, hence the primary $^{87}Sr/^{86}Sr$ rarely preserved.

$\varepsilon_{Nd}(0)$ of sediments in the Semri Group varies from -34.0 to -12.9, with the mean at -22.2, whereas that of the Kaimur Group falls in a narrow range between -18.2 and -17.1 with the mean at -17.7. The sediments from the Rewa Group have $\varepsilon_{Nd}(0)$ values varying between -17.8 and -14.6 with the mean at -16.2 and the variation in the Bhander Group is between -20.2 and -14.2, with the mean at -17.3. The range of values in the Rewa and the Bhander groups are overlapping. There are significant changes in the values of $\varepsilon_{Nd}(0)$ at the boundaries between various groups. Interestingly, it is difficult to differentiate the average ε_{Nd} values of the Rewa (-16.4) and the Bhander groups (-16.8) in the Chittorgarh sector, while in the Bundi sector they are different: ε_{Nd} -16.0 and -17.4, respectively. The main mode of $\varepsilon_{Nd}(0)$ variations in the Vindhyans of Rajasthan is at -17, and more than 70% of samples fall in the range of -20 to -14 (Fig. 3.26A).

The variations of average ε_{Nd} in various groups also reveal an important aspect of the depositional conditions in the Vindhyan Basin. The observation that there is an appreciable change in average ε_{Nd} with time suggests that each group (e.g. Semri, Kaimur, Rewa and Bhander) of rocks had distinct sediment sources, which in turn implies that either there were distinct breaks in sedimentation in the basin or there were major tectono-climatic changes in the provenances sbsequent to the deposition

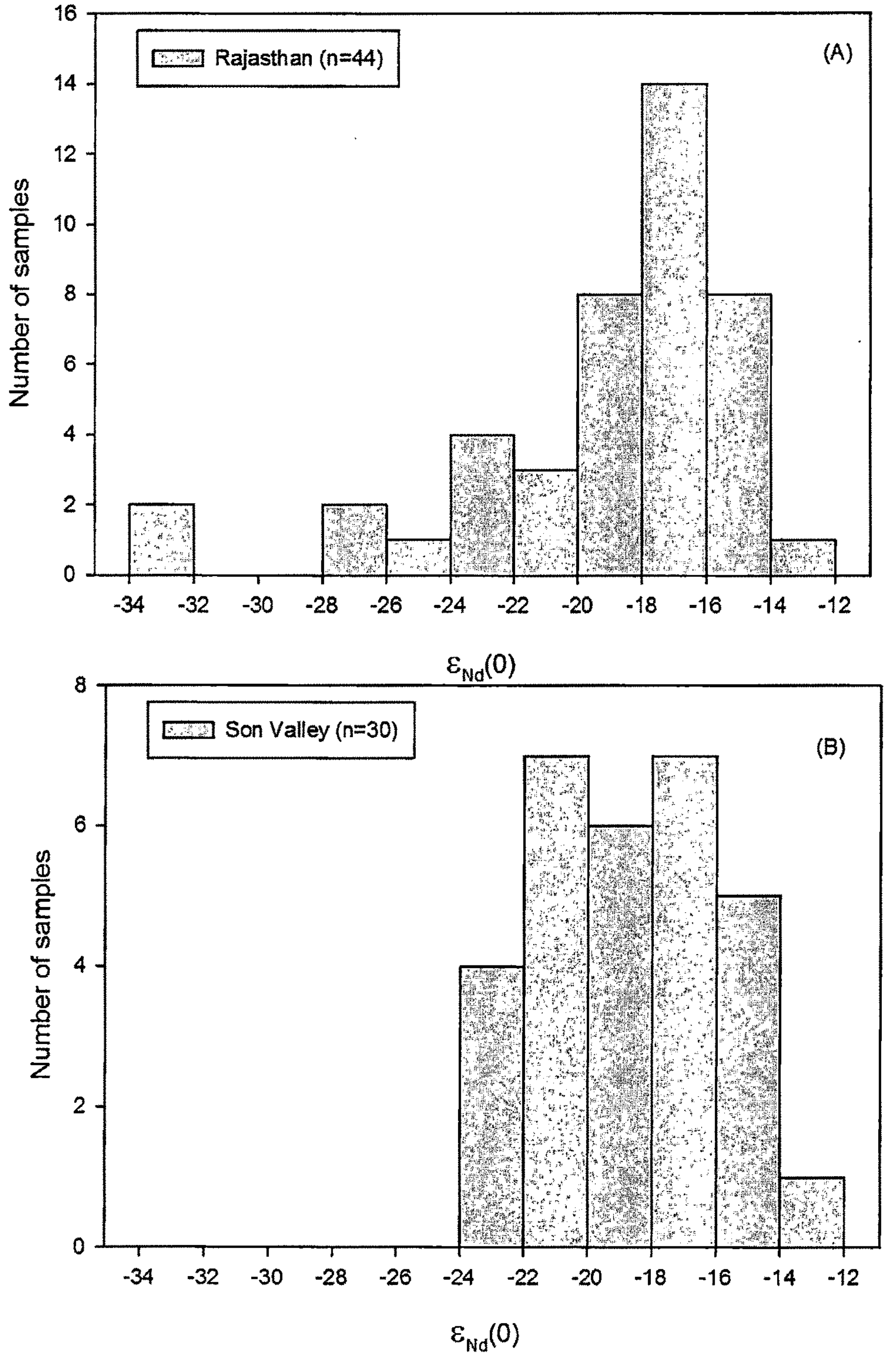

Fig. 3.26: Histograms showing frequency distributions $\varepsilon_{Nd}(0)$ in the Vindhyans of Rajasthan (A) and the Son Valley (B). Data source for the Son Valley: Chakrabarti et al. (2007).

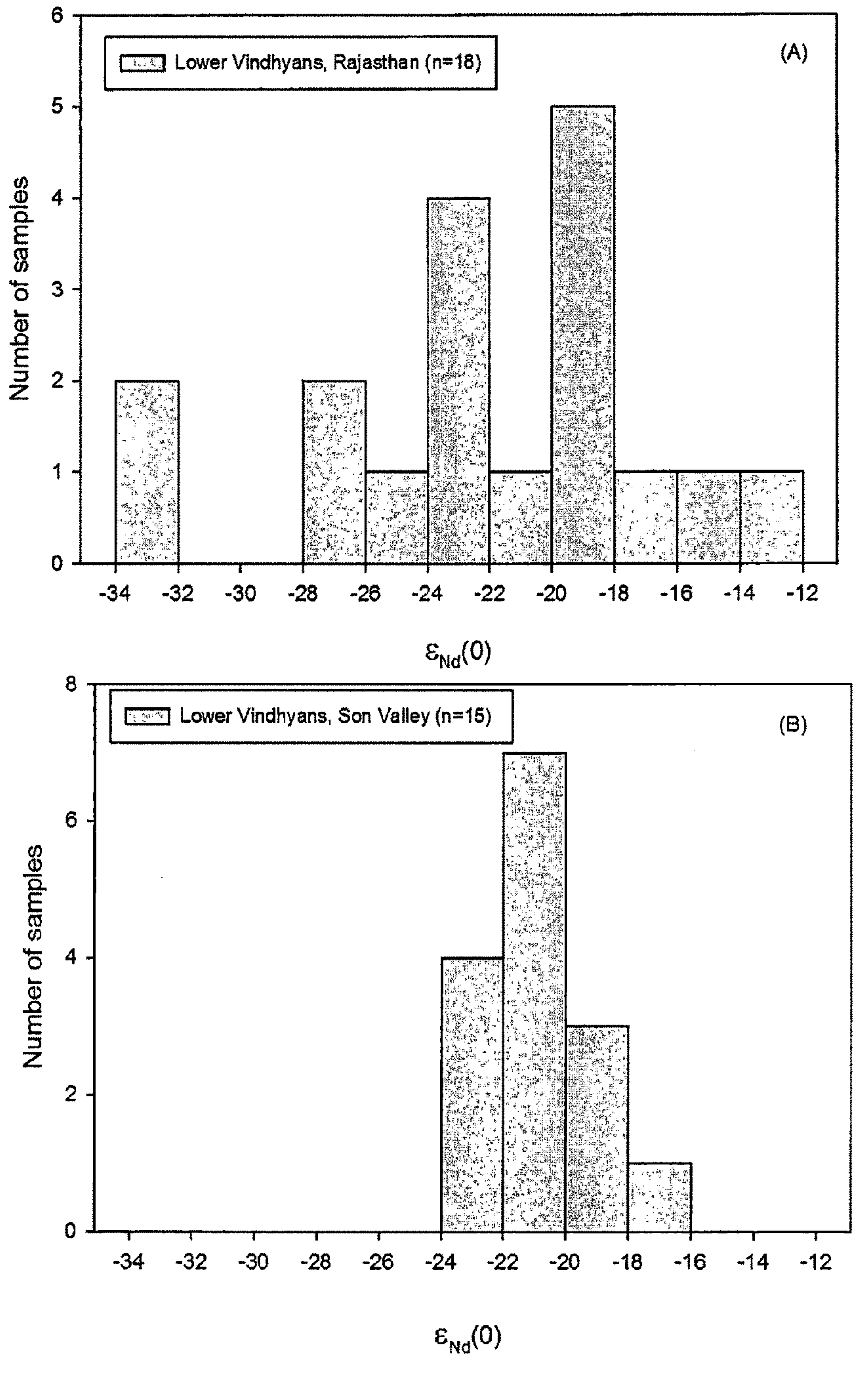

Fig. 3.27: Histograms showing frequency distributions $\varepsilon_{Nd}(0)$ in the Lower Vindhyan formations of Rajasthan (A) and the Son Valley (B). Data source for the Son Valley: Chakrabarti et al. (2007).

of each group of rocks. A closer look at the change in ε_{Nd} reveals that all the breaks, except for the one between the Semri Group and the Kaimur Group did not have a basin-wide presence. The distributions of the $\varepsilon_{Nd}(0)$ in the Vindhyans of Rajasthan (our data) are compared with that in the Vindhyans of the Son Valley (Chakrabarti et al., 2007) in Fig. 3.26 and 3.27.

We find that Chakrabarti et al. (2007)'s $\varepsilon_{Nd}(0)$ for Vindhyan formations in the Son Valley values are comparable to our data from equivalent formations in Rajasthan. Cakrabarti et al. (2007) reported $\varepsilon_{Nd}(0)$ values for the Porcellanite Formation in the range of -22.7 to -16.7, which overlaps with the range of values (-25.8 to -19.2) we find in equivalent formations in Rajasthan (Sawa Sandstones, Sawa Shales and Porcellanite). The average values of $\varepsilon_{Nd}(0)$ for the Semri Group calculated from Chakrabarti et al. (2007) is found to be -20.5, which is slightly higher than that of the Semri Group in Rajasthan (-22.2). The drastic difference in the epsilon value across the Lower and the Upper Vindhyan transition as observed by Chakrbarti et al. (2007) (from -20.5 to -17.4) is not seen in the Vindhyans of Rajasthan, where it changes from -16.7 in the Suket Shale to -17.1 in the Kaimur Sandstone. This observation corroborates the findings that unlike the Vindhyans of the Son Valley the transition between the Lower Vindhyans and the Upper Vindhyans in Rajasthan is not sharp. The overall variation in $\varepsilon_{Nd}(0)$ in Rajasthan(-34.0 to -12.9) is large in comparison to restricted variation in the Son Valley (-24 to -12). The Vindhyan sediments from both the sectors show a prominent mode at $\varepsilon_{Nd}(0)$ = -17 (Fig. 3.26). In both the sectors this mode appears only in the Upper Vindhyans. The $\varepsilon_{Nd}(0)$ of the Lower Vindhyans of Rajasthan show bimodal distribution, with modes at -23 and -19, whereas that of the Lower Vindhyans of the Son valley has a mode at -21. These observations suggest that a majority of the original sediments for the Upper Vindhyans of Rajasthan and of the son Valley came from similar type of magmatic rocks and that for the Lower Vindhyans in both the sectors came entirely from different types of sources.

Considering that the depositional age of the Lower Vindhyans is now well constrained in the Son Valley sector (e.g. Ray, 2006) we calculated $\varepsilon_{Nd}(T)$ for various equivalent/correlatable formations of the Semri Group in Rajasthan. The same exercise was also done for the formations of the Upper Vindhyans assuming approximate ages for them. The data presented in form of histograms in Fig. 3.28. $\varepsilon_{Nd}(T)$ varies from -20.4 to +5.1 in the Vindhyans of Rajasthan. If we exclude one sample from the Suket Shale (CGB-07-22A) that has a $\varepsilon_{Nd}(T)$ value of -20.4, then the range of $\varepsilon_{Nd}(T)$ of the entire Vindhyans reduces to -14.4 to +5.1. $\varepsilon_{Nd}(T)$ goes on increasing as one follows the stratigraphic younging direction in the Lower Vindhyans, e.g. it increases to +2.4 in the Suket Shale from -9.9 in the Sawa Grit Formation. Such a change clearly points to the increased addition of sediments from juvenile material. The value of +3.1 in the Sawa Sandstone clearly indicates influence of young igneous sources.

$\varepsilon_{Nd}(T)$ for the rocks of the Upper Vindhyans were calculated assuming the following the depositional ages: 1) Kaimur Group: 1200Ma (the age of Bijaygarh Shale), 2) Rewa Group: 1000Ma (younger than the Kimberlite intrusion) and 3) Bhander Group: 750 Ma for the lower part and 650 Ma in the upper part (based on Sr-isotope stratigraphy). These assumptions are based on existing reliable geochronological information (Ray, 2006). The value $\varepsilon_{Nd}(T)$ for the Kaimur Group varies from +3.9 to +5.1 (av. +4.5), for the Rewa Group from -8.8 to -1.5 (av. -6.0) and for the Bhander Group from -12.7 to -3.5 (av. -7.8). Positive $\varepsilon_{Nd}(T)$ values clearly indicate a significant presence of juvenile mantle derived material in these sediments, whereas the high negative values indicate large continental crustal contribution.

The $f_{Sm/Nd}$, which is a measure of Sm and Nd fractionation with respect to Sm/Nd of CHUR, is −0.45 and -40 for the tow Berach granite samples and for the mafic igneous

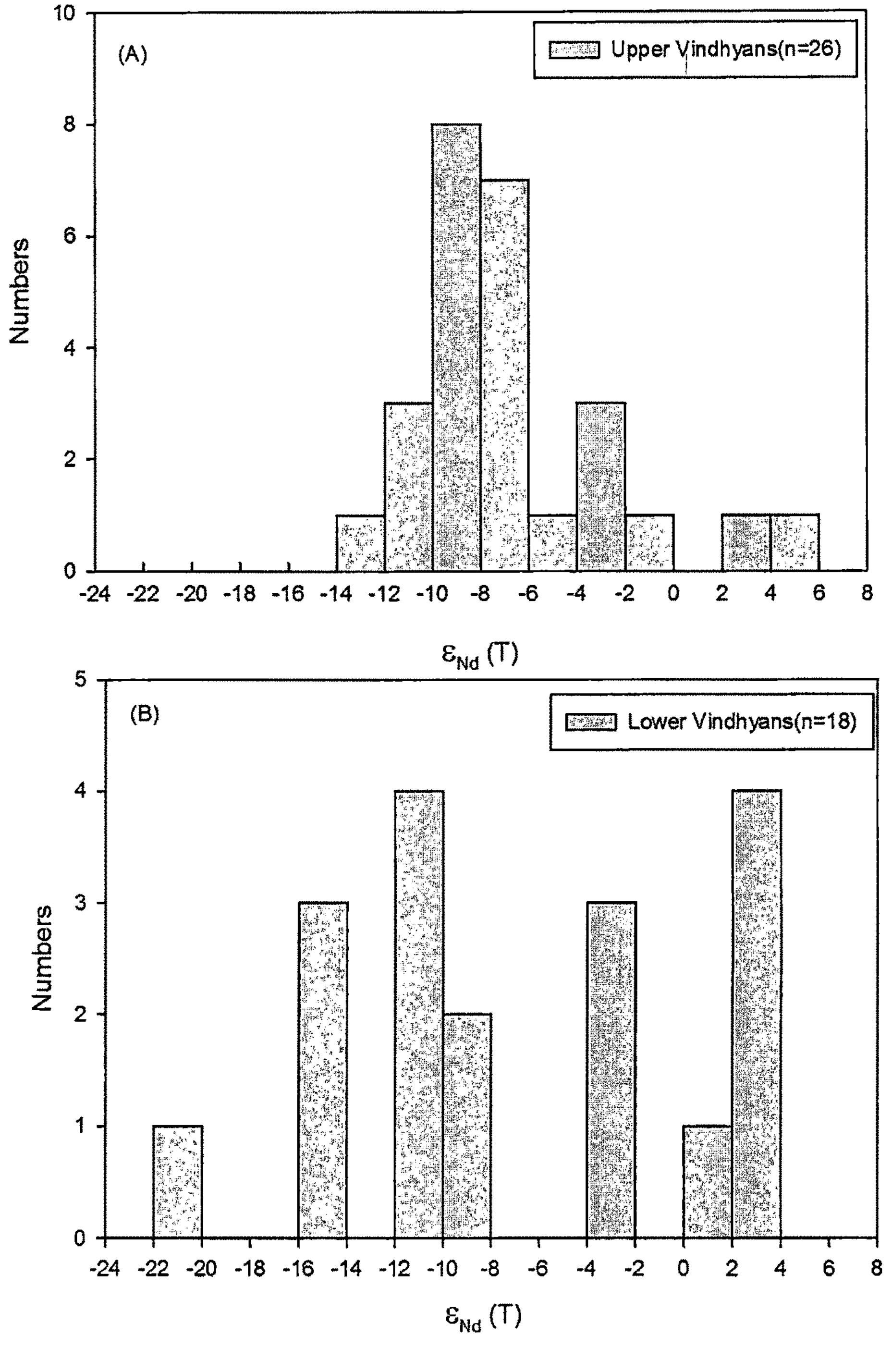

Fig. 3.28: Frequency distributions diagram for ε_{Nd}(T) in the Upper Vindhyan (A) and the Lower Vindhyans (B) of Rajasthan.

rocks it varies between -0.45 and -0.25. It varies between -0.64 and -0.25 (av. -0.41) in the Semri Group and decreases to -0.69 in the Kaimur Group. In the Rewa Group the value varies between -0.56 and -0.30 (av. -0.42) and in the Bhander Group between -0.62 and -0.24 (av. -0.50). These variations suggest that the source of material remained almost same for most part of the deposition of the supergroup, except for abrupt changes across the transitions between groups.

The calculated model ages (T_{DM}) for the Vindhyan formations from Rajasthan are plotted in histograms in Fig. 3.29. T_{DM} age of a sedimentary rock essentially represents an average mantle extraction ages of the original igneous protoliths from which the sediments have been derived, and therefore are older than the age of deposition. The distribution of T_{DM} in the Lower Vindhyans shows a prominent mode at ~1500 Ma. The distribution pattern shows that there is a general decrease in T_{DM} from the Lower to the Upper Vindhyans. The decrease/increase in T_{DM} or an increase/decrease in ε_{Nd} corresponds to an increased/decreased contribution of radiogenic Nd to the sedimentary sequences. The increase in ε_{Nd} can be attributed to incorporation of juvenile material or termination of contributions from old crustal sources. In general, the addition of juvenile sediments is associated with tectonic activity, in the form of crustal uplift or renewed volcanism (Andersen and Samson, 1995). It is generally observed that the Archean and early to mid-Proterozoic sediments have T_{DM} ages close to their stratigraphic ages, and in the case of younger sediments these ages are much older (as much as 2.0 Ga) than their stratigraphic ages (O'Nions et al., 1983).

T_{DM} distributions in Rajasthan and that in the Son valley (Fig. 3.30) show a prominent mode at ~2300 Ma, which could be attributed to derivation of sediments from two prominent igneous sources; one from a >2300 Ma source and other from a <2300 Ma source. Interestingly, T_{DM} values of this mode are observed predominantly in the formations of the Lower Vindhyans. In Rajasthan, this value could be attributed to the mixing of sediments derived from the ~2500 Ma old basement rocks (e.g. Berach granite) with those derived from younger igneous rocks, the ~1850 Ma old Hindoli Group and/or the Khairmalia volcanics, whereas, in the Son Valley the sediments appear to have been derived from the ~2500 Ma old basement (e.g. Bundelkhand Granite) and the ~1630 Ma old rhyolitic volcanics that formed the Porcellanite Formation.

Interestingly, the model age (T_{DM}) of the Kaimur Sandstone of Rajasthan is found to be the lowest (~1.3 Ga) while that of the same in the Son Valley is 2.5 Ga (Chakrabarti et al. 2007). The T_{DM} of the Kaimur Sandstone of Rajasthan appears to be close to its depositional age (~1200 Ma) as inferred from the available geochronological data (see Table 2.4).

The second and the highest mode in the T_{DM} distribution in Rajasthan is observed at ~ 1500 Ma (Fig. 3.29), which is seen only in this part of the Vindhyans, and mostly in the Upper Vindhyans. This age can be interpreted as mixing of sediments derived from various igneous sources: 1) the ~ 1850 Ma old Hindoli volcanics which is most prominent in the Pb-Pb age distribution of detrital zircons from the uppermost Vindhyan sandstone formation (Malone et al., 2008), and 2) other magmatic events as observed in the age distribution of detrital zircons (1020, 1140, 1260 and 1380 Ma, Malone et al., 2008) whose sources might be located within the Aravalli-Delhi fold belt. It might also be possible that the mixing of sediments from the Malani Igneous Suite (~750 Ma) and from the Hindoli Group of rocks or other unidentified sources whose zircons have been observed by Malone et al. (2008) could have generated the T_{DM} at 1500Ma in the Upper Vindhyans younger than 750 Ma. If true, this goes against the claim by Malone et al. (2008) that the Vindhyan Basin did not receive sediments from the Malani Igneous Suite (MIS) and therefore, is older than 1000 Ma. Here, it is to be noted that the population density curves (vs. age) in Fig. 15 of Malone et al. (2008) contain a small peak below 1000 Ma and therefore, their conclusion about the non-inclusion of material from MIS is not unequivocal. Furthermore, the appearance of zircons in sediments from magmatic sources depends on several processes including the distance between the source and basin,

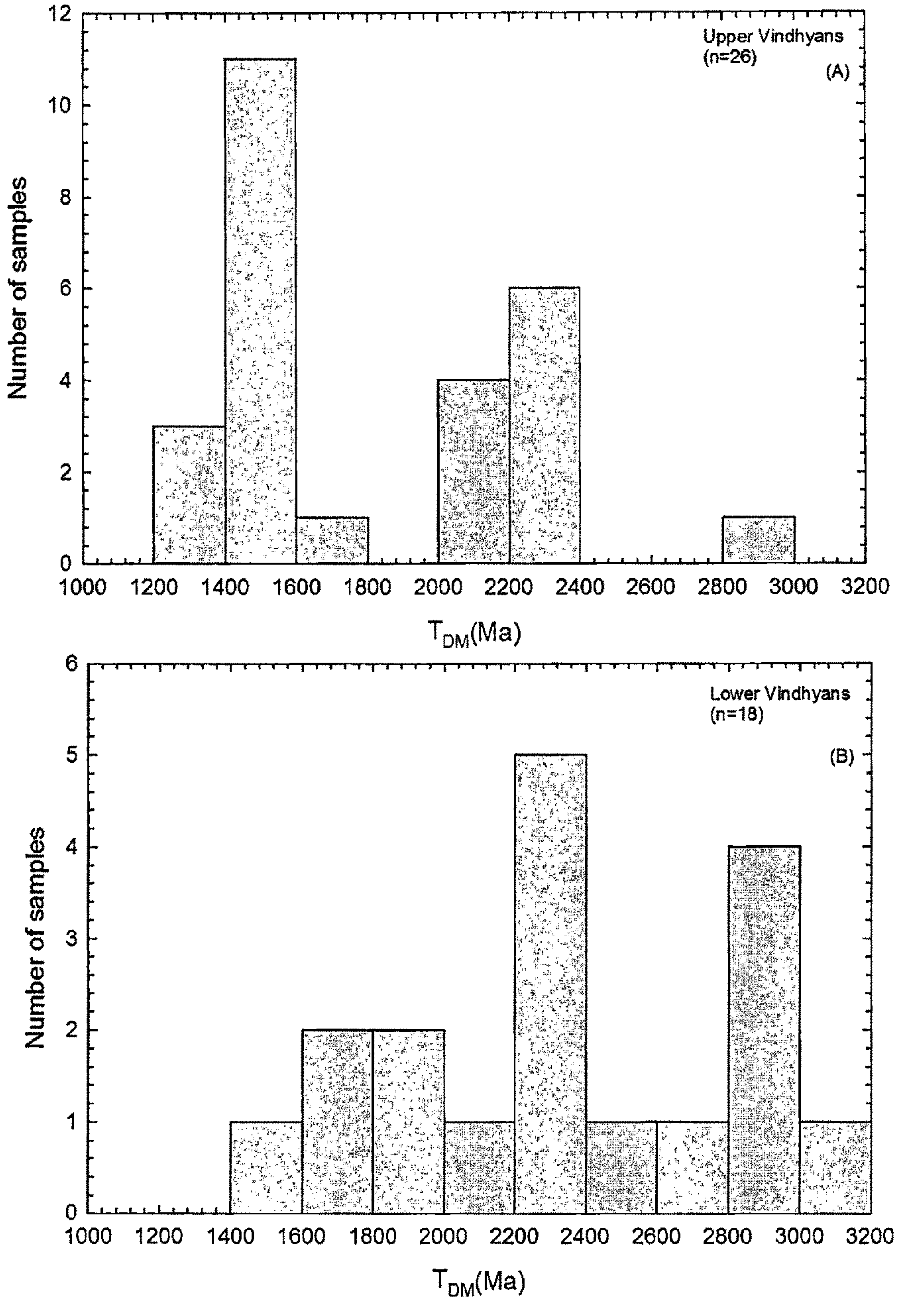

Fig 3.29: T_{DM} frequency distributions in the formations of the Upper Vindhyans (A) and the Lower Vindhyans (B) of Rajasthan.

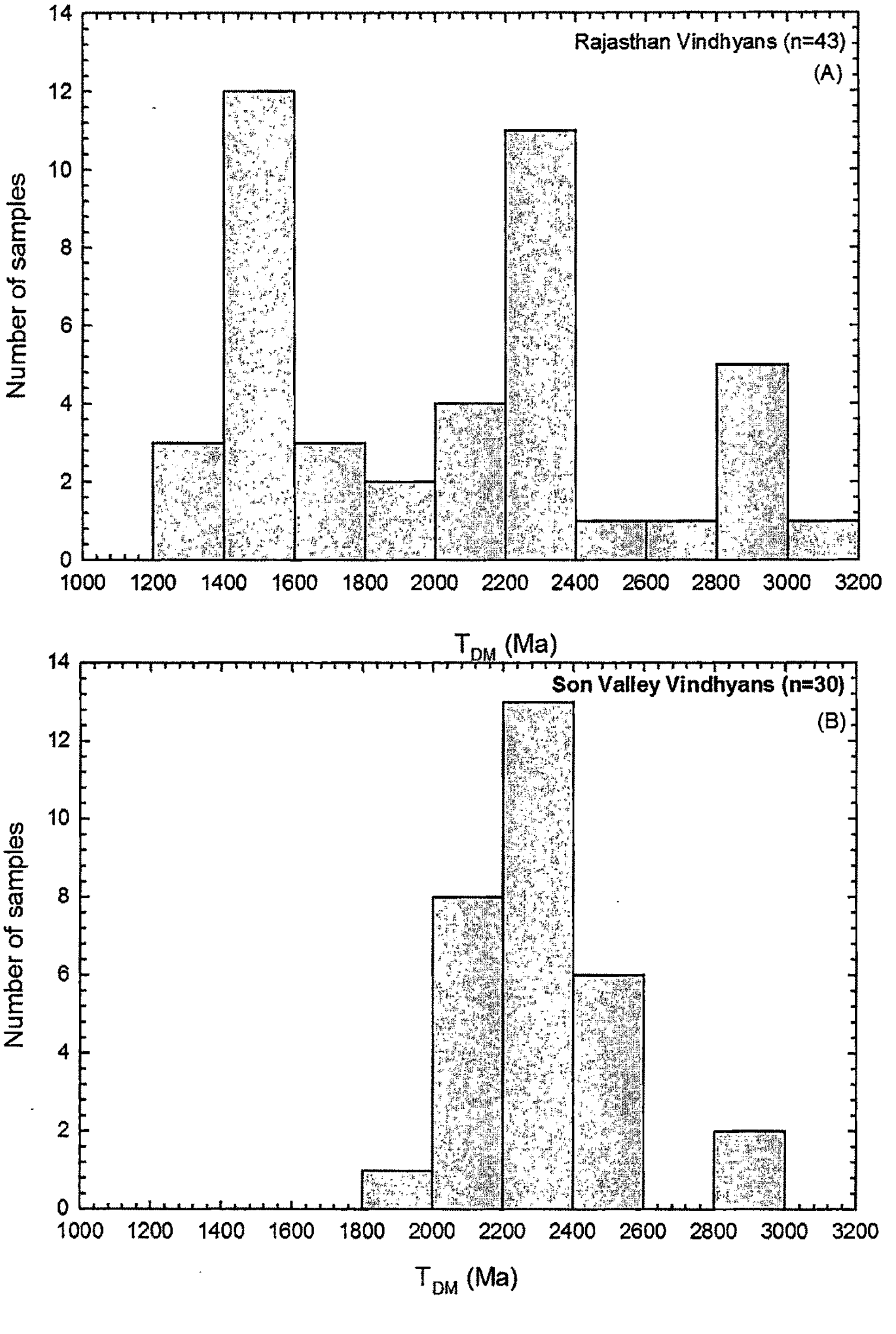

Fig. 3.30: Histograms showing T_{DM} distributions in the Vindhyans of Rajasthan (A) and of the Son Valley (B).

		Chittorgarh			Bundi			Son Valley		
		$\varepsilon_{Nd}(0)$	$\varepsilon_{Nd}(T)$	T_{DM}(Ma)	$\varepsilon_{Nd}(0)$	$\varepsilon_{Nd}(T)$	T_{DM}(Ma)	$\varepsilon_{Nd}(0)$	$\varepsilon_{Nd}(T)$	T_{DM}(Ma)
Upper Vindhyans	Bhander (<620 Ma)	-16.8	-9.7	2.3	-17.4	-6.6	1.6	-15.6	-9.8	2.3
	Rewa (~1000 Ma)	-16.4	-7.1	2.2	-16	-5.3	1.5	-17.8	-8.13	2.1
	Kaimur (~1200 Ma)	-17.7	4.5	1.3				-17.6	-5.8	2.2
Lower Vindhyans	Semri (2240-1600Ma)	-20.8	-6.7	2.4				-20.5	-14.3	2.4
	Khairmalia Basalt	-12.2	2.2	2.22						
	Andesite (2240-1850Ma)	-26.3	-5.7	2.85						
Archeans								-34	2.3	2.5
	Berach Granite ~2440 Ma	-32	-1.3	2.7						
		-30.2	-6.4	3.1						

Fig. 3.31: The variation of the average values of the $\varepsilon_{Nd}(0)$, $\varepsilon_{Nd}(T)$ and T_{DM} across the stratigraphical column and the basin.

hence the absence of zircons from MIS cannot be claimed as direct evidence against a younger age for the Upper Vindhyans. It is quite possible that the high mountain ranges of the Aravallis to the east of MIS created a barrier for any sediment (zircon) contribution from it to the Vindhyan Basin.

One of the most important observations in the T_{DM} distributions is that the formations in the Son Valley have T_{DM} ≥1800 Ma, whereas that in Rajasthan is as low as ~1200 Ma (Fig.3.30). This observation means that either the sources in the west (Rajasthan) did not contribute sediments to the deposition of Vindhyans in the east (Son Valley), or that there existed a physical barrier within the basin which did not allow sediments to move from west to east.

Fig. 3.31 presents the three important parameters ($\varepsilon_{Nd}(0)$, $\varepsilon_{Nd}(T)$ and T_{DM}) related to the Nd-isotope systematics across the stratigraphical column in various sectors of the Vindhyan Basin. As discussed earlier the average values of ε_{Nd} for various groups are distinct and vary widely across the basin. The T_{DM} of the Upper Vindhyans are younger in the Bundi sector compared to that in the Chittorgarh sector and the Kaimur Group has the youngest model age of ~1.3 Ga. Comparing our results from Chittorgarh with that of Chakrabarti et al. (2007) from Son Valley we find that except for the Kaimur Group rocks average T_{DM} values are identical in both the sectors (Fig. 3.31) even though the ε_{Nd} values for the Rewa and the Bhander groups are different in both the sectors. The Lower Vindhyans in both the sectors are geochemically correlatable through identical ε_{Nd} and T_{DM}. These observations suggest that the Vindhyans in both the sectors, to a large extent, are contemporaneous and had similar type of sediment sources. Upper Vindhyans in Bundi sector, however, appear to have contributions from much younger sources as reflected in their T_{DM} values.

3.2.3 Geochronological studies

An attempt was made to date possible datable horizons within the Rajasthan sector of the Vindhyan Basin. For this purpose, the porcellanite layer sandwiched between the Sawa Sandstone and Sawa Shale (Prasad, 1984) was chosen to constrain the age of the Lower Vindhyans (Semri Group). Petrography of these samples did not reveal any volcaniclastic material, hence, we believe that most likely these represent the Sawa Sandstone. Detrital zircons were separated from these samples and analyzed for their ^{207}Pb-^{206}Pb ages following the method described in the previous chapter. For dating the Upper Vindhyans, Sr-isotope stratigraphy technique was utilized in the topmost limestone formation, i.e. Balwan Limestone. The implications of these results are discussed below along with the Nd model ages.

3.2.3.1 Detrital Zircon Geochronology of the Sawa Sandstone

The results of our study (Table 3.6) suggest that there is no correlation between the age of the grains and their morphological types. A probability distribution of the grains with their respective ages are presented in Fig. 3.32. Most of the grains are concordant and their ^{207}Pb-^{206}Pb ages show a bimodal distribution. As expected, the oldest zircon population present in the rock was found to have been derived from the ~2.5 Ma old basement granites and older crustal rocks present in this part of the Indian shield. The zircons showing mode at ~1.9 Ga are apparently derived from magmatic activities of these ages (Hindoli Group), and can be linked to the timing of the base metal mineralization (Roy and Jakhar, 2002). On the basis of this work the youngest event recorded by the zircons is a 1616 Ma event and the yougest mode is at 1660 Ma (Ray et al., 2007). This clearly suggests that parts of the Sawa Sandstone may actually be correlatable with the Deonar Porcellanite Formation in the Son Valley. This would mean that, even though there is no lateral continuity of the Lower Vindhyans of the Son Valley into Rajasthan, the formations of Semri Group in the west were deposited contemporaneously with those in the east within the

Vindhyan Basin. These observations suggest that Vindhyan sediments were depositing simultaneously in western as well as in eastern parts of the basin. Such an inference is also supported by ε_{Nd} and T_{DM} data from both the sectors.

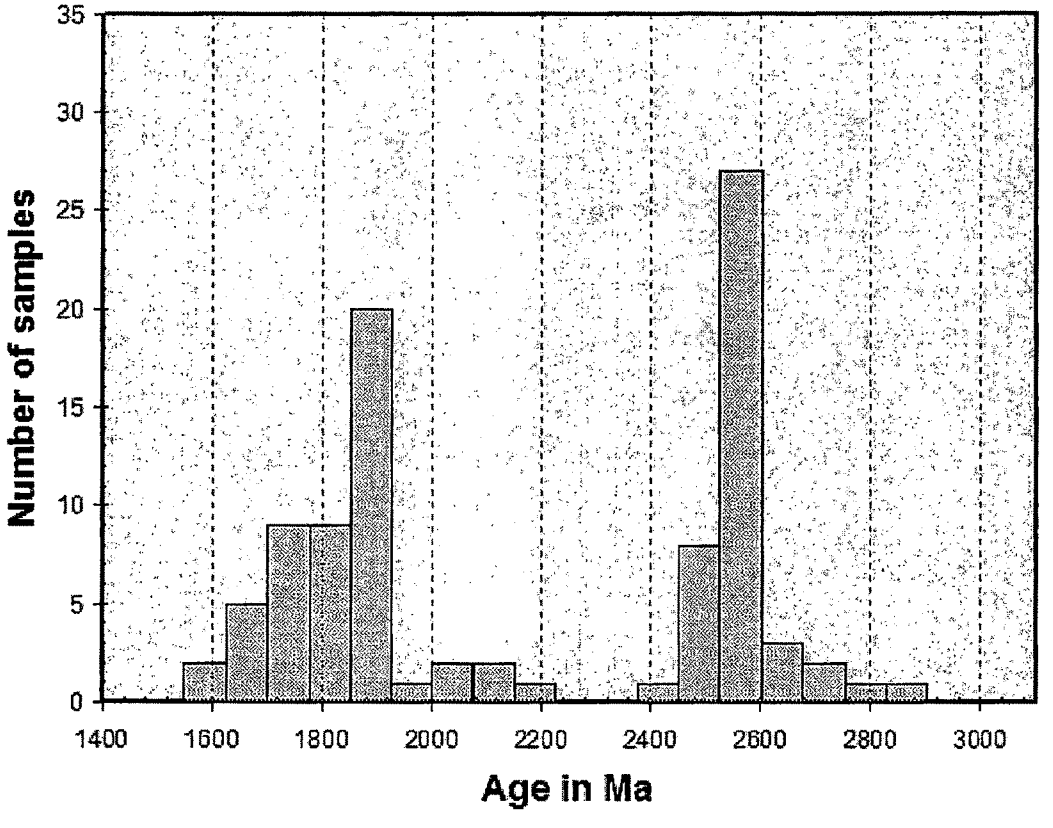

Fig. 3.32: Histogram showing distribution of ^{207}Pb-^{206}Pb ages for detrital zircons from the Sawa Formation, Semri Group, Chittorgarh.

3.2.3.2 *Nd model ages (T_{DM})*

The calculated Nd-model ages of the sediments discussed earlier can give clues to the ages of the sediments. Since, the model ages are the ages derived from the Nd isotopic ratios, which have been behaving like close system after their incorporation in the basin, the age calculated reflects an age which is resultant of mixing of the sources ages. Therefore, the age calculated may be older than the actual depositional age of the sediments because of the differential mixing of older and younger material, which were originally derived from the Earth's mantle. In any case these ages could not be younger than their actual depositional age or rather than the youngest igneous material added to the sediments. But the distribution of the model ages through the stratigraphical column may give some relative age information of any sedimentary basin.

As already discussed the average T_{DM} values of the Vindhyans of Rajasthan vary from 1.3 to 2.4 Ga, with the youngest age coming from the Kaimur Group. The T_{DM} of ~ 1.3 Ga for Kaimur suggest that the age of the sedimentation in this group is younger than 1.3 Ga and contributions from a younger igneous activity (1200 <Age<1300 Ma) could have been responsible for such a low model age. The Semris in both the sectors have average T_{DM} of 2.4 Ga, which means that the Vindhyan sedimentation did not start until 2.4 Ga. Following the same line of argument we infer that the Rewa and Bhander groups of rocks are younger than 1.5 Ga in the Bundi sector, however, considering the T_{DM} of the Kaimur Group we can safely conclude that the Upper Vindhyans of Rajasthan are younger than 1.3 Ga.

3.2.3.3 *Sr-isotope stratigraphy*

Strontium isotope stratigraphy is a relative dating method for limestones formed out of ocean water. This method can be very useful to provide first order depositional age brackets in sedimentary sequences where absolute ages are meager. This method is based on the use of $^{87}Sr/^{86}Sr$ in unaltered marine carbonates and the $^{87}Sr/^{86}Sr$ evolution curve for the global seawater (e.g. McArthur, 1994, Veizer et al., 1999, Burke et al., 1982). By tying $^{87}Sr/^{86}Sr$ of discrete stratigraphic levels to the global seawater evolution curve tied to the geomagnetic polarity time scale or absolute ages; approximate time gaps and relative depositional ages can be estimated. Since the evolution curve in Precambrian is not robust, the ages obtained through this method should be treated as minimum ages. Such a method can only work if Sr in the samples has remained unaffected by diagenesis and subsequent alteration. Therefore, care must be taken to recover samples from the least altered portions of a rock or isotopic analysis. We make an attempt to use this method to constrain the age of the Lakheri and the Balwan Limestones of the Upper Vindhyans of Rajasthan.

The $^{87}Sr/^{86}Sr$ data generated on these limestones are presented in Table 3.11. The ratios obtained for the Lakheri Limestone was higher than the value reported by Ray et al. (2003) (0.70678), and hence deemed to be useless for stratigraphic purpose. In the case of the Balwan Limestone Formation, however, we were able to get much lower $^{87}Sr/^{86}Sr$ values (e.g. 0.70676 and 0.70684) normalized to NBS 987 value of 0.71025. The lowest value of 0.70676 for the Balwan carbonates was projected onto the Sr-evolution curve of Shields and Veizer (2002) and a minimum age of 620Ma was obtained. This means that the Balwan Limestone is at least 620 million years old and that it could have been deposited prior to this date but later than 650 Ma (Sr stratigraphy age for the Lakheri Limestone, Ray et al., 2003). This age estimate for the Balwan Limestone is in tune with the biostratigraphic inferences made by Kumar and Pandey (2008) for the same formation.

The fossil findings of the Neoproterozoic age from the Sirbu Shales (Srivastava, 2009) and the Balwan Limestone (Kumar and Pandey, 2008) support the Neoproterozoic age for the Bhander Group. Here, we would like to emphasize that the minimum age of 620Ma of the Balwan Limestone, which is the second topmost lithounit (below Dholpur Shale) of the Vindhyan in Rajasthan, indicates that the deposition of the Vindhyan Supergroup was over much before the Precambrian-Cambrian transition.

It is also highly likely that these sediments could have recorded the events of Cryogenian period (750-600Ma) of the Neoproterozoic. With these new information we have made an attempt to correlate the Vindhyans of Rajasthan with those in the Son valley (Fig. 3.33).

3.2.4 Provenance of the Vindhyan Sediments

The geochemical investigations of the Vindhyan sediments from the Rajasthan reveal that the provenance of these sediments lie in the pre-Aravalli, Aravalli, Hindoli and Delhi Supergroup of rocks exposed to the west or southwest of the Vindhyan Basin. The identification of magmatic arc type multi-element patterns (typical Nb-Ta-Sr depletions and Pb enrichment) within various formations of the Vindhyan Supergroup and their similarity to the patterns observed in the Khairmalia volcanics and other mafic igneous rocks in the vicinity, hints at the existence of a subduction zone to the west of the basin prior to the initiation of deposition. It is highly likely that this part of the Vindhyan Basin probably was formed as a result of subduction zone related tectonic events.

Sediments of the Semri Group show increased incorporation of mafic igneous material as one goes up stratigraphically. The association of Sawa Grit/Sandstone with volcaniclastics (porcellanite) and high positive $\varepsilon_{Nd}(T)$ of some of the formations clearly points to direct contribution of volcanic/volcaniclastic sediments to the Vindhyan Basin, but mostly prior to and during the deposition of Kaimur Formation (~1.3 Ga). It is highly likely that the youngest zircon populations seen in the Sawa Grit/Sandstone Formation (~1616 Ma) represents the felsic volcanism in the eastern part of the basin (or its equivalents in the west) that formed the Deonar Porcellanite Formation. The trace element chemistry of sediments also suggests input from subduction zone magmatic sources such as the Khairmalia type andesites in almost all the formations in Rajasthan. Chemical and isotopic compositions clearly indicate that the major igneous sources for the sediments were the Berach Granites and the mafic igneous rocks, that occur in the basal part of the Aravalli Supergroup (Ahmad et al., 2008b) and the Khairmalia type volcanics that occurred just before the deposition of the Vindhyans (Fig. 3.34). We also observe sediment contributions from much older (T_{DM}> 2.5 Ga) mafic igneous rocks ($f_{Sm/Nd}$ >-0.4) (Fig. 3.34) to the Lower Vindhyans. Such sources could be komatiites of Aravalli craton (Ahmad et al. 2008b). From Fig. 3.34, one can also see that apart from the above sources there were other igneous sources, with low $f_{Sm/Nd}$ and low T_{DM} (< 1.3 Ga), which contributed sediments to the Vindhyan Basin, especially during the deposition of the Upper Vindhyans. Such sources, most likely, were felsic (highly differentiated) in nature and we believe that these are the granitic and rhyolitic rocks of 1300 to 750 Ma age and present in the Aravalli craton.

The sedimentation in the Vindhyan Basin appears to have lasted for more than 1 billion years. The lithological boundaries identified in between the groups are found to be times of changes in the chemistry of sediments (Fig. 3.35). The drastic changes in T_{DM}, ε_{Nd} and $f_{Sm/Nd}$ across boundary between the Lower Vindhyan and Upper Vindhyans indicate the change in provenance. The difference in the model ages of the Rewa and Bhander Groups in the Chittorgarh and Bundi districts suggests that the younger sources contributed substantially in the Bundi sector. This could be attributed to the Delhi orogeny in the vicinity.

Various important geochemical and isotopic proxies ($^{87}Sr/^{86}Sr$, $f_{Sm/Nd}$, $\varepsilon_{Nd}(0)$, $\varepsilon_{Nd}(T)$ and T_{DM}) have been plotted across the stratigraphical column in the Fig. 3.35. The $^{87}Sr/^{86}Sr$ ratios as expected, is highly radiogenic (Fig. 3.35A) and vary widely, hence are not suitable for provenance study. The $\varepsilon_{Nd}(0)$ and $\varepsilon_{Nd}(T)$ show increasing trends with stratigraphy in the Semri Group, whereas T_{DM} shows a decreasing trend (Fig. 3.35C, D, & E). Combining these findings it can be postulated that higher contribution from juvenile igneous components masked the supply of sediments from older crustal sources towards the top of the Lower Vindhyan.

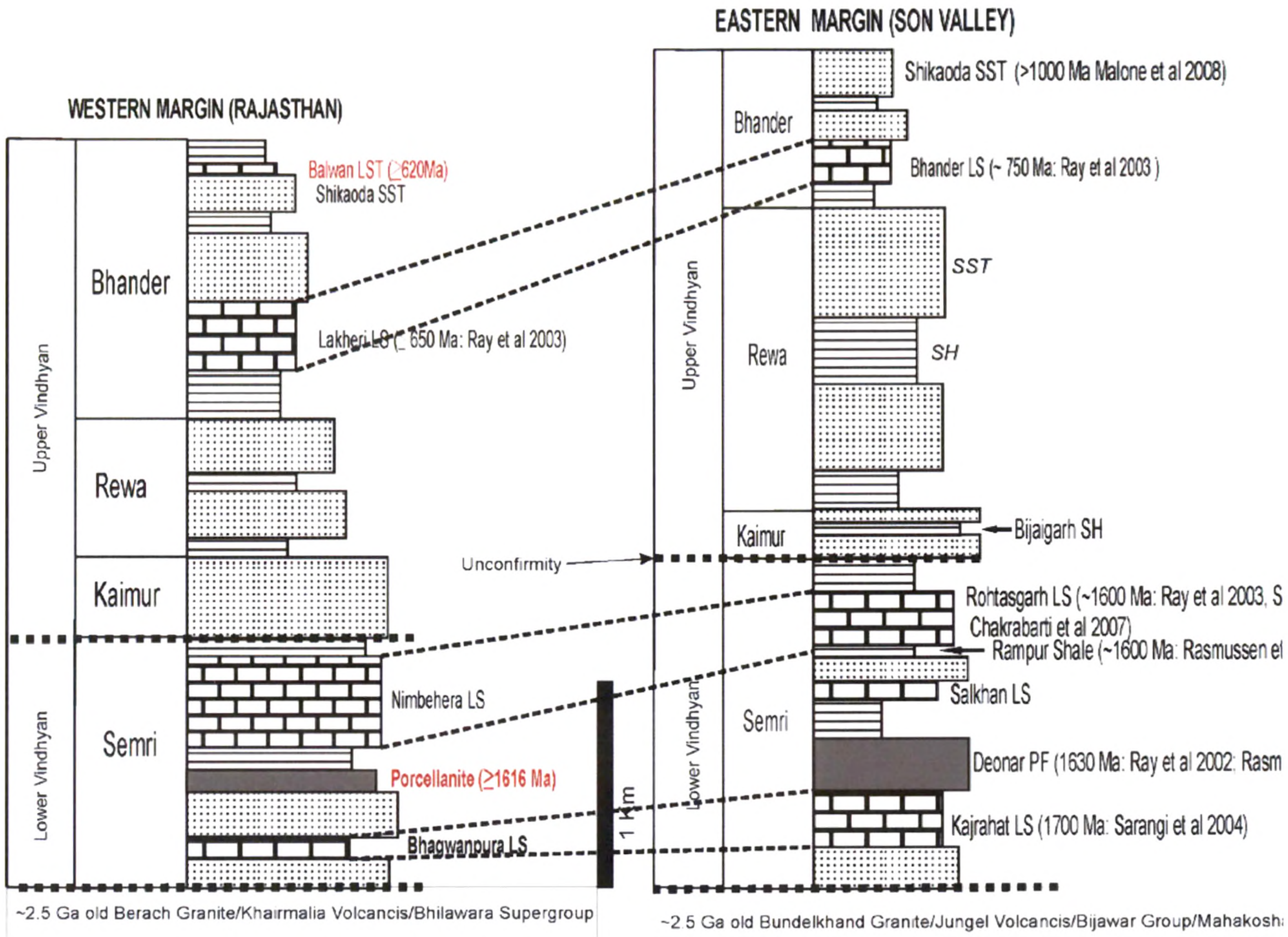

Fig.3.33: Geochronological correlation between Rajasthan and the Son Valley Vindhyans based on the present work. Results from present work are marked in red.

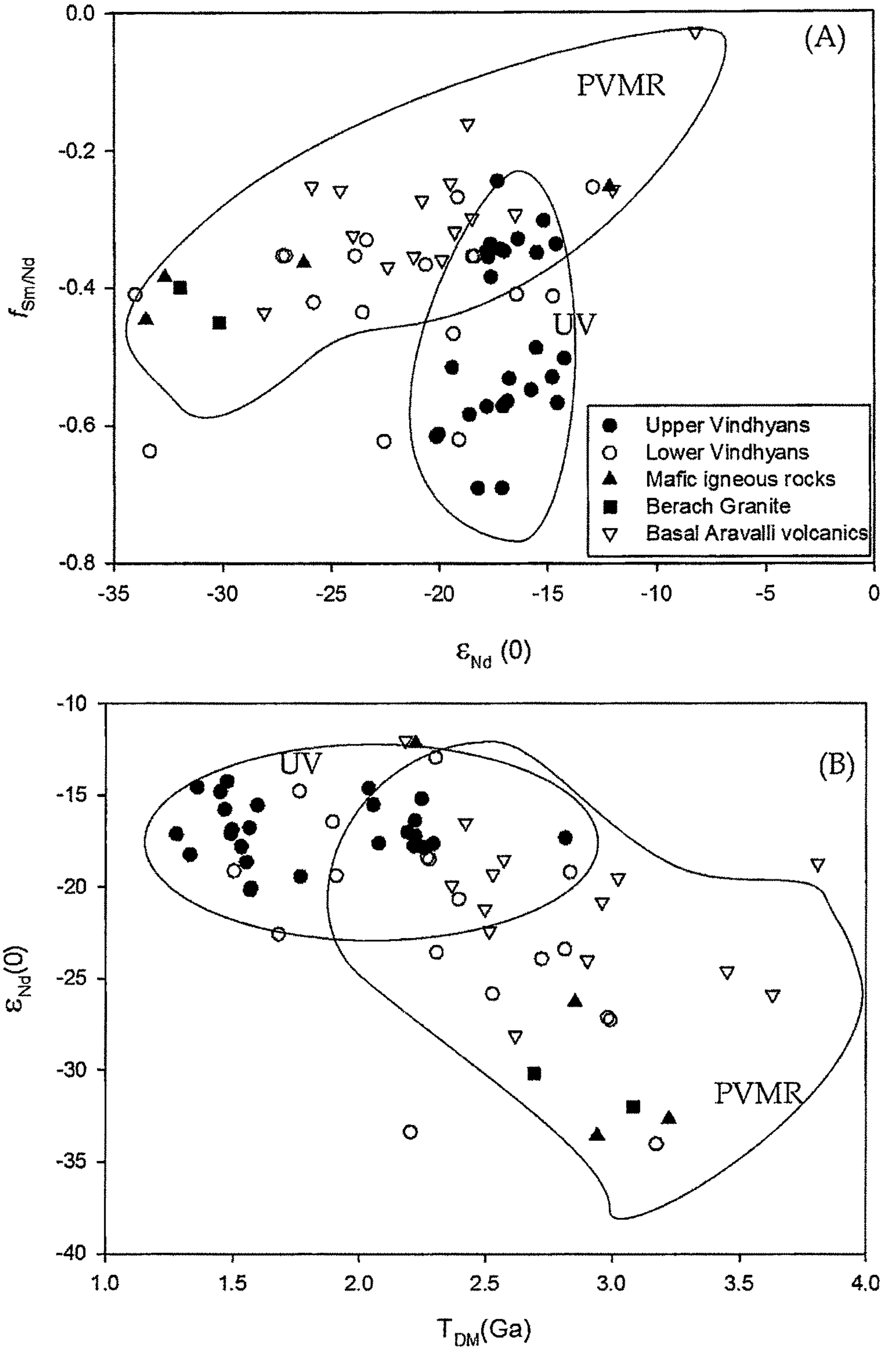

Fig. 3.34: Plots of $f_{Sm/Nd}$ vs. $\varepsilon_{Nd}(0)$ (A) and ε_{Nd} (0) vs. T_{DM} (B) showing data for sediments from the Lower and the Upper Vindhyans, pre-Vindhyan mafic igneous rocks, Berach Granite and volcanics from the Aravalli Supergroup. Data source for Aravalli volcanics: Ahmad et al. (2008b). PVMR: Pre-Vindhyan Mafic Rocks; UV: Upper Vindhyans.

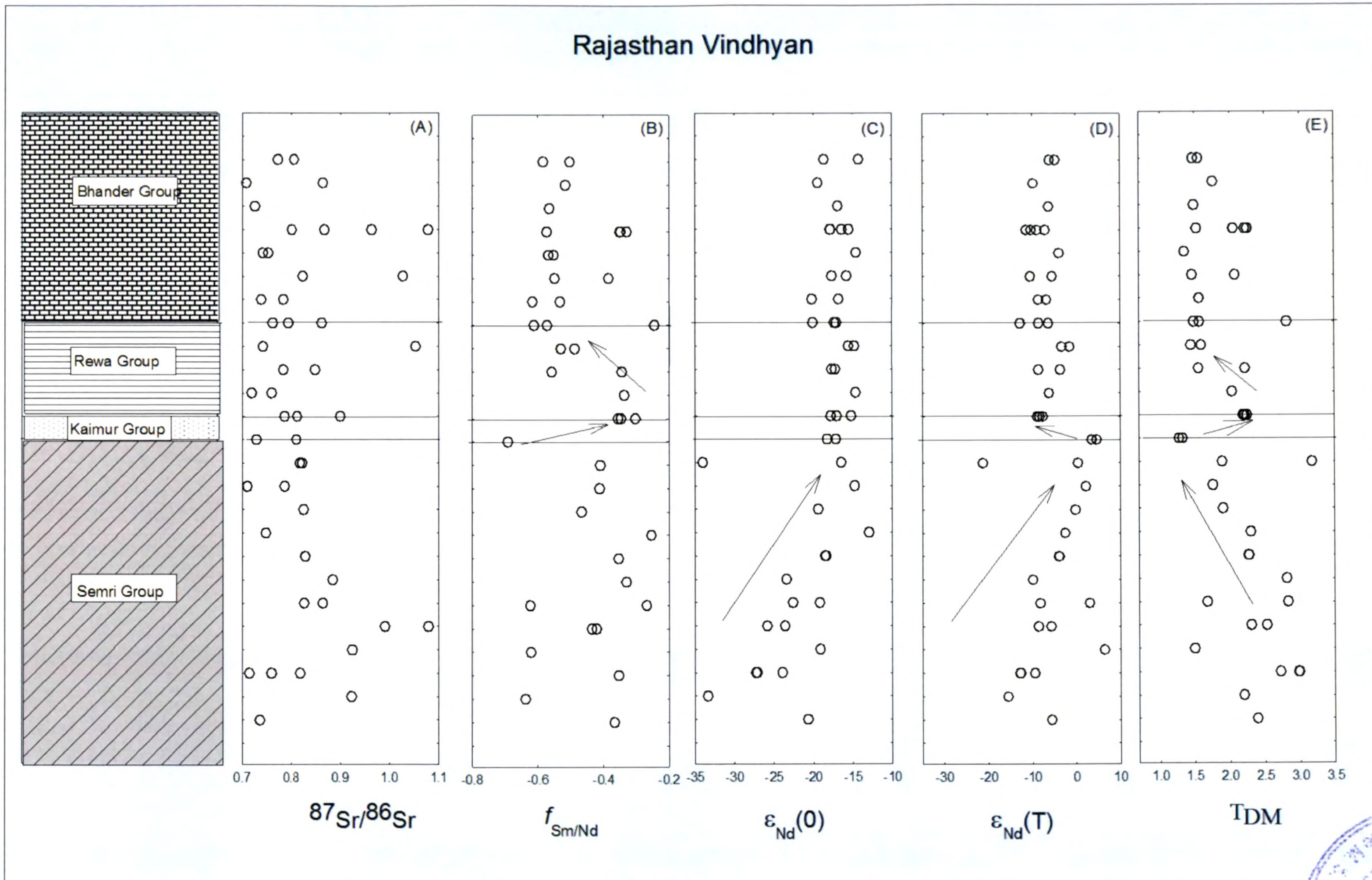

Fig. 3.35: Variation of various geochemical proxies across the stratigraphical column in the Vindhyan Supergroup of Rajasthan.

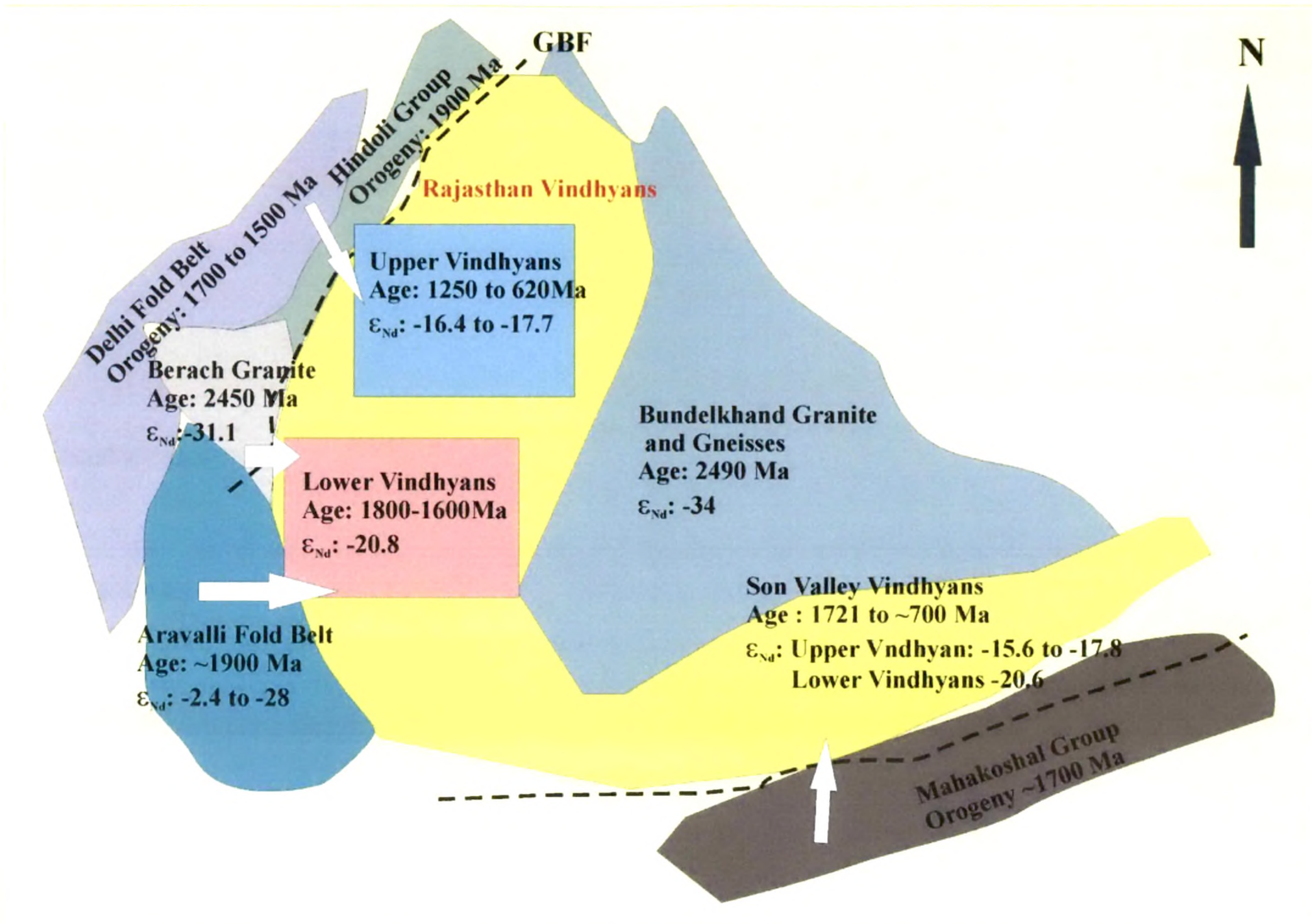

Fig. 3.36: A schematic of Vindhyan Basin during the deposition of Vindhyan Supergroup and the inferred provenances of sediments.

The young model ages and positive ε_{Nd} (T) of the Kaimur Formation clearly demands direct incorporation of young mantle derived components into the sediments. Just prior to the deposition of the Rewa Group all chemical parameters revert back to the average values observed within the Semri Group, possibly meaning similar sediment sources continued to contribute. However, the reduction in $f_{Sm/Nd}$ starting within the Rewa Group hints at contributions from more felsic (or differentiated) sources to the Upper Vindhyans. Based on the above observations and observations made by Chakrabarti et al. (2007) a sketch of the Vindhyan Basin configuration is presented in Fig. 3.36 along with the location of possible source regions for sediments.

3.2.5 $\delta^{13}C$ and $\delta^{18}O$ variations in limestones

Major inquiries related to the evolution of the Earth's atmosphere, climate, the sedimentary cover and the life are believed to be answered through the study of isotopic variations in chemical sediments hence, in the seawater through time. Numerous studies in the recent past have demonstrated the usefulness of carbon and oxygen isotope compositions of Phanerozoic marine carbonate sediments in this regard (e.g., Veizer et al., 1980; Burke et al., 1982; Holser, 1984; Richter et al., 1992; Strauss, 1997; Veizer et al., 1999). Such studies have substantially improved our knowledge about the evolution of our planet during the last 540 million years. Variations of C isotopes reflect a series of complex biogeochemical interactions that document equilibrium between net burial of organic matter and oxidation of their reduced forms (e.g., Berner & Raiswell, 1983; Popp et al., 1997; Kump & Arthur, 1999). The O isotopic variation through time, if considered primary, tells us either that the ancient oceans were warmer compared to their modern counterparts or the isotopic composition of the oceans became progressively higher (Veizer et al., 1999).

In recent times, the use of above isotopic tracers has been extended into Precambrian in an attempt to understand the evolution of Earth's nascent ocean-atmosphere systems and life (e.g., DesMarais, 1994; Hall & Veizer, 1996; Frank et al., 1997; Jacobsen & Kaufman, 1999). Also, there have been efforts to generate seawater $\delta^{13}C$ isotopic evolution curve that can be used as tools for stratigraphic correlation, for most part of the Precambrian that lacks biostratigraphic framework. In spite of all the earlier research, not enough data has yet been generated either to carry out isotope stratigraphy or critically understand the co-evolution of life and environment during Precambrian in a global scenario.

To strengthen the existing database and to fill the gaps in our knowledge about various global events that occurred during Earth's early history during the Proterozoic we studied the C and O isotopic records preserved in Lakheri and Balwan Limestone formations of the Upper Vindhyans in Rajasthan that are believed to have been deposited during the Neoproterozoic time (Ray et al. 2003).

3.2.5.1 The Lakheri Limestone

The Bhander Group in Rajasthan is comprised mostly of sandstones (see Table 2.1) and two limestone formations and four shale formations (Fig.2.2). The Lakheri Limestone that occurs at the bottom part of the Bhander Group is has a gradational contact with the overlying shale formation (Ganurgarh). In an earlier work Kumar et al. (2002) had observed a negative excursion in $\delta^{13}C$ variation in these carbonates at Satur near Bundi town hypothesized it to represent one of the Neoproterozoic global glaciations. The authors also had reported a physical evidence for glaciation in form of tilloid bed at the base of the formation near the town of Lakheri, however, this could not be located during the present study. Ray et al. (2003) also reported a negative excursion in $\delta^{13}C$ but in the equivalent formation in the Son Valley and had hinted at a possible correlation with one of these glacial events.

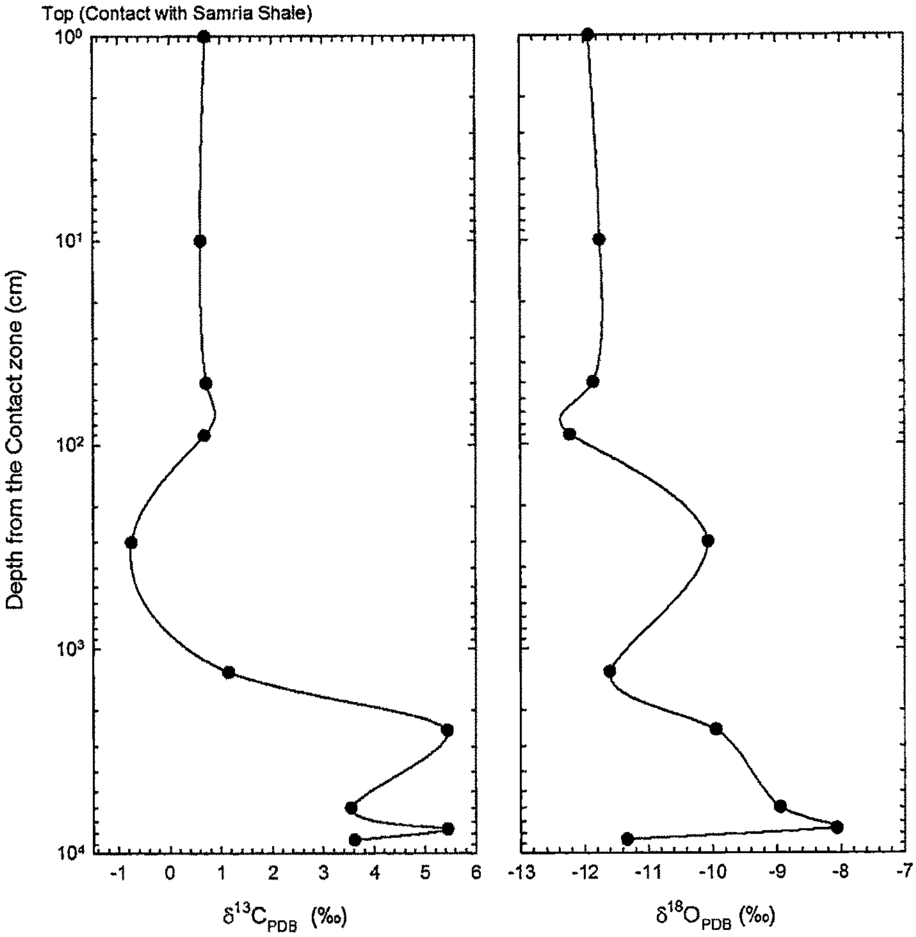

Fig. 3.37: $\delta^{13}C$ and $\delta^{18}O$ profiles in the Lakheri Limestone at Gandoli on the Bundi-Indergarh Road.

To contribute to this discussion we decided to carry out carbon isotope studies on this formation at Gandoli, where the entire width of the Lakheri Formation is exposed. The stable isotope data are presented in Table 3.8 and plotted in Fig. 3.37. $\delta^{13}C$ value appears to decrease with height, from ~5‰ to 0‰, from bottom to top. Although not very significant by itself, this change if combined with the data of Kumar et al. (2002) hints at a large variation from -5.2‰ to +6‰. Such a change (about 11‰) could be attributed either to 1) facies variation within the basin, with the deeper facies having more negative $\delta^{13}C$ values or 2) to an overall decrease in biology towards the end of deposition.

3.2.5.2 The Balwan Limestone

The Balwan Limestone Formation is the topmost carbonate unit of the Vindhyan Supergroup and is exposed only in the Rajasthan sector near Lakheri. It overlies the Shikaoda Sandstone Formation and is exposed in a ~100m thick band along a 15 km section (Fig. 2.4) and truncated by folds and faults on both ends of the length. The formation contains molar tooth structures near the bottom and is stromatolitic at the top. The most interesting aspect of this formation is the presence of a ~20m thick conglomerate band in the middle. The conglomerate is mostly intraclastic and at places contains flat pebbles of the bottom beds of the same formation. Immediately below and above the conglomerate zone the limestone beds contain chert pebbles. We feel that this zone is a result of a storm and/or slope failure close to the shoreline of the basin.

High resolution of carbonate sampling was done in the formation (Table 2.6) and visually least altered components were analysed for C and O isotopic ratios compositions (Table 3.10A). Since there is no apparent positive correlation between the $\delta^{13}C$ and $\delta^{18}O$ in the samples (Fig. 3.38) and negative correlation between Mn/Sr and $\delta^{18}O$ (Fig. 3.39), these isotopic compositions are deemed least altered (i.e. almost pristine) following the arguments given by Veizer at al. (1999). The profiles of $\delta^{13}C$ and $\delta^{18}O$ are plotted in Fig. 3.40 for transect 2 (Table 2.6). The profiles of $\delta^{13}C$ and

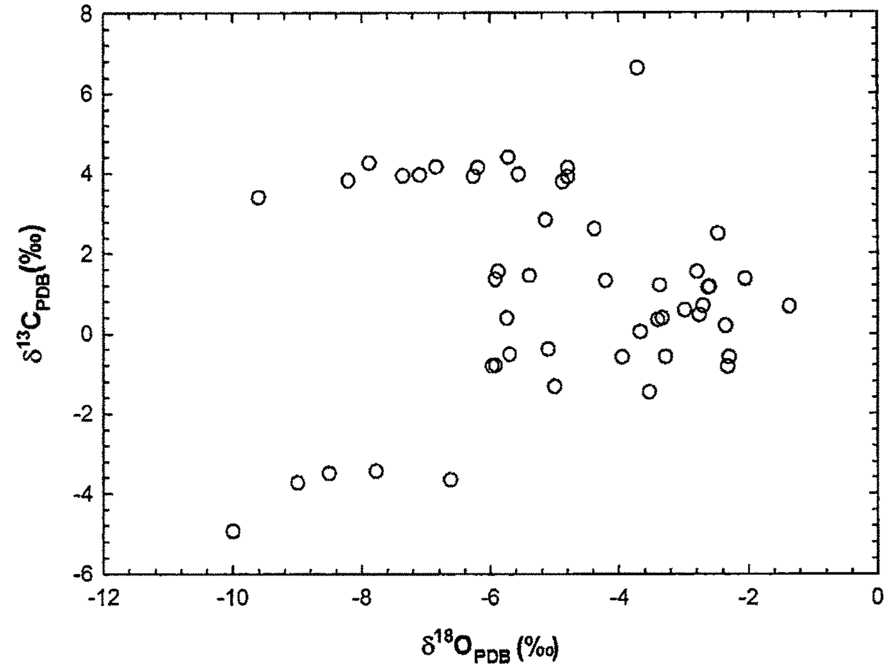

Fig. 3.38: $\delta^{13}C$ vs. $\delta^{18}O$ of carbonate components from the Balwan Limestone.

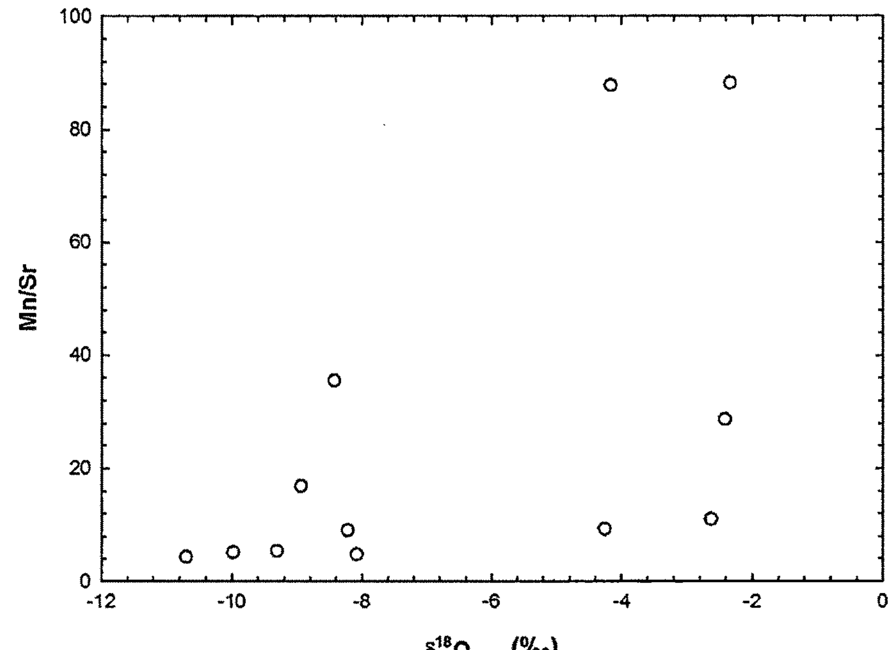

Fig. 3.39: Mn/Sr vs. $\delta^{18}O$ in carbonate components from the Balwan Limestone.

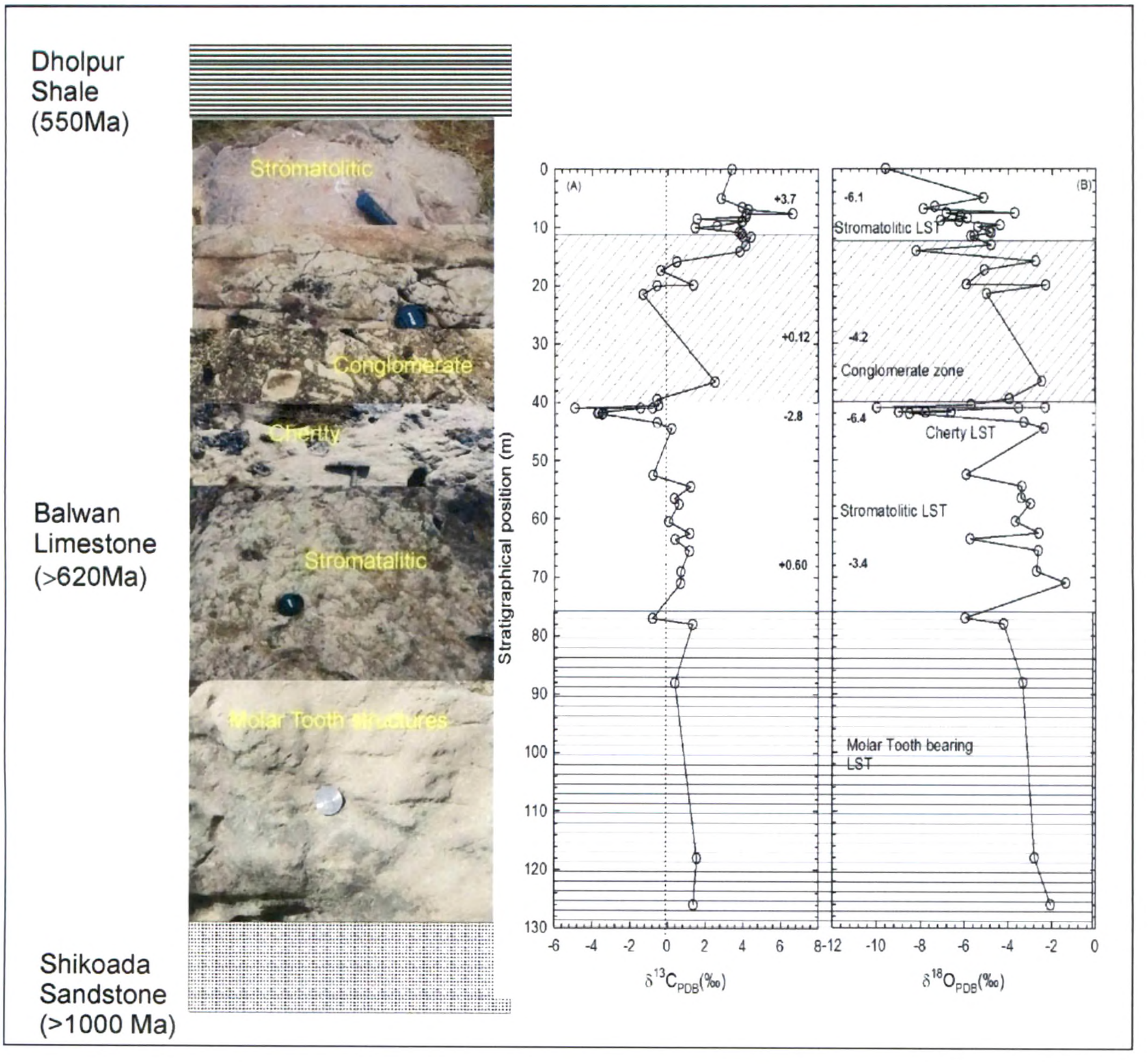

Fig.3.40: $\delta^{13}C$ and $\delta^{18}O$ profiles across the Balwan Limestone near Lakheri Town, Bundi, Rajasthan.

$\delta^{18}O$ are plotted in Fig. 3.40 for transect 2 (Table 2.6). It was found that the beds below the conglomerate bearing horizon has the lowest $\delta^{13}C$ composition (-4.9‰) whereas the bed immediate above the conglomerate horizon has the highest $\delta^{13}C$ (+6.6‰).

As can be seen from the profile in Fig. 3.40, the $\delta^{13}C$ hovers between values of -1 ‰and +2‰ below the cherty horizon, but becomes more negative (up -5‰) within it. It comes back to slightly positive values within the conglomerate zone but becomes highly positive (up +6.6‰) in layers above this zone. Such trends are not confined along to one transect, in fact, we have observed this in three transects, along the length of the entire formation, separated by more than a few kilometers (>7km). We, therefore, believe that the negative and positive excursions of $\delta^{13}C$ in the Balwan Limestone are not a result of any facies variation, instead represent basin wide, if not global, changes in organic matter burial. The negative excursion probably reflects large scale reduction in biology just before the storm or slope failure event and the positive excursion reflects sudden change in biodiversity. Considering the Sr-isotope stratigraphic age for the Balwan Limestone we strongly feel that this storm event could possibly be related to the latest global glaciation event of the Neoproterozoic. However, more research is necessary to substantiate such an inference, since, we have not observed any diamictite horizon within this formation.

3.2.6 Evolution of the Vindhyan Basin in Rajasthan

The geochemical and isotopic studies in the Rajasthan Vindhyans suggest that the sources of the sediments were located in adjoining Aravalli-Delhi fold belt and in the Archean basements. Variations in chemical parameters across the supergroup support classification of the Vindhyan Supergroup into various groups. In general, the boundaries between the four groups are characterized by changes in provenance. The difference in the model ages of the Semri Group and the Kaimur Group in Rajasthan reflects the dynamic nature of tectono-geomorphic setting in this part of the basin compared that in the Son Valley sector. The protoliths of the Vindhyan sediments, most likely, were located within a magmatic arc setting, the remnants of which may now be located within the pre-Vindhyan fold belts to the west of the basin. The presence of a subduction zone in the Aravalli-Delhi belt during Neoarchean and Paleoproterozoic time has also been proposed by earlier workers (Sarkar et al. 1989; Mishra et al. 2000; Leelanandam et al. 2006). Based on the inferences of Chakrabarti et al. (2007) and our results from Rajasthan, and the concept of a Central Indian Suture Zone resulting from a mid Proterozoic collision (Sinha-Roy et al., 1998; Yedekar et al., 1990; Jain et al., 1991; Sinha-Roy and Mohanti, 1988; Sudgen et al., 1990; Raza et al., 1993), a model for the tectono-stratigraphic evolution of the Vindhyan Basin in Rajasthan is proposed below.

The tectonic configuration of the Vindhyan Basin before the deposition began could be understood from the geophysical investigations of Mishra et al. (2000), where they suggested for a collisional zone for the Aravalli and Satpura fold belts during Paleoproterozoic time. This model is a two stage model. During the first stage ~1900Ma, (age of Dharwal granites) due to the Aravalli orogeny, a foreland setting got generated in the eastern flank of the Aravalli mountain chain. Aravalli orogeny also resulted in mafic igneous intrusion, obduction of ophiolites sequences and development of a magmatic arc with andesite volcanism e.g. Khairmalia (Fig. 3.41). These rocks supplied the sediments to the Lower Vindhyans for about 200 million years. The presence of a volcaniclastic sedimentary member (Porcellanite) and evidence for direct input from volcanic ejecta to the Lower Vindhyan sediments and particularly to the Kaimur Group of rocks in the Upper Vindhyans hint at the presence of a very active subduction zone. The initiation of Delhi orgoney in the western flank of the Aravalli Mountain marks the closing of the Lower Vindhyans. After completion of the major Delhi folding at ~ 1400 Ma, the second stage sets in and the Upper Vindhyans start getting deposited. This appears plausible in the light of available geochronological age estimates of the Kaimur Group. The low T_{DM} age of ~1.3 Ga which is similar to the age estimated for the Bijaygarh Shale in the Son Valley supports the inferences that there exists a gap in the sedimentation between the Lower and the Upper Vindhyans. The low T_{DM} ages of the Rewa and the Bhander groups (~1.5 Ga and 1.6 Ga) in the Bundi district, which is closer to the Delhi Fold belt, also support the conclusion that the sedimentation in the groups postdates the Delhi orogeny.

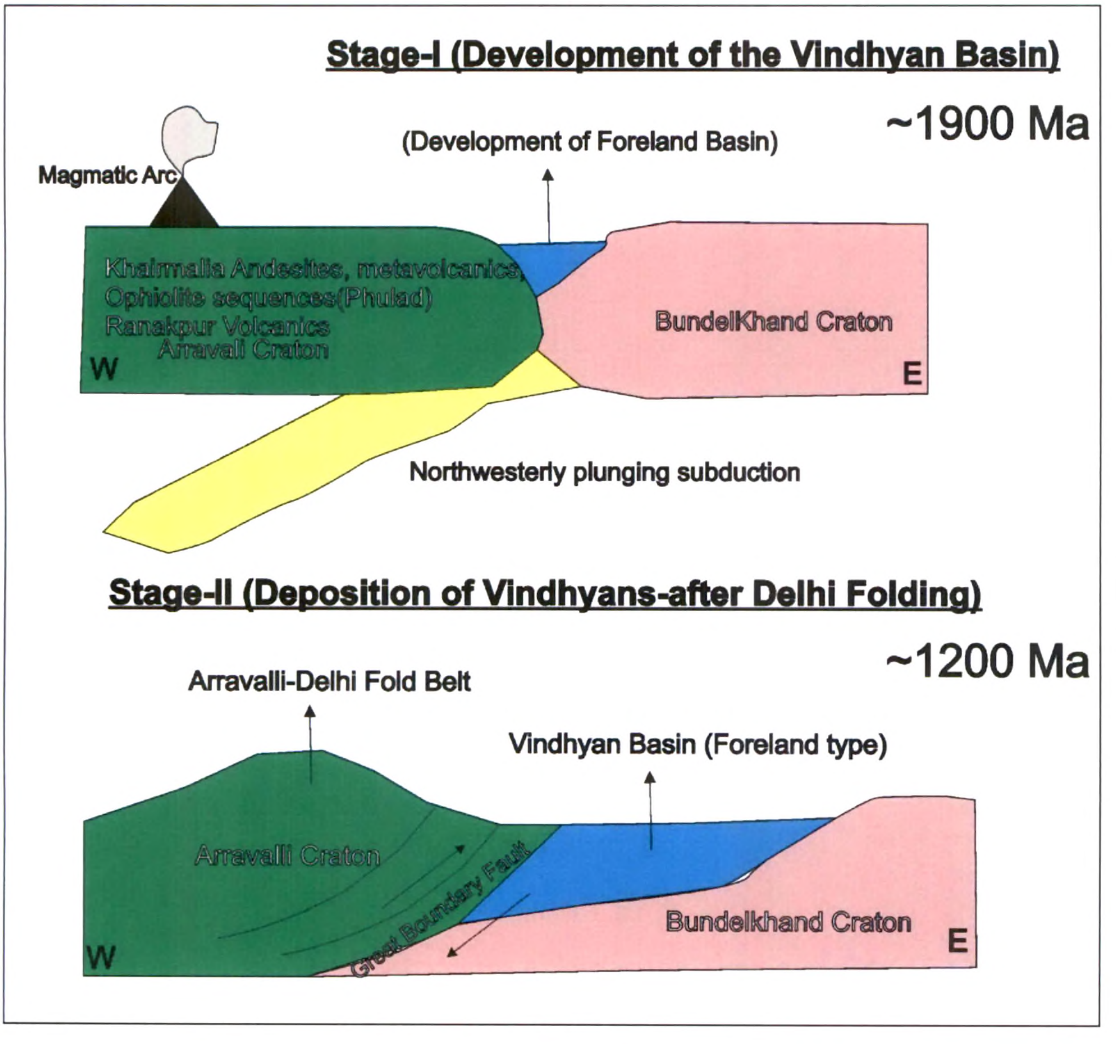

Fig. 3.41: A schematic diagram of our proposed evolutionary model for the Vindhyan Basin in Rajasthan. The collision between the Bundelkhand craton and the Aravalli craton resulted in the formation of the Aravalli-Delhi Mountain Belts subsequent to the subduction of the pre-Vindhyan oceanic crust. The present day GBF and associated faults might be the expressions of this tectonic process.

Chapter-4

SUMMARY AND CONCLUSIONS

The present study is an attempt to understand the Proterozoic evolutionary history of the Indian shield by unraveling the evidences preserved in sedimentary sequences. The existence of several large and contemporaneous sedimentary basins (Purana Basins) in India always puzzled the geosciencetist community about the locations of the sources of sediments for the basins. It has, therefore, become necessary to decipher the provenance of sediments deposited in these basins for formulation of any geodynamic model for the evolution of the Indian subcontinental landmass. The Vindhyan Basin, being the largest of the basins, is selected for such a study. Additional interesting problems in the basin that attracted our attention and needed scientific investigations are: 1) the lack of accurate stratigraphic correlations between various sectors; 2) the lack of any physical evidence for Neoproterozoic glacial events; and 3) the lack of proper understanding of the reasons behind gaps in sedimentation in the supergroup. To find answers to these questions a geochemical approach through the use of major, trace elements and radiogenic isotope ratios in siliciclastics rocks was taken. To establish chronology of depositions, we utilized U-Pb dating of the detrital zircons and Sr-isotope stratigraphy (in carbonate horizon). The major conclusions of this study are listed below. The answers to the major objectives of thesis and other inferences achieved are summarized below:

1. Geochemical and isotopic data from siliciclastic formations of the Vindhyan Supergroup of Rajasthan suggest that most of their sediments were derived from a magmatic arc located to the west of the basin. We believe that the magmatic rocks of the Hindoli Group, Delhi and the Aravalli Supergroups formed part of this arc. The basement rocks of the Vindhyans such as the Berach Granite and the Khairmalia volcanics also appear to have been generated by this arc.
2. Normalized trace element patterns of the Vindhyan Shales mimic that of average continental crust which essentially indicates that the sources for the

sediments came from stabilized craton. This could also mean that all major tectonic activities, related to continental crust formation, were over in this part of the Indian shield prior to the deposition of the Vindhyans.

3. Bimodal distribution of $\varepsilon_{Nd}(0)$ in the Lower Vindhyan sediments (of Rajasthan) suggests involvement of two major groups of magmatic source rocks, whose average $\varepsilon_{Nd}(0)$ values are -23 and -19. The T_{DM} age distribution for these also support this inference by showing modes at 2.9 Ga and 2.3 Ga. Taking cue from the detrital zircon geochronology, which shows peaks of magmatism at 2.5 Ga and 1.9 Ga, we conclude that the older sediments (T_{DM} = 2.9 Ga) represent a mixture of sediments from ~2.5 Ga old granites (e.g. Berach) and >3.0 Ga old volcanics from the Archean basement (e.g. Mangalwar complex, BGC). The younger group represents mixture of sediments from again the ~ 2.5 Ga old granites and the 2.2 - 1.9 Ga old volcanics from the Hindoli Group and or the Aravalli/Delhi Supergroups and the Khairmalia volcanics.
4. History of sedimentation in the Upper Vindhyans of Rajasthan is very interesting, since the original sediment sources appear to have been different in the southwest (near Chittorgarh) and northwest (near Bundi-Lakheri) sectors of the basin. While the southwest sector, except for when the Kaimur Group was getting deposited, received sediments from same/similar sources as in the case of the Lower Vindhyans (T_{DM} = 2.3 Ga), the northwest sector received sediments from much younger (1.6 Ga to 1.0 Ga) magmatic rocks. This is very clearly evident from the mode of $\varepsilon_{Nd}(0)$ distribution at -17 and mode of T_{DM} at 1.5 Ga. The Kaimur Group sandstone (T_{DM}=1.3 Ga) in the southwest sector seems to share the same history. The sediments for these formations are believed to have come predominantly from the 1.9 - 1.6 Ga old volcanics (the Hindoli Group; Deonar Rhyolites and its equivalent in Rajasthan) and from much younger magmatism (1.2 Ga to ~ 800 Ma). Again, taking clues from the detrital zircon geochronology data (of Malone et al. 2008) it is inferred that the latter source could be the 1.4 -1.2 Ga old magmatic

activities in the Aravalli/Delhi Supergoups (for the Kaimur sediments) or the 0.9 - 0.8 Ga old magmatism in the Aravallis and in the Mailani Igneous Suite.

5. The absence of sediments with T_{DM} <1.2 Ga in the Upper Vindhyans of the Son Valley could either suggest that the sources in the west (Rajasthan) did not contribute sediments to the east (Son Valley) or that there existed a physical barrier within the basin. This could be the reason why it has always been difficult to correlate Vindhyans in various sectors.
6. Comparing the present results with those of Chakrabarti et al. (2007) it is concluded that, except for the formation of the Kaimur Group, most siliciclastic formations of the Vindhyan Supergroup in the Son Valley are broadly correlatable with those in Rajasthan, both in terms of time of deposition and type of provenance. The Kaimur Group in Rajasthan, however, appears to be chemically very different from its counterpart in the Son Valley.
7. The long recognized basin-wide unconformity between the Lower and the Upper Vindhyans appears to have a chemical signature too. Across this discontinuity there is a clear evidence for change in provenance of sediments, as discussed above. A similar change is also observed across the boundary between the Kaimur and the Rewa groups in Rajasthan.
8. With the help of detrital zircon geochronology it is established that the Sawa Sandstone Formation is younger than 1616±50 Ma and may contain volcanics similar to the ~ 1630 Ma rhyolites of the Deonar Formation in the Son Valley.
9. The results from Sr-isotope stratigraphy in the Balwan Limestone Formation of the Bhander Group suggest a minimum age of ~ 620 Ma. This age clearly confines the Vindhyan Supergroup to the Proterozoic Eon and increases the likelihood of finding physical evidences for one or more of the Neoproterozoic global glacial events.
10. The variations of $\delta^{13}C$ and $\delta^{18}O$ in the Balwan Limestone are not the result of any facies variation, instead represent basin wide, if not global, changes in organic matter burial. The negative excursion observed within the formation probably reflects a large scale reduction in biology and the positive excursion reflects sudden change in biodiversity.

11. Based on this study a two stage model for the evolution of the Vindhyan Basin in Rajasthan has been proposed. At first stage ~1900 Ma due to the Aravalli Orogeny a foreland setting got generated in the eastern flank of the Aravalli mountain chain which supplied the sediments to the Lower Vindhyans for about 200 million years. The initiation of Delhi orgoney in the western flank of the Aravalli Mountain marks the closing of the Lower Vindhyans. After completion of the major Delhi folding at ~ 1400 Ma, the second stage sets in and the Upper Vindhyans start getting deposited.

Future Scope

The present work carried out on the Vindhyan Supergroup of rocks in Rajasthan Vindhyans demands a thorough study of these sediments at various places in the basin for developing a comprehensive evolutionary model for the Vindhyan Basin. In view of this, future studies that can be pursued are as follows:

1. Identification of locations of the subduction zones in the Aravalli-Delhi mountain chain.
2. The basal volcanics such as Khairmalia in the Rajasthan and Jungel in the Son Valley should be studied in greater detail for their contributions to the sediments for the Vindhyan Basin.
3. The geochronological attempts should be made to date volcanism in the basement.
4. Nd isotope fingerprinting of various basement rocks should be done in the Aravalli-Delhi mountain chain, especially in the Hindoli Group and the Delhi Group of rocks.
5. More field and isotopic work should be done on the limestone formations to look for the physical and chemical evidences for the Neoproterozoic glacial events.

REFERENCES

Abbey S. (1983) Studies in "Standard Samples" of Silicate Rocks and Minerals 1969-1982, *Canadian Geological Survey paper* 83-15, p-114.

Acharyya S. K. (2003) The nature of Mesoproterozoic Central Indian tectonic zone with exhumed and reworked older sediments, *Gond. Res.* 6, 197–214.

Ahmad T, Deb M., Tarney J. and Raza M. (2008a) Proterozoic mafic volcanism in the Aravalli-Delhi Orogen, Northwestern India: Geochemistry and tectonic framework, *Jour. Geol. Soc. India* 72, 93-111.

Ahmad T, Dragusanu C. and Tanaka T. (2008b) Provenance of Late Archean Aravalli mafic rocks from Rajasthan, Northwestern India: Nd isotopes, evidence for enriched mantle reservoirs, *Precam. Res.* 162, 150-159.

Anbarasu K. (2001) Acritarch from Mesoproterozoic Chitrakoot Formation, Semri group, Chitrakoot Area, Central India, *Jour. Geol. Soc. India* 57, 179-183.

Andersen C. B. and Samson S. D. (1995) Temporal changes in Nd isotopic composition of sedimentary rocks in the Sevier and Taconic foreland basins: Increasing influence of juvenile sources, *Geology* 23, 983-986.

Azmi R. J., Joshi D., Tiwari B. N., Joshi M. N., Mohan K. and Srivastava S. S. (2006) Age of the Vindhyan Supergroup of Central India: An exposition of biochronology vs. radiochronology, *In*: Micropalaeontology: Application in Stratigraphy and Palaeoceanography (Ed. D.K. Sinha), Narosa Publishing House, New Delhi, India, 29-62.

Azmi, R. J. (1998) Discovery of Lower Cambrian Small Shelly Fossils and Brachiopods from the Lower Vindhyan of Son Valley, Central India, *Jour. Geol. Soc. of India 52, 381-389.*

Banerjee A. and Banerjee D. M. (2010) Modal analysis and geochemistry of two sandstones of the Bhander Group (Late Neoproterozoic) in parts of the Central Indian Vindhyan basin and their bearing on the provenance and tectonics, *J. Earth Syst. Sci.* 119, 825-839.

Banerjee A. K. and Singh H. J. M. (1981) Paleogeography and sedimentation of Vindhyans in eastern Rajasthan, *Misc. Publ. Geol. Surv. India* 50, 89-94.

Banerjee I. (1974) Barrier coastline sedimentation model and Vindhyan example, *Geol. Min. Metal. Soc. India* 46, 101-127.

Basu A. R., Sharma M. and DeCelles P. G. (1990) Nd, Sr-isotopic provenance and trace element geochemistry of Amazonian Foreland Basin Fluvial Sands, Bolivia and Peru: implications for Ensialic Andean Orogeny, *Earth Planet. Sci. Lett.* 105, 149–169.

Bengtson S., Belivanova V., Rasmussen B. and Whitehouse M. (2009) The controversial "Cambrian" fossils of the Vindhyan are real but more than a billion years older, *Proc. National Acad. Sci. 106, 7729–7734.*

Berner R. A. and R. Raiswell (1983) Burial of organic carbon and pyrite sulphur in sediments over Phenerozoic time: A new theory, *Geochim. Cosmochim. Acta* 47, 855-862.

Bhatia M. R. (1983) Plate Tectonics and geochemical composition of sandstone, *J. Geology* 91, 611-627.

Bhatia M. R. and Crook K. A. W. (1986) Trace element characteristics of graywackes and tectonic discrimination of sedimentary basins, *Contrib. Mineral. Petrol.* 92,181-193.

Bhattacharyya A. (1996) *Recent advances in Vindhyan Geology, Mem. Geol. Soc. India* 36, 331p.

Blatt H. (1985) Provenance studies and mudrocks, Jour. *Sedi. Petrol.* 55, 69–75.

Bock B., McLennan S. M. and Hanson G. N. (1994) Rare earth element redistribution and its effects on the neodymium isotope system in the Austin Glen Memberof the Normanskill Formation, New York, USA, *Geochim. Cosmochim. Acta* 58, 5245–5253.

Bose P. K., Banerjee S. and Sarkar S. (1997) Slope-controlled seismic deformation and tectonic framework of deposition, Koldaha Shale, India. *Tectonophysics* 269, 151–169

Bose P.K., Sarkar S., Chakraborty S. and Banerjee S. (2001) Overview of the Meso-to-Neoproterozoic evolution of the Vindhyan basin, central India. *Sedimentary Geology* 141–142, 395–419.

Burke W.H., Denison R.E., Hetherington E.A., Koep nick R.B., Nelson H.F. and Otto, J.B. (1982) Variation of seawater $^{87}Sr/^{86}Sr$ throughout Phanerozoic time, *Geology* 10, 516–519.

Catling D.C., and Claire M.W. (2005) How Earth's atmosphere evolved to an oxic state: A status report, *Earth Planet. Sci. Lett.* 237, 1-20.

Chakrabarti R., Basu A.R. and Chakrabarti A. (2007) Trace element and Nd-isotopic for sediment sources in the mid-Proterozoic Vindhyan Basin, central India, *Precam. Res.* 159, 260-274.

Chakraborty C. (2006) Proterozoic intracontinental basin: The Vindhyan example. *J. Earth Sys. Sci.* 115(1), 3-22.

Chakraborty C. and Bhattacharyya A. (1996) The Vindhyan Basin: An overview in the light of current perspectives, *Mem. Geol. Soc. India* 36,301-312.

Chakraborty P. P., Dey S. and Mohanti S. P. (2010) Proterozoic platform sequences of Peninsular India: Implications towards basin evolution and supercontinent assembly, *J. Asian Earth Sci.* 39, 589-607.

Chanda S. K. and Bhattacharyya A. (1982) Vindhyan sedimentation and paleogeography: Post-Auden developments, In K. S. Valdiya, S.B. Bhatia and V. K. Gaur (Eds.) *Geology of Vindhyachal*, Hindustan Pub. Corp. Delhi, 88-101.

Condie K. C. (1982) Plate Tectonics and crustal evolution, 2nd edidition, Pergaman Press.

Condie K. C. (1993) Chemical composition and evolution of the Upper continental crust: contrasting results from surface samples and shales, *Chem. Geol.* 104, 1–37.

Condie K. C. (1991) Another look at rare earth elements in shales, *Geochim. Cosmochim Acta* 55, 2527-2531.

Crawford, A.R., and Compston, W. (1970) Age of Vindhyan System of peninsular India, *J. Geol. Soc. London* 125, 351–372.

Daly R. A. (1909) First calcareous fossils and the evolution of limestones, *Geol. Soc. Am. Bull.* 20, 153-170.

Das L. K., Mishra D. C., Ghosh D. and Banerjee B. (1990) Geomorphotectonics of the basement in a part of upper Son Valley of the Vindhyan Basin, *J. Geol. Soc. India* 35, 445–458.

De C (2003) Possible organisms similar to Ediacaran forms from the Bhander Group, Vindhyan Supergroup, Late Neoproterozoic of India, *J. Asian Earth Sci.* 21, 387–395.

De C (2006) Ediacaran Fossil assemblage in the Upper Vindhyans of Central India and its significance, *J. Asian Earth Sci.* 27, 660–683.

Deb M., Thorpe R. and Krstic D. (2002) Hindoli Group of Rocks in the Eastern Fringe of the Aravalli-Delhi Orogenic Belt-Archean Secondary Greenstone Belt or Proterozoic Supracrustals? *Gond. Res.* 5(4), 879-883.

DePaolo D. J. and Wasserburg G. J. (1976) Nd isotopic variations and petrogentic models, *Gephys. Res. Letters* 3, 249-252.

DePaolo D. J. (1988) Age dependence of the composition of continental crust as determined from Nd isotopic variations in igneous rocks, *Earth Planet. Sci. Lett.* 59, 263-271.

Des Marais D. J. (1994) The Archean atmosphere: its composition and fate. *In*: K.D. Condie, Editor, *Archean Crustal Evolution*, Elsevier, Amsterdam (1994), 505–523.

Dia A., Dupre B., Gariepy C., and Allegre C. J. (1990) Sm-Nd and trace element characterization of shales form the Abitibi Belt, Labrador Trough, and Appalachian Belt: Consequences for crustal evolution through time, *Canad. J. Earth Sci.* 27, 758-766.

Dickinson W. R. (1970) Interpreting detrital modes of greywacke and arkose, *J.Sediment. Petrol.* 40, 695–707.

Evans D. A. D. (2000) Stratigraphic, geochronological, and paleomagnetic constraints upon the Neoproterozoic climatic paradox, *Am. J. Sci.* 300, 347-433.

Evans D. A. D. (2009) The palaeomagnetically viable, long-lived and all-inclusive Rodinia supercontinent reconstruction, In Murphy J. B., Keppie J. D. & Hynes A. J. (eds.) *Ancient Orogens and Modern Analogues*, Geol. Soc. London, Sp. Publ. 327, 371-404.

Faure G. (1986) *Principles of isotope geology*, 2nd edition, John Wiley & Sons, Singapore, 589p.

Fedo C. M., Nesbitt H. W. and Young, G. M. (1995) Unraveling the effects of K-metasomatism in sedimentary rocks and paleosols, with implications for paleoweathering conditions and provenance, *Geology* 23, 921–924.

Fermor L. L. (1930) On the age of the Aravalli Range, *Record Geol. Surv. India*, 62, 391-409.

Flanagan F.J. (1976) 1972 Compilation of data on USGS, *U.S. Geol. Surv. Prof. Paper* 840, 131-183.

Foley S., Tiepolo M. and Vannucci R. (2002) Growth of early continental crust controlled by melting of amphibolite in subduction zones, *Nature*, 417, 837–840.

Folk R.L. and Ferm J. C. (1966) A portrait of Paul D. Krynine, *J. Sediment. Petrol.* 36, 851- 863.

Frank T. D., Lyons T. W. and Lohmann K. C. (1997) Isotopic evidence for the paleoenvironmental evolution of the Mesoproterozoic Helena Formation, Belt Supergroup, Montana, USA, *Geochim. Cosmochim. Acta* 61, 5023–504.1

Friedman I. and O'Neil J. R. (1977) Compilation of stable isotope fractionation factors of geochemical interest, *U.S. Geol. Surv.Prof. Pap.* 440-KK, 49.

Gao S., Liu X. M., Yuan H. L., Hattendorf B., Gunther D., Chen L. and Hu S. H. (2002) Determination of forty two major and trace elements in USGS and NIST SRM glasses by laser ablation-inductively coupled plasma-mass spectrometry, *Geostand. Newsl.* 26, 181–196.

Ghosh A. and Bose A. (1950) Microfossils from the Vindhyans, *Science and Culture* 15, 330-331.

Gladney E. S. and Roelandts I. (1988) 1987 Compilation of Elemental Concentration Data for USGS BHVO-1, MAG-1, QLO-1, RGM-1, SCo-1, SDC-1, SGR-1, and STM-1, *Geostand. Newsl.* 12, 253-362.

Gleason J. D., Patchett P. J. and Ruiz W. R. D. (1994) Nd isotopes link Ouachita turbidites to Appalachian sources, *Geology* 22, 347-350.

Gokaran S. G., Rao C. K. and Singh B. P. (1995) Crustal structure in southeast Rajasthan using magneto-telluric technique, Mem. *Geol. Soc. India* 31, 373-383.

Goldstein S. J. and Jacobsen S. B. (1988) Nd and Sr isotope systematics of river water suspended material: Implications for crustal evolution, Earth Planet. Sci. Lett 87,249-265.

Govindaraju K. (1994) 1994 Compilation of Working Values and sample Descriptions for 383 Geostandards, *Geostand. Newslett.* 18, 1-158.

Graver J. I. and Scott T. J. (1995) Trace elements in shale as indicators of crustal province and terrain accretion in the southern Canadian Cordillera, *Geol. Soc. Am. Bull.* 107, 440-453.

Gregory L. C. (2008) India in the Proterozoic : two key spatial and temporal constraints, *A MS Thesis University of Florida*.78p.

Gupta B. C. (1934) The geology of central Mewar, *Mem. Geol. Surv. India* 65,107-168.

Hacket C. A. (1881) On the geology of Aravalli region Central and Eastern Rajputana, *Rec. Geol. Surv. India* 44, 97-102.

Hall S.M. and Veizer J. (1996) Geochemistry of Precambrian carbonates. VII. Belt Supergroup, Montana and Idaho, USA, *Geochim. Cosmochim. Acta* 60, 667-977.

Hannigan R. E. and Basu A. R. (1998) late diagenetic trace element remobilization in organic-rich Black Shales of the Taconic Foreland basin Quebec, Ontario and New York, *In*: Jurgen W. Z. S. and Sethi P. S. (eds.), *Shales and Mudstones II*, 209-233.

Heron A. M. (1936) Geology of south-eastern Rajputana, *Mem. Geol. Surv. India*, 68, 1-120.

Herron M. M. (1988) Geochemical classification of terrigenous sands and shales from core or log data, *Jour. of Sed. Pet.* 30, 841-883.

Hoffman H. J. (2005) Paleoproterozoic dubiofossils from India revisited-Vindhyan *Triploblastic* animal burrows or pseudofossils, *J. Palaeont. Soc. India*, Golden Jubilee Volume 50(2), 113-120.

Hoffman P.F., and Schrag D.P. (2002) The snowball Earth hypothesis: testing the limits of global change, *Terra Nova* 14,129-155.

Hoffman P.F., Kaufman A.J., Halverson G.P., and Schrag D.P. (1998) A Neoproterozoic snowball earth, *Science*, 281, 1342-1346.

Holser W.T. (1984) Gradual and abrupt shifts in ocean chemistry during Phanerozoic time. *In*: Holland, H.D., Trendall, A.F. (Eds.), *Patterns of Change in Earth Evolution*. Springer, Berlin, 123-143.

Hussain M. F., Mondal M. E. A. and Ahmad T. (2004) Geodynamic evolution and crustal growth of the central Indian Shield: Evidence from geochemistry of gneisses and granitoids, *Proc. Indian Acad. Sci. (Earth Planet. Sci.)* 113(4), 699-714.

Iqbaluddin, Pasad B., Sharma S. B., Mathur R. K., Gupta S. N. and Sahai T. N. (1978) Genesis of the Great Boundary Fault of Rajasthan, India, *Proc. 3rd Reg. Conf. Geol. Min. Resour.* South East Asia, Bangkok, 145-149.

Jacobsen S. B. and Kaufman A. J. (1999) The Sr, C and O isotopic evolution of Neoproterozoic seawater, *Chemical Geology* 161, 37-57.

Jain S. C., Yedekar D. B. and Nair K. K. K. (1991) Central Indian Shear Zone: A major Precambrian crustal boundary, *J. Geol. Soc. India* 37, 521-532.

Jarvis K. E. (1988) Inductively coupled plasma mass spectrometry; a new technique for the rapid or ultra-trace level determination of the rare-earth elements in geological materials, *Chem. Geol.* 68, 31-39.

Javaux E. J., Knoll A. H., and Walter M. R. (2001) Morphological and ecological complexity in early eukaryotic ecosystems, *Nature* 412, 66-69.

Jokhan Ram, Shukla S. N., Pramanik A. G., Varma B. K., Chandra G. and Murthy M. S. N. (1996) Recent Investigations in the Vindhyan Basin: Implications for Basin Tectonics, *Mem. Geol. Soc. India* 36, 267-286.

Kaila K. L. and Krishna V. G. (1992) Deep Seismic sounding studies in India and major discoveries, *Curr. Sci.*, 62, 117-154.

Kaila K. L., Murty P. R. K. and Mall D. M. (1989) The evolution of the Vindhyan Basin vis-à-vis the Narmada-Son Lineament, central India, from deep seismic soundings, *Tectonophysics* 162 (3/4), 277–289.

Kaufman A. J., Corsetti F. A. and Varni M. A. (2007) The effect of atmospheric oxygen on carbon and sulphur isotope anomalies in the Neoproterozoic Johnnie Formation, *Chem. Geol.* 237, 47-63.

Kent A. J. R., Jacobsen B., Peate D. W., Waight T. E. and Baker J.A. (2004) isotope dilution MC-ICPMS-Ms Rare Earth Element analysis of Geochemical Reference Materials NIST SRM610, NIST SRM 612,NIST SRM614, BHVO-2G,BHVO-2, BCR-2G, JB-2, WS-E, W-2, AGV-1 and AGV-2, *Geostand. Geoanalyt. Res.* 28 (3), 417-429.

Klootwijk C.T., Nazirullah R. and de Jong K.A. (1986) Paleomagnetic constraints on formation of the Mianwali reentrant, Trans-Indus and western Salt range,Pakistan, *Earth Planet. Sci. Lett.* 80, 394-414.

Kopp R. E., Kirschvink J. L., Hilburn I. A., and Nash C. Z. (2005) The paleoproterozoic snowball Earth: A climate disaster triggered by the evolution of oxygenic photosynthesis: *Proc. Nat. Acad. Sci. USA* 102, 11131-11136.

Krishnan M. S. (1968) *Geology of India and Burma*. Tata McGraw Hill Publication, New Delhi.

Krumbein W. C. and Pettijohn F. J. (1938) *Manual of Sedimentary Petrography*. Appleton-Century-Crofts, New York. 549 pp.

Kulkarni K. G. and Borakar V. D. (1996) A significant stage of metazoan evolution from the Proterozoic rocks of the Vindhyan Supergroup, *Curr. Sci.* 70, 1096-1100.

Kumar A., Gopalan K. and Rajgopalan G. (2001) Age of the Lower Vindhyan sediments, Central India. *Curr. Sci.* 81, 806–809.

Kumar A., Kumari P., Dayal A.M., Murthy D.S.N. and Gopalan K. (1993) Rb–Sr ages of Proterozoic kimberlites of India: evidence for contemporaneous emplacements. *Precam. Res.* 62, 227–237.

Kumar B. Das sharma S., Sreenivas B., Dayal A. M., Rao M. N., Dubey N and Chawla B. R. (2002) Carbon oxygen and strontium isotope geochemistry of Proterozoic carbonate rocks of the Vindhyan Basin, central India. *Precam. Res.* 113, 43-63.

Kumar S. (1995) Megafossils from the Mesoproteroozic Rohtas Formation (the Vindhyan Supergroup), Katni area, Central India, *Precam. Res.* 72, 171-184.

Kumar S. (1999) Siliceous sponge spicule-like forms from the Neoproterozoic Bhander Limestone, Maihar area, Madhya Pradesh. *J. Palaeon. Soc. India* 44, 141-148.

Kumar S. (2001) Mesoproterozoic megafossils *Chuaria-Tawuia* association may represents parts of a multicellular plant, Vindhyan Supergroup, Central India, *Precam. Res.* 106, 187-211.

Kumar S. and Pandey S. K. (2008) Discovery of organic-walled microbiota from the black-bedded chert, Balwan Limestone, the Bhander Group, Lakheri area, Rajasthan. *Curr. Sci.* 94, 797-800.

Kumar S., Schidlowski M. and Joachi M. M. (2005) Carbon isotope stratigraphy pf the palaeo-Neoproteroozic Vindhayn Super group, Central India: implications for basin evolution and intrabasinal correlation, J. Palaeont. Soc. India 50, 65-81.

Kumar S. and Srivastava P. (1997) A note on the carbonaceous megafossils from Neoproterozoic Bhander Group, Maihar area, Madhya Pradesh, *Jour. Paleo. Soc. India* 42, 141-146.

Kumar S. and Srivastava P. (2003) Carbonaceous megafossils from the Neoproterozoic Bhander Group, central India, *Jour. Paleo. Soc. India* 48, 139-154

Kumar S. and Srivastava P.(1992) Microfossils from the black the chert of Bhagwanpura Limestone (Middle Proterozoic), Vindhyan Supergroup, Chittorgarh area, Rajasthan, West India, *Curr. Sci.* 62, 371-372.

Kump L. R. and Arthur M. A.(1999) Interpreting carbon-isotope excursions: carbonates and organic matter , *Chemical Geology* 161, 181–198.

Le Bas M. J., LeMaitre R. W., Streckeisen A. and Zanettin P. (1986) A chemical classification of volcanic rocks based on the total alkali-silica diagram. *Jour. Petrol.* 27, 745-750

Leelanandam C., Burke K., Ashwal L.D. and Webb S.J. (2006) Proterozoic mountain building in Peninsular India: an analysis based primarily on alkaline distribution, *Geol. Mag.* 143 (2), 195-212.

Lev S. M and Filer J. K. (2004) Assessing the impact of black shale processes on REE and the U–Pb isotope system in the southern Appalachian Basin, Chem. Geol. 206 , 393–406.

Lev S. M., McLennan S. M. and Hanson G. N. (1999) Mineralogic controls on REE mobility during black shale diagenesis, *Jour. Sed. Res.* 69, 1071–1082.

Lichte F. E., Meier A. L., and Crock J. G. (1987) Determination of the rare-earth elements in geological materials by inductively coupled plasma mass spectrometry, *Anal. Chem.* 59, 1150-1157.

Longerich H. P. Jenner G.A. Fryer B. J. and Jackson S. E. (1990) Inductively coupled plasma-mass spectrometric analysis of geological samples: A critical evaluation based on case studies, *Chemical Geology* 83, 105-118.

Ludwig K. R. (2003) User's Manual for Isoplot/Ex. 3.00: A Geochronological Toolkit for Microsoft Excel. *Berkeley Geochronology Centre (Special Publication 1a)*, 55 p.

Luhr J. F. and Haldar D. (2006) Barren Island Volcano (NE Indian Ocean): Island-arc high-alumina basalts produced by troctolite contamination, *J. Volcano. Geothermal Res.* 149, 177– 212.

Mackie W. (1899a) The sands and sandstones of eastern Moray, *Trans. Edinb. Geol. Soc.* 7, 148–172.

Mackie W. (1899b) The feldspars present in sedimentary rocks as indicators of the conditions of contemporaneous climates, *Trans.Edinb. Geol. Soc.* 7, 443–468

Maithy P. K. and Babu R. (1988) The mid-Proterozoic Vindhyan macrobiota from Chopan, south-east, Uttar Pradesh, *J. Geol. Soc. India* 31, 584–590.

Maitra A. K. and De C. (1998) Primitive trace fossils from Vindhyans. *Geol. Surv. India News*, 29, 47-48.

Mallet F. R. (1869) The Vindhyan Series as exhibited in north-western and central provinces of India, *Mem. Geol. Surv. of India*, 7, (1), 1-129.

Malone S. J., Meert J. G., Banerjee D. M., Pandit M. K., Tamrat E., Kamenov G. D., Pradhan V. R. and Sohl L. E. (2008) Paleomagnetism and Detrital Zircon Geochronology of the Upper Vindhyan Sequence, Son Valley and Rajasthan, Indian: A ca. 1000 Ma Closure age for the Purana Basins?, *Precam. Res.* 164, 137-159.

Mathur S. M., Narian K. and Srivastava J. P. (1958) Algal structure from Fawn Limestone, Semri Series (Lower Vindhyans) in the Mirzapur district, *Rec. Geol. Surv. India* 87,819-822.

McArthur J. M. (1994) Recent trends in strontium isotope stratigraphy, *Terra Nova* 6, 331-358.

McCulloch M. T. and Wasserburg G. (1978) Sm-Nd and Rb-Sr chronology of continental crust formation, *Science* 200, 1003-1011.

McDonough W. F. and Sun S-s. (1995) The composition of the Earth, *Chem. Geol.* 120,223-253.

McLennan S. M., Nance W. B. and Taylor S. R. (1980) Rare earth element-thorium correlations in sedimentary rocks, and the composition of the continental crust, *Geochim. Cosmochim. Acta* 44, 1833-1839.

McLennan S. M. and Hemming S. (1992) Samarium/neodymium elemental and isotopic systematics in sedimentary rocks, *Geochim. Cosmochim. Acta* 56, 887-898.

McLennan S. M., Bock B., Hemming R., Hurowitz J. A., Lev S. M. and McDaniel D. K. (2003) The roles of provenance and sedimentary processes in the geochemistry of sedimentary rocks. *In*: Lenz, D.R. (Ed.), *Geochemistry of Sediments and Sedimentary Rocks*, Geological Association of Canada, Newfoundland (Geotext4.), 7–31.

McLennan S. M., Hemming S., Taylor S. R. and Erikson (1995) Early Proterozoic crustal evolution: Geochemical and Nd-Pb isotopic evidence from metasedimentary rocks southwestern North America, *Geochim. Cosmochim. Acta* 59, 1153-1177.
McLennan S. M. and Hemming S. (1992) Samarium/neodymium elemental and isotopic systematics in sedimentary rocks, *Geochim. Cosmochim. Acta* 56, 887-898.
McLennan S. M., Hemming S., McDaniel D. K. and Hanson G. N. (1993) Geochemical approaches to sedimentation, provenance and tectonics, *Geol. Soc. Am. Sp. Paper* 284, 21-40.

McLennan S. M. (1989) Rare Earth Elements in sedimentary rocks: influence of provenance and sedimentary processes, *In*: B. R. Lipin and G. A. McKay (eds.), Geochemistry and mineralogy of rare earth elements, *Reviews in Mineralogy* 21,169-200.

McElhinny M.W., Cowley J.A. and Edwards D.J. (1978) Paleomagnetism of some rocks from Peninsular India and Kashmir, *Tectonophysics* 50, 41-54.

Medlicott H. B. (1859) Vindhyan rocks and their associates in Bundelkhand, *Mem. Geol. Surv. India* 2, part 1.

Meert J.G. and Torsvik T.H. (2003) The making and unmaking of a supercontinent:Rodinia revisited, *Tectonophysics* 375, 261-288

Michard A., Gurriet P., Soudant M. and Albarede F. (1985) Nd isotopes in French Phanerozoic shales: External and internal aspects of crustal evolution, *Geochim. Cosmochim. Acta* 49, 601-610.

Milodowski A. E., Zalasiewicz J. A. (1991) The origin and sedimentary, diagenetic and metamorphic evolution of chlorite-mica stacks in Llandovery sediments of central Wales, U.K. *Geol. Mag.*, 128 (3), 263-278

Miller D. M., Goldstein S. L. and Langmuir C. H. (1994) Cerium/lead and lead isotope ratios in arc magmas and the enrichment of lead in the continents. *Nature* 368, 514–520.

Miller R. G. and O'Nions R. K. (1984) The provenance and crustal residence ages of British sediments in relation to palaeogeographic reconstructions. *Earth Planet. Sci. Lett.* 68, 459–470.

Mishra D. C., Singh B., Tiwari V. M., Gupta S. B. and Rao M.B.S.V. (2000) Two cases of continental collisions and related tectonics during the Proterozoic period in India — insights from gravity modeling constrained by seismic and magnetotelluric studies, *Precam. Res.* 99, 149-169.

Mishra M. and Sen S. (2010) Geochemical signatures of Mesoproterozoic silliciclastic rocks of the Kaimur Group of the Vindhyan Supergroup, *Central India, Chin. J. Geoch.* 29, 21-32.

Mishra R. C. (1969) The Vindhyan System, Presidential Address *56th Indian science Congress*, Kolkata, 1-32.

Mondal M. E. A., Goswami J. N., Deomurari M. P. and Sharma K. K. (2002) Ion microprobe $^{207}Pb/^{206}Pb$ ages of zircons from the Bundelkhand massif, northern India: implications for crustal evolution of the Bundelkhand-Aravalli protocontinent, *Precam. Res.* 117, 85-100.

Murthy T. V. V. G. R. K. and Mishra S. K. (1981) The Narmada-Son lineament and structure of the Narmada rift system, *Jour. Geol. Soc. India*, 22,112-120.

Naqvi S. M. and Rogers J. J. W. (1987) *Precambrian Geology of India*. Oxford University Press, Oxford, 223 pp.

Naqvi S. M., Sawkar R. H., Subbarao D. V., Govil P. K. and Rao T. G. (1988) Geology, geochemistry and tectonic setting of Archean Greywacke from Karnataka nucleus, India, *Precam. Res.* 39, 193-216.

Narian H. (1987) Geophysical constraints on the evolution of Purana basins of India with special reference to Cuddapah, Godavari and Vindhyan basins, *Mem. Geol. Soc. India* 6, 5-12.

Nelson B. K. and DePaolo D. J. (1988) Application of Sm–Nd and Rb–Sr isotope systematics to studies of provenance and basin analysis. *Jour. Sed. Petrol.* 58, 348–357.

Nesbitt H.W. and Young G. M. (1982) early Proterozoic climates and plate motions inferred from major element chemistry of lutites, *Nature* 299, 715-717.

Nesbitt H.W. and Young G.M. (1984) Prediction of some weathering trends of plutonic and volcanic rocks based on thermodynamic and kinetic considerations, *Geochim. Cosmochim Acta* 48, 1523-1534.

Ohr M., Halliday A. N. and Peacor D. R. (1994) Mobility and fractionation of rare earth elements in argillaceous sediments: Implications for dating diagenesis and low-grade metamorphism, *Geochim Cosmochim. Acta* 58, 289-312.

O'Nions R.K., Hamilton P. J. and Hooker P. J. (1983) A Nd isotope investigation of sediments related to crustal development in the British Isles, *Earth Planet. Sci. Lett.* 63, 229–240.

Oldham T. (1856) Remarks on the classification of the rocks of central India resulting from investigations of Geological Survey, *Jour. Asiatic. Soc. Bengal,* 25,224-256.

Oldham T. (1893) *Manual of Geology of India*, 2nd edition, Govt. Printing Press, 543p.

Paikaray S., Banerjee S. and Mukherji S. (2008) Geochemistry of shales from the Paleoproterozoic to Neoproterozoic Vindhyan Supergroup: implications on provenance, tectonics and paleoweathering, *J. Asian Earth Sci.* 32, 34-48.

Patranabis-Deb, S., Bickford, M.E., Hill, B., Chaudhuri, A.K. and Basu, A. (2007) SHRIMP Ages of Zircon in the Uppermost Tuff in Chattisgarh Basin in Central India Require ~500-Ma Adjustment in Indian Proterozoic Stratigraphy, *J. Geol.* 115, 407-415.

Popp B. N., Parekh P., Tilbrook B., Bidigare R. R. and Laws E. A. (1997) Organic carbon $\delta^{13}C$ variations in sedimentary rocks as chemostratigraphic and paleoenvironmental tools, *Palaeogeogr. Palaeoclimat. Palaeoecology* 132, 119–132.

Prasad B. (1980) Vindhyan stromatolites stratigraphy in SE Rajasthan, *Misc. Pub. Geol. Surv. India* 44,201-206.

Prasad B. (1981) A review of the Vindhyan Supergroup in southeastern Rajasthan, *Misc. Pub. Geol. Surv. India* 50, 31-40.

Prasad B. (1984) Geology, sedimentation and paleogeography of the Vindhyan Supergroup, S.W. Rajasthan, *Mem. Geol. Surv. India* 116 (1), 1–107.

Prasad B. R. and Rao V. V. (2006) Deep seismic reflection study over the Vindhyans of Rajasthan: Implications for geophysical setting of the basin, *J. Earth Syst. Sci.* 115 (1),135-147.

Raczek I., Jochum K. P. and Hofmann A. W. (2003) Neodymium and Strontium Isotope Data for USGS Reference Materials BCR-1, BCR-2, BHVO-1, BHVO-2, AGV-1, AGV-2, GSP-1, GSP-2 and Eight MPI-DING Reference Glasses, *Geostand. Newsl.* 27(2), 173–179.

Radhakrishna B. P. and Naqvi S. M. (1986) Precambrian continental crust of India and its evolution, *J. Geology* 94, 145-166.

Rai V. and Singh V. K. (2004) Discovery of *Obruchevella* Reitlinger, 1948 from the Late Palaeoproterozoic Lower Vindhyan succession and its significance, *Jour. Palaeont. Soc. India,* 49, 189-196.

Rai V., Shukla M. and Gautam R. (1997) Discovery of carbonaceous megafossils (*Chuaria-Tawuia* assemblage) from the Neoproterozoic Vindhyan succession (Rewa Group), Allahabad-Rewa area, India, *Curr. Sci.* 73, 783-788.

Ramakrishnan M. and Vaidyanadhan R. (2008) *Geology of India*, Volume 1, Bangalore, India, Geological Society of India, 556 p.

Rasmussen B., Bose P. K., Sarkar S., Banerjee S., Fletcher I. R., and McNaughton N. J. (2002) 1.6 Ga U-Pb zircon age for the Chorhat Sandstone, lower Vindhyan, India: Possible implications for early evolution of animals, *Geology* 30, 103–106,

Ray J. S., Davis W. J. and Shukla A. D. (2007) Age of lower Vindhyans of Rajasthan, Presented at *International Conference on Precambrian Sedimentation and Tectonics,* December 10-12, 2007, IIT Bombay, India.

Ray J. S. (2006) Age of the Vindhyan Supergroup: A review of recent findings. *J. Earth Sys. Sci.* 115(1,) 149-160.

Ray J. S., Martin M. W., Veizer J., and Bowring S. A. (2002) U-Pb zircon dating and Sr isotope systematics of the Vindhyan Supergroup, India, *Geology* 30, 131–134.

Ray J. S., Veizer J. and Davis W. J. (2003) C, O, Sr and Pb isotope systematics of carbonate sequences of the Vindhyan Supergroup, India: age, diagenesis, correlations and implications for global events, *Precam. Res.* 132, 103-140.

Ray R., Shukla A. D., Sheth H. C., Ray J. S., Duraiswami R. A., Vanderkluysen L., Rautela C.S. and Mallik J. (2008) Highly heterogeneous Precambrian basement under the central Deccan Traps, India: Direct evidence from xenoliths in dykes, *Gond. Res.* 13, 375-385.

Raza M., Jafari S. G., Alvi S. H. and Khan A. (1993) Geodynamic evolution of Indian shield during Proterozoic: Evidence from mafic volcanic rocks, *J. Geol. Soc. India* 41, 455-469.

Raza M., Casshyap S. M. and Khan A. (2002) Geochemistry of Mesoproterozoic Lower Vindhyan Shales from Chittaurgarh, Rajasthan and its Bearing on Source Rock Composition, Palaeoweathering Conditions and Tectono-sedimentary Environments, *Jour. Geol. Soc. India*, 60, 505-518.

Raza M., Dayal A. M., Khan A., Bhardwaj V. R. and Rais S. (2010) Geochemistry of lower Vindhyan clastic sedimentary rocks of Northwestern India shield: Implications for composition and weathering history of Proterozoic continental crust, *J. Asian Earth Sci.* 39, 51-61.

Raza M., Khan A. and Khan M. S. (2009) Origin of Late Palaeoproterozoic Great Vindhyan basin of North Indian shield: Geochemical evidence from mafic volcanic rocks, *J. Asian Earth Sci.* 34, 716-730.

Richter F.M., Rowley D.B. and DePaolo D.J. (1992) Sr isotope evolution of seawater: the role of tectonics, *Earth Planet. Sci. Lett.* 109, 11–23.

Rogers J. J. W. (1986) The Dharwar craton and the assembly of the Peninsular India, *J. Geol.* 94, 145-166.

Rosenbaum J. and Sheppard S. M. F. (1986) An isotopic study of siderites, dolomites and ankerites at high temperatures, *Geochim. Cosmochim. Acta* 50, 1147–1150

Roser B. P. and Korsch R. J. (1986) Determination of tectonic settings of sandstone-mudstone suits using SiO_2 content and K_2O/Na_2O ratio. *J. Geol.* 94, 635–650.

Roy A. and Bandyopadhyay B. K. (1990) Cleavage development in Mahakoshal Group of rocks of Sleemanabad-Sihora area, Jabalpur District, Madhya Pradesh. *Indian Mineral* 44, 111–128.

Roy A. B. and Jakhar S. R. (2002) *Geology of Rajasthan (Northwest India) Precambrian to recent*, Scientific Publishers (India), Jodhpur,421p.

Roy A. B. (1988) Framework of the Aravalli mountain range. *In:* Roy, A.B. (Ed.), Precambrian of the Aravalli Mountain Rajasthan, India. *Mem. Geol. Soc. India* 7, 3–31.

Rye R., and Holland H.D. (1998) Paleosols and the evolution of atmospheric oxygen: A critical review, *American Journal of Science* 298, 621-672.

Sahay A. and Srivastava D. C. (2005) Ductile shearing along the Great Boundary Fault: An example from the Berach river section, Chittaurgarh, Rajasthan, *Curr. Sci.* 88, 557-560.

Sahni M. R. (1936) *Fermoria minima*: A revised classification of the organic remains from Vindhyans of India, *M. Rec. Geol. Surv. India*, 458-468.

Sarangi S., Gopalan K. and Kumar S. (2004) Pb–Pb age of earliest megascopic, eukaryotic alga bearing Rhotas Formation, Vindhyan Supergroup, India: implications for Precambrian atmospheric oxygen evolution. *Precam. Res.* 132, 107–121.

Sarkar A., Chakraborty P.P., Mishra B., Bera M. K., Sanyal P. and Paul S. (2009) Mesoproterozoic sulphidic ocean, delayed oxygenation and evolution of early life: sulphur isotope clues from Indian Proterozoic basins, *Geol. Mag.* 147 (2), 1–13.

Sarkar G., Barman T.R. and Corfu F. (1989) Timing of Continental Arc-Type Magmatism In Northwest India; Evidence from U-Pb Zircon Geochronology, *J. Geol.* 97, 607-612.

Sarkar S., Banerjee S. and Bose P. K. (1996) Trace fossils in the Mesoproterozoic Koldaha Shale, central India and their implications, *N. Jb. Geol. Paleont. Mh.* 7, 425-436.

Sarkar S., Chakraborty P.P., Bhattacharya, S.K. and Banerjee S. (1998) C^{12} enrichment along intraformational unconformities within Proterozoic Bhander limestone, Son valley, India and its implication. *Carbonates and Evaporites* 13, 108–114.

Sastry M. V. A. and Moitra A. K. (1984) Vindhyan Stratigraphy-A review, *Mem. Geol. Surv. India* 116(2), 109-148.

Schieber J. (1992) A combined petrographical-geochemical provenance study of the Newland formation, Mid-Proterozoic of Montana, *Geological Magazine* 129, 223–237.

Schopf J. W. and Klein C. (1992) *The Proterozoic Biosphere - A Multidisciplinary Study*. Cambridge University Press, 1348p.

Seilacher A., Bose P.K., and Pfluger F., (1998) Triploblastic animals more than 1 Billion years ago: trace fossil evidence from India, *Science* 282, 80–83.

Sharma M. (1996) Microbiolites (stromatolites) from the Mesoproterozoic Salkhan Limestone, Semri Group, Rohtas, Bihar: their systematics and significance, *Geol. Soc. India, Mem.* 36, 167-196.

Sharma M. (2006) Paleobiology of Mesoproterozoic Salkhan Limestone, Semri group, Rohtas, Bihar, India, Synthesis and significance, J. *Earth Syst. Sci.*115 (1),67-98.

Shield G. and Veizer J. (2002) Precambrian marine carbonate isotope database version 1.1, G^3, doi: 10.1029/2001GC/000266.

Sinha-Roy S., Malhotra G. and Mohanty M. (1998) *Geology of Rajasthan*, Geological Society of India, Bangalore, 278p.

Sinha-Roy S. and Mohanti M. (1988) Blue schist facies metamorphism in ophiolitic mélange of the late Proterozoic Delhi belt, Rajasthan, India, *Precam. Res.* 42, 97-105.

Sinha-Roy S., Kirmani I. R., Reddy B. V. R., Sahu R. L. And Patel S. N. (1986) Fold pattern in the Vindhyan sequence in relation to the Great Boundary Fault: Example from Chittaurgarh area, Rajasthan, *Quart. Jour. Geol. Min. Metal. Soc. India* 558(4), 241-251.

Sircombe K.N. (2004) Age Display: an EXCEL workbook to evaluate and display univariate geochronological data using binned frequency histograms and probability density distributions, *Comp. & Geosci.* 30, 21-31.

Soni M. K., Chakraborty S. and Jain V. K. (1987) Vindhyan Super Group- A Review, *Mem. Geol. Soc. India* 6, 87-138.

Sorby, H.C., 1880. On the structure and origin of non-calcareous stratified rocks. *Proc. Geol. Soc. Lond.* 36, 46– 92.

Srivastava A. K. and Rajgopalan G. (1986) F-T Dating of Precambrian deposits of Vindhyan Group at Chitrakut, Banda district (U.P.-M.P.), *In* K. K. Sharma (ed.) *Nuclear Tracks*, 41-52.

Srivastava D. C. and Sahay A. (2003) Brittle tectonics and pore-fluid conditions in the evolution of the Great Boundary Fault around Chittaurgarh, Northwestern India. *Struc. Geol.* 25, 1713–1733.

Srivastava, P. (2002) Carbonaceous megafossils from the Dholpura Shale, Uppermost Vindhyan Supergroup, Rajasthan: An age implication, *J. Palaeontol. Soc. India* 47, 97-105.

Srivastava P. (2009 *Trachyhystrichoshaera*: An age-marker acanthomorph from the Bhander group, upper Vindhyan, Rajasthan, *J. Earth Sys. Sci.* 118, 575-582.

Srivastava H. B. and Gyanchand (1984) Geological and sedimentalogical studies of rocks, south of Chittaurgarh, Rajasthan, *Rec. Geol. Surv. India* 114(2), 1-14.

Stern R. A. (1997) The GSC Sensitive High Resolution Ion Microprobe (SHRIMP): analytical techniques of zircon U-Th-Pb age determinations and performance evaluation. In: Age and Isotopic Studies: *Report 10. Geol. Surv. Canada (Current Research 1997-F*, 1-31.

Stern R. A. and Amelin Y. (2003) Assessment of errors in SIMS zircon U-Pb geochronology using a natural zircon standard and NIST SRM 610 glass, *Chem. Geol.* 197 (1-4), 111-146.

Strauss H. (1997) The isotopic composition of sedimentary sulfur through time. *Paleo. Paleo. Paleo.* 132, 97-118.

Sudgen T. J., Deb M. and Windley B. E. (1990) Tectonic setting of mineralization in the Proterozoic Aravalli-Delhi orogenic belt, NW India, In : *Developments in Precambrian Geology*, 8, Elsevier, Amsterdam, 367-390.

Tanaka T., Togashi S., Kamioka H., Amakawa H., Kagami H., Hamamoto T., Yuhara M., Orihashi Y., Yoneda S., Shimizu H., Kunimaru T., Takahashi K., Yanagi T., Nakano T., Fujimaki H., Shinjo R., Asahara Y., Tanimizu M., Dragusanu C. (2000) JNdi-1: a neodymium isotopic reference in consistency with La Jolla neodymium, *Chem. Geol.* 168, 279-281.

Tandon S. K., Pant C. C. and Casshyap S.M. (1991) *Sedimentary basins of India – Tectonic context*. Gyanodaya Prakashan, Nainital.

Taylor S. R. and McLennan S. M. (1985) *The Continental Crust: its Composition and Evolution*. Blackwell scientific publications, 312 pp.

Tewari A. P. (1968) A new concept of paleotectonic setup of a part of a part of northern peninsular India with special reference to the great boundary faults. *Geol. Mijnbouw* 47, 21-27.

Thurach H. (1884) U¨ ber das Vorkommen mikroskopischer Zirkoneund Titanmineralien in den, *Gesteinen. Verh. Phys. Med. Ges. Wurzbrg.* 18, 203- 284.

Tucker M., Wright V. P. and Dickson J. A. D. (1990) *Carbonate Sedimentalogy*, Wiley Blackewell,482p

Turner C. C., Meert J. G., Kamenov G.D., and Pandit M.K.(2010) A Detrital zircon transect across the Son Valley sector of the Vindhyan Basin, India: Further constraints on Basin Evolution Geological Society of America *Abstracts with Programs*, 42, # 5, p. 195.

Valdiya K. S. (1969) Stromatolites of Lesser Himalayan carbonate formations and Vindhyan, *J. Geol. Soc. India* 10, 1-25.

Veizer J., Ala D., Azmy K., Bruckschen P., Buhl D., Bruhn F., Carden G.A.F., Diener A., Ebneth S., Godderis Y., Jasper T., Korte C., Pawellek F., Podlaha O.G. and Strauss H. (1999) $^{87}Sr/^{86}Sr$, $\delta^{13}C$ and $\delta^{18}O$ evolution of Phanerozoic seawater, *Chem. Geol.* 161, 59-88.

Veizer J., Holser W. T. and Wilgus C. K. (1980) Correlation of $^{13}C/^{12}C$ and $^{34}S/^{32}S$ secular variations. *Geochim. Cosmochim. Acta* 44, 579-587.

Venkatachala B. S., Sharma M., Shukla M. (1996) Age and life of the Vindhyans-facts and conjecture. In: Bhattacharyya, A. (Ed.), *Recent Advances in Vindhyan Geology, Mem. Geol. So. India* 36, 137-165.

Verma P. K. (1996) Evolution and Age of the Great Boundary fault of Rajasthan, *Mem. Geol. Soc. India*, 36, 197-212.

Verma, P. K. and Greiling, R. O. (1995) Tectonic evolution of the Aravalli orogen (NW India): an inverted Proterozoic rift basin? *Geol Rundsch.* 84, 683-696.

Verma R. K (1991) *Geodynamics of the Indian Peninsula and the Indian Plate Margin*, Oxford and IBH, 357p.

Vinogradov A., Tugarinov A., Zhykov C., Stapnikova N., Bibikova E., and Khorre K. (1964) Geochronology of Indian Precambrian: New Delhi, *International Geological Congress*, 10, 553-567.

Vredenburg E. (1906) Suggestions for a classification of the Vindhyans system, *Rec. Geol. Surv. India* 23,254-260.

Wang Y. L., Liu Y. G. and Schmitt R. A. (1986) Rare earth element geochemistry of south Atlantic deep sea sediments: Ce anomaly change at -54 My, *Geochim. Cosmochim. Acta* 50,1337-1355.

Weltje G. J and Eynatten H. V. (2004) Quantitative provenance analysis of sediments: review and outlook, Sed. Geol. 171,1-11.

Weidenbeck M., Goswami J.N. and Roy A.B. (1996) Stabilization of the Aravalli craton of the northwestern India at 2.5 Ga, an ion microprobe zircon study, *Chem. Geol.* 129, 325-340.

Winter J. D. (2001) *An Introduction to Igneous and Metamorphic Petrology*, Printice Hall, New Jersey, USA, 697p.

Wronkiewicz D. J. and Condie K. C. (1987) Geochemistry of archean shales from the Witwatersand supergroup, South Africa: source-area weathering and provenance, *Geochim. Cosmochim. Acta* 51, 2401-2416.

Yedekar D. B., Jain S. C., Nair K. K. K. and Dutta K. K. (1990) The Central Indian collision suture, *Spec. Pub. Geol. Surv. India* 28, 1-43.

Yin L. M., Zhu M. Y., Knoll A. H., Yuan X.L., Zhang J.M. and Hu J. (2007) Doushantuo embryos preserved inside diapauses egg cysts, *Nature* 446, 661-663.